frontiers | Research Topics

Molecular diagnostic methods for bacteria and fungi detection

Edited by
Laura Cerqueira and Carina Almeida

Published in
Frontiers in Cellular and Infection Microbiology

ISSN 1664-8714
ISBN 978-2-8325-5026-7
DOI 10.3389/978-2-8325-5026-7

About Frontiers

Frontiers is more than just an open access publisher of scholarly articles: it is a pioneering approach to the world of academia, radically improving the way scholarly research is managed. The grand vision of Frontiers is a world where all people have an equal opportunity to seek, share and generate knowledge. Frontiers provides immediate and permanent online open access to all its publications, but this alone is not enough to realize our grand goals.

Frontiers journal series

The Frontiers journal series is a multi-tier and interdisciplinary set of open-access, online journals, promising a paradigm shift from the current review, selection and dissemination processes in academic publishing. All Frontiers journals are driven by researchers for researchers; therefore, they constitute a service to the scholarly community. At the same time, the *Frontiers journal series* operates on a revolutionary invention, the tiered publishing system, initially addressing specific communities of scholars, and gradually climbing up to broader public understanding, thus serving the interests of the lay society, too.

Dedication to quality

Each Frontiers article is a landmark of the highest quality, thanks to genuinely collaborative interactions between authors and review editors, who include some of the world's best academicians. Research must be certified by peers before entering a stream of knowledge that may eventually reach the public - and shape society; therefore, Frontiers only applies the most rigorous and unbiased reviews. Frontiers revolutionizes research publishing by freely delivering the most outstanding research, evaluated with no bias from both the academic and social point of view. By applying the most advanced information technologies, Frontiers is catapulting scholarly publishing into a new generation.

What are Frontiers Research Topics?

Frontiers Research Topics are very popular trademarks of the *Frontiers journals series*: they are collections of at least ten articles, all centered on a particular subject. With their unique mix of varied contributions from Original Research to Review Articles, Frontiers Research Topics unify the most influential researchers, the latest key findings and historical advances in a hot research area.

Find out more on how to host your own Frontiers Research Topic or contribute to one as an author by contacting the Frontiers editorial office: frontiersin.org/about/contact

Molecular diagnostic methods for bacteria and fungi detection

Topic editors

Laura Cerqueira — University of Porto, Portugal

Carina Almeida — National Institute for Agricultural and Veterinary Research (INIAV), Portugal

Citation

Cerqueira, L., Almeida, C., eds. (2024). *Molecular diagnostic methods for bacteria and fungi detection*. Lausanne: Frontiers Media SA.

doi: 10.3389/978-2-8325-5026-7

Table of contents

frontiers | Frontiers in Cellular and Infection Microbiology

TYPE Editorial
PUBLISHED 04 June 2024
DOI 10.3389/fcimb.2024.1430630

OPEN ACCESS

EDITED AND REVIEWED BY
Rodolfo García-Contreras,
National Autonomous University of Mexico, Mexico

*CORRESPONDENCE
Laura Cerqueira
lcerqueira@fe.up.pt

RECEIVED 10 May 2024
ACCEPTED 24 May 2024
PUBLISHED 04 June 2024

CITATION
Almeida C and Cerqueira L (2024) Editorial: Molecular diagnostic methods for bacteria and fungi detection.
Front. Cell. Infect. Microbiol. 14:1430630.
doi: 10.3389/fcimb.2024.1430630

Editorial: Molecular diagnostic methods for bacteria and fungi detection

Carina Almeida[1,2,3] and Laura Cerqueira[2,3]*

[1]Food Safety Unit, National Institute for Agrarian and Veterinary Research (INIAV), Vila do Conde, Portugal, [2]LEPABE – Laboratory for Process Engineering, Environment, Biotechnology and Energy, Faculty of Engineering, University of Porto, Porto, Portugal, [3]AliCE – Associate Laboratory in Chemical Engineering, Faculty of Engineering, University of Porto, Porto, Portugal

KEYWORDS

diagnostic methods, bacteria, fungi, molecular methods, pathogens detection

Editorial on the Research Topic
Molecular diagnostic methods for bacteria and fungi detection

In recent years, a multitude of emerging pathogens and resistance determinants have highlighted the growing urgency for rapid and multiplex testing to address a spectrum of challenges of public health, veterinary, and environmental sectors. Currently, cutting-edge technologies in molecular diagnostics have emerged as indispensable tools to effectively address: the great diversity of agents that need to be detected in different matrices, the need to provide a fast and more informative response; the need for low detection limits to allow early detection; and/or the need to produce deployable methods that can be used *in loco* or in low-resource contexts. These needs set the foundation for a broad range of molecular-based technologies that could expedite the diagnosis and provide a precise intervention.

In this Research Topic, researchers were encouraged to submit innovative works describing new molecular methodologies, or comparing existing ones, with the purpose of improving microbial detection/diagnosis. This Research Topic provides examples of diverse molecular methods, from conventional PCR, to digital PCR or isothermal amplification techniques, that proved to be good alternatives to standard culturing techniques either in terms of time to result, limit of detection or type of information obtained.

Beginning with a study on the evaluation of different methodologies; Chatelard at al. has provided a comparison of three early blood culture testing protocols in terms of their ability to shorten the time to result and implement timely/appropriate antibiotic therapy. Positive blood cultures were tested using either a multiplex PCR panel (GenMark ePlex), a combination of MRSA/SA PCR, β-Lacta and oxidase tests (multi test), or conventional identification and susceptibility testing (as the gold standard). The delay between a blood culture positivity and initial results was more pronounced in the multitest protocol. More importantly, the proportion of patients receiving appropriate antibiotic therapy within 48 h of blood sampling was higher when either multiplex PCR and multitest were implemented (90% and 88%, respectively) comparing to the conventional method (71%).

Moving to another comparison study, now on tuberculosis diagnostics, Boldi et al. has provided an important 10-year retrospective study on the performance of microscopy, PCR and culture on different respiratory specimens (sputum, induced sputum, bronchial

aspirate and bronchoalveolar lavage). Culture displayed the highest sensitivity and specificity, while PCR has shown higher sensitivity and specificity than microscopy for all respiratory specimens. The diagnosis yield of bronchial aspirate was higher than that of bronchoalveolar lavage. Overall, results suggest that PCR should be systematically performed on bronchial aspirates, when available, to expedite diagnosis without significantly compromising the diagnostic accuracy.

Another subject of great relevance when dealing with significant infectious agents/diseases, such as Tuberculosis, is the availability quality control materials for appropriate proficiency testing. Early diagnosis is essential for proper treatment, especially in low- and middle-income countries that register 98% of the Tuberculosis cases worldwide, and reference materials are crucial for proper training and assessment of laboratories. Guan et al. provided us with a quality control library to be used with Xpert MTB/RIF test, a worldwide implemented assay (endorsed by the World Health Organization) that provides detection and simultaneous rifampicin resistance testing. The panel covers various probe patterns of Xpert MTB/RIF for the resistance detection. The library was constructed in two non-pathogenic bacterial strains, *E. coli* and *Bacillus subtilis*, which eliminate biosafety risks.

Still within the tuberculosis diagnostics, Owusu et al. propose a new multiplex PCR assay that allows the differentiation of *Mycobacterium tuberculosis* complex, specifically *M. tuberculosis*, *M. africanum* Lineages 5/6 and *M. bovis*, in low resource settings. No cross-reaction with other respiratory pathogens was observed and the detection limit for the different primers sets ranged between 620 and 2479 copies/ul. Validation was performed in sputum samples from 341 confirmed tuberculosis patients previously analysed by sputum smear microscopy, GeneXpert MTB/RIF assay and culture (BD BACTEC) methods. This multiplex PCR assay allowed the speciation of MTBC lineages in clinical samples, as well as the identification of mixed-lineage tuberculosis infections that can difficult treatment.

Other interesting PCR methodologies were proposed by Jiang et al. to detect two relevant fungal genera, *Aspergillus* and *Mucorales*, into paraffin-embedded tissue samples collected from patients with suspected invasive mold disease. The methodologies targeted the 18S and the 28S rRNA and presented sensitivity values ranging from 65% to 75% and specificity ranging from 82 to 97%. Interestingly, Wei et al. studied an alternative, non-invasive, approach to detect pulmonary aspergillosis (PA) without resorting to bronchoalveolar lavage fluid (BALF). They stated that the use of ultra high-performance liquid chromatography coupled with high-resolution mass spectrometry (UHPLC-HRMS) ascertain the metabolic profile of exhaled breath condensate (EBC) samples in PA patients and can be used as a non-invasive alternative method. They have identified five biomarkers for the diagnosis of PA. Compared with other methods (sputum smear and culture, BALF galactomannan assay and mNGS), the EBC method was accurate and efficient.

A promising molecular alternative in terms of sensitivity/detection limit certainly rests in digital PCR, for its ability to split the sample/reaction mix into thousands of single partitions. Tak et al. have developed an innovative droplet digital PCR (ddPCR) method to detected low number of infectious bacteria during early stages of prosthetic joint infection. The bacterial pathogen adheres and then forms microcolonies and biofilms that are very difficult to eradicate. Most often diagnosis resorts to a combined approach but depends mostly on the culture of patient-derived samples (typically tissue samples obtained during joint aspiration) which often contain very low number of cells, ending up on false negative results (due to low sensitivity). These authors make use of the ddPCR ability to provide absolute quantification of the target (without standard calibration curve), as well as its very high sensitivity, to detect early bacterial infection. They have found that ddPCR limit if detection was approximately 10 times lower than that of real-time PCR.

Within amplification-based molecular methods, isothermal techniques have evolved very quickly in the last years, especially due to the pressure of the SARS-CoV-2 pandemic crisis that boosted the development of point-of-need solutions, for which isothermal amplification is well suited. Recombinase polymerase amplification (RPA) is one the most studied isothermal alternatives, and here we provide two manuscripts addressing RPA applications. A practical example of an RPA application to a relevant clinical pathogen is provided by Liu et al. They have devised an RPA methodology to detect *Pseudomonas aeruginosa*, a pathogen involved in a wide range of clinical infections. They have combined RPA with a sequence-specific CRISPR-Cas biosensing system and, after optimization, the solution was validated in clinical samples. It was able to detect as low as 60 fg (~8 copies) of *P. aeruginosa* genomic DNA per reaction, no cross-reactivity was observed with 17 other species/strains. Performance on clinical samples was evaluated in 96 clinical samples, by comparison with a microfluidic chip. All results (19 positive and 77 negative for *P. aeruginosa*) were consistent with the microfluidic method.

The manuscript by Tan et al. reviews the principle and the different variations of RPA techniques, and it further provides a comparison with other amplification-based strategies. Clearly this technique holds great promise for future deployable solutions, with very short reaction times (5 to 20 minutes) and simple protocols and primers design. Further improvements on reagents availability and overall sensitivity, will certainly take these techniques to the next level of development.

All these works clearly show that the array of molecular techniques available today have the potential to improve, guide and expedite diagnosis, increasing the odds of a successful treatment and saving costs and, eventually, human lives. While, this Research Topic of articles showcases a limited diversity of molecular techniques/technologies that are today available in most of the research and routine laboratories; many more examples could be highlighted, with equal value and with great potential of application. Molecular diagnostics are reshaping our understanding of the microbial world and these new emerging alternatives are pushing the boundaries on our ability to quickly detect microorganisms with high accuracy. This research field will certainly bring exciting advances in the next years for diagnostic laboratories.

Author contributions

CA: Writing – review & editing, Writing – original draft. LC: Writing – review & editing, Writing – original draft.

Conflict of interest

The authors declare that the research was conducted in the absence of any commercial or financial relationships that could be construed as a potential conflict of interest.

The author(s) declared that they were an editorial board member of Frontiers, at the time of submission. This had no impact on the peer review process and the final decision.

Publisher's note

frontiers | Frontiers in Cellular and Infection Microbiology

TYPE Original Research
PUBLISHED 08 September 2022
DOI 10.3389/fcimb.2022.1008924

OPEN ACCESS

EDITED BY
Laura Cerqueira,
University of Porto, Portugal

REVIEWED BY
Malcolm D. Richardson,
The University of Manchester,
United Kingdom
András Bikov,
The University of Manchester,
United Kingdom

*CORRESPONDENCE
Shuo Wei
15846079@qq.com
Yi Shi
shiyi56@126.com

†These authors have contributed equally to this work and share first authorship

SPECIALTY SECTION
This article was submitted to Clinical Microbiology, a section of the journal Frontiers in Cellular and Infection Microbiology

RECEIVED 01 August 2022
ACCEPTED 22 August 2022
PUBLISHED 08 September 2022

CITATION
Wei S, Chen Y-s and Shi Y (2022) Metabolomic profiling of exhaled breath condensate for the diagnosis of pulmonary aspergillosis.
Front. Cell. Infect. Microbiol.
12:1008924.
doi: 10.3389/fcimb.2022.1008924

Metabolomic profiling of exhaled breath condensate for the diagnosis of pulmonary aspergillosis

Shuo Wei[1*†], Yi-sheng Chen[2†] and Yi Shi[3*]

[1]Department of Infectious Disease, Shengli Clinical Medical College of Fujian Medical University, Fujian Provincial Hospital, Fuzhou, China, [2]Department of Clinical Laboratory, Shengli Clinical Medical College of Fujian Medical University, Fujian Provincial Hospital, Fuzhou, China, [3]Department of Respiratory Medicine, Jinling Hospital, Nanjing, China

Objective: This study aims to ascertain the unique metabolic profile of exhaled breath condensate (EBC) samples in pulmonary aspergillosis (PA) patients, and explore their usefulness for the diagnosis of PA.

Methods: A total of 133 patients were included in the study, including 66 PA patients (invasive pulmonary aspergillosis, n=3; chronic pulmonary aspergillosis, n=60; allergic bronchopulmonary aspergillosis, n=3) and controls (n=67). Ultra high-performance liquid chromatography coupled with high-resolution mass spectrometry(UHPLC-HRMS) was used to analyze EBC samples. Metabolic profiling of EBC samples that were collected from 22 CPA patients at various times during treatment (before treatment, <1 month, 1–2 months, 2–3 months, 3–6 months, and ≥6 months after treatment initiation) were performed using UHPLC-HRMS. Potential biomarkers were evaluated using cluster analysis, Venn diagram and receiver operating characteristic analysis (ROC).

Results: A total of 47 metabolites of potential interest were detected in the EBC samples. Further investigation showed that Asperpyrone C, Kotanin, Terphenyllin, Terrelumamide B, and Cyclotryprostatin D could be used as a diagnostic biomarker for PA. The classification between metabolic profiling of EBC samples from PA patients and controls was good with a sensitivity of 100%, specificity 89.6% for patients with PA, respectively. Venn diagram analysis of these biomarker candidates displayed three main types of compounds, which could be used for the further discrimination of aspergilloma and chronic cavitary PA. In addition, antifungal treatment had a limited influence on the value of the EBC results.

Conclusions: This metabolomic approach using UHPLC-HRMS could be used as a noninvasive method for the diagnosis of PA.

KEYWORDS

pulmonary aspergillosis, exhaled breath condensate, ultra high-performance liquid chromatography, high-resolution mass spectrometry, diagnosis

Background

The diagnosis of pulmonary aspergillosis (PA) remains a challenge. Currently, diagnosis is mainly based on routine testing, such as pathological evidence,culture and direct microscopic examination. However, these routine methods have poor sensitivities (Patterson et al., 2016). Although bronchoalveolar lavage fluid (BALF) has been applied to galactomannan (GM) which is a component of the cell wall of *Aspergillus* assay and quantitative polymerase chain reaction (PCR) for diagnosis of PA and some progress has been made (Johnson et al., 2014; Patterson et al., 2016; Ullmann et al., 2018; Donnelly et al., 2020), the bronchoscopy examination is an invasive procedure and unsuitable for repeated use in practice.

Although exhaled breath analysis of volatile organic compounds (VOCs) by electronic nose (eNose) technology has been evaluated for the diagnosis of invasive aspergillosis and showed a good performance where the eNose discriminated *Aspergillus fumigatus* from bacteria/yeasts, or *Rhizopus arrhizus* with an accuracy of 92.9% and 100%, respectively (de Heer et al., 2016); However, this method requires special expensive equipment and is not available in most centers. In another study conducted in 2014, VOCs in exhaled breath was analyzed using gas chromatography mass spectrometry and the VOCs could be used to differentiate invasive pulmonary aspergillosis (IPA) from other pneumonias (Koo et al., 2014). Unfortunately, this study had several disadvantages, such as inconvenient sample preparation, expensive machines, and only invasive PA was included not chronic pulmonary aspergillosis (CPA). Recently, several studies have reviewed the application of exhaled breath condensate (EBC) samples in the assessment of pulmonary diseases, such as asthma, obstructive sleep apnea, and malignant pleural mesothelioma (De Luca Canto et al., 2015; Horváth et al., 2017; Peel et al., 2017; Treyin et al., 2020).

To date, few studies have been conducted to investigate the application of EBC samples in the diagnosis of PA. In 2018 a study reported that GM was detectable in EBC for the diagnosis of IPA in immunocompromised patients, however, this study did not include CPA patients (Bhimji et al., 2017).Therefore, this prospective study aims to ascertain the unique metabolic profile of EBC samples in PA patients and explore their usefulness for the diagnosis of PA.

Methods

Ethics

The study was conducted at Fujian Provincial Hospital in Southeast China. This study was approved by the Ethics Committees of Fujian Provincial Hospital (Ethical approval number K2021-03-041). Written informed consent was obtained from all suspected patients before the study started.

Patients

Between January 2018 and November 2019, PA patients who admitted to the center were included for further analysis, including IPA, Allergic Bronchopulmonary Aspergillosis (ABPA), and CPA [Simple aspergilloma, Aspergillus nodule, Chronic cavitary pulmonary aspergillosis (CCPA), Chronic fibrosing pulmonary aspergillosis (CFPA), Subacute invasive pulmonary aspergillosis formerly called chronic necrotizing pulmonary aspergillosis (CNPA)]. Controls were also set, including pneumonia (community acquired pneumonia (CAP), hospital acquired pneumonia (HAP)), chronic respiratory tract infection (such as COPD and bronchiectasis), and healthy volunteers. In addition, *Aspergillus* respiratory tract colonization control was also set. Then, clinical specimens, such as serum, sputum, BALF, and lung tissues, were collected from patients or healthy volunteers. Routine assays, such as culture, smear, GM, and 1-3-β-D glucan assays, metagenomic next-generation sequencing (mNGS), and histological examinations, were performed at various times during treatment (before treatment, <1 month, 1–2 months, 2–3 months, 3–6 months, and ≥6 months after treatment initiation), and EBC samples were collected in parallel to determine metabolic profiles for comparison. According to the 2016 consensus reached by the IDSA of PA, PA patients received voriconazole (6 mg/kg IV every 12 h for 1 d, followed by 4 mg/kg IV every 12 h; oral therapy can be used at 200–300 mg every 12 h or weight based dosing on a mg/kg basis) (Patterson et al., 2016). The detailed study protocol is shown in Figure 1.

The diagnostic criteria for patients were described briefly, as follows: proven or probable IPA were defined according to the revision and update of the European Organization for Research and Treatment of Cancer and the Mycoses Study Group Education and Research Consortium (Donnelly et al., 2020). The criteria for ABPA diagnosis was adapted from a review published in "*The Journal of Allergy and Clinical Immunology*" (2012) (Knutsen et al., 2012). The diagnosis of CPA requires a combination of characteristics: one or more cavities with or without a fungal ball present or nodules on thoracic imaging, direct evidence of *Aspergillus* infection (microscopy or culture from biopsy) or an immunological response to *Aspergillus* spp. and exclusion of alternative diagnoses, all present for at least 3 months (Denning et al., 2015). In addition, CPA was further classified as: Simple aspergilloma, Aspergillus nodule, CCPA, CFPA, CNPA (Denning et al., 2015). Colonization with *Aspergillus* spp. in respiratory samples was defined based on: without any evidence for *Aspergillus*- associated infection, and one or more criteria necessary for a diagnosis of putative PA are

absent. Patients were excluded due to unavailable EBC samples and requirement of mechanical ventilation.

EBC samples

At the same site, EBC was collected using a commercially available condenser (RTube, Respiratory Research, Charlottesville, Virginia, USA). No fasting required before sampling. It is a portable Collection Devices for the Study of Respiratory Droplets in Exhaled Breath Condensate. Large "Tee" section separates saliva from the exhaled breath and prevents it from entering the condensation tube Custom duckbill valve/nozzle enhances condensation efficiency and produces high condensate volumes. Exhaled Breath Condensate (EBC) is composed of droplets of Airway Lining Fluid (ALF) evolved by turbulence from all lung compartments and held in a matrix of condensed moisture from the breath. These droplets contain numerous biomarkers including DNA, RNA, mRNA, proteins, metabolites, and volatile organic compounds (VOC). Typical condensate fluid yield is 200 microliters/minute for an adult at normal tidal breathing effort. 7-10 minute collection time is commonly employed. EBC Volume of Condensate Collected at least 1000 microliters. Prepare the cooling sleeve before taking samples. The cooling sleeve is necessary for efficient condensate collection. Usually stored in a laboratory freezer Temperature(-80°) until needed. After sample collection has been completed and the sample stored properly and place the cooling sleeve back into the protective bag and refreeze. This unique feature allows for easy integration of the RTube into existing studies and allows large amounts of EBC data to be collected with ease from subjects in the clinic, hospital, home, workplace, school, or any other reasonable environment. Then, EBC samples were preserved in aliquots and stored at −80°C until analysis. Ultra high-pressure liquid chromatography (UHPLC) and electrospray ionization (ESI) coupled with high-resolution mass spectrometry (HRMS) (UHPLC/ESI–HRMS) analyses were performed using a Waters Acquity Ultra-Performance Liquid Chromatography (LC) (UPLC) system (Waters, Milford, MA, USA) and Waters Xevo G2-XS Q-TOF system, as outlined in the Supplementary Methods. (Supplementary Material 1). After removing background noise, all compounds identified with a mass spectrometry response value of > e^4 were selected for further analysis. Then, a comparison between PA patients and healthy volunteers was performed to identify potential compounds for the diagnosis of PA. In addition, based on the existing literature, a dataset of the metabolites of *Aspergillus* sp. was manufactured and then differential compounds found in the EBC samples were determined if they had the same m/z value (differences <0.05 Da) was matched. The investigators that performed the metabolite identification were blinded to clinical data.

Venn diagram analysis of the EBC metabolites that were identified and cluster analysis of PA patients was then performed. The diagnostic performance of the EBC method was evaluated and compared with routine methods, or BALF GM assay combined with mNGS. In addition, the potential of the EBC method during antifungal treatment was investigated.

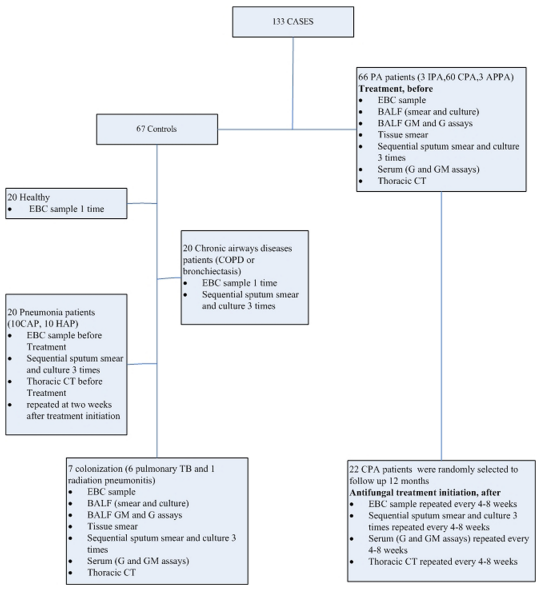

FIGURE 1
Flow chart of study protocol.

Statistical analysis

Statistical analyses were performed by SPSS 23.0. Venn diagrams (OriginPro 2019, version 9.6.0.172; OriginLab) and cluster analyses were used to screen out the differential metabolomic profiling of EBC between patients with different aspergillosis. Then, clinical characteristics aspects were compared between PA patients and controls and among PA subgroups. Continuous variables were presented with mean ± standard deviation and compared with ANOVA. Categorical variables were presented with percentages (frequency) and compared with Chi-squared (χ^2) or Fisher's exact tests. Quantitative analysis was performed by UHPLC/ESI–HRMS, sensitivity and specificity were calculated, respectively. The receiver operating characteristic (ROC) analysis was used to compare different diagnostic methods, and the agreement between them was assessed using Cohen's kappa coefficient. A two-sided *p*-value of <0.05 was considered significant.

Results

Patients

During the study, a total of 66 PA patients (IPA, n=3; CPA, n=60; ABPA, n=3) were included. Then, twenty two of CPA cases were selected randomly and followed-up for 1 year. Controls (n=67) that included pneumonia (n=20; CAP), n=10; HAP, n=10), chronic airway disease (n=20), *Aspergillus* respiratory tract colonization (n=7; pulmonary tuberculosis, n=6; radiation pneumonitis, n=1), and healthy volunteers (n=20) were included. No significant differences existed between the five groups (PA, colonization, pneumonia, chronic airway disease, and healthy) in clinical characteristics aspects included number, age, gender, risk factor, and APACHEII (Table 1).

Comparison between healthy and PA groups

By literature review, a data set of primary *Aspergillus* metabolites and secondary metabolites were constructed with at least 500 compounds for the identification of candidates (Supplementary Material 2). A comparison of UHPLC/ESI–HRMS results between healthy (n = 20) and PA (n = 66) groups was performed. Approximately 47 metabolites were different between groups which were selected for further analysis. Among the PA group, 10 of the 47 metabolites were positive in >80% of cases (Table 2). Owing to the high analyte sensitivity of UHPLC/ESI–HRMS revealed by ion responses and chromatographic peak shape, five metabolites were excluded and the remaining five were included, as follows: Asperpyrone C, Terphenyllin, Kotanin, Terrelumamide B, and Cyclotryprostatin D. Asperpyrone C was detected in all cases with PA, UHPLC/ESI–HRMS analysis revealed that Terphenyllin was more abundant compared with the others, and all five metabolites previously mentioned could easily be identified (Figures 2, 3). In addition, the five metabolites were absent in 40 patients with pneumonia and chronic respiratory tract infection. However, one or more metabolite of the five metabolites mentioned above could be detected in the EBC samples among the seven cases with *Aspergillus* colonization.

Hierarchical cluster analysis

First, PA patients were divided into seven groups: invasive PA, Aspergilloma, Aspergillus nodule, chronic cavitary PA, chronic fibrosis PA, chronic necrotizing PA, and allergic bronchopulmonary aspergillosis. Then, a Venn diagram was constructed for the 47 metabolites to show the similarities between the EBC signature for the metabolic panel. No significant difference in the clinical characteristics was observed between the seven groups (Table 3, $p>0.05$). The cluster analysis identified three groups: (1) chronic cavitary PA, chronic fibrotic aspergillosis; (2) invasive PA, allergic bronchopulmonary aspergillosis, aspergillus nodule, chronic necrotizing PA; and (3) aspergilloma (Figure 4A). The Venn diagram identified three main types of metabolites that partially overlapped (Figure 4B).

Diagnostic performance of metabolic panels of EBC

For the diagnosis of PA, the role of metabolic panels of EBC were assessed using Cohen's kappa coefficient (κ), sensitivity, specificity, positive and negative predictive values and were reported as follows: 0.895, 100% (66/66), 89.6% (60/67), 90.4% (66/73), and100% (66/66), respectively (Table 4). Between the 133 patients included in the study, the EBC method agreed with the clinical diagnosis in most patients [n = 126 (94.7%)] and disagreements between the two were found in seven cases, which showed confirmed colonization.

In addition, ROC analysis was used to compare the performance between the EBC method and routine methods [e.g., tissue examination, culture and smear (e.g., sputum, BALF, bronchial brushing, and tissues)] or BALF GM assay combined with mNGS (BALF GM+ mNGS). The positive results of each methods: (1) EBC method: PA patients (100%, 66/66), controls, (10.4%, 7/67); (2) Combination of tissue examination and culture and smear using several specimens (e.g., sputum, bronchoalveolar lavage fluid, bronchial brushing, and tissue): PA patients (45.5%, 30/66), controls (0%, 0/67); (3) BALF GM + mNGS: PA patients (81.8%, 54/66), controls (10.4%, 7/67). The area under the ROC curve of the EBC method was 0.948 and was

TABLE 1 Clinical characteristics of subjects included in this study.

Variables	PA	Aspergillus colonization [a]	Pneumonia[c]	Chronic airway disease[d]	Healthy	*p*-value
Number	66	7	20	20	20	
Age (years)	56.86 ± 11.08	62.86 ± 8.80	57.20 ± 10.40	60.35 ± 9.64	58.65 ± 10.79	0.500
Gender [male (%)]	38 (57.6)	3 (42.9)	10 (50.0)	12 (60.0)	10 (50.0)	0.888
[b]Risk factor [(n) %]	5 (7.6)	1 (14.3)	1 (5.0)	1 (5.0)	0 (0.0)	0.771
[e]APACHEII	6 (4.75,7)	8 (3,9)	6 (4.25,8)	7 (5,7.75)	N/A	0.204

[a]colonization (6 pulmonary TB and 1 radiation pneumonitis).
[b]The risk factors for PA include prolonged neutropenia, hematologic malignancy, allogeneic HSCT recipients, solid organ transplant (SOT) recipients, corticosteroid use, T or B-cell immunosuppressants use, inherited severe immunodeficiency, and acute graft-versus-host disease grade III or IV (Donnelly et al., 2020).
[c]Sputum culture for pneumonia (n=20): Streptococcus pneumoniae pneumonia (n = 1), Stenotrophomonas maltophilia (n = 1), Pseudomonas aeruginosa (n = 1), methicillin resistant Staphylococcus aureus (n = 1), and others (-).
[d]Chronic respiratory tract infection: Stenotrophomonas maltophilia (n=1), Pseudomonas aeruginosa (n=1), and others (-).
[e]APACHE II, acute physiology and chronic health evaluation scoring system; Healthy group, N/A.

TABLE 2 Positive rates for 47 metabolites identified in EBC samples among patients with PA.

No	Compound	m/z value	Positive rate (%)
1	2-hydroxy-3-methyl-1,4-benzoquinone, C7H6O3	138.121	6.1
2	Penicillic acid, C8H10O4	170.163	83.3
3	Naphthalic anhydride, C12H6O3	198.174	93.9
4	Aspergillomarasmine B, C9H14N2O8	278.216	3.0
5	aflatoxicol (Aflatoxin Ro), C17H14O6	314.289	22.7
6	3-hydroxyterphenyllin, C20H18O6	354.353	92.4
7	JBIR-138, C19H23O7	363.382	3.0
8	Demethylasterriquinone, C24H20N2O5	416.426	13.6
9	Arugosin E, C25H26O6	422.470	4.5
10	Kotanin, C24H22O8	438.427	97.0
11	Terrelumamide B, C19H18O7N6	442.382	81.8
12	Terrelumamide A, C20H20O7N6	456.409	42.4
13	territrem A, C28H30O9	510.532	4.5
14	Dianhydro-aurasperone C, C31H24O10	556.516	19.7
15	Asperpyrone C, C32H26O10	570.543	100.0
16	Emestrin, C27H22N2O10S2	598.601	4.5
17	Flufuran, C6H6O4	142.109	22.7
18	Terphenyllin, C20H18O5	338.354	83.3
19	Asterriquinone (1), C25H22N2O5	430.453	16.7
20	Fumitremorgin C/Tryptoquivaline C, C29H30N4O7	546.571	13.6
21	Nigerapyrone B, C21H20O3	320.382	81.8
22	Cyclotryprostatin D, C21H21N3O4	379.409	80.3
23	Candidusin A 804, C20H16O6	352.337	72.7
24	Folipastatin, C23H24O5	380.434	74.2
25	Asparvenone, C12H14O4	222.237	62.1
26	Erythroglaucin, C16H12O6	300.263	3.0
27	versiconal acetate, C20H16O9	400.336	1.5
28	Pseurotin B, C22H25NO9	447.435	22.7
29	cis-4-Hydroxymellein, C10H10O4	194.184	1.5
30	phthalide or chromanol (3), C11H12O5	224.210	1.5
31	Bianthrone and secoanthraquinone secondary metabolite 1, C16H14O7	318.278	4.5
32	phthalide or chromanol (7), C16H20O7	324.326	4.5
33	Phenylahistin, C20H22N4O2	350.414	4.5

(Continued)

10.3389/fcimb.2022.1008924

TABLE 2 Continued

No	Compound	m/z value	Positive rate (%)
34	Sydoxanthone C, C17H14O7S	362.354	4.5
35	5,6-dimethoxysterigmatocystin, C20H16O8	384.336	4.5
36	Kipukasin H, C18H20N2O9	408.359	7.6
37	Butyrolactone I, C19H16O7	356.326	7.6
38	Emerixanthone D, C27H30O8	482.522	9.1
39	Phomaligin A, C16H25NO5	311.373	28.8
40	brevianamide M, C18H15N3O3	321.330	3.0
41	Viriditoxin, C34H30O14	662.594	37.9
42	Neosartorin, C34H32O15	680.609	13.6
43	Cryptoechinuline E, C20H19N3O3	349.383	4.5
44	Xanthoascin (2), C22H16N2O4	372.373	10.6
45	tryptoquivaline E, C22H18N4O5	418.402	3.0
46	Fumiquinazoline K, C26H23N5O4	469.492	6.1
47	Fumiquinazoline C, C24H21N5O4	443.455	3.0

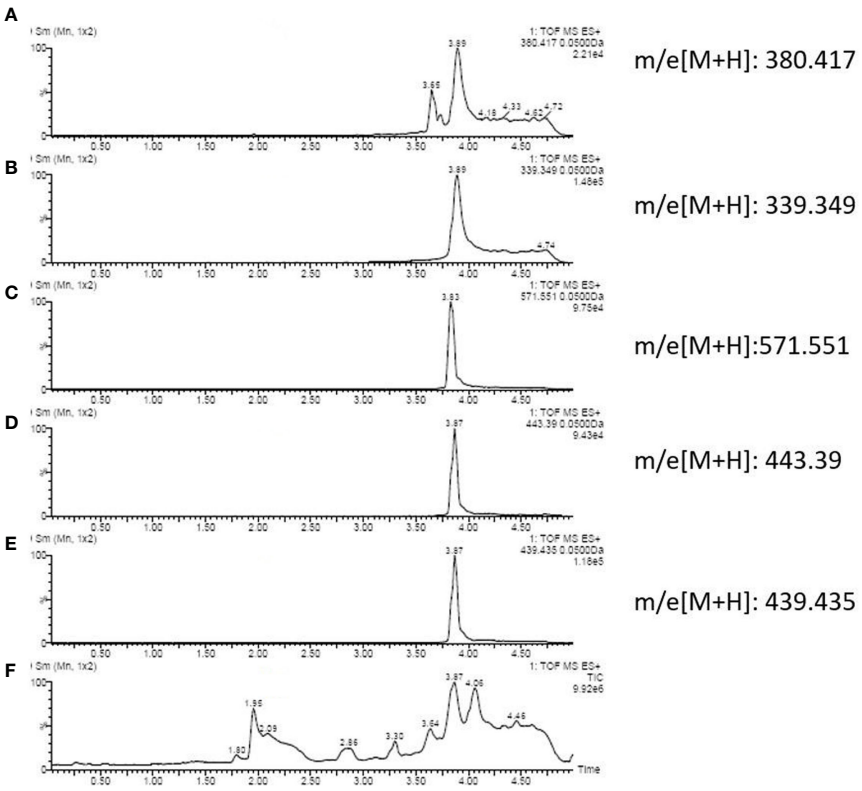

FIGURE 2
Ion chromatography of an EBC sample that consists of: **(A)** Cyclotryprostatin D; **(B)** Terphenyllin; **(C)** Asperpyrone C; **(D)** Terrelumamide B; **(E)** Kotanin; and **(F)** total metabolites.

10.3389/fcimb.2022.1008924

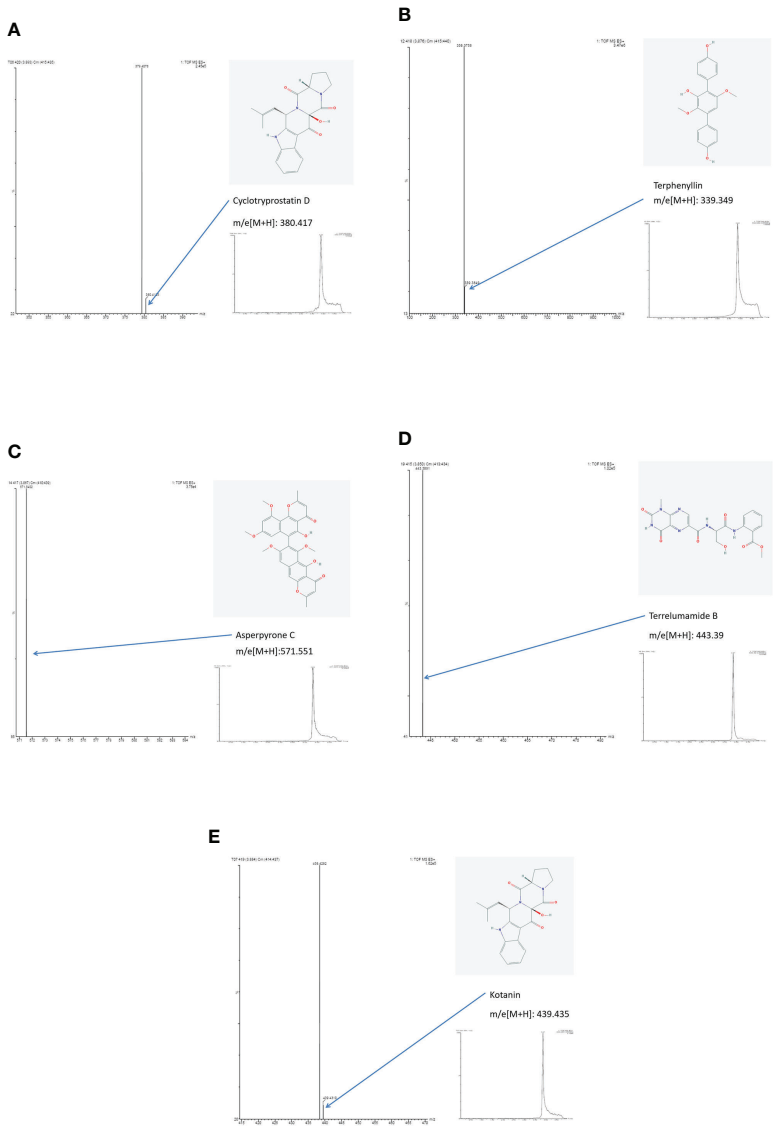

FIGURE 3
Results of ion chromatography and mass spectrometry: **(A)** Cyclotryprostatin D; **(B)** Terphenyllin; **(C)** Asperpyrone C; **(D)** Terrelumamide B; **(E)** Kotanin.

higher than that of the routine methods (0.723), or BALF GM assay combined with mNGS [0.863; $p<0.05$ (Figure 5)].

Impact of antifungal therapy

In total, 22 CPA patients were followed-up for 1 year. Routine (sputum culture and smear) and EBC methods were tested after 1, 2 and 3 months, 3–6 months, 6–9 months, 9–12 months, and ≥12 months of antifungal therapy. The sensitivity of the EBC method was always 100% (Figure 6). In addition, considering corresponding conditions, patients were administrated with 6-9 months, 9-12 months, or ≥12 months antifungal therapy separately, all EBC samples were tested as negative at the therapy termination. In contrast, the sensitivity of routine methods appeared to decrease during the treatment, only 20% were positive in routine methods after 6 months of therapy and none of them were positive when the study was completed.

TABLE 3 Clinical characteristics of patients between seven groups.

	IPA	Aspergillus globules	Aspergillus nodule	chronic cavitary PA	chronic fibrosis PA	chronic necrotizing PA	allergic bronchopulmonary aspergillosis	*p*-value
Number (n)	**3**	**10**	**6**	**22**	**4**	**18**	**3**	
Age (years, mean ± SD	58.00 ± 5.00	57.90 ± 10.91	52.17 ± 13.24	57.55 ± 12. 13	57.50 ± 14.34	56.17 ± 9.33	60.00 ± 17.35	0.340
Gender [n (%)]								0.987
Male	2 (66.7)	6 (60.0)	4 (66.7)	13 (59.1)	2 (50.0)	9 (50.0)	2 (66.7)	
[a]Risk factors [n (%)]	1 (33.3)	0 (0.0)	0 (0.0)	2 (9.1)	0 (0.0)	1 (5.6)	1 (33.3)	0.277
APACHE II	9 (6),	4 (3.75,6.5)	4.5 (3,6.75)	5 (4,6.25)	6.5 (5.25,7.75)	7 (4.75,9)	6 (6),	0.097
Smear (sputum or BALF)	1 (33.3)	1 (10.0)	1 (16.7)	3 (13.6)	1 (25.0)	2 (11.1)	0 (0)	0.969
Culture (sputum or BALF)	2 (66.7)	3 (30.0)	2 (33.3)	8 (36.3)	2 (50.0)	5 (27.8)	2 (66.7)	0.787
BALF GM≥1.0	1 (33.3)	4 (40.0)	3 (50.0)	15 (68.2)	3 (75.0)	11 (61.1)	2 (66.7)	0.741

[a]Risk factors for PA include prolonged neutropenia, hematologic malignancy, allogeneic HSCT recipients, solid organ transplant (SOT) recipients, corticosteroid use, T or B-cell immunosuppressants use, inherited severe immunodeficiency, and acute graft-versus-host disease grade III or IV (Donnelly et al., 2020). Five patients had ≥1 risk factors, including one renal transplant (n = 1) and corticosteroid use (n = 4).
Of the 66 PA patients, 40 were tested for tissue culture and pathological examination and 18 have positive results, 12 were tested for immunoCAP Aspergillus-specific IgG test and 10 have positive results, nine were tested for BALF mNGS and three have positive results, and no BALF PCR was performed.

Discussion

In this study, metabolites produced by *Aspergillus* sp. were exhaled and absorbed into the condensing breath. Using a condenser RTube EBC samples were collected for UHPLC/ESI– HRMS analysis and metabolites, such as Asperpyrone C, Kotanin, Terphenyllin, Terrelumamide B, and Cyclotryprostatin D5 demonstrated a significant difference between the PA group (IPA, CPA, and ABPA) and healthy volunteers, pneumonia, or chronic respiratory tract infection. Further analysis showed the metabolic panels of EBC samples had a sensitivity of 100% and specificity of 89.6% for the diagnosis of PA.

Over the last decades, several assay, such as GM assay, *Aspergillus* IgG antibodies serology test, and molecular methods (eg, PCR, and mNGS) were evaluated in the field of IPA and CPA diagnosis. According to the guidelines, mycological evidence for probable IPA includes the following items: 1) GM assays (at least one): single serum or plasma: ≥1.0; BAL fluid: ≥1.0; single serum or plasma: ≥0.7 and BAL fluid ≥0.8. 2) *Aspergillus* PCR (at least one): plasma, serum, or whole blood (+, 2 or more consecutive PCR tests); BAL fluid (+, 2 or more duplicate PCR tests); plasma, serum, or whole blood (+, at least 1) and BAL fluid (at least 1). 3) *Aspergillus* culture: sputum (+), BAL(+), bronchial brushing (+), or bronchial aspirate (+) (Donnelly et al., 2020). Besides, if patients have one or more cavities, characteristic are consistent with CPA, and other diagnosis has been excluded, a diagnosis of CPA can be confirmed when met the following items: *Aspergillus* IgG antibodies serology or precipitins (+), GM (+) or *Aspergillus* DNA (+) in respiratory fluids (Denning et al., 2015). Recently, mNGS was introduced in practice and presented as a promising diagnostic tool for the diagnosis of infectious lesions. This method detected and identified a large variety of pathogens during pulmonary infection, including *Aspergillus* sp (Huang et al., 2020).

In this study, a comparison of diagnostic performance between EBC method、BALF GM +mNGS, and routine methods were assessed. It was found that the EBC method has the highest AUC value with about 1.0 and further ROC curve analysis demonstrated that the EBC method was superior to the other two methods for the diagnosis of PA. The data suggested that the sensitivity of the EBC method was higher than that of the other two other methods and BALF GM +mNGS and EBC methods had similar specificities without significant difference. Due to the small number of IPA, and ABPA enrollment, and the fact that the diagnosis of ABPA (without routine methods and GM assay) (Knutsen et al., 2012) the diagnostic performance of IPA, CPA, and ABPA for EBC was not further analyzed separately compared with routine methods and with BALF GM + mNGS tests. It was reported that, in patients with impaired immunity of having IPA, serum GM had a sensitivity of 0.71 and specificity of 0.89. BAL GM had a sensitivity of 0.84 and specificity of 0.88. Serum or whole blood PCR had a sensitivity of 0.81 and specificity of 0.79. BAL PCR had a high sensitivity of 0.90 and specificity of 0.96 (Haydour et al., 2019). Regarding the role of GM assay in CPA, serum GM appears to have limited value for CPA diagnosis. This is because the sensitivity of serum GM was only 23% (Shin et al., 2014). In addition, the performance of GM assay for CPA diagnosis depended on the cut off value selected. For example, the sensitivity and specificity of GM assay in BAL fluid specimens was 77.2% and 77.0%,

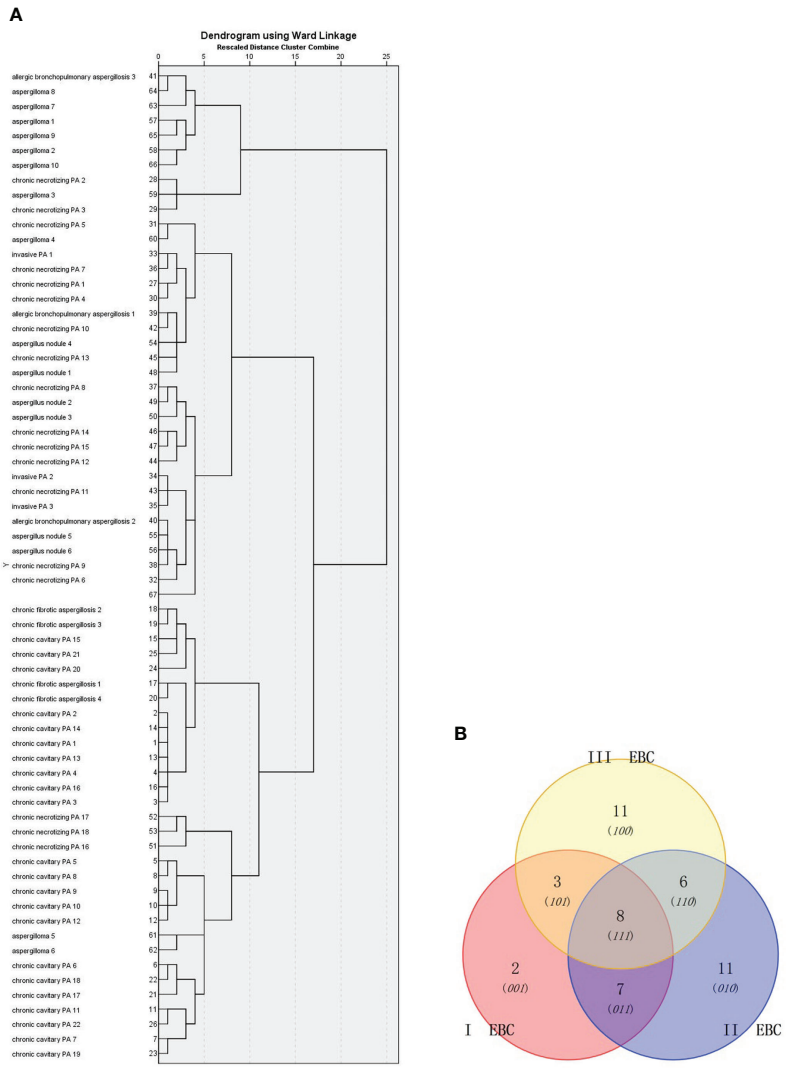

FIGURE 4
Cluster analysis of: **(A)** 66 PA patients based on Ward chain; and **(B)** Venn diagram analysis of the EBC metabolites identified from these patients. I EBC : Table 2 (26, 27). II EBC: Table 2 (29-35, 38,40- 42). III EBC: Table 2 (1, 4, 7, 9,13,16, 43-47).

respectively (with a cut-off level of 0.4) (Izumikawa et al., 2012). In another study the BAL GM-antigen detection test had a sensitivity and specificity of 85.7% and 76.3%, respectively, with a cut-off level of >0.5 (Kono et al., 2013). In a recent study, the best cut off value for serum and BALF-GM was 0.55 (area under the ROC curve [AUROC], 0.605; sensitivity, 38%; specificity, 87%) and 1.375 (AUROC, 0.836; sensitivity, 68%; specificity, 93%), respectively. At a cutoff value of 2.5, BALF GM had a sensitivity and specificity of 50% and 100%, respectively (Sehgal et al., 2019).

TABLE 4 Performance of EBC method in the diagnosis of PA.

	PA	Controls	Total	Kappa indices	Agreement
EBC method (+)	66	7	73	0.895	94.7%
EBC method (-)	0	60	60		
Total	66	67	133		

Kappa indices, 0.895 (0.821–0.969, 126/133); Sensitivity, 100% (0.821–0.969, 66/66); Specificity, 89.6% (79.1%– 95.3%, 60/67); Negative predictive value, 100% (92.5%–100.0%, 66/66); Positive predictive value, 90.4% (80.7%–95.7%, 66/73).

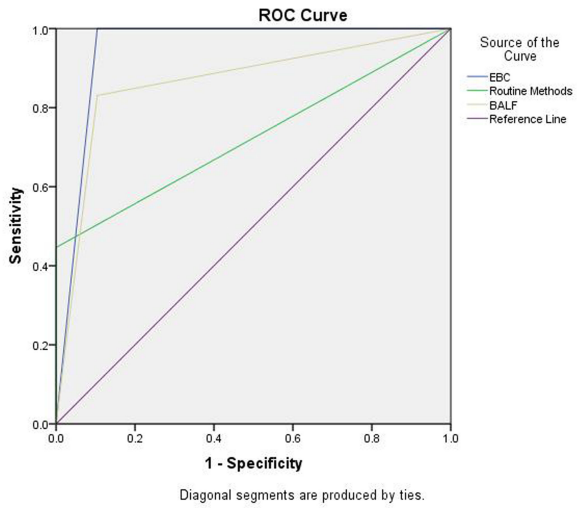

FIGURE 5
ROC analysis for EBC method, routine assays, and BALF GM + mNGS in the diagnosis of PA. Area under ROC curve: EBC, 0.948 (0.904, 0.991); routine method, 0.723 (0.634, 0.812); and BALF GM + mNGS 0.863(0.795,0.931).

Of the 66 PA patients, three groups were identified by cluster analysis: (1) CCPA,CFPA; (2) IPA, ABPA, aspergillus nodule, CNPA; and (3) aspergilloma. It is noted that according to the results previously mentioned, cluster analysis is associated with infectious severity and is not related to the immune responses to *Aspergillus* sp. and the length of the clinical course of aspergillosis. The findings suggested that pathological evidence was not associated with the cluster analysis and patients with different pathological conditions (e.g., IPA, CPA, and ABPA) could be allocated to the same group. In this study, the result of cluster analysis might be explained by: (1) the first group (CCPA, CFPA) had the same infectious severity that both had a longer length of the clinical course (>6 months); (2) the second group might all be involved with the distribution of fungal agents within the respiratory airways and similar EBC metabolites were found. Due to its invasive nature, IPA and CNPA could cause invasion of the respiratory tract. Aspergillus nodule might be caused by the distribution of *Aspergillus* sp. along the respiratory tract. ABPA is a type of reactive airway diseases; and (3) aspergilloma usually presents with no or mild symptoms, or no radical changes within at least 3 months. Due to mild symptoms, patients usually resolve without any treatment. Unfortunately, if CCPA presents in a single cavity, it is difficult to discriminate it from aspergilloma, and further information, such as clinical symptoms, progression revealed by radiological imaging, and inflammatory biomarkers are required for the discrimination. However, the findings suggested a potential diagnostic tool for discriminating between chronic cavitary PA and aspergilloma. This was because some compounds are associated with the severity of *Aspergillus* sp. infection.

For the diagnosis of PA (IPA, CPA, and ABPA), the panels of metabolites in the EBC samples have several advantages. First, the EBC sample was easy to prepare and could be stored and transferred for analysis. Most importantly, this method is noninvasive. Second, the control group included pneumonia and chronic respiratory tract infections, such as *Pseudomonas aeruginosa* and *Stenotrophomonas maltophilia* colonization. the EBC method could easily differentiate them. This implied that the metabolites found in this study were specific to PA patients. Third, the sensitivity of routine methods appeared to decrease during treatment, only 20% were positive using routine methods after 6 months of therapy and none were positive using routine

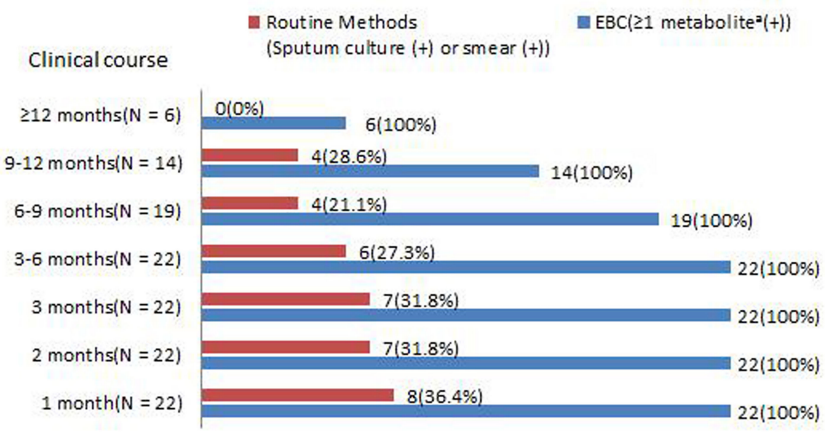

FIGURE 6
Positive rates of (sputum culture and smear) and ≥1 metabolite in EBC samples among PA patients during antifungal therapy. [a]Asperpyrone C, Kotanin, Terphenyllin, Terrelumamide B, and Cyclotryprostatin D.

methods when patients were censored. Unlike routine methods, the sensitivity of the EBC method remained high and was always 100% during the treatment. In addition, even in patients that were free of abnormal radiological features, ≥1 metabolite in the EBC samples could be detected. Similar finding could be found in *Aspergillus* colonization controls. These finding has equal significance with a positive *Aspergillus* PCR in BALF (Denning et al., 2015), which supports the diagnosis, but are not enough alone for a confirmed diagnosis of PA as numerous other conditions can yield *Aspergillus* in the airways. However, after antifungal therapy termination, the target metabolites couldn't be detected. This study has several limitations. First, due to the superior sensitivity of mass spectrometry, levels of metabolites in the EBC samples varied significantly between each run. Therefore, this study was conducted based on qualitative data. In addition, the level of metabolites found in the study was not further analyzed and investigated for their potential significance. Second, for *Aspergillus* sp. infection, several clinical presentations, such as invasive PA, allergic bronchopulmonary aspergillosis, and chronic PA might occur in one patient. This might contribute to a significant influence on the accuracy of cluster analysis. Third, Aspergillus-specific IgG antibodies serology test, which is known as a superior test to other diagnostic methods for CPA confirmation, was infrequently used in the cohort. Therefore, a comparison with EBC method wasn't evaluated, this point should be paid an caution. Fourth, small sample is another limitation. For example, due to few cases of IPA and ABPA included, our results may not reflect the true metabolic profile of EBC samples. If more controls with *Aspergillus* colonization were included, metabolite for the discrimination between *Aspergillus* colonization and diseases may be identified. In the next, further analysis is required to validate the findings in a larger population.

This study investigated the EBC metabolic profile of PA patients using UHPLC/ESI–HRMS and five biomarkers for the diagnosis of PA were identified. Compared with other methods (e.g., sputum smear and culture, BALF GM assay, and mNGS), the EBC method was accurate and efficient. More importantly, the EBC method remained positive for a long time, up to 1 year later. In addition, the metabolite profiling of EBC samples could reveal the metabolite signatures in patients with different clinical presentations of PA. These findings suggested that the EBC method could be a potentially safe, noninvasive approach for the diagnosis of patients with PA.

Data availability statement

The original contributions presented in the study are included in the article/Supplementary Material. Further inquiries can be directed to the corresponding authors.

Ethics statement

The study was conducted at Fujian Provincial Hospital in Southeast China. This study was approved by the Ethics Committees of Fujian Provincial Hospital. Written informed consent was obtained from all suspected patients before the study started.

Author contributions

SW contributed to the study design, data collection, data analysis, data interpretation, funding acquisition, and figures and wrote the manuscript. Y-sC contributed to the data curation, data analysis, data interpretation, and figures. YS contributed to the conceptualization and design of the study. SW and Y-sC contributed equally to this work and should be considered co-first authors. SW is the first corresponding author. YS is the co-corresponding authors. All authors contributed to the article and approved the submitted version.

Funding

This study was funded by the Natural Science Foundation of Fujian Province (2021J01377).

Conflict of interest

The authors declare that the research was conducted in the absence of any commercial or financial relationships that could be construed as a potential conflict of interest.

Publisher's note

Supplementary material

The Supplementary Material for this article can be found online at: https://www.frontiersin.org/articles/10.3389/fcimb.2022.1008924/full#supplementary-material

References

Bhimji, A., Bhaskaran, A., Singer, L. G., Kumar, D., Humar, A., Pavan, R., et al, et al. (2017). Aspergillus galactomannan detection in exhaled breath condensate compared to bronchoalveolar lavage fluid for the diagnosis of invasive aspergillosis in immunocompromised patients. *Clin. Microbiol. Infection* 24 (6), 640–645. doi: 10.1016/j.cmi.2017.09.018

de Heer, K., Vonk, S. I., Kok, M., Kolader, M., Zwinderman, A. H., Oers van, M. H. J., et al. (2016). eNose technology can detect and classify human pathogenic molds*in vitro*: a proof-of-concept study ofAspergillus fumigatus and rhizopus oryzae. *J. Breath Res.* 10 (3), 36008. doi: 10.1088/1752-7155/10/3/036008

Denning, D. W., Cadranel, J., Beigelman-Aubry, C., Ader, F., Chakrabarti, A., Blot, S., et al. (2015). Chronic pulmonary aspergillosis: Rationale and clinical guidelines for diagnosis and management. *Eur. Respir. J.* 47 (1), 45–68. doi: 10.1183/13993003.00583-2015

Donnelly, J. P., Chen, S. C., Kauffman, C. A., Steinbach, W. J., Baddley, J. W., Verweij, P. E., et al. (2020). Revision and update of the consensus definitions of invasive fungal disease from the European organization for research and treatment of cancer and the mycoses study group education and research consortium. *Clin. Infect. Dis.* 71 (6), 1367–1376. doi: 10.1093/cid/ciz1008

De Luca Canto, G., Pachêco-Pereira, C., Aydinoz, S., Major, P. W., Flores-Mir, C., Gozal, D., et al. (2015). Diagnostic capability of biological markers in assessment of obstructive sleep apnea: A systematic review and meta-analysis. *J. Clin. Sleep Med. Jcsm Off. Publ. Am. Acad. Sleep Med.* 11 (1), 27–36. doi: 10.5664/jcsm.4358

Haydour, Q., Hage, C. A., Carmona-Porquera, E. M., Epelbaum, O., Evans, S. E., Gabe, L. M., et al. (2019). Diagnosis of fungal infections. a systematic review and meta-analysis supporting American thoracic society practice guideline. *Ann. Am. Thorac. Soc.* 16 (9), 1179–1188. doi: 10.1513/AnnalsATS.201811-766OC

Horváth, I., Barnes, P. J., Loukides, S., Sterk, P. J., Högman, M., Olin, A. -C., et al. (2017). A European respiratory society technical standard: exhaled biomarkers in lung disease. *Eur. Respir. J.* 49 (4), 1600965. doi: 10.1183/13993003.00965-2016

Huang, J., Jiang, E., Yang, D., Wei, J., Zhao, M., Feng, J., et al. (2020). Metagenomic next-generation sequencing versus traditional pathogen detection in the diagnosis of peripheral pulmonary infectious lesions. *Infection Drug Resistance* 13, 567–576. doi: 10.2147/IDR.S235182

Izumikawa, K., Yamamoto, Y., Mihara, T., Takazono, T., Morinaga, Y., Kurihara, S., et al. (2012). Bronchoalveolar lavage galactomannan for the diagnosis of chronic pulmonary aspergillosis. *Med. Mycol.* 50 (8), 811–817. doi: 10.3109/13693786.2012.682228

Johnson, G., Ferrini, A., Dolan, S. K., Nolan, T., Agrawal, S., Doyle, S., et al. (2014). Biomarker for invasive aspergillosis: the challenges continue. *Biomarkers Med.* 8 (3), 429–451. doi: 10.2217/bmm.13.129

Knutsen, A. P., Bush, R. K., Demain, J. G., Denning, D. W., Dixit, A., Fairs, A., et al. (2012). Fungi and allergic lower respiratory tract diseases. *J. Allergy Clin. Immunol.* 129 (2), 280–291. quiz 292-3. doi: 10.1016/j.jaci.2011.12.970

Kono, Y., Tsushima, K., Yamaguchi, K., Kurita, N., Soeda, S., Fujiwara, A., et al. (2013). The utility of galactomannan antigen in the bronchial washing and serum for diagnosing pulmonary aspergillosis. *Respir. Med.* 107 (7), 1094–1100. doi: 10.1016/j.rmed.2013.04.007

Koo, S., Thomas, H. R., Daniels, S. D., Lynch, R. C., Fortier, S. M., Shea, M. M., et al. (2014). A breath fungal secondary metabolite signature to diagnose invasive aspergillosis. *Clin. Infect. Dis.* 59 (12), 1733–1740. doi: 10.1093/cid/ciu725

Patterson, T. F., Thompson, G. R. 3rd, Denning, D. W., Fishman, J. A., Hadley, S., Herbrecht, R., et al. (2016). Practice guidelines for the diagnosis and management of aspergillosis: 2016 update by the infectious diseases society of America. *Clin. Infect. Dis.* 63 (4), e1-e60. doi: 10.1093/cid/ciw326

Peel, A. M., Crossman-Barnes, C. -J., Tang, J., Fowler, S. J., Davies, G. A., Wilson, A. M., et al. (2017). Biomarkers in adult asthma: a systematic review of 8-isoprostane in exhaled breath condensate. *J. Breath Res* 11 (1), 016011. doi: 10.1088/1752-7163/aa5a8a

Sehgal, I. S., Dhooria, S., Choudhary, H., Aggarwal, A. N., Garg, M., Chakrabarti, A., et al. (2019). Utility of serum and bronchoalveolar lavage fluid galactomannan in diagnosis of chronic pulmonary aspergillosis. *J. Clin. Microbiol* 57 (3), e01821-18. doi: 10.1128/JCM.01821-18

Shin, B., Koh, W.-J., Jeong, B.-H., Yoo, H., Park, H. Y., Suh, G. Y., et al. (2014). Serum galactomannan antigen test for the diagnosis of chronic pulmonary aspergillosis. *J. Infect.* 68 (5), 494–499. doi: 10.1016/j.jinf.2014.01.005

Töreyin, Z. N., Ghosh, M., Göksel, ö., Göksel, T., Godderis, L., et al. (2020). Exhaled breath analysis in diagnosis of malignant pleural mesothelioma: Systematic review. *Int. J. Environ. Res. Public Health* 17 (3), 1110. doi: 10.3390/ijerph17031110

Ullmann, A. J., Aguado, J. M., Arikan-Akdagli, S., Denning, D. W., Groll, A. H., Lagrou, K., et al. (2018). Diagnosis and management of aspergillus diseases: executive summary of the 2017 ESCMID - ECMM - ERS guideline. *Clin. Microbiol. Infection* 24(Suppl 1), e1–e38. doi: 10.1016/j.cmi.2018.01.002

frontiers | Frontiers in Cellular and Infection Microbiology

TYPE Review
PUBLISHED 28 November 2022
DOI 10.3389/fcimb.2022.1019071

OPEN ACCESS

EDITED BY
Laura Cerqueira,
University of Porto, Portugal

REVIEWED BY
Bo Pang,
National Institute for Communicable Disease Control and Prevention (China CDC), China
Alejandro Castellanos-Gonzalez,
University of Texas Medical Branch at Galveston, United States
Shulu Zhang,
Agdia, United States

*CORRESPONDENCE
Guijiang Wei
weiguijiang2021@163.com

†These authors have contributed equally to this work

SPECIALTY SECTION
This article was submitted to Clinical Microbiology, a section of the journal Frontiers in Cellular and Infection Microbiology

RECEIVED 14 August 2022
ACCEPTED 03 November 2022
PUBLISHED 28 November 2022

CITATION
Tan M, Liao C, Liang L, Yi X, Zhou Z and Wei G (2022) Recent advances in recombinase polymerase amplification: Principle, advantages, disadvantages and applications. *Front. Cell. Infect. Microbiol.* 12:1019071. doi: 10.3389/fcimb.2022.1019071

Recent advances in recombinase polymerase amplification: Principle, advantages, disadvantages and applications

Meiying Tan†, Chuan Liao†, Lina Liang†, Xueli Yi, Zihan Zhou and Guijiang Wei*

Center for Clinical Laboratory Diagnosis and Research, The Affiliated Hospital of Youjiang Medical University for Nationalities, Baise, China

After the outbreak of SARS-CoV-2, nucleic acid testing quickly entered people's lives. In addition to the polymerase chain reaction (PCR) which was commonly used in nucleic acid testing, isothermal amplification methods were also important nucleic acid testing methods. Among several common isothermal amplification methods like displaced amplification, rolling circle amplification, and so on, recombinase polymerase amplification (RPA) was recently paid more attention to. It had the advantages like a simple operation, fast amplification speed, and reaction at 37-42°C, et al. So it was very suitable for field detection. However, there were still some disadvantages to RPA. Herein, our review mainly summarized the principle, advantages, and disadvantages of RPA. The specific applications of RPA in bacterial detection, fungi detection, virus detection, parasite detection, drug resistance gene detection, genetically modified food detection, and SARS-CoV-2 detection were also described. It was hoped that the latest research progress on RPA could be better delivered to the readers who were interested in RPA.

KEYWORDS

isothermal amplification, recombinase polymerase amplification, pathogenic microorganism, genetically modified food, SARS-CoV-2

Introduction

Among the nucleic acid-based molecular diagnostic methods, the polymerase chain reaction (PCR) invented in the 1980s (Mullis et al., 1986) was the most widely used. However, due to the excessive dependence of PCR on temperature control equipment, time-consuming, and professional operation, it was difficult to apply PCR in on-site detection (Yan et al., 2014). In 2006, Piepenburg et al. developed a isothermal

amplification method named by recombinase polymerase amplification (RPA) (Piepenburg et al., 2006). Due to its advantages like a simple operation, fast amplification speed, reaction at 37-42°C and, so on (Li et al., 2018), it was expected to replace PCR. Since RPA was established over ten years, it had been widely used in various fields like the detection of bacteria, fungi, parasites, viruses, drug resistance genes, and so on. Nowadays, through the continuous improvement of the sample treatment process, amplification system, and result detection system, RPA seemed to be more and more popular in molecular diagnosis. In particular, the outbreak of SARS-CoV-2 in 2019 further promoted the application of RPA in nucleic acid detection (Bai et al., 2022). Our review summarized the latest RPA research in the past five years that mainly cover several fields, including the detection of bacteria, fungi, parasites, viruses, drug resistance genes, genetically modified food, and SARS-CoV-2. It was hoped to provide a reference for further study of RPA.

The principle of RPA

The principle of basic RPA

RPA technology mainly includes two enzymes: recombinant enzyme T4 UvsX and bacillus subtilis Pol I (Piepenburg et al., 2006). Moreover, the RPA reaction system also needed amplification templates, primers, and various raw materials. The basic reaction process of RPA was as follows: First, in the presence of ATP and polyethylene glycol, the recombinase protein UvsX combined with RPA primers to form a recombinase-primer complex. Then, the complex could find the homologous sequence in the double-strained DNA template. Once the homologous sequence was found, it would insert into the template chain to form a D-ring structure and start the chain replacement reaction. To prevent the inserted primer from being expelled through branch migration, the replaced template chain was bound to the Single-stranded binding protein to maintain the stability of the single chain. Finally, the recombinase was isolated from the complex. In the presence of dNTPs, DNA polymerase was bound to the 3`-OH end of the primer for chain elongation to form a new complementary chain. Repeat the above steps to achieve exponential amplification of the target region on the template. The whole RPA process was very fast. Generally, detectable amplification products could be obtained in about 20 min. The basic principle of RPA was shown in Figure 1 (Lobato and O'Sullivan, 2018). The RPA amplification products could be displayed by conventional agarose gel electrophoresis. In addition, the commonly used RPA methods were mainly exo-RPA and LFS-RPA.

The principle of exo-RPA

Real-time RPA was an assay that combines RPA with a fluorescent probe. This method allowed for the rapid detection of target genes while allowing real-time monitoring of the amplification process. According to the probe design requirements of the TwistAmp™Exo kit, a segment of sequence with a length of about 46-52 bases was first selected, and then a probe was synthesized according to the principle of complementary pairing. The probe was labeled by a fluorophore and had a quencher near the fluorophore to temporarily block the fluorescent signal. There was a blocker at the 3′ end that was used to prevent the polymerase from extending from the 3′ end. Real-time detection was based on the cleavage of the fluorescent probe at the abasic site between the fluorophore and the quencher. Abasic site could be tetrahydrofuran (THF) or a dSpacer (a derivative of the THF). The E. coli exonuclease III cleaved the probe at THF or dSpacer site, separating the fluorophore and quencher, thus releasing the fluorescent signal (Li et al., 2018). The fluorescence amplification curve could be obtained by continuously collecting fluorescence. The principle of exo probe detection was shown in Figure 2.

The principle of LFS-RPA

The RPA combined with lateral flow strip assay (LFS-RPA) was a method that combined basic RPA amplification technology, test strips, and immunoassay technology to enable visual detection. The principle of LFS-RPA detection was as follows: A sequence of about 46-52 bases in length was selected and a corresponding sequence was synthesized according to the principle of complementary pairing. The THF(or dSpacer) site was labeled in the middle of the sequence, carboxyfluorescein (FAM) and blocker were labeled at both ends, and biotin was labeled at the 5 'end of the reverse primer. During amplification, the Nfo endonucleases recognized the THF(or dSpacer) site and cleaved it, a double-stranded DNA labeled with FAM on one end and biotin on the other end was obtained. During LFS chromatography, RPA amplification products with colloidal gold nanoparticles(AuNPs) were first produced when the sample flows through the conjugate pad because the FAM-RPA amplification products could bind to anti-FAM antibodies with AuNPs. As the RPA amplified fragments moved forward with the AuNPs, their biotin group could bind to the anti-biotin antibody on the test line. The test line turned red due to the accumulation of AuNPs (Wang B et al., 2021). Colloidal gold complexes not captured by the anti-biotin antibody were captured by the secondary antibody on the control line, showing a red line indicating the validity of the LFS (Wang F et al., 2021a). The working principle of RPA

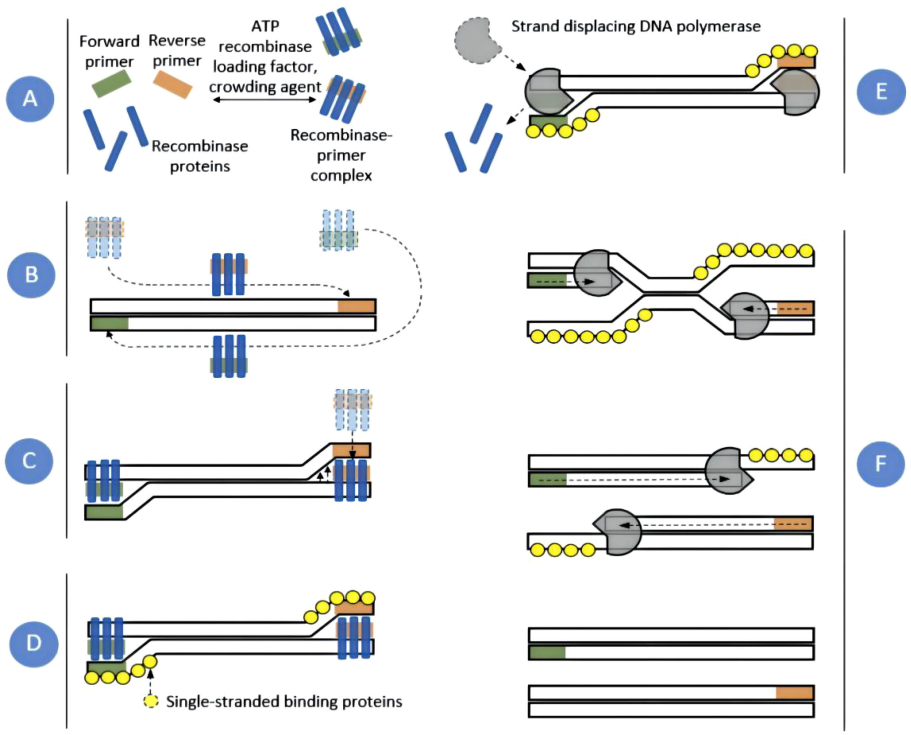

FIGURE 1
RPA amplification scheme. Recombinase proteins formed complexes with each primer **(A)**, which scanned DNA for homologous sequences **(B)**. The primers were then inserted at the cognate site by the strand-displacement activity of the recombinase **(C)** and single-stranded binding proteins stabilized the displaced DNA chain **(D)**. The recombinase then disassembled leaving the 3` end of the primers accessible to a strand displacing DNA polymerase **(E)**, which elongated the primer **(F)**. Exponential amplification was achieved by cyclic repetition of this process (Lobato and O'Sullivan, 2018).

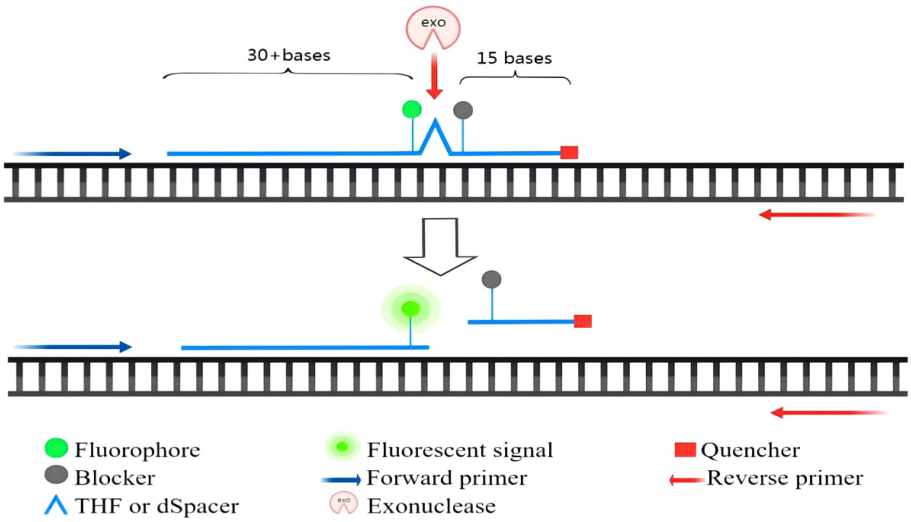

FIGURE 2
The principle of exo probe detection.

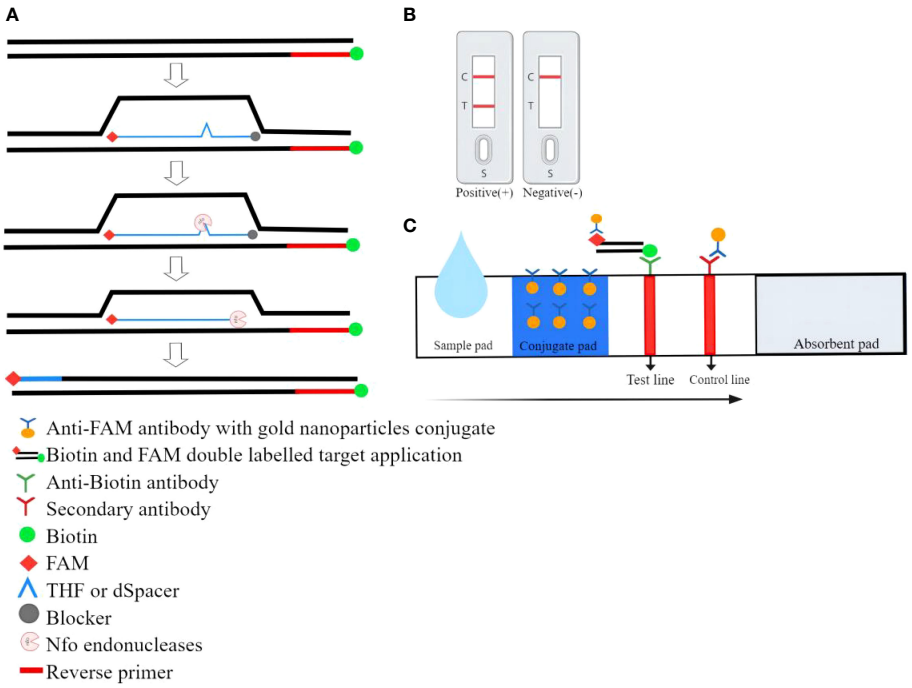

FIGURE 3
The working principle of RPA combined with lateral flow strip (LFS) assay. **(A)** During LFS-RPA, the reverse primer carries the biotin at the 5′ end and a modified probe was added to the reaction. Both ends of the probe were labeled with FAM and blocker respectively. Only when the probe was fully bound to the homologous sequence the endonuclease was able to cut the DNA double-strand and release the blocker. Thereby polymerase extended the substrate and chain synthesis continues leading to double-labeled amplicons. **(B)**Positive/negative results. **(C)** Schematic diagram of the RPA combination with lateral flow strip.

combined with lateral flow strip (LFS) assay was shown in Figure 3.

Comparison of RPA and PCR, other isothermal amplification methods

Comparison of RPA and PCR

RPA, which emerged in 2006, was a new nucleic acid amplification technology that claims to replace PCR. Compared with PCR, its biggest advantage was that it could perform isothermal amplification at 37-42°C. Table 1 compared RPA and PCR.

Comparison of RPA and other isothermal amplification methods

In recent years, with the continuous development of nucleic acid-based amplification technology, the scientific community had been trying to find an isothermal amplification method that did not need PCR instruments. At present, the isothermal amplification technology that had been developed includes RPA, strand displaced amplification(SDA), rolling circle amplification(RCA), helicase-dependent isothermal DNA amplification(HDA), nucleic acid sequence-based amplification (NASBA), and loop-mediated isothermal amplification(LAMP), et al. Among these isothermal amplification methods, RPA was a relatively simple method.

The comparison between RPA and other isothermal amplification techniques was shown in Table 2.

The application of RPA

The application of RPA in bacteria detection

The traditional bacterial detection methods were mainly based on the biochemical characteristics of culture method. The culture method took a long time, and some non-culturable bacteria could enter the living state and the bacteria with strict requirements for culture conditions were difficult to detect by the culture method. Therefore, we urgently needed to find a rapid and simple bacterial detection method. Wang et al.

TABLE 1 Comparison of RPA and PCR.

Method	RPA	PCR
Origin	2006	1980s
Enzyme	Recombinase; DNA polymerase	Taq enzyme
Temp.	37-42°C	95°CDenaturation-55°Cannealing-72°Cextension
Time	5-20 min	1.5-2h
Number of primers	2	2
Reagent	Lyophilized or liquid	Liquid
Product detecting methods	Gel electrophoresis, real-time fluorescence, colloidal gold	Gel electrophoresis, real-time fluorescence, colloidal gold
Performance	Considerable sensitivity and specificity	High sensitivity and specificity
Advantage	Isothermal amplification; Short time; Low operation and instrument requirements Resistance to inhibitors; Tolerate more mismatches	Many conventional laboratories; Many commercial kits and wide applications; Mature technology; Reagents are relatively cheap; Ideal for quantification purposes
Disadvantage	High reagent price; There are few commercial kits, which is not conducive to large-scale detection; No special primer design software; Not used in clinical, only for scientific research; Prone to non-specific amplification; Poor quantitative separation rate	Need expensive instruments; The operation is highly specialized and requires special operation training; Intolerance to some substances
References	(Rohrman and Richards-Kortum, 2015; Oliveira et al., 2021; Xu et al., 2021; Munawar, 2022)	(Schrader et al., 2012; Oliveira et al., 2021; Munawar, 2022)

TABLE 2 Comparison of RPA and other common isothermal amplification methods.

Method	RPA	SDA	RCA	HDA	NASBA	LAMP
Template	DNA/RNA	DNA	DNA/RNA	DNA/RNA	RNA	DNA/RNA
Time	5-20min	1-2h	1h	0.5-2h	1.5-2h	1h
Temp.	37-42°C	37-60°C	37-65°C	60-65°C	41°C	60-65°C
Number of primers	2	4	2	2	2	4-6
Number of enzymes	2	2	2	2	3	1
Advantage	Short reaction time; Tolerance of certain mismatches; Simple primer design and support for multiplex amplification reactions	Mild reaction conditions; Rapid amplification	Easy exponential amplification; Locked probe can make it have high specificity	Constant temperature reaction; Simple reaction structure	High selectivity to RNA molecules, free from background DNA interference; No additional cDNA processing required	High specificity; Simple colorimetric detection; Resistance to inhibitors
Disadvantage	No special primer design software; High reagent prices; Fewer reagent kits;	Low amplification efficiency for long targets; Strong non-specific background reaction; Thermal denaturation is required at first	Low purity annular template makes it difficult to control connection efficiency; The template needs to be a single chain ring structure;	Complicated buffer optimization	The reaction components are complex and require many enzymes; Not suitable for DNA virus detection	The primer design is complex; Easy to produce nonspecific amplification
References	(Xu et al., 2021; Munawar, 2022)	(Walker et al., 1992; Walker, 1993)	(Xu et al., 2021; Gao et al., 2022)	(Yan et al., 2014; Barreda-Garcia et al., 2018)	(Simpkins et al., 2000; Honsvall and Robertson, 2017; Gao et al., 2022)	(Yan et al., 2014; Reuter et al., 2020; Oliveira et al., 2021)

established a dual detection biosensor based on RPA and three-segment lateral flow strips to detect Vibrio cholerae and Vibrio vulnificus. This biosensor had the advantages of high sensitivity and specificity, short reaction time, and simple equipment, which was very suitable for detection in primary hospitals and on-site (Wang P et al., 2021). The RPA-lateral flow strips (RPA-LFS) method established by Wang et al. could be used to distinguish capsulated and non-capsulated Haemophilus influenzae, with a detection limit of 1 cfu/μl (Wang et al., 2022). In addition, the RPA-LFS for the detection of Pseudomonas aeruginosa (Yang et al., 2021) and Vibrio parahaemolyticus (Jiang et al., 2020) had also been experimentally verified. Hu et al. developed a detection method combining RPA with polymer flocculation sedimentation. This method could detect as low as 13fg genomic DNA of Staphylococcus aureus and could be directly judged by naked eyes within 20 min (Hu et al., 2020). The double RPA reaction system constructed by Tran et al. could simultaneously detect Staphylococcus aureus and Pseudomonas aeruginosa. It could detect genomic DNA of Staphylococcus aureus as low as 10 fg/reaction and Pseudomonas aeruginosa as 30 fg/reaction (Tran et al., 2022), the sensitivity of Staphylococcus aureus detection was higher than RPA combined with polymer flocculation sedimentation method.

Unlike other bacteria, Vibrio vulnificus could enter a viable but nonculturable state, making it difficult to be detected by conventional methods. Yang et al. established real-time RPA (RT-RPA) for the extracellular metalloproteinase gene of Vibrio vulnificus. This method could be detected only in 2-14 min at 39°C. The detection limit was 17 copies/reaction, and the detection results of clinical samples were 100% consistent with qPCR (Yang et al., 2020). In addition, the vvhA gene could also be used as a specific gene for RT-RPA detection of Vibrio vulnificus (Zhu et al., 2021). Gumaa et al. established RT-RPA and RPA-LFS to detect Brucella. The detection limits of RT-RPA and RPA-LFS were 4 and 6 copies/reaction, respectively (Gumaa et al., 2019). The application of dual RPA could also detect and identify Brucella melitensis and Brucella abortus (Gumaa et al., 2020). Garrido-Maestu et al. established the built-in IAC multiple RT-RPA to detect Listeria monocytogenes. The sensitivity and specificity of the multiple RT-RPA were equivalent to the European reference method (ISO 11290-1), and this method could complete the detection in one working day while using the ISO method took six days (Garrido-Maestu et al., 2020). In addition, Streptococcus pneumoniae (Clancy et al., 2015)and Streptococcus suis serotype 2 (Jiang et al., 2022) could also be quickly detected by RT-RPA.

CRISPR refers to clustered regularly interspaced short palindromic repeats, it was often combined with isothermal amplification methods for nucleic acid detection. An et al. established a one-tube and two-step reaction system to detect Salmonella spp. by combining RPA and Clustered Regularly Interspaced Short Palindromic Repeats associated protein 13a (CRISPR-Cas13a). One-tube and two-step RPA-CRISPR-Cas13a could be detected within 20 min and 45 min, respectively. The detection limits of the two reaction systems were 10^2 copies and 10^0 copies, respectively (An et al., 2021). Luo et al. developed an RPA/Cas12a-based system to detect Xanthomonas arboricola pv. prun(Xap). The method could detect as low as 10^{-18} M Xap gDNA with a mini-UV torch, while the sensitivity was 10^{-17} M with LFS (Luo et al., 2021). In addition, the integration of bio-barcode immunoassay, RPA, and CRISPR-Cas12a cleavage into a reaction system could be very sensitive and intuitive to detect Salmonella typhimurium (Cai et al., 2021). In these bacterial detection experiments, RPA showed high specificity, sensitivity, and detection efficiency. Selecting the corresponding RPA results reading method according to different bacteria and detection environments would make bacterial detection more rapid, convenient, and efficient. It could be seen that RPA had its unique advantages in the rapid detection of bacteria.

The application of RPA in fungi detection

At present, the detection of fungi in medicine was mainly through their morphological and physiological phenotypes. These methods had a long detection time and a low positive detection rate. Cryptococcus neoformans was a conditional pathogen. Most patients had symptoms of central nervous system infection and had high mortality. The common methods to detect Cryptococcus neoformans were ink staining and pathogen culture. The culture method was the gold standard of detection, but the long culture time was not conducive to rapid clinical diagnosis. The ink staining method was limited by the type of specimen, and the positive detection rate was low. Based on this situation, Ma et al. designed high-specific primers and probes for the internal transcribed spacer of Cryptococcus neoformans and established an RPA-LFS for visual and rapid detection of Cryptococcus neoformans/C. gattii. It could detect 0.64 pg of Cryptococcus neoformans genomic DNA, and the sensitivity and specificity were 95.2% and 95.8%, respectively (Ma et al., 2019). When the capsule-associated gene CAP64 of Cryptococcus neoformans/C. gattii was used as the detection target of RPA-LFS, its detection limit was 10cfu/ml or 1 fg/ml (Wang L et al., 2021). Candida albicans was another common clinical pathogenic fungi. Although most people infected with Candida albicans in skin and mucosa were generally not life-threatening, it seriously reduced people's quality of life and increased people's economic burden. Wang et al. established RPA-LFS to detect Candida albicans. The detection limit of this method was 1 cfu/reaction, and the detection accuracy was 100% (Wang F et al., 2021a). Leptosphaeria maculans was a highly aggressive fungus that could cause severe phoma stem canker of Brassica napus. After successfully establishing a dual real-time

fluorescence RPA to detect L. maculans and L. biglobosa (Lei et al., 2019), Lei et al. further developed an RPA-CRISPR/Cas12a method to detect Leptosphaeria maculans. This method could be completed in 45 min with a minimum detection limit of 4.7 genomic DNA copies (Lei et al., 2022a). With the gradual popularity of RPA, in the field of fungi detection, using visual LFS as the reading method of amplification results was more popular.

The application of RPA in virus detection

RPA combined with the CRISPR system was widely used in virus detection. Gong et al. developed an integrated trinity test with RPA-CRISPR/Cas12a-fluorescence assay system to detect the respiratory syncytial virus(RSV) A or RSV B. This method could detect the target sequence of 1.38×10^{1} copies/μl and could distinguish RSV A or RSV B infection within 37 min (Gong et al., 2022). Qian et al. established RPA-CRISPR/Cas12a to rapid detection Human norovirus. In this method, CRISPR/Cas12a combined with fluorescence or LFS was used to detect RPA products. The minimum detection limit was 9.65×10^{2} copies/ml, and the detection coincidence rate with qRT-PCR was 98.3%(Qian et al., 2021b). RPA-CRISPR/Cas12a could also detect Human metapneumovirus (Qian et al., 2021a). CRISPR/lwCas13a was another protein that could be used for nucleic acid detection, it had been successfully combined with RPA to detect the African swine fever virus (ASFV) (Ren et al., 2021a) and rabies virus (Ren et al., 2021b). CRISPR/Cas12a and CRISPR/Cas13a systems could be used not only for virus detection alone but also for multiple RPA detection at the same time. Tian et al. developed a dual-gene diagnostic technique for SARS-CoV-2 and ASFV by using the orthogonal collateral cleavage activity of CRISPR/Cas12a and CRISPR/Cas13a system, which showed 100% sensitivity and specificity in the analysis of clinical samples (Tian et al., 2022).

RT-RPA and RPA-LFS methods, which were applied earlier than the RPA-CRISPR, were also widely used in virus detection. Huang et al. successfully developed RT-RPA to detect decapod iridescent virus 1, with a lower detection limit of 2.3×10^{1} copies/reaction (Huang et al., 2022). RPA-LFS could quickly read the test results with the naked eye, so it was very popular in virus detection. Zhang et al. developed RPA-LFS to detect the hepatitis B virus, with a minimum detection limit of 10 copies/reaction and no cross-reaction with other common pathogens (Zhang et al., 2021). RPA-LFS could also jointly detect Epizootic hemorrhagic disease virus and Palyam serogroup viruses, the analytical sensitivity was 7.1 copies/μl and 6.8 copies/μl respectively (Li et al., 2021). RPA-LFS could also be used to detect respiratory syncytial virus (Xu et al., 2020). Because piper yellow mottle virus had two stages of DNA and RNA in its replication cycle, Mohandas et al. established RPA and reverse transcription RPA to detect the virus. The sensitivity of RPA using crude DNA extract as template was equivalent to that of PCR. When using cetyltrimethyl ammonium bromide to extract DNA, the sensitivity of both RPA methods was 10 times higher than that of PCR (Mohandas and Bhat, 2020). Ivanov et al. developed an RPA-LFS method to detect alfalfa mosaic virus and compared two methods for generating labeled RPA amplicons after LFS detection. The results showed that the primer labeled RPA-LFS method could detect 10^{3} copies of RNA within 30 min, and its half-maximal binding concentration was 22 times lower than the probe-dependent RPA-LFS (Ivanov et al., 2021). RPA could also detect tomato apical stunt viroid (Kovalskaya and Hammond, 2022) and barley yellow dwarf virus (Kim et al., 2022) in plants. The application of RPA in virus detection often required reverse transcription first. If reverse transcription and RPA amplification were divided into two steps, there was an increased risk of aerosol generation and contamination.

The application of RPA in parasite detection

Malaria was a vector infectious disease caused by Plasmodium infection. Early and rapid diagnosis was the key to malaria control. Kersting et al. amplified the 18SrRNA gene fragment of Plasmodium falciparum by RPA-LFS. The detection results were obtained in less than 20 min at 38°C. It could detect the genomic DNA of Plasmodium falciparum as low as 100fg, which was very suitable for on-site detection in remote areas and promoted the progress of global malaria control (Kersting et al., 2014). RPA-LFS could also detect Trichinella spiralis DNA as low as 100 fg, and its sensitivity was about 10 times that of the conventional PCR (Li et al., 2019). When the RPA-LFS method was used to detect Babesia microti, it could detect 0.25 parasite/μl blood, which was 40 times more sensitive than the conventional PCR and had no cross-reactions with DNA of related apicomplexan parasites and their host (Nie et al., 2021). To assess the validity of RPA-LFS for the diagnosis of cutaneous leishmaniasis, Travi et al. used RPA-LFS to test samples from 226 patients. RPA-LFS had a sensitivity of 91.2% and a positive predictive value of 93%. It had potential point of care in cutaneous leishmaniasis endemic areas but may miss positive samples with very low parasite levels (Travi et al., 2021). Molina-Gonzalez et al. successfully used RPA-LFS to detect Giardia duodenalis DNA in stool samples collected in the field. However, the problem of how to extract high-purity DNA from stool samples hindered on-site detection (Molina-Gonzalez et al., 2020). In addition, RPA-LFS had been applied to detect Entamoeba histolytica (Nair et al., 2015) and Trypanosoma evansi (Li Z et al., 2020). RPA-LFS was mainly used for the on-site detection of parasites, and it was important to find simpler methods for high-concentration DNA extraction.

The combination of RPA and real-time fluorescence allowed for real-time detection of the process and had a lower risk of

cross-contamination than RPA-LFS. Rostron et al. established RT-RPA targeting the repeat region of Schistosoma haematobium Dra1 genomic. This method could detect 1fg Schistosoma japonicum gDNA, and the results could be obtained within 10 min using a small portable battery-powered tube scanner device (Rostron et al., 2019). RT-RPA could also design primer probes for specific genes of different parasites to establish multiple RT-RPA. Multiple RT-RPA had been successfully applied to the simultaneous rapid detection of Theileria equi and Babesia caballi (Lei et al., 2020). In addition to conventional fluorescent probes, fluorescent dye SYBR Green I combined with RPA was also commonly used in the detection of parasites, such as Plasmodium knowlesi (Lai and Lau, 2020). The SYBR Green I was cheaper than the fluorescent probe. Yu et al. combined RPA with CRISPR/Cas12a to detect Cryptosporidium parvum IId-subtype-family, and the results could be read by the naked eye under blue light or with LFS. This method had robust specificity, showing sensitivities of 1 and 10 copies in pure and complex samples, respectively (Yu et al., 2021). Lei et al. established a portable one-pot assay for Toxoplasma gondii using RPA-CRISPR/Cas2a with a lower limit of detection of 3.3Copes/μl. A portable suitcase was also designed to meet the needs of on-site detection (Lei et al., 2022b). RPA had been successfully applied to detect many parasites, but the application was not yet widespread. Most of the current studies were relatively simple RPA-LFS, real-time fluorescent RPA, etc. Further studies of RPA combined with other methods were relatively rare.

The application of RPA in drug resistance gene detection

The overuse of antibiotics would lead to bacterial resistance, which would bring great challenges to the diagnosis and treatment of clinical diseases. The monitoring of bacterial drug resistance was of great significance for guiding clinical medication and avoiding or delaying the production of drug-resistant strains. Liu et al. established a 15 μl RPA reaction system to detect carbapenem-resistance genes blaoxa-23 of Acinetobacter baumannii. The test results showed that 90% of the strains showed positive amplification signals, and only 10% of the strains showed negative amplification signals, which was consistent with the results of the PCR (Liu et al., 2020). Methicillin-resistant staphylococci (MRS) was a common drug-resistant strain in the clinic. Srirattakarn et al. established RPA-LFS to monitor MRS, the sensitivity and specificity of RPA-LFS were 92.1% and 100% respectively (Srisrattakarn et al., 2020). RPA-LFS could also be used to detect vancomycin-resistant enterococci (Panpru et al., 2021). Singpanomchai et al. established an allele-specific RPA-SYBR amplification system to detect multidrug-resistant tuberculosis, this method designed specific primers for the alleles of four major mutations rpoB516, rpoB526, rpoB531, and katG315. The experimental results showed that RPA-SYBR had 100% sensitivity and specificity compared with DNA sequencing, and its detection limit for these special mutation sites was 5 ng (Singpanomchai et al., 2021). Wang et al. developed RPA-LFS based on the four most common carbapenemase genes: bla_{KPC}, bla_{NDM}, $bla_{OXA-48-like}$, and bla_{IMP} for rapid on-site detection of carbapenemase-producing Enterobacterales. The lowest detection limit of this method was 100 fg/reaction (bla_{KPC}, bla_{NDM}, $bla_{OXA-48-like}$) or 1000 fg/reaction (bla_{IMP}), and its sensitivity was 10 times that of PCR (Wang F et al., 2021b). The combination of RPA and real-time fluorescence could also be applied to detect bla_{NDM} gene (Wang X et al., 2021). The rapid, efficient, and simple advantages of RPA could play an important role in the detection of resistance genes. The RPA had the detection ability equivalent to PCR, and sometimes its sensitivity was even higher than that of PCR.

The application of RPA in detection of genetically modified food

With the development of genetically modified technology and more genetically modified food entering the market, the safety of genetically modified food had attracted more and more attention. At present, there were mainly two kinds of methods for detecting transgenic crops based on protein level and nucleic acid level. The former was limited by protein denaturation, detection reagents, and other reasons and could not meet the detection of large-scale transgenic crops. The PCR method in the latter had high sensitivity and specificity, but PCR required a complex and expensive thermal circulator. Its operation process was complex, which was not suitable for on-site detection. Establishing a rapid convenient detection method would greatly improve the detection efficiency of genetically modified food. Due to the characteristics of isothermal amplification, convenient operation, and fast amplification speed, RPA had been gradually introduced into the field of genetically modified food detection. Li et al. combined single universal primer RPA with LFS to establish an isothermal paper biosensor for multiple detection of genetically modified maize. The biosensor enabled the simultaneous detection of MON810, MON863, and MON89034. The whole analysis process was completed in 30 min without any large instruments, and its detection limit was 50 copies (Li K et al., 2020). Wang et al. combined the advantages of RPA and fluorescence detection, and established a fast, sensitive, specific, and simple MON863 corn field detection platform, with a detection limit of 20 copies (Wang et al., 2020). Different from traditional transgenic technology, RNA interference (RNAi) provided gene silencing at the transcriptional level, which also posed new challenges to traditional detection methods. To improve the stability and amplification efficiency of RPA reaction, Li et al. developed an isothermal fluorescent

biosensor based on graphene oxide nanomaterials to enhance RPA, which was used to detect RNAi transgenic plants. The detection limit of this method was 1.5 ng (Li et al., 2022). RPA was convenient and efficient, which was very suitable for on-site transgenic detection in grassroots units, warehouses, and fields. However, only one company sold RPA reagent, which limited its application in large-scale screening of genetically modified food.

The application of RPA in the detection of SARS-CoV-2

Since the outbreak of SARS-CoV-2, the number of confirmed cases of SARS-CoV-2 continued to rise globally. At present, there was no effective antiviral drug for SARS-CoV-2, so the most important thing for the prevention and control of the SARS-CoV-2 epidemic was still early diagnosis and early isolation. The outbreak of SARS-CoV-2 had made nucleic acid detection well-known. Nowadays, the main methods for detecting SARS-CoV-2 included qRT-PCR, digital PCR, and various isothermal amplification methods. Among them, qRT-PCR was the most widely used method, but PCR had high requirements for equipment, detection condition, and personnel operation. In large-scale detection of pathogens, the speed and simplicity of detection methods were very important, so found a fast and simple method to detect SARS-CoV-2 had become a hot spot. Sun et al. established a double-stranded RPA-LFS detection platform, it could simultaneously realize the rapid visual screening of SARS-CoV-2 and influenza virus, which was conducive to distinguishing patients with SARS-CoV-2 and influenza virus infection with similar clinical symptoms (Sun Y et al., 2022). Shelite et al. established the RPA-LFS for rapid detection of SARS-CoV-2 using the cDNA nucleocapsid gene as the target, with a detection limit of 35.4 viral cDNA nucleocapsid gene copies/μL. The RPA-LFS was 100% consistent with the reverse transcription-qPCR reference test (Shelite et al., 2021). Cherkoui et al. used RPA to simultaneously detect the E gene and RdRp gene of SARS-CoV-2 and designed two optional product detecting methods (real-time fluorescence and test strip) so that the most appropriate method could be selected according to different field environments. The analytical sensitivity of the fluorescence test for the E gene and RdRp gene was 9.5 and 17 RNA copies/reactions respectively, and the analytical sensitivity of the test paper method was 130 RNA copies/reactions (Cherkaoui et al., 2021). A microfluidic-integrated lateral flow RPA for rapid detection of SARS-CoV-2 was established by integrating RPA and LFS detection systems into a single microfluidic chip. The closed microfluidic chip overcame aerosol contamination and the convenient analysis system reduced expensive equipment costs and labor costs (Liu et al., 2021). Choi et al. combined the rkDNA graphene oxide probe system with RPA to detect the SARS-CoV-2 virus within 1h (Choi et al., 2021). The design of RPA as a mobile suitcase laboratory was conducive to the mobile detection of SARS-CoV-2 in the resource-deficient environment (El Wahed et al., 2021). RPA could also monitor SARS-CoV-2 in real-time or at the end point by adding fluorescent dye SYBR Green I. Used SYBR Green I as the fluorescent reporting group did not need to open the tube that may cause aerosol pollution, and this method could observe the test results with the naked eye, and the cost was also lower than RPA-LFS and RT-RPA (Lau et al., 2021).

With the rapid development of the CRISPR system, more and more scholars combined the CRISPR system with RPA to detect SARS-CoV-2. Sun et al. combined RPA with CRISPR/Cas12a to develop a single-tube method to detect SARS-CoV-2. CRISPR/Cas12a detection was carried out in one tube to reduce the liquid transfer step and reduce the risk of aerosol pollution. It could detect SARS-CoV-2 as low as 2.5 copies/μl, and the detection results were 100% consistent with qRT-PCR (Sun et al., 2021). In the single tube reaction, the amplification template loss caused by RPA-CRISPR/Cas12a cleavage would lead to low detection efficiency, Lin et al. found that glycerol additive could significantly improve the detection efficiency of one-pot RPA-CRISPR/Cas12a, and its sensitivity was nearly 100 times higher than that of the method without glycerol. This optimized RPA-CRISPR/Cas12a had been successfully used to detect SARS-CoV-2 and ASFV (Lin et al., 2022). During the establishment of a one-pot detection method based on RPA-CRISPR/cas12a, the development and optimization of methodology could be accelerated by using the statistical design of experiments (Malci et al., 2022). RPA-CRISPR/Cas12a detection system could not only detect SARS-CoV-2 alone but also realize multiple detection of SARS-CoV-2 and other viruses. Sun et al. established the RCD platform based on RPA-CRISPR/cas12a and digital microfluidics. RCD platform showed high sensitivity and specificity and could realize automation and multiplexing. It has been successfully used to detect influenza virus and SARS-CoV-2 (Sun Z et al., 2022).

The 2019 pandemic coronavirus disease generated a huge demand for sensitive and rapid detection of SARS-CoV-2. In recent years, more and more technologies for SARS-CoV-2 detection combined with RPA had been developed. Based on the high peroxidase-like activity of the FeS2 nanozymes, Meng et al. combined RPA and FeS2 nanoenzyme strips to achieve nucleic acid amplification and subsequent colorimetric signal enhancement. The method had a detection limit of 200 copies/ml for SARS-CoV-2 (Meng et al., 2022). Hu et al. established a light-controlled CRISPR-RPA method to detect SARS-CoV-2. The crRNA was designed to be temporarily inactivated and the CRISPR-Cas12a detection system was activated under rapid light irradiation after the RPA reaction was completed. RPA and CRISPR/Cas12 system integrated into a completely closed tube to avoid the risk of contamination. Compared with the conventional OnePot detection, the sensitivity was improved by more than two orders of magnitude (Hu et al., 2022). Park et al. developed the first digitization-enhanced CRISPR/Cas-assisted

one-pot virus detection (deCOViD) method and applied it to detect SARS-CoV-2. The deCOViD was based on RPA-CRISPR/Cas12a, which enabled qualitative detection in 15 min and quantitative detection in 30 min. It was highly sensitive and could detect down to 1 genome equivalent (GE) μL^{-1} of SARS-CoV-2 RNA and 20 GE μL^{-1} of heat-inactivated SARS-CoV-2. This method was one of the fastest and most sensitive SARS-CoV-2 detection methods based on CRISPR/Cas (Park et al., 2021). Some new methods combined with RPA were not very mature at present, but they showed great advantages in improving detection sensitivity. In conclusion, RPA had low requirements for equipment and field detection environment and was very suitable for on-site screening of SARS-CoV-2.

Conclusion

As a technology that could complete nucleic acid detection at 37-42°C, RPA had been greatly developed in recent years. Compared with PCR and other isothermal amplification methods, RPA had the advantages of simple operation, fast reaction speed, and low requirements for equipment. In terms of sensitivity, RPA could detect trace-level nucleic acid in samples at the lowest level. In some studies, RPA could even detect low concentrations of DNA that could not be detected by PCR. In terms of specificity, RPA could identify and amplify target genes from the genomic DNA of different species and specimen types. It had a strong anti-interference ability, the detection results were highly consistent with PCR. In addition, RPA could run at 37-42°C without complex temperature control equipment, which was very suitable for on-site detection in low resource environment. And RPA could get test results within 20 min, which was conducive to large-scale screening and rapid detection of samples. The mild reaction conditions and high amplification efficiency of RPA made it very suitable for rapid clinical diagnosis, food detection, epidemic prevention and control, industrial application, and on-site real-time detection. Especially after the outbreak of SARS-CoV-2, nucleic acid testing had become normalized, and the scale of testing had become larger and larger. A rapid, accurate, and efficient detection method would play an important role in epidemic prevention and control. To make RPA more efficient and convenient, people had taken various optimization and improvement measures in the amplification system and detection result reading system of RPA, such as adding glycerol that could improve the detection sensitivity, simple visual product detecting method, portable suitcase laboratory, and so on. Of course, as an emerging method with a short development time, RPA also had certain limitations. For example, no specialized software had been developed for the design of RPA primers, and only PCR software could be used for design and screening. The primers of RPA were longer than PCR primers. Sometimes the RPA could amplify the corresponding fragments with PCR primers, but it might not achieve the optimal amplification effect. At present, RPA technology has not been widely used mainly because it is not an open technology and is only used for scientific research. In addition, only one company sells RPA kit, which is expensive and costable for the detection of large-scale samples. Although RPA technology still has some limitations, it is expected to become the mainstream technology of nucleic acid amplification in the future by further exploring it and amplifying its advantages.

Author contributions

MT: Collect data, write and revise articles; CL: Collect information and assist in writing articles; XY: Guidance; ZZ: Article revision; LL: Guidance; GW: Review and modification of final draft. All authors contributed to the article and approved the submitted version.

Funding

Our research was granted by Natural Science Foundation of China (82260418), Natural Science Foundation of Guangxi (2019JJB140034), First Batch of High-level Talent Scientific Research Projects of the Affiliated Hospital of Youjiang Medical University for Nationalities (R202011701) and Baise Scientific Research and Technology Development Project (20193121).

Conflict of interest

The authors declare that the research was conducted in the absence of any commercial or financial relationships that could be construed as a potential conflict of interest.

Publisher's note

References

An, B., Zhang, H., Su, X., Guo, Y., Wu, T., Ge, Y., et al. (2021). Rapid and sensitive detection of salmonella spp. using CRISPR-Cas13a combined with recombinase polymerase amplification. *Front. Microbiol.* 12. doi: 10.3389/fmicb.2021.732426

Bai, Y., Ji, J., Ji, F., Wu, S., Tian, Y., Jin, B., et al. (2022). Recombinase polymerase amplification integrated with microfluidics for nucleic acid testing at point of care. *Talanta* 240, 123209. doi: 10.1016/j.talanta.2022.123209

Barreda-Garcia, S., Miranda-Castro, R., de-Los-Santos-Alvarez, N., Miranda-Ordieres, A. J., and Lobo-Castanon, M. J. (2018). Helicase-dependent isothermal amplification: a novel tool in the development of molecular-based analytical systems for rapid pathogen detection. *Anal. Bioanal. Chem.* 410 (3), 679–693. doi: 10.1007/s00216-017-0620-3

Cai, Q., Wang, R., Qiao, Z., and Yang, W. (2021). Single-digit salmonella detection with the naked eye using bio-barcode immunoassay coupled with recombinase polymerase amplification and a CRISPR-Cas12a system. *Analyst* 146 (17), 5271–5279. doi: 10.1039/d1an00717c

Cherkaoui, D., Huang, D., Miller, B. S., Turbe, V., and McKendry, R. A. (2021). Harnessing recombinase polymerase amplification for rapid multi-gene detection of SARS-CoV-2 in resource-limited settings. *Biosensors Bioelectron.* 189, 113328. doi: 10.1016/j.bios.2021.113328

Choi, M. H., Lee, J., and Seo, Y. J. (2021). Combined recombinase polymerase amplification/rkDNA-graphene oxide probing system for detection of SARS-CoV-2. *Analytic. Chim. Acta* 1158, 338390. doi: 10.1016/j.aca.2021.338390

Clancy, E., Higgins, O., Forrest, M. S., Boo, T. W., Cormican, M., Barry, T., et al. (2015). Development of a rapid recombinase polymerase amplification assay for the detection of streptococcus pneumoniae in whole blood. *BMC Infect. Dis.* 15, 481. doi: 10.1186/s12879-015-1212-5

El Wahed, A. A., Patel, P., Maier, M., Pietsch, C., Ruster, D., Bohlken-Fascher, S., et al. (2021). Suitcase lab for rapid detection of SARS-CoV-2 based on recombinase polymerase amplification assay. *Analytic. Chem.* 93 (4), 2627–2634. doi: 10.1021/acs.analchem.0c04779

Gao, Y., Huang, K., Wang, F., Hou, Y., Xu, J., and Li, G. (2022). Recent advances in biological detection with rolling circle amplification: design strategy, biosensing mechanism, and practical applications. *Analyst.* 147 (15), 3396–3414. doi: 10.1039/d2an00556e

Garrido-Maestu, A., Azinheiro, S., Fucinos, P., Carvalho, J., and Prado, M. (2020). Comparative study of multiplex real-time recombinase polymerase amplification and ISO 11290-1 methods for the detection of listeria monocytogenes in dairy products. *Food Microbiol.* 92, 103570. doi: 10.1016/j.fm.2020.103570

Gong, L., Wang, X., Li, Z., Huang, G., Zhang, W., Nie, J., et al. (2022). Integrated trinity test with RPA-CRISPR/Cas12a-fluorescence for real-time detection of respiratory syncytial virus a or b. *Front. Microbiol.* 13. doi: 10.3389/fmicb.2022.819931

Gumaa, M. M., Cao, X., Li, Z., Lou, Z., Zhang, N., Zhang, Z., et al. (2019). Establishment of a recombinase polymerase amplification (RPA) assay for the detection of brucella spp. *infection. Mol. Cell. Probes* 47, 101434. doi: 10.1016/j.mcp.2019.101434

Gumaa, M. M., Li, Z., Cao, X., Zhang, N., Lou, Z., Zhou, J., et al. (2020). Specific detection and differentiation between brucella melitensis and brucella abortus by a duplex recombinase polymerase amplification assay. *Front. Veterin. Sci.* 7. doi: 10.3389/fvets.2020.539679

Honsvall, B. K., and Robertson, L. J. (2017). From research lab to standard environmental analysis tool: Will NASBA make the leap? *Water Res.* 109, 389–397. doi: 10.1016/j.watres.2016.11.052

Huang, Q., Chen, Y., Liu, H., St-Hilaire, S., Gao, S., MacKinnon, B., et al. (2022). Establishment of a real-time recombinase polymerase amplification (RPA) for the detection of decapod iridescent virus 1 (DIV1). *J. Virol. Methods* 300, 114377. doi: 10.1016/j.jviromet.2021.114377

Hu, M., Qiu, Z., Bi, Z., Tian, T., Jiang, Y., and Zhou, X. (2022). Photocontrolled crRNA activation enables robust CRISPR-Cas12a diagnostics. *Proc. Natl. Acad. Sci. U.S.A.* 119 (26), e2202034119. doi: 10.1073/pnas.2202034119

Hu, J., Wang, Y., Ding, H., Jiang, C., Geng, Y., Sun, X., et al. (2020). Recombinase polymerase amplification with polymer flocculation sedimentation for rapid detection of staphylococcus aureus in food samples. *Int. J. Food Microbiol.* 331, 108691. doi: 10.1016/j.ijfoodmicro.2020.108691

Ivanov, A. V., Safenkova, I. V., Zherdev, A. V., and Dzantiev, B. B. (2021). Recombinase polymerase amplification assay with and without nuclease-dependent-labeled oligonucleotide probe. *Int. J. Mol. Sci.* 22 (21), e11885. doi: 10.3390/ijms222111885

Jiang, W., Ren, Y., Han, X., Xue, J., Shan, T., Chen, Z., et al. (2020). Recombinase polymerase amplification-lateral flow (RPA-LF) assay combined with immunomagnetic separation for rapid visual detection of vibrio parahaemolyticus in raw oysters. *Analytic. Bioanal. Chem.* 412 (12), 2903–2914. doi: 10.1007/s00216-020-02532-9

Jiang, X., Zhu, L., and Zhan, D. (2022). Development of a recombinase polymerase amplification assay for rapid detection of streptococcus suis type 2 in nasopharyngeal swab samples. *Diagn. Microbiol. Infect. Dis.* 102 (2), 115594. doi: 10.1016/j.diagmicrobio.2021.115594

Kersting, S., Rausch, V., Bier, F. F., and von Nickisch-Rosenegk, M. (2014). Rapid detection of plasmodium falciparum with isothermal recombinase polymerase amplification and lateral flow analysis. *Malaria J.* 13, 99. doi: 10.1186/1475-2875-13-99

Kim, N.-K., Lee, H.-J., Kim, S.-M., and Jeong, R.-D. (2022). Rapid and visual detection of barley yellow dwarf virus by reverse transcription recombinase polymerase amplification with lateral flow strips. *Plant Pathol. J.* 38 (2), 159–166. doi: 10.5423/PPJ.NT.01.2022.0009

Kovalskaya, N., and Hammond, R. W. (2022). Rapid diagnostic detection of tomato apical stunt viroid based on isothermal reverse transcription-recombinase polymerase amplification. *J. Virol. Methods* 300, 114353. doi: 10.1016/j.jviromet.2021.114353

Lai, M., and Lau, Y. (2020). Detection of plasmodium knowlesi using recombinase polymerase amplification (RPA) combined with SYBR green I. *Acta Tropica* 208, 105511. doi: 10.1016/j.actatropica.2020.105511

Lau, Y. L., Ismail, I. B., Mustapa, N. I. B., Lai, M. Y., Tuan Soh, T. S., Haji Hassan, A., et al. (2021). Development of a reverse transcription recombinase polymerase amplification assay for rapid and direct visual detection of severe acute respiratory syndrome coronavirus 2 (SARS-CoV-2). *PloS One* 16 (1), e0245164. doi: 10.1371/journal.pone.0245164

Lei, R., Kong, J., Qiu, Y., Chen, N., Zhu, S., Wang, X., et al. (2019). Rapid detection of the pathogenic fungi causing blackleg of brassica napus using a portable real-time fluorescence detector. *Food Chem.* 288, 57–67. doi: 10.1016/j.foodchem.2019.02.089

Lei, R., Li, Y., Li, L., Wang, J., Cui, Z., Ju, R., et al. (2022a). A CRISPR/Cas12a-based portable platform for rapid detection of leptosphaeria maculans in brassica crops. *Front. inPlant Sci.* 13. doi: 10.3389/fpls.2022.976510

Lei, R., Li, L., Wu, P., Fei, X., Zhang, Y., Wang, J., et al. (2022b). RPA/CRISPR/Cas12a-based on-site and rapid nucleic acid detection of toxoplasma gondii in the environment. *ACS Synthetic Biol.* 11 (5), 1772–1781. doi: 10.1021/acssynbio.1c00620

Lei, R., Wang, X., Zhang, D., Liu, Y., Chen, Q., and Jiang, N. (2020). Rapid isothermal duplex real-time recombinase polymerase amplification (RPA) assay for the diagnosis of equine piroplasmosis. *Sci. Rep.* 10 (1), 4096. doi: 10.1038/s41598-020-60997-1

Li, K., Lei, Z., Zhang, C., Zhu, L., Huang, K., Shang, Y., et al. (2022). Graphene oxide nanosheet-mediated fluorescent RPA "turn-on" biosensor for rapid RNAi transgenic plant detection. *Analytic. Chim. Acta* 1189, 339222. doi: 10.1016/j.aca.2021.339222

Li, K., Luo, Y., Huang, K., Yang, Z., Wan, Y., and Xu, W. (2020). Single universal primer recombinase polymerase amplification-based lateral flow biosensor (SUP-RPA-LFB) for multiplex detection of genetically modified maize. *Analytic. Chim. Acta* 1127, 217–224. doi: 10.1016/j.aca.2020.06.001

Li, J., Macdonald, J., and von Stetten, F. (2018). Review: a comprehensive summary of a decade development of the recombinase polymerase amplification. *Analyst* 144 (1), 31–67. doi: 10.1039/c8an01621f

Lin, M., Yue, H., Tian, T., Xiong, E., Zhu, D., Jiang, Y., et al. (2022). Glycerol additive boosts 100-fold sensitivity enhancement for one-pot RPA-CRISPR/Cas12a assay. *Analytic. Chem.* 94 (23), 8277–8284. doi: 10.1021/acs.analchem.2c00616

Li, Z., Pinto Torres, J. E., Goossens, J., Stijlemans, B., Sterckx, Y. G.-J., and Magez, S. (2020). Development of a recombinase polymerase amplification lateral flow assay for the detection of active trypanosoma evansi infections. *PloS Negl. Trop. Dis.* 14 (2), e0008044. doi: 10.1371/journal.pntd.0008044

Liu, S., Huang, G., Gong, Y., Jin, X., Meng, Y., Peng, Y., et al. (2020). Rapid and accurate detection of carbapenem-resistance gene by isothermal amplification in acinetobacter baumannii. *Burns Trauma* 8, tkaa026. doi: 10.1093/burnst/tkaa026

Liu, D., Shen, H., Zhang, Y., Shen, D., Zhu, M., Song, Y., et al. (2021). A microfluidic-integrated lateral flow recombinase polymerase amplification (MI-IF-RPA) assay for rapid COVID-19 detection. *Lab. Chip* 21 (10), 2019–2026. doi: 10.1039/d0lc01222j

Li, T., Wang, J., Zhang, N., Li, W., Yan, H., Li, L., et al. (2019). Rapid and visual detection of trichinella spp. using a lateral flow strip-based recombinase polymerase amplification (LF-RPA) assay. *Front. Cell. Infection Microbiol.* 9. doi: 10.3389/fcimb.2019.00001

Li, Z., Yang, Z., Li, Z., Gao, X., Hu, Z., Yang, H., et al. (2021). Development and evaluation of recombinase polymerase amplification combined with lateral flow dipstick assays for co-detection of epizootic haemorrhagic disease virus and the palyam serogroup virus. *BMC Veterin. Res.* 17 (1), 286. doi: 10.1186/s12917-021-02977-9

Lobato, I. M., and O'Sullivan, C. K. (2018). Recombinase polymerase amplification: Basics, applications and recent advances. *Trends Analytic. Chem.* 98, 19–35. doi: 10.1016/j.trac.2017.10.015

Luo, M., Meng, F., Tan, Q., Yin, W., and Luo, C. (2021). Recombinase polymerase amplification/Cas12a-based identification of xanthomonas arboricola pv. *pruni peach. Front. Plant Sci.* 12. doi: 10.3389/fpls.2021.740177

Malci, K., Walls, L. E., and Rios-Solis, L. (2022). Rational design of CRISPR/Cas12a-RPA based one-pot COVID-19 detection with design of experiments. *ACS Synthetic Biol.* 11 (4), 1555–1567. doi: 10.1021/acssynbio.1c00617

Ma, Q., Yao, J., Yuan, S., Liu, H., Wei, N., Zhang, J., et al. (2019). Development of a lateral flow recombinase polymerase amplification assay for rapid and visual detection of cryptococcus neoformans/C. gattii in cerebral spinal fluid. *BMC Infect. Dis.* 19 (1), 108. doi: 10.1186/s12879-019-3744-6

Meng, X., Zou, S., Li, D., He, J., Fang, L., Wang, H., et al. (2022). Nanozyme-strip for rapid and ultrasensitive nucleic acid detection of SARS-CoV-2. *Biosensors Bioelectron.* 217, 114739. doi: 10.1016/j.bios.2022.114739

Mohandas, A., and Bhat, A. I. (2020). Recombinase polymerase amplification assay for the detection of piper yellow mottle virus infecting black pepper. *Virusdisease* 31 (1), 38–44. doi: 10.1007/s13337-019-00566-x

Molina-Gonzalez, S. J., Bhattacharyya, T., AlShehri, H. R., Poulton, K., Allen, S., Miles, M. A., et al. (2020). Application of a recombinase polymerase amplification (RPA) assay and pilot field testing for giardia duodenalis at lake Albert, Uganda. *Parasit. Vectors* 13 (1), 289. doi: 10.1186/s13071-020-04168-1

Mullis, K., Faloona, F., Scharf, S., Saiki, R., Horn, G., and Erlich, H. (1986). Specific enzymatic amplification of DNA *in vitro*: the polymerase chain reaction. *Cold Spring Harbor Symp. On Quantitative Biol.* 51 Pt 1, 263–273. doi: 10.1101/sqb.1986.051.01.032

Munawar, M. A. (2022). Critical insight into recombinase polymerase amplification technology. *Expert Rev. Mol. Diagn.* 22 (7), 725–737. doi: 10.1080/14737159.2022.2109964

Nair, G., Rebolledo, M., White, A. C. J., Crannell, Z., Richards-Kortum, R. R., Pinilla, A. E., et al. (2015). Detection of entamoeba histolytica by recombinase polymerase amplification. *Am. Soc. Trop. Med. Hygiene* 93 (3), 591–595. doi: 10.4269/ajtmh.15-0276

Nie, Z., Zhao, Y., Shu, X., Li, D., Ao, Y., Li, M., et al. (2021). Recombinase polymerase amplification with lateral flow strip for detecting babesia microti infections. *Parasitol. Int.* 83, 102351. doi: 10.1016/j.parint.2021.102351

Oliveira, B. B., Veigas, B., and Baptista, P. V. (2021). Isothermal amplification of nucleic acids: the race for the next "Gold standard". *Front. Sensors* 2. doi: 10.3389/fsens.2021.752600

Panpru, P., Srisrattakarn, A., Panthasri, N., Tippayawat, P., Chanawong, A., Tavichakorntrakool, R., et al. (2021). Rapid detection of enterococcus and vancomycin resistance using recombinase polymerase amplification. *PeerJ* 9, e12561. doi: 10.7717/peerj.12561

Park, J. S., Hsieh, K., Chen, L., Kaushik, A., Trick, A. Y., and Wang, T. (2021). Digital CRISPR/Cas-assisted assay for rapid and sensitive detection of SARS-CoV-2. *Advanced Sci.* 8 (5), 2003564. doi: 10.1002/advs.202003564

Piepenburg, O., Williams, C. H., Stemple, D. L., and Armes, N. A. (2006). DNA Detection using recombination proteins. *PloS Biol.* 4 (7), e204. doi: 10.1371/journal.pbio.0040204

Qian, W., Huang, J., Wang, T., He, X., Xu, G., and Li, Y. (2021a). Visual detection of human metapneumovirus using CRISPR-Cas12a diagnostics. *Virus Res.* 305, 198568. doi: 10.1016/j.virusres.2021.198568

Qian, W., Huang, J., Wang, X., Wang, T., and Li, Y. (2021b). CRISPR-Cas12a combined with reverse transcription recombinase polymerase amplification for sensitive and specific detection of human norovirus genotype GII.4. *Virology* 564, 26–32. doi: 10.1016/j.virol.2021.09.008

Ren, M., Mei, H., Zhou, M., Fu, Z. F., Han, H., Bi, D., et al. (2021b). Development of a super-sensitive diagnostic method for african swine fever using CRISPR techniques. *Virol. Sin.* 36 (2), 220–230. doi: 10.1007/s12250-020-00323-1

Ren, M., Mei, H., Zhou, J., Zhou, M., Han, H., and Zhao, L. (2021a). Early diagnosis of rabies virus infection by RPA-CRISPR techniques in a rat model. *Arch. Virol.* 166 (4), 1083–1092. doi: 10.1007/s00705-021-04970-x

Reuter, C., Slesiona, N., Hentschel, S., Aehlig, O., Breitenstein, A., Csaki, A., et al. (2020). Loop-mediated amplification as promising on-site detection approach for legionella pneumophila and legionella spp. *Appl. Microbiol. Biotechnol.* 104 (1), 405–415. doi: 10.1007/s00253-019-10286-3

Rohrman, B., and Richards-Kortum, R. (2015). Inhibition of recombinase polymerase amplification by background DNA: a lateral flow-based method for enriching target DNA. *Analytic. Chem.* 87 (3), 1963–1967. doi: 10.1021/ac504365v

Rostron, P., Pennance, T., Bakar, F., Rollinson, D., Knopp, S., Allan, F., et al. (2019). Development of a recombinase polymerase amplification (RPA) fluorescence assay for the detection of schistosoma haematobium. *Parasites Vectors* 12 (1), 514. doi: 10.1186/s13071-019-3755-6

Schrader, C., Schielke, A., Ellerbroek, L., and Johne, R. (2012). PCR inhibitors - occurrence, properties and removal. *J. Appl. Microbiol.* 113 (5), 1014–1026. doi: 10.1111/j.1365-2672.2012.05384.x

Shelite, T. R., Uscanga-Palomeque, A. C., Castellanos-Gonzalez, A., Melby, P. C., and Travi, B. L. (2021). Isothermal recombinase polymerase amplification-lateral flow detection of SARS-CoV-2, the etiological agent of COVID-19. *J. Virol. Methods* 296, 114227. doi: 10.1016/j.jviromet.2021.114227

Simpkins, S. A., Chan, A. B., Hays, J., Popping, B., and Cook, N. (2000). An RNA transcription-based amplification technique (NASBA) for the detection of viable salmonella enterica. *Lett. Appl. Microbiol.* 30 (1), 75–79. doi: 10.1046/j.1472-765x.2000.00670.x

Singpanomchai, N., Akeda, Y., Tomono, K., Tamaru, A., Santanirand, P., and Ratthawongjirakul, P. (2021). Rapid detection of multidrug-resistant tuberculosis based on allele-specific recombinase polymerase amplification and colorimetric detection. *PloS One* 16 (6), e0253235. doi: 10.1371/journal.pone.0253235

Srisrattakarn, A., Tippayawat, P., Chanawong, A., Tavichakorntrakool, R., Daduang, J., Wonglakorn, L., et al. (2020). Direct detection of methicillin-resistant in staphylococcus spp. in positive blood culture by isothermal recombinase polymerase amplification combined with lateral flow dipstick assay. *World J. Microbiol. Biotechnol.* 36 (11), 162. doi: 10.1007/s11274-020-02938-8

Sun, Z., Lin, K., Zhao, Z., Wang, Y., Hong, X., Guo, J., et al. (2022). An automated nucleic acid detection platform using digital microfluidics with an optimized Cas12a system. *Sci. China Chem.* 65 (3), 630–640. doi: 10.1007/s11426-021-1169-1

Sun, Y., Qin, P., He, J., Li, W., Shi, Y., Xu, J., et al. (2022). Rapid and simultaneous visual screening of SARS-CoV-2 and influenza virufses with customized isothermal amplification integrated lateral flow strip. *Biosensors Bioelectron.* 197, 113771. doi: 10.1016/j.bios.2021.113771

Sun, Y., Yu, L., Liu, C., Ye, S., Chen, W., Li, D., et al. (2021). One-tube SARS-CoV-2 detection platform based on RT-RPA and CRISPR/Cas12a. *J. Transl. Med.* 19 (1), 74. doi: 10.1186/s12967-021-02741-5

Tian, T., Qiu, Z., Jiang, Y., Zhu, D., and Zhou, X. (2022). Exploiting the orthogonal CRISPR-Cas12a/Cas13a trans-cleavage for dual-gene virus detection using a handheld device. *Biosensors Bioelectron.* 196, 113701. doi: 10.1016/j.bios.2021.113701

Tran, D. H., Tran, H. T., Pham, T. N. M., and Phung, H. T. T. (2022). Direct multiplex recombinase polymerase amplification for rapid detection of s taphylococcus aureus and p seudomonas aeruginosa in food. *Mol. Biol. Res. Commun.* 11 (1), 1–10. doi: 10.22099/mbrc.2021.41503.1664

Travi, B. L., Delos Santos, M. B., Shelite, T. R., Santos, R. P., Rosales, L. A., Castellanos-Gonzalez, A., et al. (2021). Diagnostic efficacy of recombinase-polymerase-amplification coupled with lateral flow strip reading in patients with cutaneous leishmaniasis from the amazonas rainforest of peru. *Vector Borne Zoonotic Dis.* 21 (12), 941–947. doi: 10.1089/vbz.2021.0038

Walker, G. T. (1993). Empirical aspects of strand displacement amplification. *PCR Methods Appl.* 3 (1), 1–6. doi: 10.1101/gr.3.1.1

Walker, G. T., Little, M. C., Nadeau, J. G., and Shank, D. D. (1992). Isothermal *in vitro* amplification of DNA by a restriction enzyme/DNA polymerase system. *Proc. Natl. Acad. Sci. U.S.A.* 89 (1), 392–396. doi: 10.1073/pnas.89.1.392

Wang, F., Ge, D., Wang, L., Li, N., Chen, H., Zhang, Z., et al. (2021a). Rapid and sensitive recombinase polymerase amplification combined with lateral flow strips for detecting candida albicans. *Analytic. Biochem.* 633, 114428. doi: 10.1016/j.ab.2021.114428

Wang, P., Liao, L., Ma, C., Zhang, X., Yu, J., Yi, L., et al. (2021). Duplex on-site detection of vibrio cholerae and vibrio vulnificus by recombinase polymerase amplification and three-segment lateral flow strips. *Biosensors* 11 (5). doi: 10.3390/bios11050151

Wang, Y., Liu, A., Fu, M., Guo, J., Wang, L., Zuo, X., et al. (2022). Establishment and clinical application of a RPA-LFS assay for detection of capsulated and non-capsulated haemophilus influenzae. *Front. Cell. Infection Microbiol.* 12. doi: 10.3389/fcimb.2022.878813

Wang, F., Wang, L., Chen, H., Li, N., Wang, Y., Li, Y., et al. (2021b). Rapid detection of bla KPC, bla NDM, bla OXA-48-like and bla IMP carbapenemases in enterobacterales using recombinase polymerase amplification combined with lateral flow strip. *Front. Cell. Infection Microbiol.* 11. doi: 10.3389/fcimb.2021.772966

Wang, L., Wang, Y., Wang, F., Zhao, M., Gao, X., Chen, H., et al. (2021). Development and application of rapid clinical visualization molecular diagnostic technology for cryptococcus neoformans/C. gattii based on recombinase polymerase amplification combined with a lateral flow strip. *Front. Cell. Infection Microbiol.* 11. doi: 10.3389/fcimb.2021.803798

Wang, X., Xie, S., Chen, X., Peng, C., Xu, X., Wei, W., et al. (2020). A rapid and convenient method for on-site detection of MON863 maize through real-time fluorescence recombinase polymerase amplification. *Food Chem.* 324, 126821. doi: 10.1016/j.foodchem.2020.126821

Wang, X., Xu, L., Zuo, X., Lin, J., Jin, Z., Shen, R., et al. (2021). Rapid detection of the new Delhi metallo-beta-lactamase (NDM) gene by recombinase polymerase amplification. *Infection Genet. Evol.* 87, 104678. doi: 10.1016/j.meegid.2020.104678

Wang, B., Zhang, C., Liu, F., Li, R., Wang, Y., and Chen, G. (2021). Development of a recombinase polymerase amplification combined with lateral flow dipstick assay for rapid and sensitive detection of heterosigma akashiwo. *J. Appl. Phycol.* 33 (5), 3165–3178. doi: 10.1007/s10811-021-02538-5

Xu, L., Duan, J., Chen, J., Ding, S., and Cheng, W. (2021). Recent advances in rolling circle amplification-based biosensing strategies-a review. *Analytic. Chim. Acta* 1148, 238187. doi: 10.1016/j.aca.2020.12.062

Xu, Y., Fang, D., Chen, F., Zhao, Q., Cai, C., and Cheng, M. (2020). Utilization of recombinase polymerase amplification method combined with lateral flow dipstick for visual detection of respiratory syncytial virus. *Mol. Cell. Probes* 49, 101473. doi: 10.1016/j.mcp.2019.101473

Yang, H., Wang, Y., Yang, Q., Fan, H., Wang, L., Zhang, T., et al. (2021). A rapid and sensitive detection method for pseudomonas aeruginosa using visualized recombinase polymerase amplification and lateral flow strip technology. *Front. Cell. Infection Microbiol.* 11. doi: 10.3389/fcimb.2021.698929

Yang, X., Zhang, X., Wang, Y., Shen, H., Jiang, G., Dong, J., et al. (2020). A real-time recombinase polymerase amplification method for rapid detection of vibrio vulnificus in seafood. *Front. Microbiol.* 11. doi: 10.3389/fmicb.2020.586981

Yan, L., Zhou, J., Zheng, Y., Gamson, A. S., Roembke, B. T., Nakayama, S., et al. (2014). Isothermal amplified detection of DNA and RNA. *Mol. Biosyst.* 10 (5), 970–1003. doi: 10.1039/c3mb70304e

Yu, F., Zhang, K., Wang, Y., Li, D., Cui, Z., Huang, J., et al. (2021). CRISPR/Cas12a-based on-site diagnostics of cryptosporidium parvum IId-subtype-family from human and cattle fecal samples. *Parasit. Vectors* 14 (1), 208. doi: 10.1186/s13071-021-04709-2

Zhang, B., Zhu, Z., Li, F., Xie, X., and Ding, A. (2021). Rapid and sensitive detection of hepatitis b virus by lateral flow recombinase polymerase amplification assay. *J. Virol. Methods* 291, 114094. doi: 10.1016/j.jviromet.2021.114094

Zhu, P., Cui, Y., Pang, J., Xiong, Z., Huang, Z., Guo, S., et al. (2021). Sensitively and quickly detecting vibrio vulnificus by real time recombinase polymerase amplification targeted to vvhA gene. *Mol. Cell. Probes* 57, 101726. doi: 10.1016/j.mcp.2021.101726

frontiers | Frontiers in Cellular and Infection Microbiology

TYPE Original Research
PUBLISHED 02 March 2023
DOI 10.3389/fcimb.2023.1131241

OPEN ACCESS

EDITED BY
Carina Almeida,
Instituto Nacional Investigaciao Agraria e Veterinaria (INIAV), Portugal

REVIEWED BY
Liang-jun Chen,
Wuhan University, China
Abhishek Mishra,
Houston Methodist Research Institute, United States

*CORRESPONDENCE
Onya Opota
onya.opota@chuv.ch

SPECIALTY SECTION
This article was submitted to Clinical Microbiology, a section of the journal Frontiers in Cellular and Infection Microbiology

RECEIVED 24 December 2022
ACCEPTED 03 February 2023
PUBLISHED 02 March 2023

CITATION
Boldi M-O, Denis-Lessard J, Neziri R, Brouillet R, von-Garnier C, Chavez V, Mazza-Stalder J, Jaton K, Greub G and Opota O (2023) Performance of microbiological tests for tuberculosis diagnostic according to the type of respiratory specimen: A 10-year retrospective study.
Front. Cell. Infect. Microbiol. 13:1131241.
doi: 10.3389/fcimb.2023.1131241

Performance of microbiological tests for tuberculosis diagnostic according to the type of respiratory specimen: A 10-year retrospective study

Marc-Olivier Boldi[1], Justin Denis-Lessard[1], Rina Neziri[1], René Brouillet[2], Christophe von-Garnier[3], Valérie Chavez[1], Jesica Mazza-Stalder[3], Katia Jaton[2], Gilbert Greub[2,4] and Onya Opota[2*]

[1]Faculty of Business and Economics, University of Lausanne, Lausanne, Switzerland, [2]Institute of Microbiology, Lausanne University and University Hospital of Lausanne, Lausanne, Switzerland, [3]Division of Pulmonology, Department of Medicine, Lausanne University Hospital, University of Lausanne, Lausanne, Switzerland, [4]Infectious Diseases Service, Lausanne University and University Hospital of Lausanne, Lausanne, Switzerland

Background: The microbial diagnosis of tuberculosis (TB) remains challenging and relies on multiple microbiological tests performed on different clinical specimens. Polymerase chain reactions (PCRs), introduced in the last decades has had a significant impact on the diagnosis of TB. However, questions remain about the use of PCRs in combination with conventional tests for TB, namely microscopy and culture. We aimed to determine the performance of microscopy, culture and PCR for the diagnosis of pulmonary tuberculosis according to the type of clinical specimen in order to improve the diagnostic yield and to avoid unnecessary, time and labor-intensive tests.

Methods: We conducted a retrospective study (2008-2018) on analysis (34'429 specimens, 14'358 patients) performed in our diagnostic laboratory located in the Lausanne University Hospital to compare the performance of microbiological tests on sputum, induced sputum, bronchial aspirate and bronchoalveolar lavage (BAL). We analysed the performance using a classical "per specimen" approach and a "per patient" approach for paired specimens collected from the same patient.

Results: The overall sensitivities of microscopy, PCR and culture were 0.523 (0.489, 0.557), 0.798 (0.755, 0.836) and 0.988 (0.978, 0.994) and the specificity were 0.994 (0.993, 0.995), 1 (0.999, 1) and 1 (1, 1). Microscopy displayed no significant differences in sensitivity according to the type of sample. The sensitivities of PCR for sputum, induced sputum, bronchial aspirate and BAL were, 0.821 (0.762, 0.871), 0.643 (0.480, 0.784), 0.837 (0.748, 0.904) and 0.759 (0.624, 0.865) respectively and the sensitivity of culture were, 0.993 (0.981, 0.998), 0.980 (0.931, 0.998), 0.965 (0.919, 0.988), and 1 (0.961, 1) respectively. Pairwise comparison of specimens collected from the same patient reported a significantly higher sensitivity of PCR on bronchial aspirate over BAL ($p < 0.001$)

and sputum ($p < 0.05$) and a significantly higher sensitivity of culture on bronchial aspirate over BAL ($p < 0.0001$).

Conclusions: PCR displayed a higher sensitivity and specificity than microscopy for all respiratory specimens, a rational for a smear-independent PCR-based approach to initiate tuberculosis microbial diagnostic. The diagnosis yield of bronchial aspirate was higher than BAL. Therefore, PCR should be systematically performed also on bronchial aspirates when available.

KEYWORDS

tuberculosis, PCR, mycobacterial culture, bronchoalveolar lavage (BAL), bronchial aspirate, sputum, induced-sputum, acid-fast bacilli (AFB)

1 Introduction

With over ten million new cases in 2020 and about 1,5 million deaths, tuberculosis represents a major public health concern (WHO, 2021a). Rapid and reliable diagnosis is important to reduce morbidity and mortality associated with tuberculosis and to control transmission. When tuberculosis is suspected based on clinical symptoms, epidemiological information and radiological findings, microbial confirmation is key to establish the diagnosis. Despite progress during the last decades, the microbiological diagnosis of tuberculosis continues to be a challenge particularly in paucibacillary disease. Historically, the diagnosis of tuberculosis was based on microscopy and culture. Mycobacterial culture represents the reference method due to a low limit of detection (< 10 organisms for liquid cultures) and because it gives access to the strain for phenotypic antibiotic susceptibility test (van Zyl-Smit et al., 2011; WHO, 2021a). However, culture is challenging due to the slow growth of *Mycobacterium tuberculosis* and because it requires biosafety level three (BSL3) laboratories (Palomino, 2005; Pfyffer and Wittwer, 2012). Microscopy based on the visualization of acid-fast bacilli provides rapid results (<30 minutes) but has a limited sensitivity and specificity (limit of detection between 10^3 and 10^4 bacilli per ml) (Opota et al., 2019b). In order to increase their sensitivity, these tests may need to be repeated over several clinical specimen (Boehme et al., 2010; Campelo et al., 2021; WHO, 2021a).

More recently, molecular diagnosis, in particular polymerase chain reaction (PCR) have improved the diagnosis of tuberculosis with a limit of detection between 10 and 10^3 colony forming units per ml and a turnaround time between two to six hours (Boehme et al., 2010; van Zyl-Smit et al., 2011; Opota et al., 2016; WHO, 2021b). PCR was initially available in laboratories specialized in molecular diagnostics, through methods developed in-house assays (Greub et al., 2016; WHO, 2021c). Commercial all-inclusive systems, such as the GeneXpert system, now allow a greater number of laboratories to perform this analysis independently of a specialized infrastructure (Boehme et al., 2010; Opota et al., 2016; Dorman et al., 2018; WHO, 2021b). The GeneXpert system not only improved the initial diagnostic of tuberculosis but can be used to assess patient's infectious potential, on the basis of the semi-quantitative results (van Zyl-Smit et al., 2011; Opota et al., 2016; Opota et al., 2019b). In addition, rapid molecular test also shortens airborne isolation for hospitalized patients with presumptive tuberculosis (Lippincott et al., 2014)

More than 70% of the tuberculosis infections are pulmonary tuberculosis, for which sputum is the usual specimen collected in adults and older children who are able to collaborate. Other respiratory specimens can be considered when patients are not able to provide sputum or to increase microbial diagnostic yield (WHO, 2021c). This includes induced sputum, obtained by nebulization of sterile hypertonic saline (3% or 7% saline solution inhaled) followed by coughing and expectoration of airway secretions, bronchial aspirate, and bronchoalveolar lavages (Schaaf and Reuter, 2009; Weiszhar and Horvath, 2013).

In this study, we aimed to assess the performance of the different tests for the microbial diagnostic of tuberculosis according to the type of clinical specimen. Providing robust updated data may enable to choose optimal combination of test and specimen to: i) reach the maximum sensitivity, specificity and negative and predicative value, ii) prioritize the tests and specimens in the situation of limited resources or shortage of material and iii) reduce unnecessary costs.

There is no standard method to address the performance of diagnostic tests, particularly for tuberculosis where several microbiological tests on multiple clinical samples are frequently required. We applied data analytics methods that integrate multiple parameters, including, the type of microbiological test, the type of specimens, the sampling period, and the patients. In this study, we performed both a classical "per specimen" method to determine the performance of each diagnostic test and a "per patient" approach comparing paired specimens collected from the same patient.

This study provides data to establish diagnostic stewardship guidelines and diagnostic protocols. These data will help to establish more effective strategies to diagnose pulmonary tuberculosis in order to increase the rate of documentation, to accelerate the diagnosis and avoid unnecessary testing. In addition, it should provide analytical strategies that may also be suitable to study other infectious diseases while keeping associated medical, social and economic costs to a strict minimum.

2 Material and methods

2.1 Study design and data

Our laboratory is located in the Lausanne University Hospital (CHUV), a 1'500 beds tertiary-care hospital in a low-tuberculosis-prevalence country (Switzerland), with approximately six new cases per year per 100,000 population (Federal Office of Public Health; http://www.bag.admin.ch/). The data included microbiology analyses for patients with suspected mycobacterial infection from 2008 to 2018. They were automatically extracted from the Laboratory Information System (MOLIS, CGM).

For all specimens, information regarding the microbial diagnostic of mycobacteria were extracted. This included information regarding microscopy, PCR, cultures, molecular and phenotypic resistance genes together with the type of specimen and the date of collection. Each specimen was given a unique coded number. Similarly, each patient was given a unique coded number. The database was generated to allow analysis by date of sampling and by patients (see Section 2.4). For the microbial diagnostic of the disease, we generated a composite gold standard including microbiological findings and epidemiological and clinical data (see Section 2.3). The initial database included 34'429 specimens corresponding to 14'358 patients, including 8'587 sputum, 2'257 induced sputum, 8'610 bronchial aspirate and 4'576 bronchoalveolar lavages (BAL). Demographic data that correspond to the distribution of ages at first consultation by gender and TB status are presented in Figure 1.

2.2 Clinical specimens and mycobacterial diagnostic test

This study focuses on three microbial diagnostic tests commonly used for the diagnostic of mycobacterial infections, namely (i) microscopy (also named smear microscopy) for the direct detection of acid-fast bacilli (AFB) in clinical specimen, (ii) PCR for the detection of DNA of *M. tuberculosis* complex directly from clinical specimen and (iii) mycobacterial culture. Microscopy consists in acid-fast bacillus staining achieved through a fluorescent auramine-thiazine red staining on a heat-fixed smear as described in (Opota et al., 2016). PCR consisted of either an in-house TaqMan PCR targeting the multicopy *M. tuberculosis* IS6110 sequence, named PCR "MYTU" (Greub et al., 2016) or using the all-inclusive rapid molecular test Xpert MTB/RIF and Xpert MTB/RIF Ultra (herafter named Xpert) (Cepheid, Ca, USA) (Boehme et al., 2010; Opota et al., 2016; Chakravorty et al., 2017). Mycobacterial culture was achieved using mycobacterial growth indicator tube (MGIT) that consists in culture tubes containing tris 4, 7-diphenyl-1, 10-phenonthroline ruthenium chloride pentahydrate, an oxygen-quenched fluorochrome embedded in silicone at their bottom. Utilization of free oxygen for growing bacteria alleviates the fluorochrome quenching, resulting in fluorescence within the tube that can be visualized under UV light, as explained in a previous publication (Opota et al., 2016). Antibiotic resistance was determined using a combination of molecular and phenotypic testing as previously described (Opota

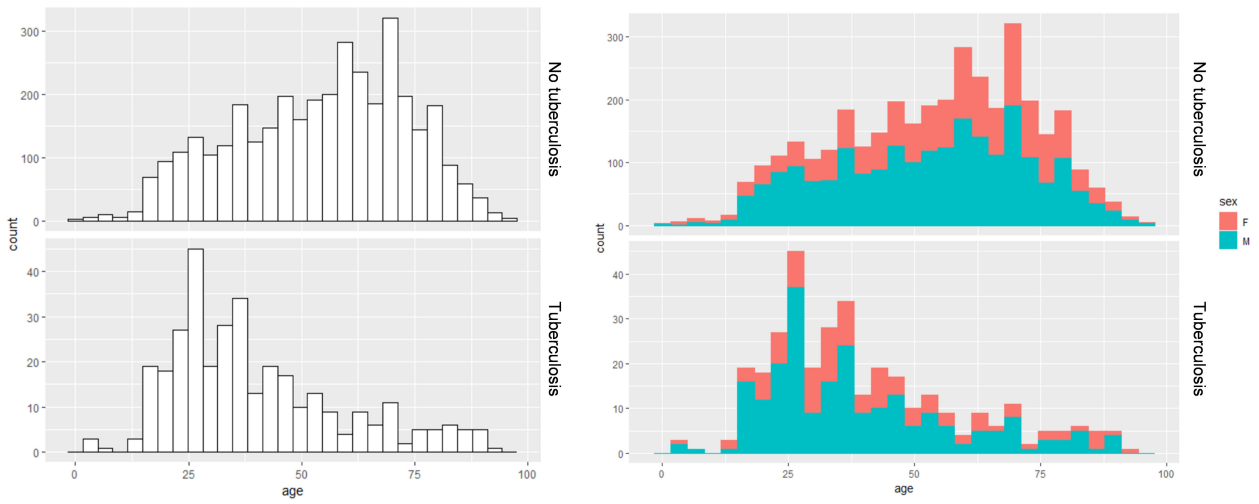

Age (years old)

Disease	Median	Mean	SD	Patients (n)
No tuberculosis	57	54.2	19.1	3634
Tuberculosis	35	39.9	19.2	337
Gender				
Female	58	54.9	19.2	1507
Male	53	51.8	19.6	2464
Total	**55**	**53**	**19.5**	**3971**

Proportions

Disease	Female	Male	Total
No tuberculosis	35.21% (1398)	56.31% (2236)	91.51% (3634)
Tuberculosis	2.74% (109)	5.74% (228)	8.49% (337)
Total	**37.95% (1507)**	**62.05% (2464)**	**100.00% (3971)**

FIGURE 1
Patient's demographic. The figure shows the patient's distribution of ages at first consultation by gender and disease status. A composite gold standard based on microbiological results and clinical data was used for disease status.

et al., 2016); overall ten strains of 296 positive cultures (3.37%) exhibited rifampicin resistant.

All the microbial analyses were performed on the same sample after splitting it for AFB staining, Xpert analysis and mycobacterial culture (Opota et al., 2016). Sputum, induced sputum, bronchial aspirate and bronchoalveolar lavage were processed as previously described (Opota et al., 2016). In particular, samples with a volume exceeding 3 mL were concentrated by centrifugation (30 minutes, 3000 g). In addition, to increase the homogeneity of the sample before smear preparation, purulent sputum or bronchial aspirates were solubilized with the mucolytic agent N-acetyl-L-cysteine (2% v/v pH 6.8) (Opota et al., 2016).

2.3 Composite gold standard

Mycobacterial culture is the gold standard for the diagnosis of *M. tuberculosis* because of its lowest limit of detection (LOD < 10 organisms). However, it can be impaired by situation that affect mycobacterial growth such as the introduction of an antibiotic treatment before sampling (van Zyl-Smit et al., 2011). We therefore used a composite gold standard based on microbiological results and clinical data. Discrepant results in the diagnostic of active tuberculosis, especially specimen with positive MTBC PCR and negative culture for *M. tuberculosis* complex, were manually cured based on clinical and epidemiological data found in medical records. Specimens for which the culture was contaminated by bacteria of the flora were excluded. Specimens with culture positive with nontuberculous mycobacteria qualified as "MOTT" (Mycobacteria other than tuberculosis) were considered negative for *M. tuberculosis*. This resulted in the "Gold Standard" (GS) reference.

2.4 Performance of the test depending on the clinical specimens and statistical methods

We used two different approaches to determine the performance of microbiological tests depending on the clinical specimens. We first used a common "per specimen" approach to determine the global performance of microscopy, PCR, and culture according to the four types of specimens and independently of the patient using the GS as reference. Then, in order to provide more robust data we performed a "per patient" approach. It consists in pairwise comparison for specimens collected the same day or during a window of 72 hours for the same patient; indeed, samples from the same patient might not be collected the same day. For each patient, the first sample was paired to the following sample if it was of a different type and within a 72-hour window. All the combinations of the four types of specimens were analyzed using this pairwise approach i) to measure the dependence between each pair of types of specimens and ii) to calculate the performance of one sample type to predict a positive of any of the two sample types.

For both approaches, the performance measures include accuracy, sensitivity, specificity, positive and negative predictive values (PPV and NPV). They were computed using the gold-standard (GS) as reference. Their respective 95% confidence intervals were computed using the Clopper–Pearson method. The comparisons of proportions were assessed with a two-sided proportion test with Yates' continuity correction. The dependence between pairs of types of specimens for the "per patient" approach was measured by the Cohen's Kappa.

2.5 Ethics committee approval

This study was approved by the relevant ethics committee, the *Commission Cantonale d'Éthique de la Recherche sur l'Être Humain* (*CER-2020-00136).*

3 Results

3.1 Global performance of microscopy, PCR and culture for the diagnostic of pulmonary tuberculosis

We first determined the global performance of microscopy. The sensitivity, 0.523 (0.489 – 0.557) and the PPV, 0.767 (0.730, 0.800) of microscopy were limited. The specificity, 0.994 (0.993, 0.995), and the NPV 0.982 (0.981, 0.984) were high but must be interpreted according to the low prevalence of microscopy positive specimen 0.036 (0.034, 0.038) (Tables 1; S1).

Regarding PCR, we first estimated the individual performance of the in-house TaqMan PCR and the rapid molecular test Xpert. The sensitivity of the in-house TaqMan PCR, 0.799 (0.743, 0.848) and Xpert 0.812 (0.760, 0.858) were not significantly different (Tables S2, S3). The specificity for both the in-house TaqMan PCR >0.999 (0.999, 1) and Xpert 0.999 (0.997, 1) were both very high. The NPV were also high but probably increased by the low prevalence of PCR positive specimen (Table S7). Because the two PCR tests displayed similar performance, we considered them as equal for the rest of the study and grouped them as "PCR". The global performance of PCR were: sensitivity 0.798 (0.755, 0.836), specificity 1 (0.999, 1), PPV 0.997 (0.983, 1) and NPV 0.988 (0.985, 0.990) (Tables 2; S2).

The culture displayed the highest performance for the diagnostic of tuberculosis using the GS reference with a sensitivity of 0.988 (0.978, 0.994) and a specificity of 1 (1, 1) (Tables 3; S3). In summary when considering all the clinical specimen, microscopy displays limited sensitivity, PCR displays a higher sensitivity than microscopy and an excellent specificity and culture displayed the highest sensitivity and specificity.

3.2 Performance of microbiological tests according to the type of specimen using a "per sample" approach or using "per patient" pairwise comparisons.

We next measured the dependence between the specimens using the "per patient" approach and the Cohen's kappa. Though

TABLE 1 Performance of smear microscopy for the diagnostic of pulmonary tuberculosis according of the type of specimen.

	Accuracy	Sensitivity	Specificity	Prevalence	PPV	NPV
All specimens	0.977 (0.975,0.979) 23219/23763	0.523 (0.489, 0.557) 447/855	0.994 (0.993, 0.995) 22772/22908	0.036 (0.034, 0.038) 855/23763	0.767 (0.730, 0.800) 447/583	0.982 (0.981, 0.984) 22772/23180
Sputum	0.967 (0.963, 0.971) 8132/8409	0.605 (0.562, 0.647) 320/529	0.991 (0.989, 0.993) 7812/7880	0.063 (0.058, 0.068) 529/8409	0.825 (0.783, 0.861) 320/388	0.974 (0.970, 0.977) 7812/8021
Induced sputum	0.966 (0.957, 0.973) 2119/2194	0.362 (0.265, 0.467) 34/94	0.993 (0.988, 0.996) 2085/2100	0.043 (0.035, 0.052) 94/2194	0.694 (0.546, 0.817) 34/49	0.972 (0.964, 0.979) 2085/2194
Bronchial aspirate	0.985 (0.982, 0.988) 8463/8591	0.362 (0.283, 0.447) 51/141	0.996 (0.994, 0.997) 8412/8450	0.016 (0.014, 0.019) 141/8591	0.573 (0.464, 0.677) 51/89	0.989 (0.987, 0.991) 8412/8502
BAL	0.986 (0.982, 0.989) 4505/4569	0.462 (0.356, 0.569) 42/91	0.997 (0.994, 0.998) 4463/4478	0.020 (0.016, 0.024) 91/4569	0.737 (0.603, 0.845) 42/57	0.989 (0.986, 0.992) 4463/4512

All p.values in Supplementary Material.

TABLE 2 Performance of PCR for the diagnostic of pulmonary tuberculosis according to the type of specimen.

	Accuracy	Sensitivity	Specificity	Prevalence	PPV	NPV
All specimens	0.988 (0.986, 0.991) 7009/7091	0.798 (0.755, 0.836) 320/401	1 (0.999, 1) 6689/6690	0.057 (0.051, 0.062) 401/7091	0.997 (0.983, 1) 320/321	0.988 (0.985, 0.990) 6770/7091
All specimens smear microscopy negative	0.988 (0.985, 0.991) 6982/7066	0.585 (0.513, 0.654) 117/200	1 (0.999, 1) 6865/6866	0.028 (0.025, 0.032) 200/7066	0.992 (0.954, 1) 117/118	0.988 (0.985, 0.990) 6865/6948
All specimens smear microscopy positive	1 (0.987, 1) 286/286	1 (0.983, 1) 210/210	1 (0.953, 1) 76/76	0.734 (0.679, 0.785) 210/286	1 (0.983, 1) 210/210	1 (0.953, 1) 76/76
Sputum	0.986 (0.980, 0.990) 2525/2562	0.821 (0.762, 0.871) 170/207	>0.999 (0.998, 1) 2355/2355	0.081 (0.071, 0.092) 207/2562	1 (0.979, 1) 170/170	0.985 (0.979, 0.989) 2355/2562
Induced sputum	0.977 (0.962, 0.987) 636/651	0.643 (0.480, 0.784) 27/42	>0.999 (0.994, 1) 609/609	0.065 (0.047, 0.086) 42/609	1 (0.872, 1) 27/27	0.976 (0.961, 0.986) 609/624
Bronchial aspirate	0.993 (0.988, 0.996) 2256/2273	0.837 (0.748, 0.904) 82/98	>0.999 (0.997, 1) 2174/2175	0.043 (0.035, 0.052) 98/2273	0.988 (0.935, 1) 82/83	0.993 (0.988, 0.996) 2174/2175
BAL	0.992 (0.986, 0.996) 1592/1605	0.759 (0.624, 0.865) 41/54	>0.999 (0.914, 1) 1551/1551	0.034 (0.025, 0.044) 54/1605	1 (0.914, 1) 41/41	0.992 (0.986, 0.996) 1551/1564

All p.values in Supplementary Material.

the Cohen's kappa is itself difficult to interpret and the confidence intervals shown in the table were not corrected for multiple comparisons, a large value of kappa means that the two sample bring the same information to some extent and thus provides little "complementary" information and are so-called "supllementary", i.e not really needed. Conversely, a kappa close to zero means that the two sample are "complementary". The results are shown in Tables S8–S11. The data suggested that for each technique, microscopy, PCR, and culture, most samples are supplementary (i.e. not all needed), except i) for microscopy, induced sputum versus bronchial aspirate and BAL, ii) for PCR, sputum versus induced sputum and iii) for the culture, induced sputum versus BAL. Because of their low robustness, we do not want to over interpret these results by concluding that the so-called "supplementary" tests don't need to be performed, but this question has to be tackled in additional work since it is however to our knowledge the first study showing such high dependence & redundancy of the various tests.

10.3389/fcimb.2023.1131241

TABLE 3 Performance of culture for the diagnostic of pulmonary tuberculosis according to the type of specimen.

	Accuracy	Sensitivity	Specificity	Prevalence	PPV	NPV
All specimens	>0.999 (0.999, 1) 24019/24030	0.988 (0.978, 0.994) 871/882	1 (1, 1) 23148/23148	0.037 (0.034, 0.039) 882/24030	1 (0.996, 1) 871/871	1 (0.999, 1) 23148/23159
Sputum	>0.999 (0.999, 1) 8583/8587	0.993 (0.981, 0.998) 543/547	1 (1, 1) 8040/8040	0.064 (0.059, 0.069) 547/8587	1 (0.993, 1) 543/543	1 (0.999, 1) 8040/8044
Induced sputum	1 (0.997, 1) 2255/2257	0.980 (0.931, 0.998) 100/102	1 (0.998, 1) 2155/2155	0.045 (0.037, 0.055) 102/2155	1 (0.964, 1) 100/100	1 (0.997, 1) 2155/2157
Bronchial aspirate	>0.999 (0.999, 1) 8605/8610	0.965 (0.919, 0.988) 136/141	1 (1, 1) 8469/8469	0.016 (0.014, 0.019) 141/8610	1 (0.973, 1) 136/136	0.999 (0.999, 1) 8469/8474
BAL	1 (0.999, 1) 4576/4576	1 (0.961, 1) 92/92	1 (0.999, 1) 4484/4484	0.020 (0.016, 0.025) 92/4576	1 (0.961, 1) 92/92	1 (0.999, 1) 4484/4484

All p.values in Supplementary Material.

3.3 Performance of microscopy according to the type of respiratory specimen

Using the classical "per specimen" approachthe sensitivities of microscopy for all specimen, sputum, induced sputum, bronchial aspirate and BAL were 0.523 (0.489, 0.557), 0.605 (0.562, 0.647), 0.362 (0.265, 0.467), 0.362 (0.283, 0.447) and 0.462 (0.356, 0.569) respectively. The sensitivity of sputum was higher than induced sputum (p-value < 0.0001) and bronchial aspirate (p-value < 0.0001) (Tables 4; S4). However, using the "per patient" comparison approach, for paired specimens collected within a window of 72h for the same patient, no significant difference was observed for the various specimens (Tables 4; S4, S9). Altogether, these data suggested a limited benefit of microscopy for tuberculosis microbial diagnosis in a low prevalence setting.

3.4 Performance of PCR according to the type of respiratory specimen.

Using the classical "per specimen" approachthe sensitivities of PCR for all specimen, sputum, induced sputum, bronchial aspirate and BAL were 0.798 (0.755, 0.836), 0.821 (0.762, 0.871), 0.643 (0.480, 0.784), 0.837 (0.748, 0.904) and 0.759 (0.624, 0.865) respectively. Using the

TABLE 4 Sensitivity of microscopy to predict tuberculosis according to the type of specimen using a 72-hours pairing window in the same patient.

	Sensitivity	NPV
Sputum versus induced sputum		
Sputum	0.923 (0.640, 0.998) 12/13 $^{n.s}$	0.997 (0.986, 1) 390/391 $^{n.s}$
Induced Sputum	0.769 (0.462, 0.950) 10/13 $^{n.s}$	0.992 (0.978, 0.998) 390/393 $^{n.s}$
Sputum versus bronchial aspirate		
Sputum	0.692 (0.386, 0.909) 9/13 $^{n.s}$	0.988 (0.970, 0.997) 337/341 $^{n.s}$
Bronchial aspirate	0.846 (0.546, 0.981) 11/13 $^{n.s}$	0.994 (0.979, 0.999) 337/339 $^{n.s}$
Sputum versus BAL		
Sputum	1 (0.631, 1) 8/8 $^{n.s}$	1 (0.987, 1) 280/280 $^{n.s}$
BAL	0.750 (0.349, 0.968) 6/8 $^{n.s}$	0.993 (0.975, 0.999) 280/282 $^{n.s}$
Induced sputum versus bronchial aspirate		
Induced Sputum	0.500 (0.013, 0.987) 1/2 $^{n.s}$	0.982 (0.904, 1) 55/56 $^{n.s}$
Bronchial aspirate	0.500 (0.013, 0.987) 1/2 $^{n.s}$	0.982 (0.904, 1) 55/56 $^{n.s}$
Induced sputum versus BAL		
Induced Sputum	0.333 (0.008, 0.906) 1/3 $^{n.s}$	0.962 (0.868, 0.995) 50/52 $^{n.s}$
BAL	0.667 (0.094, 0.992) 2/3 $^{n.s}$	0.980 (0.896, 1) 50/51 $^{n.s}$
Bronchial aspirate versus BAL		
Bronchial aspirate	0.881 (0.744, 0.960) 37/42 $^{n.s}$	0.999 (0.997, 1.000) 3528/3533 $^{n.s}$
BAL	0.714 (0.554, 0.843) 30/42 $^{n.s}$	0.997 (0.994, 0.998) 3528/3540 $^{n.s}$

All p.values in Supplementary Material. *** < 0.01 < ** < 0.05 < * < 0.1 < n.s.

"per patient" pairwise comparison approach, no significant difference in sensitivity was seen between sputum and induced sputum. Using this approach, we found that the sensitivity of bronchial aspirate, was significantly higher than BAL with respectively 0.974 (0.865, 0.999) and 0.564 (0.396, 0.722) (p. value 0.0003). The sensitivity of bronchial aspirate was also higher than sputum with respectively 1 (0.753, 1) *versus* 0.385 (0.139, 0.684) (p-value = 0.017) (Tables 5; S5, S10).

These data suggest, no significant difference in the sensitivity of PCR between sputum and induced sputum when the patient can produce spontaneous sputum. In contrast, bronchial aspirate displays higher sensitivity than sputum and BAL. PCR displayed a high specificity for all the respiratory specimens.

3.5 Performance of culture according to the type of respiratory specimen

Using the classical "per specimen" approachthe sensitivity of culture when considering all respiratory specimen was 0.988 (0.978, 0.994). The sensitivities of culture for sputum, induced sputum, bronchial aspirate and BAL were 0.993 (0.981, 0.998), 0.980 (0.931, 0.998), 0.965 (0.919, 0.988), and 1 (0.961, 1).

Using the "per patient" comparison of paired specimens, no significant difference in sensitivity was seen between the different respiratory specimens expect a superiority of bronchial aspirate over BAL, 0.970 (0.914, 0.994) versus 0.636 (0.538, 0.731) (p. value < 0.0001) (Tables 6; S6, S11).

4 Discussion

The microbial diagnosis of tuberculosis is based on a combination of different microbiological tests that can be performed on different types of clinical samples. We aimed to identify the most efficient tests and specimen in order to guarantee an ideal sensitivity and specificity and to limit the use of unnecessary tests.

4.1 Smear independent diagnostic of tuberculosis

Our results confirm a limited sensitivity of smear microscopy (0.523). The specificity (0.994) remains high, probably because of the extremely low prevalence (0.036) of positive microscopy. Our data suggest a higher sensitivity of microscopy on sputum over the three other samples. This is probably a bias because patients for whom the microbiological diagnosis is not made on spontaneous sputum and who therefore need induced sputum or bronchial aspiration and BAL are patients with paucibacillary infections as previously reported by Cadena et al. (2017). Using a pairwise comparison method to avoid the patient effect, we do not see any significant difference in sensitivity of microscopy between the various clinical specimens. With a time to result lower than 30 minutes, microscopy remains virtually the fastest diagnostic test. However, its sensitivity and specificity is limited and it requires a lot of work by specialized

TABLE 5 Sensitivity of PCR to predict tuberculosis according to the type of specimen using a 72-hours pairing window in the same patient.

	Sensitivity	NPV
Sputum versus induced sputum		
Sputum	0.667 (0.094, 0.992) 2/3 $^{n.s}$	0.992 (0.958, 1) 129/130 $^{n.s}$
Induced sputum	0.667 (0.094, 0.992) 2/3 $^{n.s}$	0.992 (0.958, 1) 129/130 $^{n.s}$
Sputum versus bronchial aspirate		
Sputum	0.385 (0.139, 0.684) 5/13 *	0.953 (0.909, 0.979) 161/169 $^{n.s}$
Bronchial aspirate	1 (0.753, 1) 13/13 *	1 (0.977, 1) 161/161 $^{n.s}$
Sputum versus BAL		
Sputum	0.600 (0.147, 0.947) 3/5 $^{n.s}$	0.985 (0.947, 0.998) 132/134 $^{n.s}$
BAL	1 (0.478, 1) 5/5 $^{n.s}$	1 (0.478, 1) 132/132 $^{n.s}$
Induced sputum versus bronchial aspirate		
Induced sputum	0.857 (0.421, 0.996) 6/7 $^{n.s}$	0.968 (0.833, 0.999) 30/31 $^{n.s}$
Bronchial aspirate	0.714 (0.290, 0.963) 5/7 $^{n.s}$	0.938 (0.792, 0.992) 30/32 $^{n.s}$
Induced sputum versus BAL		
Induced sputum	1 (0.478, 1) 5/5 $^{n.s}$	1 (0.884, 1) 30/30 $^{n.s}$
BAL	0.600 (0.147, 0.947) 3/5 $^{n.s}$	0.938 (0.792, 0.992) 30/32 $^{n.s}$
Bronchial aspirate versus BAL		
Bronchial aspirate	0.974 (0.865, 0.999) 38/39 ***	0.999 (0.995, 1.000) 1142/1143 **
BAL	0.564 (0.396, 0.722) 22/39 ***	0.985 (0.977, 0.991) 1142/1159 **

All p.values in Supplementary Material. *** < 0.01 < ** < 0.05 < * < 0.1 < n.s.

TABLE 6 Sensitivity of culture to predict tuberculosis according to the type of specimen using a 72-hours pairing window within the same patient.

	Sensitivity	NPV
Sputum versus induced sputum		
Sputum	0.857 (0.697, 0.952) 30/35 $^{n.s}$	0.987 (0.969, 0.996) 368/373 $^{n.s}$
Induced sputum	0.800 (0.631, 0.916) 28/35 $^{n.s}$	0.981 (0.962, 0.992) 368/375 $^{n.s}$
Sputum versus bronchial aspirate		
Sputum	0.613 (0.422, 0.782) 19/31 $^{n.s}$	0.964 (0.937, 0.981) 318/330 $^{n.s}$
Bronchial aspirate	0.903 (0.742, 0.980) 28/31 $^{n.s}$	0.991 (0.973, 0.998) 318/321 $^{n.s}$
Sputum versus BAL		
Sputum	0.895 (0.669, 0.987) 17/19 $^{n.s}$	0.993 (0.974, 0.999) 268/270 $^{n.s}$
BAL	0.789 (0.544, 0.939) 15/19 $^{n.s}$	0.985 (0.963, 0.996) 268/272 $^{n.s}$
Induced sputum versus bronchial aspirate		
Induced sputum	0.692 (0.386, 0.909) 9/13 $^{n.s}$	0.915 (0.796, 0.976) 43/47 $^{n.s}$
Bronchial aspirate	0.846 (0.546, 0.981) 11/13 $^{n.s}$	0.956 (0.849, 0.995) 43/45 $^{n.s}$
Induced sputum versus BAL		
Induced sputum	0.769 (0.462, 0.950) 10/13 $^{n.s}$	0.929 (0.805, 0.985) 39/42 $^{n.s}$
BAL	0.462 (0.192, 0.749) 6/13 $^{n.s}$	0.848 (0.711, 0.937) 39/46 $^{n.s}$
Bronchial aspirate versus BAL		
Bronchial aspirate	0.970 (0.914, 0.994) 96/99***	0.999 (0.997, 1.000) 3471/3474***
BAL	0.636 (0.538, 0.731) 63/99***	0.990 (0.986, 0.993) 3471/3507***

All p.values details in Supplementary Material. *** < 0.01 < ** < 0.05 < * < 0.1 < n.s.

personnel and the performance of this test may vary depending on the experience of the examiner (Opota et al., 2016; Andenmatten et al., 2019). In a region with a low prevalence of tuberculosis, the question arises of the usefulness of this test. In 2016, we introduced in our laboratory a smear-independent algorithm for the diagnostic of tuberculosis (Opota et al., 2016). For all the suspicion of tuberculosis the microbial diagnosis is initiated by PCR; microscopy were not achieved anymore in emergency but grouped once per day. In case of suspected pulmonary tuberculosis, we initiated microbial diagnostic by the rapid molecular test Xpert MTB/RIF further replaced by Xpert MTB/RIF Ultra which is used both to detect *M. tuberculosis* DNA and to address patient infectiousness based on the semi-quantitative result; microscopic analysis was still performed after treatment start, in particular to guide contact tracing and des-isolation decisions (Opota et al., 2016; Opota et al., 2019b; Opota et al., 2019a). Another study on the diagnosis of nontuberculous mycobacteria (NTM) infection also suggested a limited added-value of microscopy when 16S broad range PCR for the detection of NTM is available (Andenmatten et al., 2019). Our data suggested that microscopy might be useful only for patients with a high pre-test probability of NTM infections, such as immunocompromised patients or patients with clinical and radiological suspicion of having NTM lung disease. In February 2020, we and other diagnostic laboratory experienced an important staff limitation triggered by the SARS-CoV-2 pandemics. Indeed, during the first wave of the SARS-CoV-2 pandemic, the biomedical technicians were reassigned for the management of the SARS-CoV-2 RT-PCR tests. In this context, we had to rapidly identify all the unnecessary analysis among which was smear microscopy. As an immediate response, we therefore push forward, in February 2020, the smear independent algorithm for the diagnostic of mycobacterial infection. Since then, microscopy for the detection of acid-fast bacilli is achieved only on specific request from clinicians or for patients with a confirmed diagnostic of tuberculosis; indeed, microscopy can be useful for treatment follow-up because PCR can remain positive for a long period in patient's respiratory specimens even when a treatment is well conducted and for contact tracing investigations. Microscopy in addition to pan-mycobacterial PCR can also be requested when there is a high pre-test probability of NTM infection (Andenmatten et al., 2019).

4.2 Towards less cultures?

PCR has improved the diagnostic of tuberculosis with a lower limit of detection than microscopy and an increased specificity for PCR targeting specific *M. tuberculosis* DNA sequences such as the IS6110. Culture, the oldest microbiological test for tuberculosis, remains the reference method with the lowest limit of detection (Palomino, 2005; van Zyl-Smit et al., 2011). The performance of mycobacterial culture, sensitivity (98.8%) and specificity (100%), was calculated using a composite gold standard including all the microbiological tests as well as clinical data. We reported few patients with positive PCR but negative culture. It will therefore

be difficult to do without culture. Further optimization strategies could be implemented by selecting the most performant tests on the most efficient clinical samples regarding pulmonary tuberculosis. Thus, we could consider only a combination of (i) samples for PCR-based diagnosis to have short time to results coupled to (ii) a selection of samples to perform the culture warranted to obtain strains for testing susceptibility towards anti-mycobacterial agents and also to guarantee an optimal sensitivity (with delayed results).

When pulmonary tuberculosis is suspected, sputum is the usual specimen that is collected. Regarding microscopy, as indicated above there is no significant difference between the different types of clinical samples. On the other hand, with regard to PCR and culture which are much more sensitive and reliable tests we observed differences between the clinical specimens. When looking at sputum and induced sputum we do not see a significant difference in terms of sensitivity for culture. Several studies reported an increased sensitivity of induced sputum over sputum (Biswas et al., 2013; Seong et al., 2014). Using the classical approach or the pairwise comparison in the same patient, we did not observe a significant increase in sensitivity with induced sputum compared to spontaneous sputum. However, the pairwise comparisons suggest an increase in the yield of positivity when performing the two specimens. This conclusion should be confirmed by further studies. BAL and bronchial aspirate are generally coupled. The pairwise comparison demonstrates that in the case of tuberculosis the bronchial aspirate (97% of sensitivity) outcompete BAL (63.6% of sensitivity) suggesting a limited added benefit of the BAL for the diagnosis of tuberculosis. Bronchial aspirate and BAL are invasive, which make prospective studies hardly conceivable. Therefore, this retrospective study, giving access to 3'570 pairwise comparison including these specimen provide important data on their performance. Bronchoscopy is not only useful for tuberculosis diagnosis but also to investigate other infectious or non-infectious disease (Sanjeevaiah et al., 2018). For instance, BAL is a very good specimen for the diagnostic of fungal infection such as *Pneumocystis jirovecii* infections or *Aspergillus fumigatus* infection (Imbert et al., 2018; Perret et al., 2020; Neofytos et al., 2021). In view of these results, it is important to consider bronchial aspiration for the diagnosis of tuberculosis, confirming previous studies (Maitre et al., 2021). A first step would therefore be to always add a search for mycobacteria on the bronchial aspiration when it is missing in laboratory order. This is what we systematically do in our lab when it is missing. This study provides data for diagnostic stewardship and guidance for physicians and clinical microbiology laboratories. Such data could also help at defining diagnostic strategies in the setting of staff or reagants shortage or to reduce costs. Indeed, even in low prevalence and high-income country, the infrastructure and trained personnel for the diagnostic of tuberculosis is limited (Cannas et al., 2013). The SARS-CoV-2 pandemics negatively impacted tuberculosis control because of the mobilization of trained staff for other activities or because of the disruption of the supply chain of reagents and compounds for tuberculosis diagnostic and treatments (Meneguim et al., 2020; Armstrong et al., 2021). In a context of shortage of reagants or other material for mycobacterial culture like the one we encountered during the COVID-19 pandemic, if a prioritization had to be made, it should be done for the benefit of bronchial aspiration; but this should be decided together with the clinician that can help guiding the decision by providing clinical information for each case.

4.3 Limits of the study and perspectives

Although this is a retrospective study from a single centre, it does contain a large amount of data over a long period of time. In comparison with the low sensitivity of smear microscopy, PCR detection of *M. tuberculosis* had higher sensitivity and specificity. In addition, compared to Ziehl-Neelsen and auramine staining, rapid PCR assays such as the Xpert systems are relatively easy to use and require less training and experience. The very short time to results of rapid PCR allows its use as a first-line method for both clinical diagnosis and patient management, as well as for rapid triage of hospitalized patients to avoid nosocomial spread. In addition, the detection of rifampicin resistance is a further advantage of such rapid PCR tests. Nevertheless, smear microscopy is still a mean of rapid diagnostic of tuberculosis in low- and middle-income countries. It is also of great importance for the detection of non-tuberculous mycobacteria, especially in the absence of real-time PCR for the detection of these pathogens. Molecular diagnostic significantly improved the microbial diagnostic of tuberculosis, in particular the initial diagnostic, but is not yet generalized worldwide (Mechai et al., 2020), mainly for economical reasons. To assess the real economic impact of the management of tuberculosis a cost-benefit analysis for the full replacement of microscopy in favor of PCR should be performed since this study demonstrates the effectiveness of PCR over microscopy (Dowdy et al., 2014). Such analysis should incorporate that, in hospital setting, patients might be isolated in specific negative pressure chambers for the duration of the investigation. Such cost-benefit study should also address the risk of nosocomial infection due to delayed diagnostic. Future studies should account for the evolution in practices that may have occurred over the ten years (2008-2018) of the study. It would be worthwhile to relate the data with the evolution of protocols and guidelines that were introduced during the studied period in order not to only add diagnostic tools but also to stop the not useful approaches. This study will also permit to address the dependence between the tests results and many other parameters such as the number of tests, the quality of the clinical specimens and patients characteristics. This will be particularly useful for results interpretation, in particular negative results. Finally, this study is based on a large amount of data over a long period, which was made possible by the fact that all the microbial result are in our LIS since 1995. Although, it may not be the case even in high income country labs, comparison of these results with those obtained at other medical centers should be performed with the view of cross-validating the robustness of the present results.

5 Conclusions

This study demonstrates that many improvements have been made in the microbiological diagnosis of tuberculosis. There is no doubt

about the added value of molecular diagnosis compared to microscopy to initiate the diagnosis of tuberculosis. The limit of a generalization of independent algorithms in microscopy lies in the access to molecular diagnosis. New technologies such as the GeneXpert, which are supposed to solve this problem, are not yet generalized. Regarding tuberculosis, the limit in this case is not technological but again, economical. This study provides data for diagnostic stewardship and for editing guidelines and diagnosis protocols with the purpose to reduce the medical, social and economic costs associated with tuberculosis. Indeed, even in low prevalence and high-income country, the infrastructure and trained personnel for the diagnostic of tuberculosis is limited. Therefore, there is a need to identify the most efficient tests and specimens in order to guarantee the sensitivity and specificity and to limit the number of unnecessary tests. In addition, it provides analytical strategies that may also be suitable for the study of other infectious diseases.

Data availability statement

The datasets presented in this article are not readily available because, the data are generated only for the present study. Any re-use would need another ethical authorisation. Requests to access the datasets should be directed to onya.opota@chuv.ch.

Author contributions

OO, KJ, and M-OB contributed to conception and design of the study. RB performed the raw data extraction. RB, M-OB and OO organized the database. JD-L, RN performed part of the statistical analysis under the supervision of M-OB, VC and OO. M-OB and OO performed the statistical analysis. OO and M-OB wrote the first draft of the manuscript. All authors contributed to manuscript revision, read, and approved the submitted version.

Funding

Open access funding provided by University of Lausanne.

Acknowledgments

We are thankful to the Laboratory of Molecular Diagnostic and Mycobacteria of the Institute of Microbiology of the University of Lausanne and Lausanne University Hospital that perform the conventional and molecular analysis for the diagnosis of tuberculosis.

Conflict of interest

The authors declare that the research was conducted in the absence of any commercial or financial relationships that could be construed as a potential conflict of interest.

Publisher's note

Supplementary material

The Supplementary Material for this article can be found online at: https://www.frontiersin.org/articles/10.3389/fcimb.2023.1131241/full#supplementary-material

References

Andenmatten, S., Opota, O., Mazza-Stalder, J., Nicod, L., Greub, G., and Jaton, K. (2019). Added diagnostic value of 16s rrna gene pan-mycobacterial pcr for nontuberculous mycobacterial infections: A 10-year retrospective study. *Eur. J. Clin. Microbiol. Infect. Dis.* 38(10):1873-1881. doi: 10.1007/s10096-019-03621-z

Armstrong, D. T., Tacheny, E. A., Olinger, G., Howard, R., Lemmon, M. M., Dasgupta, D., et al. (2021). Sars-cov-2 supply shortages and tuberculosis diagnostics: Current issues requiring immediate solutions. *J. Clin. Microbiol.* 59, e0077821. doi: 10.1128/JCM.00778-21

Biswas, S., Das, A., Sinha, A., Das, S. K., and Bairagya, T. D. (2013). The role of induced sputum in the diagnosis of pulmonary tuberculosis. *Lung India: Off. Organ Indian Chest Soc.* 30, 199–202. doi: 10.4103/0970-2113.116259

Boehme, C. C., Nabeta, P., Hillemann, D., Nicol, M. P., Shenai, S., Krapp, F., et al. (2010). Rapid molecular detection of tuberculosis and rifampin resistance. *N. Engl. J. Med.* 363, 1005–1015. doi: 10.1056/NEJMoa0907847

Cadena, A. M., Fortune, S. M., and Flynn, J. L. (2017). Heterogeneity in tuberculosis. *Nat. Rev. Immunol.* 17, 691–702. doi: 10.1038/nri.2017.69

Campelo, T. A., Cardoso de Sousa, P. R., Nogueira, L. L., Frota, C. C., and Zuquim Antas, P. R. (2021). Revisiting the methods for detecting mycobacterium tuberculosis: What has the new millennium brought thus far? *Access Microbiol.* 3, 000245. doi: 10.1099/acmi.0.000245

Cannas, A., Paglia, M. G., Sakhoo, D. C., Vairo, F., Doulla, B., Nguhuni, B., et al. (2013). Strengthening tuberculosis diagnosis in a low-resource setting: Experience learned in dodoma, tanzania. *J. Infect. Dev. Ctries* 7, 676–679. doi: 10.3855/jidc.3366

Chakravorty, S., Simmons, A. M., Rowneki, M., Parmar, H., Cao, Y., Ryan, J., et al. (2017). The new xpert mtb/rif ultra: Improving detection of mycobacterium tuberculosis and resistance to rifampin in an assay suitable for point-of-care testing. *MBio* 8 (4), e00812-17. doi: 10.1128/mBio.00812-17

Dorman, S. E., Schumacher, S. G., Alland, D., Nabeta, P., Armstrong, D. T., King, B., et al. (2018). Xpert mtb/rif ultra for detection of mycobacterium tuberculosis and rifampicin resistance: A prospective multicentre diagnostic accuracy study. *Lancet Infect. Dis.* 18, 76–84. doi: 10.1016/S1473-3099(17)30691-6

Dowdy, D. W., Houben, R., Cohen, T., Pai, M., Cobelens, F., Vassall, A., et al. (2014). Impact and cost-effectiveness of current and future tuberculosis diagnostics: The contribution of modelling. *Int. J. Tuberculosis Lung Dis.* 18, 1012–1018. doi: 10.5588/ijtld.13.0851

Greub, G., Sahli, R., Brouillet, R., and Jaton, K. (2016). Ten years of r&d and full automation in molecular diagnosis. *Future Microbiol.* 11, 403–425. doi: 10.2217/fmb.15.152

Imbert, S., Meyer, I., Palous, M., Brossas, J.-Y., Uzunov, M., Touafek, F., et al. (2018). Aspergillus pcr in bronchoalveolar lavage fluid for the diagnosis and prognosis of aspergillosis in patients with hematological and non-hematological conditions. *Front. Microbiol.* 9, 1877. doi: 10.3389/fmicb.2018.01877

Lippincott, C. K., Miller, M. B., Popowitch, E. B., Hanrahan, C. F., and Van Rie, A. (2014). Xpert mtb/rif assay shortens airborne isolation for hospitalized patients with presumptive tuberculosis in the united states. *Clin. Infect. Dis.* 59, 186–192. doi: 10.1093/cid/ciu212

Maitre, T., Ok, V., Morel, F., Bonnet, I., Sougakoff, W., Robert, J., et al. (2021). Sampling strategy for bacteriological diagnosis of intrathoracic tuberculosis. *Respir. Med. Res.* 79, 100825. doi: 10.1016/j.resmer.2021.100825

Mechai, F., Cordel, H., Guglielmetti, L., Aubry, A., Jankovic, M., Viveiros, M., et al. (2020). Management of tuberculosis: Are the practices homogeneous in high-income countries? *Front. Public Health* 8, 443. doi: 10.3389/fpubh.2020.00443

Meneguim, A. C., Rebello, L., Das, M., Ravi, S., Mathur, T., Mankar, S., et al. (2020). Adapting tb services during the covid-19 pandemic in mumbai, india. *Int. J. Tuberc. Lung Dis.* 24, 1119–1121. doi: 10.5588/ijtld.20.0537

Neofytos, D., Garcia-Vidal, C., Lamoth, F., Lichtenstern, C., Perrella, A., and Vehreschild, J. J. (2021). Invasive aspergillosis in solid organ transplant patients: Diagnosis, prophylaxis, treatment, and assessment of response. *BMC Infect. Dis.* 21, 296. doi: 10.1186/s12879-021-05958-3

Opota, O., Mazza-Stalder, J., Greub, G., and Jaton, K. (2019a). The rapid molecular test xpert mtb/rif ultra: Towards improved tuberculosis diagnosis and rifampicin resistance detection. *Clin. Microbiol. Infect.* 25, 1370–1376. doi: 10.1016/j.cmi.2019.03.021

Opota, O., Senn, L., Prod'hom, G., Mazza-Stalder, J., Tissot, F., Greub, G., et al. (2016). Added value of molecular assay xpert mtb/rif compared to sputum smear microscopy to assess the risk of tuberculosis transmission in a low-prevalence country. *Clin. Microbiol. Infect.* 22, 613–619. doi: 10.1016/j.cmi.2016.04.010

Opota, O., Zakham, F., Mazza-Stalder, J., Nicod, L., Greub, G., and Jaton, K. (2019b). Added value of xpert mtb/rif ultra for diagnosis of pulmonary tuberculosis in a low-prevalence setting. *J. Clin. Microbiol.* 57. doi: 10.1128/JCM.01717-18

Palomino, J. C. (2005). Nonconventional and new methods in the diagnosis of tuberculosis: Feasibility and applicability in the field. *Eur. Respir. J.* 26, 339. doi: 10.1183/09031936.05.00050305

Perret, T., Kritikos, A., Hauser, P. M., Guiver, M., Coste, A. T., Jaton, K., et al. (2020). Ability of quantitative pcr to discriminate pneumocystis jirovecii pneumonia from colonization. *J. Med. Microbiol.* 69, 705–711. doi: 10.1099/jmm.0.001190

Pfyffer, G. E., and Wittwer, F. (2012). Incubation time of mycobacterial cultures: How long is long enough to issue a final negative report to the clinician? *J. Clin. Microbiol.* 50, 4188–4189. doi: 10.1128/JCM.02283-12

Sanjeevaiah, S., Haranal, M. Y., and Buggi, S. (2018). Role of flexible bronchoscopy in patients with sputum-negative pulmonary tuberculosis. *Indian J. Thorac. Cardiovasc. Surg.* 34, 365–369. doi: 10.1007/s12055-018-0645-z

Schaaf, H. S., and Reuter, H. (2009). "Chapter 22 - practical approaches to ordering diagnostic tests," in *Tuberculosis*. Eds. H. S. Schaaf, A. I. Zumla, J. M. Grange, et al (Edinburgh: W.B. Saunders) 216–226.

Seong, G. M., Lee, J., Lee, J. H., Kim, J. H., and Kim, M. (2014). Usefulness of sputum induction with hypertonic saline in a real clinical practice for bacteriological yields of active pulmonary tuberculosis. *Tuberculosis Respir. Dis.* 76, 163–168. doi: 10.4046/trd.2014.76.4.163

van Zyl-Smit, R. N., Binder, A., Meldau, R., Mishra, H., Semple, P. L., Theron, G., et al. (2011). Comparison of quantitative techniques including xpert mtb/rif to evaluate mycobacterial burden. *PLoS One* 6, e28815. doi: 10.1371/journal.pone.0028815

Weiszhar, Z., and Horvath, I. (2013). Induced sputum analysis: Step by step. *Breathe* 9, 300. doi: 10.1183/20734735.042912

WHO (2021a). Global tuberculosis report 2021. Geneva: World Health Organization; 2021. Licence: CC BY-NC-SA 3.0 IGO.

WHO (2021b). WHO consolidated guidelines on tuberculosis. Module 2: screening – systematic screening for tuberculosis disease. Geneva: World Health Organization; 2021. Licence: CC BY-NC-SA 3.0 IGO.

WHO (2021c). WHO consolidated guidelines on tuberculosis. *Module 2: screening – systematic screening for tuberculosis disease* Geneva: World Health Organization; 2021. Licence: CC BY-NC-SA 3.0 IGO.

frontiers | Frontiers in Cellular and Infection Microbiology

TYPE Original Research
PUBLISHED 02 March 2023
DOI 10.3389/fcimb.2023.1082347

OPEN ACCESS

EDITED BY
Christoph Gabler,
Freie Universität Berlin, Germany

REVIEWED BY
Eman A. Gouda M. Youssef,
Lundquist Institute for Biomedical Innovation, United States
Raquel Sabino,
National Institute of Health Dr Ricardo Jorge, Portugal

*CORRESPONDENCE
Yong Jiang
implasmacell@scu.edu.cn

SPECIALTY SECTION
This article was submitted to Clinical Microbiology, a section of the journal Frontiers in Cellular and Infection Microbiology

RECEIVED 28 October 2022
ACCEPTED 17 February 2023
PUBLISHED 02 March 2023

CITATION
Jiang X, Jiang Y and Ye F (2023) Detection and identification of *Mucorales* and *Aspergillus* in paraffin-embedded samples by real-time quantitative PCR. *Front. Cell. Infect. Microbiol.* 13:1082347. doi: 10.3389/fcimb.2023.1082347

Detection and identification of *Mucorales* and *Aspergillus* in paraffin-embedded samples by real-time quantitative PCR

Xiaolin Jiang[1,2], Yong Jiang[1*] and Feng Ye[1]

[1]Department of Pathology, West China Hospital of Sichuan University, Chengdu, China, [2]Department of Pathology, Guangyuan Central Hospital, Guangyuan, China

Background: In this study, we used real-time quantitative PCR (RQ-PCR) to rapidly detect *Mucorales* and *Aspergillus* in formalin-fixed, paraffin-embedded (FFPE) samples, targeting 18SrRNA gene and 28SrRNA gene. Identification of *Mucorales* and *Aspergillus* was analysed by combining *Mucorales* RQ-PCR (*Mucorales*18SrRNA and *Mucorales*28SrRNA) with *Aspergillus* RQ-PCR (*Aspergillus*18SrRNA and *Aspergillus*28SrRNA).

Objectives: The aims of this study were to compare the diagnostic performances of four RQ-PCR assays as single and combined diagnostic and identification tools.

Methods: We collected 12 control group samples and 81 experimental group samples diagnosed by histopathology, including mucormycosis (19 patients, 21 FFPE samples), aspergillosis (54 patients, 57 FFPE samples) and mucormycosis with aspergillosis (3 patients, 3 FFPE samples). All samples were detected by four RQ-PCR tests to compare and analyze diagnostic performance.

Results: The sensitivities of *Mucorales*18SrRNA and *Mucorales*28SrRNA were both 75%, with the tests having specificities of 97.10% and 94.20%. The sensitivities of *Aspergillus*18SrRNA and *Aspergillus*28SrRNA were 73.33% and 65%, with the tests having specificities of 87.88% and 81.82%. The values of the evaluation indexes of the combined detection of *Mucorales*28SrRNA and *Aspergillus*18SrRNA (M28A18) were the highest with a kappa coefficient value of 0.353, followed by M18A18. M28A18 had a sensitivity of 67.90% and a specificity of 100%.

Conclusions: We recommend using the combination of *Mucorales* RQ-PCR and *Aspergillus* RQ-PCR as a screening tool to detect samples suspected of mucormycosis and/or aspergillosis.

KEYWORDS

***mucorales*, *aspergillus*, FFPE, RQ-PCR, 18SrRNA gene, 28SrRNA gene**

Introduction

Over the past few decades, the incidence of invasive mold disease (IMD) has increased significantly and the fungal spectrum of IMD has broadened. According to literature, over 100,000 IMD cases occur each year, and these are associated with high morbidity and mortality in immunocompromised patients who have hematological malignancy and transplantation (Ruiz-Camps and Jarque, 2014; Ruhnke et al., 2015; Pegorie et al., 2017; Springer et al., 2018).

The members of the order *Mucorales* and genus *Aspergillus* are the most common opportunistic pathogens of IMD (Oren and Paul, 2014). Because of the significantly different antifungal susceptibilities and the complexity of the population of patients at risk, management of patients with IMD which lacks typical clinical manifestations has become increasingly complex. Therefore, early and reliable diagnostic methods are necessary for effective treatment.

Currently, the gold standard for the diagnosis of invasive fungal infections depends on histopathology and culture. However, culture is time-consuming and may fail if the potential microbial causes are not considered during sample collection, so formalin-fixed, paraffin-embedded (FFPE) bioptic material is collected for subsequent histological diagnosis. FFPE tissues obtained from patients with proven IMDs are frequently used to detect the etiology of invasive mycoses (Tarrand et al., 2003; Munoz-Cadavid et al., 2010; Babouee Flury et al., 2014). While histopathology can prove invasive fungal infections, the analytical correctness of histological findings is no more than 79% (Sangoi et al., 2009). Therefore, preliminary histological results should be interpreted cautiously (Guarner and Brandt, 2011) and supported by the culture whenever possible. In addition, histopathological observations of fungal shape and arrangement may not be sufficient for accurate identification of the *Mucorales* and *Aspergillus* if only a limited quantity of fungal hyphae is present.

In recent years, considerable efforts have been made to develop more sensitive and specific tools and protocols for IMD diagnosis. It is reported that PCR-based techniques, including conventional, semi-nested and real-time PCR, can be used to identify fungal agents in FFPE tissue (Bialek et al., 2005; Rickerts et al., 2006; Walsh et al., 2011; Springer et al., 2016a). RQ-PCR is very suitable for detecting the DNA of FFPE samples which are easily degraded. There are reports using the 18SrRNA gene and the 28SrRNA gene regions to detect and distinguish mucormycosis and invasive aspergillosis (Bialek et al., 2005; Walsh et al., 2011; Springer et al., 2016a; Gade et al., 2017).

The objective of this study was to evaluate RQ-PCR protocols by the use of TaqMan technology for detection and identification of *Mucorales* and *Aspergillus* in FFPE samples, targeting the 18SrRNA gene and the 28SrRNA gene. Identification of *Mucorales* and *Aspergillus* was analyzed by the combination of *Mucorales* RQ-PCR (*Mucorales*18SrRNA and *Mucorales*28SrRNA) and *Aspergillus* RQ-PCR (*Aspergillus*18SrRNA and *Aspergillus*28SrRNA).

Materials and methods

Samples

Ethical approval was obtained from the West China Hospital Ethics Committee of Sichuan University. According to local ethics, we have applied for exemption from written informed consent. We collected 81 experimental group samples (from 76 patients) in the Department of Pathology of West China Hospital from January 2015 to January 2018 with positive histopathology results, including mucormycosis (19 patients, 21 FFPE samples), aspergillosis (54 patients, 57 FFPE samples) and mucormycosis with aspergillosis (3 patients, 3 FFPE samples).

In addition, 12 FFPE tissue specimens from patients were used as controls including 6 without IMDs and 6 with other fungal infections. All of the slides including hematoxylin-eosin (H&E), periodic acid-Schiff (PAS) and/or Gomori-methenamine-silver (GMS) from each patient were reviewed and confirmed according to European Organization for Research on Treatment of Cancer and the Mycoses Study Group (EORTC/MSG) (De Pauw et al., 2008) by two professional and experienced pathologists with consistent diagnosis independently and in duplicate.

Isolates of laboratory strains included *Aspergillus flavus*, *Aspergillus fumigatus*, *Rhizomucor miehei*, *Candida albicans*, *Cryptococcus neoformans*, and *Fusarium oxysporum*. All isolated strains were provided by the Clinical Microbiology Laboratory, West China Hospital of Sichuan University.

DNA extraction

Four FFPE tissue sections with 4-to-5-um from each specimen were used for DNA extraction. Each section was cut at a different position of the disposable knife of the microtome to prevent DNA cross-contamination due to attached cells at that position of the knife from one section to the next. If the sample surface was exposed to air, discard the first 2–3 sections. For deparaffinization, the sections were put into 1.5 mL tubes. 1 ml of xylene was added, centrifuged at full speed for 2 minutes at room temperature and discarded the supernatant by pipetting. Then, 1 ml ethanol was added, centrifuged and discarded like xylene. After incubation of the tissue at 37°C to evaporate the remains of the ethanol, DNA extraction was performed according to the manufacturer's instructions for the QIAamp DNA FFPE tissue kit (Qiagen, Germany) with the following modifications. All FFPE tissue samples were incubated over night in proteinase K and ATL buffer at 56°C. Fungal cell walls were lysed by *Arthrobacter luteus* lyticase L2524 (Sigma, USA) for 45minutes at 37°C. The DNA was eluted with 100 µl Buffer ATE and stored at -20°C.

DNA extraction of laboratory strains was performed according to the manufacturer's instructions for the QIAamp DNA Mini kit (Qiagen, Germany) with the following modifications. Fungal cell

walls were lysed by *Arthrobacter luteus* lyticase L2524 (Sigma, USA) for 30 minutes at 30°C, incubated 1 to 3 hours in proteinase K and ATL buffer at 56°C. The DNA was stored at -20°C.

Real-time PCR assays

Mucorales RQ-PCR primers and probes targeting the 18SrRNA gene and the 28SrRNA gene were described by Springer et al. (Springer et al. 2016a). *Aspergillus* RQ-PCR primers and probes targeting the 18SrRNA gene were described by Walsh et al. (Walsh et al., 2011). The protocols of RQ-PCR amplifications were performed as described previously (Walsh et al., 2011; Springer et al. 2016a) with the exception of the design of a new primer pair. For optimal design of new primers and probes, multiple sequence alignments of *Aspergillus* 28SrRNA gene (National Center for Biotechnology Information [NCBI] public genetic database [GenBank]) were created using Geneious software (Biomatters, Auckland, New Zealand). Primer Express 3.0 (Applied Biosystems, Foster City, CA) was used to help select primers and probes of optimal melting temperatures (Table 1). The primers and probes of *Aspergillus* 28SrRNA were verified for its specificity by six laboratory isolated strains and normal human DNA, which thermocycling protocol are the same as *Aspergillus* 18SrRNA. The locations of real-time PCR assay targets are shown in Figure 1.

We test all samples in triplicate. Amplification had to be reproducible, occurring in all 3 replicate wells, for a sample to be considered RQ-PCR positive. The positivity cutoff of *Mucorales*18SrRNA and *Mucorales*28SrRNA was defined as both wells having Cq values of <36. The positivity cutoff of *Aspergillus*18SrRNA and *Aspergillus*28SrRNA was defined as both wells having Cq values of <35 and <33, respectively. To validate the presence of amplifiable DNA and absence of inhibitory substances, a PCR in FFPE samples was performed using the primer set G1 and G2 targeting the human β globin gene (Bialek et al., 2005). When the result was negative, DNA extraction was repeated if enough material was available. All primers and probes were synthesized in Sangon Biotech (Sangon, Shanghai, China).

For all assays, RQ-PCR amplifications were performed in a 25 ul mixture using a StepOnePlus thermocycler (Applied Biosystems). Each reaction mixture contained 12.5 ul TaqMan Universal PCR Master Mix (Applied Biosystems), 900 nM forward and reverse primer, 200 nM probe and 5 ul extracted DNA. The DNA extracted from *Rhizomucor miehei* and *Aspergillus flavus* were serially diluted and tested for each RQ-PCR assay to determine the limit of detection (LoD). In each run, negative (FFPE tissue specimen without IMD) and positive (isolated strains of *Rhizomucor miehei and Aspergillus flavus*) controls were included.

Identification of *Mucorales* and *Aspergillus* was analyzed by *Mucorales* RQ-PCR in combination with *Aspergillus* RQ-PCR, including *Mucorales*18SrRNA and *Aspergillus*18SrRNA (M18A18), *Mucorales*18SrRNA and *Aspergillus*28SrRNA (M18A28), *Mucorales*28SrRNA and *Aspergillus*18SrRNA (M28A18), and *Mucorales*28SrRNA and *Aspergillus*28SrRNA (M28A28). True positives of *Mucorales* RQ-PCR in combination with *Aspergillus* RQ-PCR were defined as cases proven according to the following criteria: for mucormycosis samples, *Mucorales* RQ-PCR positivity and *Aspergillus* RQ-PCR negativity; for mucormycosis with aspergillosis samples, both positivity; for aspergillosis samples, *Aspergillus* RQ-PCR positivity and *Mucorales* RQ-PCR negativity. Other results were regarded as negatives.

Statistical analysis

All samples, including 81 experimental group samples and 12 control group samples, were detected by four RQ-PCR tests to compare and analyze the diagnostic performance, including

TABLE 1 Primers and probes.

Assay	Primer or probe	Primer sequence (5′-3′)
***Mucorales*18SrRNA**	Forward primer	TTACCRTGAGCAAATCAGARTG
	Reverse primer	AATCYAAGAATTTCACCTCTAGCG
	Probe	TYRR(G)G(G)B(A)T(T)T(G)T(A)TTT
***Mucorales*28SrRNA**	Forward primer	TTTGGGAATGCAGCCT
	Reverse primer	TCARAGTTCTTTTCAWCTTTCCCT
	Probe	CGARARACCGATAGCRAACAAGTACCGT
***Aspergillus*18SrRNA**	Forward primer	GTGGAGTGATTTGTCTGCTTAATTG
	Reverse primer	TCTAAGGGCATCACAGACCTGTT
	Probe	CGGCCCTTAAATAGCCCGGTCCG
***Aspergillus*28SrRNA**	Forward primer	CACTAGCCGGGCAACCG
	Reverse primer	GACAGTCAGATTCCCCTTGTC C
	Probe	GCGGGCGCTTAACGACCAACTTAG

Parentheses indicate nucleotide with locked nucleic acid modification.
Nucleotides in upper case are wobble nucleotides: R stands for a or g; W for a or t; Y for c or t; B for g, c or t.
Both probes are FAM-labelled at the 5' end and BHQ1 at the 3' end.

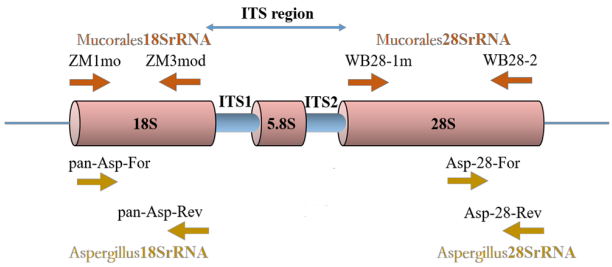

FIGURE 1
Locations of four real-time PCR assays target. An rDNA single repeat is shown. The primers ZM1mo and ZM3mod of *Mucorales*18SrRNA assay target 18SrRNA gene region. The primers WB28-1m and WB28-2 of *Mucorales*28SrRNA assay target 28SrRNA gene region. The primers pan-Asp-For and pan-Asp-Rev of *Aspergillus*18SrRNA assay target 18SrRNA gene region. The primers Asp-28-For and Asp-28-Rev of *Aspergillus*28SrRNA assay target 28SrRNA gene region.

negative predictive value (NPV), positive predictive value (PPV), sensitivity and specificity with likelihood ratios (LRs), and 95% confidence intervals (CIs) were calculated for NPV, PPV, sensitivity, and specificity. Cohen's kappa coefficient was calculated to measure the agreement between any two assays. Statistical analysis was performed using SPSS, version 20 (SPSS, Chicago, IL, USA).

Results

The study involved 76 patients (F/M, 42/34; age, 50.95 ± 17.31 years) with following comorbidities: 23 (30.26%) had diabetes, 16 (21.05%) had hypertension, 10 (13.16%) had bronchiectasis, 8 (10.53%) had solid tumor, 7 (9.21%) had Chronic obstructive pulmonary disease (COPD), 5 (6.58%) had hematological malignancy, 5 (6.58%) had tuberculosis, and 16 (21.05%) had others. Slides stained with PAS or GMS were considered, respectively, positive if magenta or brown-black fungal hyphae with morphological features were observed (Figure 2). Positive special staining with GMS and/or PAS were 24/29 (82.76%). Positive culture cases were 12/52 (23.08%). Positive 1, 3-beta-D-glucan assay cases were 9/40 (22.50%). Positive Galactomannan assay cases were 12/42 (28.57%). The principal site of infections was in lungs (61 cases), next were in other sites (including one ileum, three nasal cavity, four maxillary sinus, two trachea, one external auditory canal, one toe and three main bronchus). CT of the chest was obtained in 61 patients with pulmonary infection. There was a wide spectrum of radiological findings, with the most common being 26 nodules, followed by 20 mass, 16 cavitation, 7 consolidation, 5 pleural effusion, and 3 air crescent sign. Result of bronchofibroscopy were obtained in 56/61 patients with pulmonary infection: 18 patients were normal, and other patients were mainly necrosis, luminal stenosis, and purulent secretion.

Individual test performance

The LOD of *Mucorales*18SrRNA and *Mucorales*28SrRNA was 10^{-1}copies/ul in *Rhizomucor miehei* DNA. In *Aspergillus*RQ-PCR assays, the LOD between *Aspergillus* 18SrRNA and *Aspergillus*28SrRNA was different (10^{0}copies/ul vs. 10^{1}copies/ul) for *Aspergillus flavus* DNA. The analytical specificity of *Aspergillus*28SrRNA assays was tested by adding genomic DNA from the six isolated strains. No cross-reactivity with non-*Mucorales* species or human DNA was observed. The specificity of

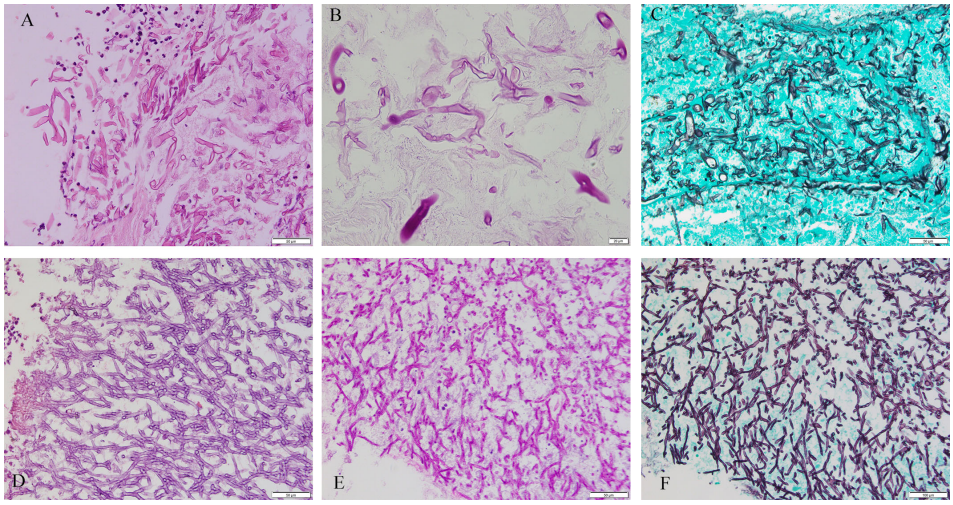

FIGURE 2
Mucorales and *Aspergillus*. Cytomorphology of *Mucorales* and *Aspergillus* in FFPE samples processed using the HE staining, PAS staining and GMS staining. The mycelium appeared magenta after PAS staining and brown-black after GMS staining. Magnification, 400×. **(A)** *Mucorales* with HE; **(B)** *Mucorales* with PAS; **(C)** *Mucorales* by GMS; **(D)** *Aspergillus* with HE; **(E)** *Aspergillus* with PAS; **(F)** *Aspergillus* with GMS. Lack of images of tissues with both *Aspergillus* and *Mucorales* infection.

*Mucorales*18SrRNA, *Mucorales*28SrRNA and *Aspergillus*18SrRNA have been tested in the previous articles (Walsh et al., 2011; Springer et al., 2016a).

Ninety-three different samples from 88 patients were analysed by the four different real-time PCR assays (Figure 3; Table 2). All control group samples were negative using the four different RQ-PCR assays. Thirteen experimental group samples were negative in all RQ-PCR assays.

The *Mucorales*18SrRNA assay was positive in 17 of 21 mucormycosis samples (80.95%), 1 of 3 mucormycosis with aspergillosis samples (33.33%), and 2 of 57 aspergillosis samples (3.51%). The *Mucorales*28SrRNA assay behaved similarly, detecting 16 out of 21 mucormycosis samples (76.19%), 2 out of 3 mucormycosis with aspergillosis samples (66.67%), and 4 out of 57 aspergillosis samples (7.02%). Only two samples were negative by two different *Mucorales* RQ-PCR despite positive histology showed fungal hyphae (F7 and F11). The *Aspergillus*18SrRNA assay was positive in 41 of 57 aspergillosis samples (71.93%), 3 of 3 mucormycosis with aspergillosis samples (100%), and 4 of 21 mucormycosis samples (19.05%). The *Aspergillus*28SrRNA assay behaved similarly, detecting 37 out of 57 aspergillosis samples (64.91%), 2 out of 3 mucormycosis with aspergillosis samples

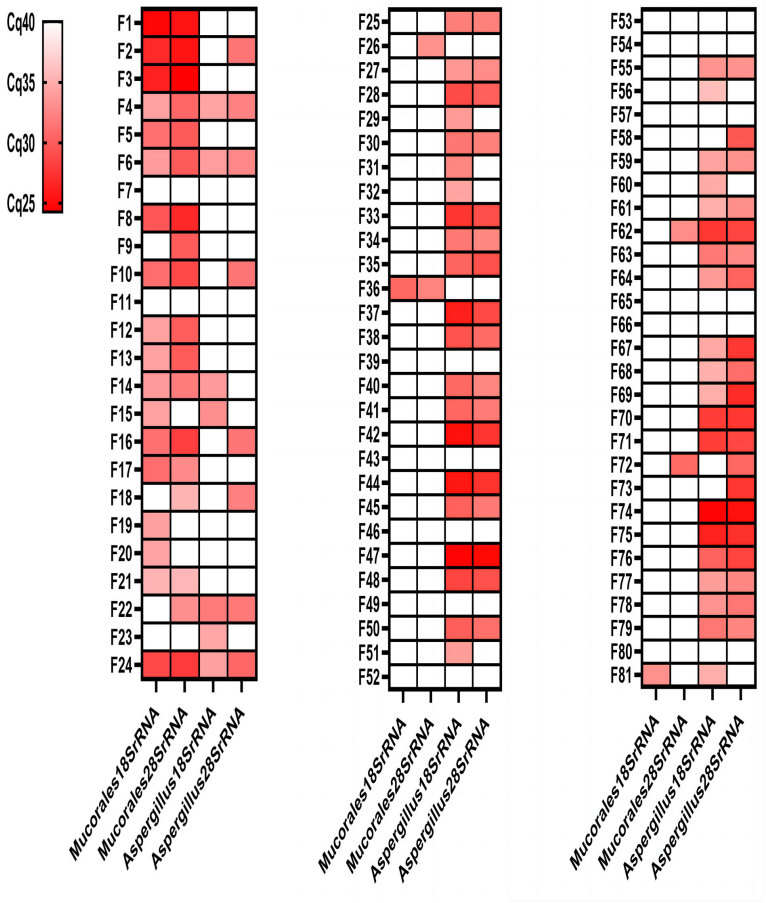

FIGURE 3
Genetic test results of the four RQ-PCR assays for 81 experimental group samples. Mucormycosis samples (F1-F21); Mucormycosis with Aspergillosis samples (F22-F24); Aspergillosis samples (F25-F81). Red: positive; White: negative.

TABLE 2 Four RQ-PCR testing results.

Samples (n)	*Mucorales*18SrRNA (%)	*Mucorales*28SrRNA (%)	*Aspergillus*18SrRNA (%)	*Aspergillus*28SrRNA (%)
mucormycosis samples (n=21)	17/21(80.95)	16/21(76.19)	4/21(19.05)	6/21(28.57)
mucormycosis with aspergillosis samples (n=3)	1/3(33.33)	2/3(66.67)	3/3(100)	2/3(66.67)
aspergillosis samples (n=57)	2/57(3.51)	4/57(7.02)	41/57(71.93)	37/57(64.91)
control group samples (n=12)	0/12	0/12	0/12	0/12

(66.67%), and 6 out of 21 mucormycosis samples (28.57%). 12 control samples were negative in each assay. A concomitant infection was diagnosed in three samples by histopathology but verified by *Mucorales* RQ-PCR and *Aspergillus* RQ-PCR in two (F22 and F24). There were some "abnormal results" in our study, e.g., 2 of aspergillosis samples were positive by *Mucorales*18SrRNA (F36 and F81); 4 of the aspergillosis samples were positive by *Mucorales*28SrRNA (F26, F36, F62 and F72); 4 of mucormycosis samples were positive by *Aspergillus*18SrRNA (F4, F6, F14 and F15); 6 of mucormycosis samples were positive by *Aspergillus*28SrRNA (F2, F4, F6, F10, F16 and F18).

The sensitivity, specificity, PPV, NPV, positive and negative LRs of all four RQ-PCR assays are shown in Table 3. The sensitivities of *Mucorales*18SrRNA and *Mucorales* 28SrRNA were both 75%, with specificity, PPV, NPV, positive LR, and negative LR of *Mucorales*18SrRNA being 97.10%, 90.00%, 91.78%, 25.86, and 0.26, respectively. *Mucorales* 28SrRNA assay showed specificity of 94.20%, PPV of 81.82%, NPV of 91.55%, positive LR of 12.93, and negative LR of 0.27. The sensitivity, specificity, PPV and NPV of *Aspergillus*28SrRNA assays were lower than *Aspergillus*18SrRNA assays, for *Aspergillus*18SrRNA assays: 73.33%, 87.88%, 91.67%, and 64.54%, respectively; for *Aspergillus*28SrRNA assays: 65%, 81.82%, 86.67%, and 56.25%, respectively. The positive LR and negative LR of *Aspergillus*18SrRNA assays and *Aspergillus*28SrRNA assays were 6.05 and 0.30 vs. 3.58 and 0.43.

Combined test performance

The true positive results of M18A18, M18A28, M28A18, and M28A28 were as follows: for mucormycosis samples, 13, 12, 13, and 10, respectively; for mucormycosis with aspergillosis samples, 1, 1, 2, and 2, respectively; for aspergillosis samples, 40, 37, 40, and 35, respectively. All combined tests were negative in control group samples (Table 4).

A pairwise comparison of the tests showed that the highest level of agreement was M28A18, with a kappa coefficient value of 0.353. All other pairs of biomarkers showed less agreement (Table 5). Any combinations of *Mucorales* RQ-PCR assays and *Aspergillus* RQ-PCR assays had the same specificity (100%), PPV (100%), and positive LR (Infinity). The sensitivity, NPV, and negative LR were as follows: for M28A18, 67.90%, 31.58%, and 0.32 respectively; for M18A18, 66.67%, 30.77%, and 0.33, respectively; for M18A28, 61.73%, 27.91%, and 0.38, respectively; for M28A28, 58.02%, 26.09%, and 0.42, respectively. In all the samples, the values of the evaluation indexes of the combined detection of M28A18 were the highest, followed by M18A18.

Discussion

The detection and identification of *Mucorales* and *Aspergillus* from FFPE samples played an important role in the diagnosis and management of aspergillosis and mucormycosis, whereas microscopy, serology, and culture were restricted by several disadvantages (Jensen et al., 1997; Frater et al., 2001; Rickerts et al., 2007; Hofman et al., 2010; Hamilos et al., 2011). Numerous RQ-PCR assays have been described for detection of *Mucorales* (Bernal-Martinez et al., 2013; Millon et al., 2013; Lengerova et al., 2014) and *Aspergillus* (Lass-Florl et al., 2011; Fricke et al., 2012; Paholcsek et al., 2014; Pini et al., 2015). In this study, we evaluated two *Mucorales* RQ-PCR assays, two *Aspergillus* RQ-PCR assays, and four combined tests to rapidly detect and identify *Mucorales* and *Aspergillus*.

More recently, the RQ-PCR of *Mucorales* from 268 serum samples and 12 FFPE samples was a promising test method with sensitivity of 91% targeting 18SrRNA gene (Springer et al., 2016b) and 86% targeting 28SrRNA gene (Springer et al., 2016a). In this study, two *Mucorales* RQ-PCR only had a sensitivity of 75%. The lower sensitivity may be relevant to small sample size and different sample types. The RQ-PCR detecting *Mucorales* also had a specificity of 100% in FFPE samples but a lower sensitivity of 56% by Hata et al. (Hata et al., 2008). The specificity of our two *Mucorales* RQ-PCR assays was 97.1% and 94.20%, respectively. As reported in the literature, the RQ-PCR specificity was 87.5% (Springer et al., 2016a). In *Mucorales* RQ-PCR assays, the diagnostic parameters and LoD values for the different assays indicated that *Mucorales*18SrRNA would provide the best diagnostic accuracy. These results support the findings of Springer et al. (Springer et al., 2016a; Springer et al., 2016b).

In our study, the specificity and sensitivity of *Aspergillus*18S rRNA were 87.88% and 73.33%, respectively, which is consistent

TABLE 3 Diagnostic performance of four RQ-PCR.

Assays	Sensitivity (%)	Specificity (%)	PPV (%)	NPV (%)	Positive LR	Negative LR
***Mucorales*18SrRNA**	75.00 (52.95, 89.40)	97.10 (88.99, 99.47)	90.00 (66.87, 98.24)	91.78 (82.35, 96.61)	25.86	0.26
***Mucorales*28SrRNA**	75.00 (52.95, 89.40)	94.20 (85.07, 98.13)	81.82 (58.99, 94.01)	91.55 (81.89, 96.52)	12.93	0.27
***Aspergillus*18SrRNA**	73.33 (60.11, 83.55)	87.88 (70.86, 96.04)	91.67 (79.13, 97.30)	64.45 (48.73, 77.71)	6.05	0.30
***Aspergillus*28SrRNA**	65.00 (51.52, 76.55)	81.82 (63.92, 92.38)	86.67 (72.51, 94.46)	56.25 (41.28, 70.23)	3.58	0.43

The sensitivities, specificities, positive predictive values, negative predictive values, likelihood ratios, and diagnostic odds ratios are displayed, with 95% confidence intervals being given in parentheses.

TABLE 4 The true positive results of *Mucorales* RQ-PCR in combination with *Aspergillus* RQ-PCR.

	mucormycosis samples (n=21)	mucormycosis with aspergillosis samples (n=3)	aspergillosis samples (n=57)	control group samples (n=12)	Total
M18A18	13	1	40	0	54
M18A28	12	1	37	0	50
M28A18	13	2	40	0	55
M28A28	10	2	35	0	47

with the results of previously published studies (Hadrich et al., 2011; Luong et al., 2011). The MycAssay™ *Aspergillus* real-time PCR kit was tested on tissues by the manufacturer with 15 different *Aspergillus* spp., including multiple strains of *Aspergillus fumigatus*, *Aspergillus niger*, *Aspergillus terreus*, and *Aspergillus nidulans*, having a sensitivity of 82% and a specificity of 79% (Lass-Florl et al., 2011). In our study, the specificity of two *Aspergillus* RQ-PCR assays was elevated, whereas sensitivity was reduced.

However, some limitations and several considerations indicate that it has some drawbacks in the *Mucorales* RQ-PCR or *Aspergillus* RQ-PCR alone. Our studies have evaluated the utility of detection of *Mucorales* RQ-PCR and *Aspergillus* RQ-PCR. Our finding, combining the results of these two tests gave optimal specificity and PPV, could be used to detect and identify *Mucorales* and *Aspergillus* and may provide a solution when gold standard tests were conflicting. Given the ubiquity of *Aspergillus* and *Mucorales* in the environment, combining *Mucorales* RQ-PCR with *Aspergillus* RQ-PCR would give clinicians greater confidence in detecting and identifying them at the same time and reduce the false positive and/or negative rate. The best combination was the M28A18, with a sensitivity of 67.90%, a specificity of 100%, which had the highest diagnostic potential with FFPE samples. This is inconsistent with the conclusion that *Mucorales*18SrRNA is better than *Mucorales*28SrRNA in diagnostic significance, which may be related to the small sample size. In all samples, the number of true positives of M18A18 was very similar to M28A18 (54 VS. 55). Their diagnostic significance needs to be further evaluated in future studies with larger sample sizes.

This study has several limitations, which may be the cause of some "abnormal results". First, the sample size is too small, especially that the mucormycosis sample is only 21 cases from 19 patients. Due to the limited number of FFPE samples and strains, the very low number of *Aspergillus* and *Mucorales* species was tested, the number of *Aspergillus* and *Mucorales* species that can be detected by these primers needs to be further evaluated. Second, RQ-PCR assays require strictly positive and negative controls. The limitations of false positive and false negative errors due to amplification and contamination for assessing the value of a molecular diagnostic test have been eloquently highlighted (Mies, 1994; Cataloluk et al., 2003). In some samples, fluorescence signals higher than the positive Cq cutoff was detected, which may be caused by false negatives due to the low number of fungal hyphae. Third, the use of mold-active drugs may affect detection result. There are conflicting reports about the effect of antifungal therapy on the performance of tests. Antifungal therapy has been reported to both decrease (Reinwald et al., 2012) and increase (Musher et al., 2004) the diagnostic performance of RQ-PCR. Furthermore, "abnormal results" may be caused by a condition other than Mucormycosis and Aspergillosis or by drug treatment. Fourthly, Formalin fixed and paraffin wax embedded tissues can cause DNA degradation, only short sequences can be amplified from this type of tissue (Bonin et al., 2003). Although the amplified sequences of the four RQ-PCRs in this study were less than 200bp, which weakened the influence of DNA fragmentation, it may still reduce the sensitivity. Fifth, due to funding reasons, we did not use commercialized kits for the detection of *Mucorales* and *Aspergillus* DNA in clinical samples. Finally, Misclassification using these inconsistent criteria of RQ-PCR can occur for many reasons, e.g., detection of pathogenic fungi may be missed due to the diversity of fungal species and test samples, and there are multiple laboratorial protocols. Each suffers from different disadvantages

TABLE 5 Diagnostic performance of dual *Mucorales* RQ-PCR and *Aspergillus* RQ-PCR testing.

	Sensitivity (%)	Specificity (%)	PPV (%)	NPV (%)	Positive LR	Negative LR	Kappa
M18A18	66.67 (55.22, 76.52)	100 (69.87, 100)	100 (91.73, 100)	30.77 (17.55, 47.73)	Infinity	0.33	0.340
M18A28	61.73 (50.22, 72.11)	100 (69.87, 100)	100 (91.11, 100)	27.91 (15.38, 43.90)	Infinity	0.38	0.294
M28A18	67.90 (56.49, 77.60)	100 (69.87, 100)	100 (91.87, 100)	31.58 (18.04, 48.79)	Infinity	0.32	0.353
M28A28	58.02 (46.54, 68.74)	100 (69.87, 100)	100 (90.59, 100)	26.09 (14.75, 41.41)	Infinity	0.42	0.263

such as vulnerability to contamination or limited detection of selected species or genera.

In conclusion, this preliminary study showed that the two *Aspergillus* RQ-PCR assays and two *Mucorales* RQ-PCR assays had high potential for the diagnosis of *Mucorales* and *Aspergillus* in FFPE samples. We envisage *Aspergillus* RQ-PCR and *Mucorales* RQ-PCR combination approach as a nearpatient test, allowing an immediate detection and identification of *Mucorales* and *Aspergillus*, with RQ-PCR results being available within a short time for samples of mucormycosis with aspergillosis. This combination approach can provide useful information when a small number of fungi are present, or the histological diagnosis is difficult in mucormycosis with aspergillosis samples. In the future, these assays may be used as a screening tool to detect other types of samples suspected of having mucormycosis and/or aspergillosis, such as serum, bronchoalveolar lavage fluid (BALF), and cytological samples. The results of our study should be validated in multicenter studies to develop tests for this clinical application.

Data availability statement

The raw data supporting the conclusions of this article will be made available by the authors, without undue reservation.

Ethics statement

The studies involving human participants were reviewed and approved by West China Hospital Ethics Committee of Sichuan University. Written informed consent for participation was not required for this study in accordance with the national legislation and the institutional requirements.

Author contributions

YJ and FY and conceived and designed the experiments. XJ analyzed the data and wrote the manuscript. All authors contributed to the article and approved the submitted version.

Funding

This work is supported by Chengdu Science and Technology Program (2019-YF05-00324-SN), West China Hospital of Sichuan University Scientific and Technological Achievements Transformation Fund (CGZH21011) and 1·3·5 project for disciplines of excellence–Clinical Research Incubation Project, West China Hospital, Sichuan University (No. 2020HXFH024).

Conflict of interest

The authors declare that the research was conducted in the absence of any commercial or financial relationships that could be construed as a potential conflict of interest.

Publisher's note

References

Babouee Flury, B., Weisser, M., Prince, S. S., Bubendorf, L., Battegay, M., Frei, R., et al. (2014). Performances of two different panfungal PCRs to detect mould DNA in formalin-fixed paraffin-embedded tissue: What are the limiting factors? *BMC Infect. Dis.* 14, 692. doi: 10.1186/s12879-014-0692-z

Bernal-Martinez, L., Buitrago, M. J., Castelli, M. V., Rodriguez-Tudela, J. L., and Cuenca-Estrella, M. (2013). Development of a single tube multiplex real-time PCR to detect the most clinically relevant mucormycetes species. *Clin. Microbiol. Infect.* 19 (1), E1–E7. doi: 10.1111/j.1469-0691.2012.03976.x

Bialek, R., Konrad, F., Kern, J., Aepinus, C., Cecenas, L., Gonzalez, G. M., et al. (2005). PCR based identification and discrimination of agents of mucormycosis and aspergillosis in paraffin wax embedded tissue. *J. Clin. Pathol.* 58 (11), 1180–1184. doi: 10.1136/jcp.2004.024703

Bonin, S., Petrera, F., Niccolini, B., and Stanta, G. (2003). PCR analysis in archival postmortem tissues. *Mol. Pathol.* 56 (3), 184–186. doi: 10.1136/mp.56.3.184

Cataloluk, O., Cakmak, E. A., Buyukberber, N., and Barlas, O. (2003). Formalin fixing and paraffin embedding may lead to extra band development in PCR. *New microbiologica* 26 (2), 193–198.

De Pauw, B., Walsh, T. J., Donnelly, J. P., Stevens, D. A., Edwards, J. E., Calandra, T., et al. (2008). Revised definitions of invasive fungal disease from the European organization for research and treatment of Cancer/Invasive fungal infections cooperative group and the national institute of allergy and infectious diseases mycoses study group (EORTC/MSG) consensus group. *Clin. Infect. Dis.* 46 (12), 1813–1821. doi: 10.1086/588660

Frater, J. L., Hall, G. S., and Procop, G. W. (2001). Histologic features of zygomycosis: emphasis on perineural invasion and fungal morphology. *Arch. Pathol. Lab. Med.* 125 (3), 375–378. doi: 10.1043/0003-9985(2001)125<0375:HFOZ>2.0.CO;2

Fricke, S., Fricke, C., Oelkrug, C., Blatz, R., Schonfelder, U., Niederwieser, D., et al. (2012). A real-time PCR for the detection and characterisation of aspergillus species. *Mycoses* 55 (5), 416–425. doi: 10.1111/j.1439-0507.2011.02161.x

Gade, L., Hurst, S., Balajee, S. A., Lockhart, S. R., and Litvintseva, A. P. (2017). Detection of mucormycetes and other pathogenic fungi in formalin fixed paraffin embedded and fresh tissues using the extended region of 28S rDNA. *Med. Mycol* 55 (4), 385–395. doi: 10.1093/mmy/myw083

Guarner, J., and Brandt, M. E. (2011). Histopathologic diagnosis of fungal infections in the 21st century. *Clin. Microbiol. Rev.* 24 (2), 247–280. doi: 10.1128/CMR.00053-10

Hadrich, I., Mary, C., Makni, F., Elloumi, M., Dumon, H., Ayadi, A., et al. (2011). Comparison of PCR-ELISA and real-time PCR for invasive aspergillosis diagnosis in patients with hematological malignancies. *Med. Mycol* 49 (5), 489–494. doi: 10.3109/13693786.2010.540724

Hamilos, G., Samonis, G., and Kontoyiannis, D. P. (2011). Pulmonary mucormycosis. *Semin. Respir. Crit. Care Med.* 32 (6), 693–702. doi: 10.1055/s-0031-1295717

Hata, D. J., Buckwalter, S. P., Pritt, B. S., Roberts, G. D., and Wengenack, N. L. (2008). Real-time PCR method for detection of zygomycetes. *J. Clin. Microbiol.* 46 (7), 2353–2358. doi: 10.1128/JCM.02331-07

Hofman, V., Dhouibi, A., Butori, C., Padovani, B., Gari-Toussaint, M., Garcia-Hermoso, D., et al. (2010). Usefulness of molecular biology performed with formaldehyde-fixed paraffin embedded tissue for the diagnosis of combined pulmonary invasive mucormycosis and aspergillosis in an immunocompromised patient. *Diagn. Pathol.* 5, 1. doi: 10.1186/1746-1596-5-1

Jensen, H. E., Salonen, J., and Ekfors, T. O. (1997). The use of immunohistochemistry to improve sensitivity and specificity in the diagnosis of systemic mycoses in patients with haematological malignancies. *J. Pathol.* 181 (1), 100–105. doi: 10.1002/(SICI)1096-9896(199701)181:1<100::AID-PATH100>3.0.CO;2-O

Lass-Florl, C., Follett, S. A., Moody, A., and Denning, D. W. (2011). Detection of aspergillus in lung and other tissue samples using the MycAssay aspergillus real-time PCR kit. *Can. J. Microbiol.* 57 (9), 765–768. doi: 10.1139/w11-064

Lengerova, M., Racil, Z., Hrncirova, K., Kocmanova, I., Volfova, P., Ricna, D., et al. (2014). Rapid detection and identification of mucormycetes in bronchoalveolar lavage samples from immunocompromised patients with pulmonary infiltrates by use of high-resolution melt analysis. *J. Clin. Microbiol.* 52 (8), 2824–2828. doi: 10.1128/JCM.00637-14

Luong, M. L., Clancy, C. J., Vadnerkar, A., Kwak, E. J., Silveira, F. P., Wissel, M. C., et al. (2011). Comparison of an aspergillus real-time polymerase chain reaction assay with galactomannan testing of bronchoalvelolar lavage fluid for the diagnosis of invasive pulmonary aspergillosis in lung transplant recipients. *Clin. Infect. Dis.* 52 (10), 1218–1226. doi: 10.1093/cid/cir185

Mies, C. (1994). Molecular biological analysis of paraffin-embedded tissues. *Hum. Pathol.* 25 (6), 555–560. doi: 10.1016/0046-8177(94)90218-6

Millon, L., Larosa, F., Lepiller, Q., Legrand, F., Rocchi, S., Daguindau, E., et al. (2013). Quantitative polymerase chain reaction detection of circulating DNA in serum for early diagnosis of mucormycosis in immunocompromised patients. *Clin. Infect. Dis.* 56 (10), e95–101. doi: 10.1093/cid/cit094

Munoz-Cadavid, C., Rudd, S., Zaki, S. R., Patel, M., Moser, S. A., Brandt, M. E., et al. (2010). Improving molecular detection of fungal DNA in formalin-fixed paraffin-embedded tissues: comparison of five tissue DNA extraction methods using panfungal PCR. *J. Clin. Microbiol.* 48 (6), 2147–2153. doi: 10.1128/JCM.00459-10

Musher, B., Fredricks, D., Leisenring, W., Balajee, S. A., Smith, C., and Marr, K. A. (2004). Aspergillus galactomannan enzyme immunoassay and quantitative PCR for diagnosis of invasive aspergillosis with bronchoalveolar lavage fluid. *J. Clin. Microbiol.* 42 (12), 5517–5522. doi: 10.1128/JCM.42.12.5517-5522.2004

Oren, I., and Paul, M. (2014). Up to date epidemiology, diagnosis and management of invasive fungal infections. *Clin. Microbiol. Infect.* 20 Suppl 6, 1–4. doi: 10.1111/1469-0691.12642

Paholcsek, M., Leiter, E., Markovics, A., and Biro, S. (2014). Novel and sensitive qPCR assays for the detection and identification of aspergillosis causing species. *Acta Microbiol. Immunol. Hung* 61 (3), 273–284. doi: 10.1556/AMicr.61.2014.3.3

Pegorie, M., Denning, D. W., and Welfare, W. (2017). Estimating the burden of invasive and serious fungal disease in the united kingdom. *J. Infect.* 74 (1), 60–71. doi: 10.1016/j.jinf.2016.10.005

Pini, P., Bettua, C., Orsi, C. F., Venturelli, C., Faglioni, L., Forghieri, F., et al. (2015). Clinical performance of a commercial real-time PCR assay for aspergillus DNA detection in serum samples from high-risk patients: comparison with a galactomannan enzyme immunoassay. *Eur. J. Clin. Microbiol. Infect. Dis.* 34 (1), 131–136. doi: 10.1007/s10096-014-2211-y

Reinwald, M., Hummel, M., Kovalevskaya, E., Spiess, B., Heinz, W. J., Vehreschild, J. J., et al. (2012). Therapy with antifungals decreases the diagnostic performance of PCR for diagnosing invasive aspergillosis in bronchoalveolar lavage samples of patients with haematological malignancies. *J. Antimicrob. Chemother.* 67 (9), 2260–2267. doi: 10.1093/jac/dks208

Rickerts, V., Just-Nubling, G., Konrad, F., Kern, J., Lambrecht, E., Bohme, A., et al. (2006). Diagnosis of invasive aspergillosis and mucormycosis in immunocompromised patients by seminested PCR assay of tissue samples. *Eur. J. Clin. Microbiol. Infect. Dis.* 25 (1), 8–13. doi: 10.1007/s10096-005-0078-7

Rickerts, V., Mousset, S., Lambrecht, E., Tintelnot, K., Schwerdtfeger, R., Presterl, E., et al. (2007). Comparison of histopathological analysis, culture, and polymerase chain reaction assays to detect invasive mold infections from biopsy specimens. *Clin. Infect. Dis.* 44 (8), 1078–1083. doi: 10.1086/512812

Ruhnke, M., Groll, A. H., Mayser, P., Ullmann, A. J., Mendling, W., Hof, H., et al. (2015). Estimated burden of fungal infections in Germany. *Mycoses* 58 Suppl 5, 22–28. doi: 10.1111/myc.12392

Ruiz-Camps, I., and Jarque, I. (2014). [Invasive mould disease in haematological patients]. *Rev. Iberoam Micol* 31 (4), 249–254. doi: 10.1016/j.riam.2014.06.002

Sangoi, A. R., Rogers, W. M., Longacre, T. A., Montoya, J. G., Baron, E. J., and Banaei, N. (2009). Challenges and pitfalls of morphologic identification of fungal infections in histologic and cytologic specimens: a ten-year retrospective review at a single institution. *Am. J. Clin. Pathol.* 131 (3), 364–375. doi: 10.1309/AJCP99OOOZSNISCZ

Springer, J., Goldenberger, D., Schmidt, F., Weisser, M., Wehrle-Wieland, E., Einsele, H., et al. (2016a). Development and application of two independent real-time PCR assays to detect clinically relevant mucorales species. *J. Med. Microbiol.* 65 (3), 227–234. doi: 10.1099/jmm.0.000218

Springer, J., Lackner, M., Ensinger, C., Risslegger, B., Morton, C. O., Nachbaur, D., et al. (2016b). Clinical evaluation of a mucorales-specific real-time PCR assay in tissue and serum samples. *J. Med. Microbiol.* 65 (12), 1414–1421. doi: 10.1099/jmm.0.000375

Springer, J., White, P. L., Kessel, J., Wieters, I., Teschner, D., Korczynski, D., et al. (2018). A comparison of aspergillus and mucorales PCR testing of different bronchoalveolar lavage fluid fractions from patients with suspected invasive pulmonary fungal disease. *J. Clin. Microbiol.* 56 (2), e01655-17. doi: 10.1128/JCM.01655-17

Tarrand, J. J., Lichterfeld, M., Warraich, I., Luna, M., Han, X. Y., May, G. S., et al. (2003). Diagnosis of invasive septate mold infections. a correlation of microbiological culture and histologic or cytologic examination. *Am. J. Clin. Pathol.* 119 (6), 854–858. doi: 10.1309/EXBV-YAUP-ENBM-285Y

Walsh, T. J., Wissel, M. C., Grantham, K. J., Petraitiene, R., Petraitis, V., Kasai, M., et al. (2011). Molecular detection and species-specific identification of medically important aspergillus species by real-time PCR in experimental invasive pulmonary aspergillosis. *J. Clin. Microbiol.* 49 (12), 4150–4157. doi: 10.1128/JCM.00570-11

frontiers | Frontiers in Cellular and Infection Microbiology

TYPE Original Research
PUBLISHED 17 March 2023
DOI 10.3389/fcimb.2023.1128337

OPEN ACCESS

EDITED BY
Carina Almeida,
Instituto Nacional Investigaciao Agraria e Veterinaria (INIAV), Portugal

REVIEWED BY
Li Zhong,
Center for Excellence in Molecular Plant Sciences, Chinese Academy of Sciences (CAS), China
Lu Zhang,
Fudan University, China

*CORRESPONDENCE
Yun Fan
fanyun@sccl.org.cn

†These authors have contributed equally to this work and share first authorship

SPECIALTY SECTION
This article was submitted to Clinical Microbiology, a section of the journal Frontiers in Cellular and Infection Microbiology

RECEIVED 20 December 2022
ACCEPTED 06 March 2023
PUBLISHED 17 March 2023

CITATION
Guan Z, Han X, Huang W, Wang X, Wang H and Fan Y (2023) Construction and application of a heterogeneous quality control library for the Xpert MTB/RIF assay in tuberculosis diagnosis. *Front. Cell. Infect. Microbiol.* 13:1128337. doi: 10.3389/fcimb.2023.1128337

Construction and application of a heterogeneous quality control library for the Xpert MTB/RIF assay in tuberculosis diagnosis

Zehao Guan[1†], Xuefei Han[1†], Weigang Huang[1], Xueliang Wang[1], Hualiang Wang[1,2] and Yun Fan[1*]

[1]R&D Laboratory of Quality Control Material, Shanghai Center for Clinical Laboratory, Shanghai, China, [2]Shanghai Academy of Experimental Medicine, Shanghai, China

Proficiency testing based on quality control materials is an important component of the quality assurance system for detection methods. However, in the detection of infectious diseases, it is a challenge to use quality control materials derived from clinical samples or pathogens owing to their infectious nature. The Xpert MTB/RIF assay, endorsed by the World Health Organization, is one of the most widely implemented assays in the detection of *Mycobacterium tuberculosis* along with rifampicin resistance and its heterogeneity. Clinical isolates are typically used as quality controls for this assay, leading to concerns about biosafety, constrained target sequence polymorphisms, and time-consuming preparation. In this study, a heterogeneous quality control library for the Xpert MTB/RIF assay was constructed based on DNA synthesis and site-directed mutation, which provides sufficient rifampicin resistance polymorphisms, enabling monitoring all five probes of Xpert MTB/RIF and its combinations. *Escherichia coli* and *Bacillus subtilis* were used as heterogeneous hosts rather than the pathogen itself to eliminate biosafety risks; thus, preparation does not require a biosafety level III laboratory and the production time is reduced from a few months to a few days. The panel was stable for more than 15 months stored at 4°C and could be distributed at room temperature. All 11 laboratories in Shanghai participating in a pilot survey identified the specimens with corresponding probe patterns, and discordant results highlighted inappropriate operations in the process. Collectively, we show, for the first time, that this library, based on heterogeneous hosts, is an appropriate alternative for *M. tuberculosis* detection.

KEYWORDS

***Mycobacterium tuberculosis*, Xpert MTB/RIF assay, quality control material, proficiency testing, heterogeneous host**

Introduction

Tuberculosis (TB), caused by *Mycobacterium tuberculosis*, is the leading lethal infection, responsible for more than 1 million deaths globally each year in the last decade. Low- and middle-income countries have the highest impact, accounting for 98% of all TB cases (World Health Organization, 2021). Drug resistance and diagnosis delay are two key challenges in effectively treating the pathogen (Dartois and Rubin, 2022; Dong et al., 2022; Liebenberg et al., 2022). In 2019, cases of development of rifampicin resistance or multiple drug resistance represented nearly half a million cases (World Health Organization, 2020a; World Health Organization, 2021). A timely diagnosis is essential for early initiation of appropriate therapy, thereby preventing drug resistance transmission and improving the treatment outcomes. However, conventional culture or phenotypic drug-susceptibility testing is time-consuming, requiring 10 weeks or longer (World Health Organization, 2011). The delay to rifampicin-resistant detection was reported to be 62 days in Shanghai, China (Wu et al., 2020). The Xpert MTB/RIF assay (Cepheid, Sunnyvale, CA, USA) is the game changer towards addressing this issue, targeting the 81-bp rifampicin resistance-determining region (RRDR) of the *rpoB* gene and identifying *M. tuberculosis* along with rifampicin resistance within only 2 h, while simultaneously reflecting RRDR heterogeneity associated with variable levels of rifampicin resistance (Shea et al., 2021; Li et al., 2022) *via* various patterns of its five probes (A-E) and recombination (World Health Organization, 2011; Uddin et al., 2020). By integrating sample processing in the cartridge, less operational skill is required, which especially favors resource-limited regions. With these superiorities, the Xpert MTB/RIF assay has been one of the most widely implemented assays to date, being used in more than 122 TB high-burden developing countries (Albert et al., 2016) and having been recommended as an initial test in adults and children with signs and symptoms of TB by the World Health Organization (2020b).

Like all diagnostic tests, a quality assurance program based on a proficiency test panel is required to ensure the quality of the Xpert MTB/RIF assay; nevertheless, the development of proficiency test panels has not kept pace with the expansion of Xpert MTB/RIF testing. A limited number of panels are available, most of them derived from *M. tuberculosis*, including clinical isolates with drug resistance (Scott et al., 2011; Scott et al., 2014; Gumma et al., 2019), which raises important biosafety concerns and constraints in transportation, especially cross-border transportation. The infectious nature of the pathogen imposes specific infrastructure requirements. A biosafety level III laboratory and associated equipment are prerequisites for preparing these panels (Gumma et al., 2019; Klein et al., 2020), which are not easily accessed in resource-limited settings, hindering the local manufacture of the proficiency test panels, especially in resource-limited regions and countries that are severely affected by TB. In practice, however, local manufactures are encouraged to improve the performance quality of the assay by reducing costs and output time, while ensuring sustainability (Gumma et al., 2019). Another critical issue needing attention is that *M. tuberculosis* has an extremely slow growth rate, leading to a period of several months in production and inactivation verification (Scott et al., 2011; Gumma et al., 2019). The long processing period prevents easy access to these panels. Furthermore, the current available panels lack variety in both rifampicin resistance polymorphisms (corresponding probe patterns in Xpert MTB/RIF) and bacterial load settings for a designated panel. Typically, the panel contains several specimens with similar bacterial loads, including a rifampicin-susceptive specimen and one or two rifampicin-resistant specimens isolated from clinical strains (Scott et al., 2014; Gumma et al., 2019) with the resistance polymorphisms confined to the dominating strains of a local epidemic. Only very few of the probe patterns in Xpert MTB/RIF can be expected in these isolates. The custom panel based on dominant strains from one region may not be suitable for all outbreak areas and could fail to reflect subdominant strains in the region.

These limitations can be attributed to the pathogen's infectious nature and extremely slow growth rate, as well as to the low numbers of strains with rifampin resistance polymorphisms collected for proficiency tests. A synthetic biology methodology—involving non-pathogenic heterogeneous hosts harboring target sequences simulating *M. tuberculosis*—seems to be a promising solution. However, few studies have investigated this issue. Scott et al. (2014), compared five external quality assessment (EQA) panels for Xpert MTB/RIF with a scoring system across various qualitative and quantitative variables. The panel based on *M. tuberculosis* DNA encapsulated in the heterogeneous host *Escherichia coli* yielded the lowest score owing to the requirement of a cold chain for transport and the inconvenience in dispensing the samples into the cartridge. Mitigating these pitfalls may make the method efficient and suitable for use in low-income countries. An improved panel based on a heterogeneous host library was developed in our laboratory. The library harbored mutants corresponding to various probe patterns of Xpert MTB/RIF for the resistance heterogeneity detection. Two non-pathogenic bacilli, *E. coli* and *Bacillus subtilis*, served as heterogeneous hosts. In this study, we investigated the features of this library and its application feasibility in the Xpert MTB/RIF assay quality control.

Materials and methods

Preparation of the mutant library based on *E. coli*

A DNA fragment, MTB-RIF-S (Table S1), containing the 81-bp core region of the *rpoB* gene and a partial 16S rDNA sequence of *M. tuberculosis* separated by EcoRI and HindIII recognition sites, was synthesized and ligated into the pUC57 plasmid, which was digested by EcoRV-BamHI to yield the plasmid p16S-S and strain EC-16S-S. The DNA fragment MTB-RIF-BDE was synthesized in the same manner as described above, including three-nucleotide mutants corresponding to probes B, D, and E of the Xpert MTB/RIF assay, yielding plasmid p16S-BDE and strain EC-16S-BDE. These two plasmids were constructed by Sangon Biotech (Shanghai, China). To remove the 16S rDNA region, p16S-S and p16S-BDE were digested by HindIII and self-ligated, yielding pRIF-S and

pRIF-BDE, respectively. The plasmid series was constructed by PCR-based mutation from these two plasmids.

PCR-induced mutagenesis was performed using QuikChange Site-Directed Mutagenesis Kit (Agilent, CA USA) according to the manufacturer instructions, with some modifications. Briefly, PrimeSTAR HS DNA polymerase (Takara Japan) was used instead of Pfu Turbo DNA polymerase, and the PCR mixture of 50 µl included 100–300 ng templates, 0.3–1 µM primer pair, 200 µM dNTPs, and 1.5 U of DNA polymerase. The extension reaction was initiated by pre-heating the reaction mixture to 98°C for 10 s, followed by 30 cycles of 98°C for 10 s and 68°C for 4 min, and incubation at 68°C for 10 min. The PCR-amplified products were purified and treated with the restriction enzyme DpnI (Takara Japan). One microliter of the product was transformed into *E. coli* DH5α competent cells and inoculated on Luria-Bertani (LB) agar plates with 100 mg/ml ampicillin. The mutants were identified by sequencing. The primers and templates used for each plasmid are listed in Tables S2 and S3, respectively.

Preparation of the mutant library based on *E. coli* and *B. subtilis*

The fragment containing the 81-bp *rpoB* core region and partial 16S rDNA sequence was amplified from p16S-S with primer 1 (flanked with a BtsI-v2 recognition site) and primer 2 (Table S2), further digested with BtsI-v2, and ligated into the shuttle plasmid pBE980a (digested with BtsI-v2 and NheI and then treated with the Klenow large fragment) to yield pBE-MTB-S.

The mutation plasmids were constructed as described above for the *E. coli* host with the primers and templates listed in Tables 1 and S2, respectively, except that 50 µg/ml kanamycin was used to screen the transformants. The shuttle plasmids were transferred to *B. subtilis* WB600 (a gift from Professor Zhiqun Lu) to prepare the mutation library based on *B. subtilis via* electroporation as described by Xue et al. (1999) with minor modifications. Trehalose (0.5 M) was added to the electroporation medium (0.5 M sorbitol, 0.5 M mannitol, 0.5 M trehalose, and 10% glycerol); the competent cells in a 1-mm electroporation cuvette were shocked using a pulser (Gene Pulser Xcell Total System; Bio-Rad, Hercules, CA, USA) at 2100 V, 25 µF, and 200 Ω; and 50 µg/ml kanamycin was used for selection of the transformants.

Sample preparation and panel distribution for the survey

A pilot survey based on the *E. coli* library was performed involving 11 participating laboratories of Shanghai, including two major TB-designated medical institutions (Shanghai Pulmonary Hospital and Shanghai Public Health Clinical Center) that are responsible for most of the diagnosis and treatment of TB in Shanghai, using the 10 GeneXpert Dx and 1 Infinity System devices.

To prepare the panel sample, the fresh colony was inoculated into 3 ml LB medium with corresponding antibiotics and incubated at 37°C overnight. The next day, the culture was centrifuged, washed, and diluted with sterile water to reach a final absorbance value (optical density at 600 nm [OD_{600}]) of 1 as the stock strain. The strain was then diluted to preset concentrations with 1 mM Tris-HCl, 1% sodium carboxymethyl cellulose, 10% glycerol, and 0.2% KroVin 600 (Seebio, Shanghai, China) as an antibacterial agent, and distributed at 1 ml per tube for storage at 4°C. The survey panel consisted of three samples varying in OD value: (1) RIF-S (OD_{600} = 10^{-4}), (2) RIF-BDE (OD_{600} = 10^{-7}), and (3) RIF-E (OD_{600} = 10^{-5}), corresponding to the wild type, the most predominant mutation, and a rare triple mutation found in India (Thirumurugan et al., 2015), respectively. These panels were couriered or hand-delivered to the participating Xpert laboratories in Shanghai. The detection reports

TABLE 1 Mutant strain based on *B. subtilis*.

Strains	Plasmids	Templates	Primers (see Table S2)
BS-S	pBE-MTB-S	\	\
BS-A	pBE-MTB-A	pBE-MTB-S	MA-F&MA-R
BS-B	pBE-MTB-B	pBE-MTB-S	MB-F&MB-R
BS-C	pBE-MTB-C	pBE-MTB-S	MC-F&MC-R
BS-D	pBE-MTB-D	pBE-MTB-S	MD-F&MD-R
BS-E	pBE-MTB-E	pBE-MTB-S	ME-F&ME-R
BS-AD	pBE-MTB-AD	pBE-MTB-D	MA-F&MA-R
BS-AE	pBE-MTB-AE	pBE-MTB-A	ME-F&ME-R
BS-BD	pBE-MTB-BD	pBE-MTB-S	MBD-F&MB-R
BS-BE	pBE-MTB-BE	pBE-MTB-E	MB-F&MB-R
BS-DE	pBE-MTB-DE	pBE-MTB-E	MD-F&MD-R
BS-BDE	pBE-MTB-BDE	pBE-MTB-E	MBD-F&MB-R
BS-ADE	pBE-MTB-ADE	pBE-MTB-DE	MA-F&MA-R

in PDF file format generated by GeneXpert software were collected for analysis.

Stability at room temperature

RIF-S samples with OD_{600} = 10^{-5} were prepared as described above; stored at room temperature (in a range of 20–30°C) for 0, 7, 10, and 20 days, respectively; and then stored at 4°C until tested in the Xpert system in triplicate. A similar test was performed at 37°C for 10 days.

Storage stability of the panel

The survey panel samples were stored at 4°C for 15 months, subjected to the Xpert MTB/RIF assay in triplicate, and compared with the results of the survey.

Chemical inactivation of bacteria with KroVin 600

KroVin 600 was used as a preservative to prolong the shelf lifetime of the panel. Meanwhile, to prevent unintended proliferation and the spread of host strains, a sterility test (bactericidal activity of KroVin 600) was performed as follows. Panel samples with *E. coli* DH5α or *B. subtilis* WB600 (OD_{600} = 1) were stored at 4°C, and 100 µl aliquots were spread on LB plates at irregular intervals following preparation for incubation at 37°C to detect the growth of bacteria.

To exclude the impaction of KroVin 600 on the test results, samples (RIF-S or BS-S, OD600 = 10-5) with or without Krovin 600 were tested with the Xpert system in triplicate. No significant differences were found (Figure S1).

Ct difference between the two chassis cells

Strains RIF-S and BS-S prepared at OD_{600} of 10^{-3}, 10^{-5}, and 10^{-7} were stored at 4°C for more than three days and then tested with the Xpert system in triplicate.

Statistical analysis

The means and standard deviations were calculated for the Ct quantitative variable for probe A. Microsoft Excel was used for all calculations, and an unpaired *t*-test was used for statistical comparisons in analyzing the stability of the specimens; $p < 0.05$ was considered statistically significant.

Results

RRDR library based on *E. coli*

An RRDR library was constructed based on *E. coli* (Figure 1), derived from two synthetic plasmids subjected to site-directed mutation with the aid of five primer pairs (Table S3). The library harbors mutants corresponding to the nine probe patterns of the Xpert MTB/RIF assay, including the wild type of the core region (RIF-S), five mutants targeting each probe of Xpert MTB/RIF (RIF-A, B, C, D, and E), two mutants corresponding to double probes (RIF-BE, RIF-DE), and one mutant corresponding to triple probes (RIF-BDE). These patterns were confirmed by the GeneXpert

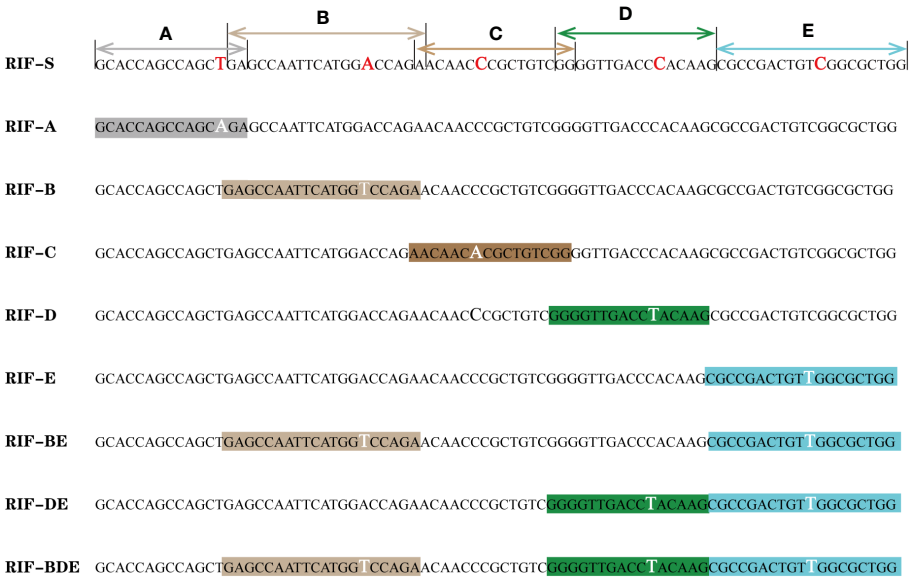

FIGURE 1
*rpo*B mutant library based on *E. coli*. **(A–E)**: probes of the Xpert MTB/RIF assay; the mutant and corresponding nucleotides are highlighted.

system with off-target effects in single, double, or triple probes reported as rifampicin-susceptible or -resistant *M. tuberculosis* with genotypic heterogeneity, whereas the *E. coli* chassis cell alone did not exhibit corresponding patterns (Figures S2, S3). In addition, all semi-quantitative scores reported for *M. tuberculosis* and detected by Xpert MTB/RIF (very low, low, medium, or high) were achieved by adjusting the bacterial OD value (Figures 2A, S2, S3).

Stability of RRDR library samples at room temperature

The specimens were stable for either more than 20 days at room temperature (Figure 3A), or more than 10 days at 37°C (Figure S4), indicating that a cold chain would not be required for transport and delivery. Typically, it takes no more than three days to deliver samples to most cities in China by courier.

EQA *via* detection of discordance among laboratories

All participating laboratories (except for site 7) detected *M. tuberculosis* in all samples and identified rifampicin resistance in specimens 2 and 3, with the heterogeneity between them responding to different probe patterns; probes B, D, and E showed off-target effects in specimen 2, whereas probe E was missing in specimen 3 (Table 2).

With respect to the semi-quantitative results in TB detection, most of the sites obtained the same or an adjacent rank for a given specimen (Figure 4). According to the dominant results, specimens 1, 2, and 3 were designated as "high," "medium/low," and "high/medium," respectively. The hierarchy was confirmed by the mean Ct values of the probes of 10.8, 21.6, and 16.3 corresponding to specimens 1, 2, and 3, respectively, using the Ct of probe A as reference; a value of 22 is set as the threshold value between "low" and "medium" and a value of 16 is set as the threshold between "medium" and "high." This ranking also showed a positive association with the OD values of the bacillus (Table 2 and Figure 4).

Sites 7 and 10 were identified to have discordant results among the 11 participating laboratories. Site 7 failed to detect TB in specimen 2 and reported a semi-quantitative ranking of "medium" rather than "high" for specimen 1. Site 10 reported a result of "low" rather than "high/medium" for specimen 3 (Figure 4). Telephone interviews were conducted for these sites to understand the nature of this discordance. Site 10 reported sample loss for specimen 3 in the interview. Site 7 indicated that they had followed the procedure for sputum sediment rather than for raw sputum as performed at the other sites, which involves additional steps, including NaOH treatment, that are not used in the raw sputum procedure. To verify that these procedural differences were the causes of the discordance, three more samples of specimen 2 were retested at Site 7 following the raw sputum procedure, resulting in a report of a "medium" rank (mean Ct_{pA} = 21.4).

Long-term stability

The survey panel was stable for more than 15 months at 4 °C, as indicated by the Ct values of probe A compared with the survey results ($p > 0.05$) (Figure 3B).

Library expansion and chassis switch

A library based on the shuttle plasmid pBE980a was first prepared in *E. coli* DH5α. The pattern number was then expanded to 13 by introducing an additional primer and extra combinations of primers and templates based on site-directed mutation. The *B. subtilis* library was then constructed after transformation, containing 12 mutants and one wild-type sequence in the RRDR (Table 1), which was confirmed by the GeneXpert system with a corresponding probe pattern. Similar to the results for the *E. coli* chassis, no *M. tuberculosis* was detected with *B. subtilis* only (Figure S5). When comparing the two chassis

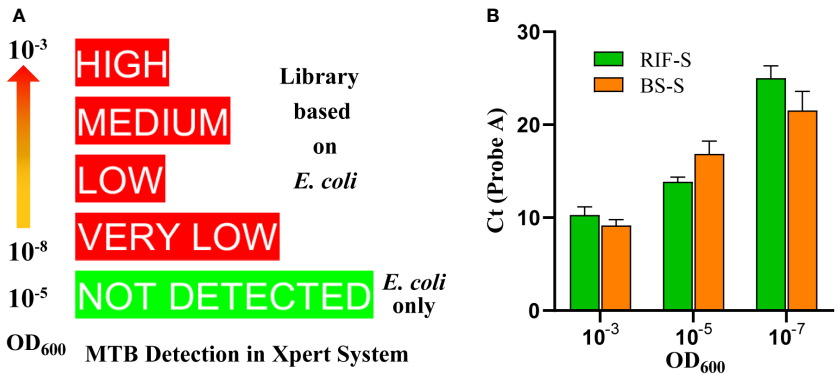

FIGURE 2
Quantitative and semi-quantitative results according to optical density values at 600 nm (OD_{600}). **(A)** Semi-quantitative readings from the library based on (*E*) *coli* in the Xpert MTB/RIF assay, showing that OD_{600} of specimens ranges from 10^{-8} to 10^{-3}. The rank is associated with the mutants and lots. **(B)** Cycle threshold (Ct) values of probe A for (*E*) *coli* and (*B*) *subtilis* with the same OD_{600} value.

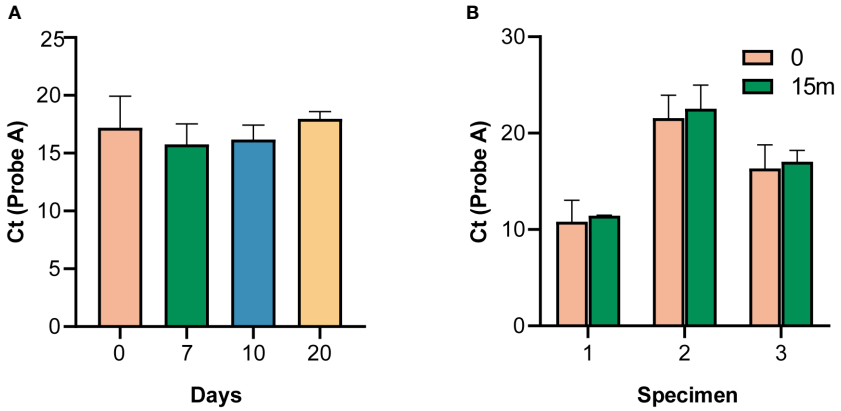

FIGURE 3
Stability of the panels. **(A)** Stability of specimens at room temperature. **(B)** Stability of specimens after 15 months of storage, according to the cycle threshold (Ct) value of probe A.

harboring the same genotype of RRDR (BS-S vs. RIF-S), similar Ct values were obtained in the set OD values (Figure 2B). Neither *E. coli* nor *B. subtilis* colonies developed on the plates after 3 days of treatment with the panel matrix. These results indicated similar features of the library based on both bacteria, demonstrating their suitability in the preparation and application as quality controls for the Xpert MTB/RIF assay.

Discussion

In this study, we developed a heterogeneous quality control library for the Xpert MTB/RIF assay with advantages of convenient preparation methods and accessibility. The library harbors mutants with sufficient RRDR polymorphisms in the Xpert MTB/RIF assay, enabling monitoring of its five probes and their combinations. The mutations in RRDR, responsible for the rifampicin resistance mechanism in 95% of cases (Helb et al., 2010; Uddin et al., 2020), are reported as single, double, or triple off-target of five probes or their combinations (Zaw et al., 2018). The mutant frequencies corresponding to different probes vary across regions, being very rare in some areas. Collecting strains with an appropriate diversity of probe patterns in the Xpert MTB/RIF assay for proficiency testing requires obtaining numerous rifampicin-resistant isolates. Out of 90 rifampicin-resistant isolates in India, only five distinct patterns in the assay are expected: three single mutations, one double mutation, and one triple mutation (Mokrousov et al., 2003). Similarly, out of 100 rifampicin-resistant isolates from 518 *M.*

TABLE 2 Discordant results identified in 11 laboratory sites participating in the survey.

	Specimen 1 (RIF-S)				Specimen 2 (RIF-BDE)				Specimen 3 (RIF-E)			
Site	MTB	Rif	Probes	Ct_A	MTB	Rif	Probes	Ct_A	MTB	Rif	Probes	Ct_A
1	High	–	All	10.4	Medium	+	AC	19.3	High	+	ABCD	13.6
2	High	–	All	10	Low	+	AC	24.9	Medium	+	ABCD	16.6
3	High	–	All	10.5	Medium	+	AC	21.4	High	+	ABCD	13.6
4	High	–	All	9.6	Low	+	AC	22.2	High	+	ABCD	14.7
5	High	–	All	11.3	Medium	+	AC	21.6	High	+	ABCD	15.6
6	High	–	All	12.7	Low	+	AC	26	Medium	+	ABCD	16.9
7	Medium*	–	All	16.7	NEG*	\	\	\	Medium	+	ABCD	18.8
8	High	–	All	9.8	Medium	+	AC	21.7	High	+	ABCD	14.7
9	High	–	All	9.6	Medium	+	AC	18.8	Medium	+	ABCD	16.7
10	High	–	All	8.7	Medium	+	AC	19.2	Low*	+	ABCD	22.1
11	High	–	All	9.6	Medium	+	AC	20.4	Medium	+	ABCD	16.4
			Mean	10.8			Mean	21.6			Mean	16.3

*Discordant results.
MTB, Mycobacterium tuberculosis; Rif, rifampicin resistance; Probes, positive probes; Ct_A, cycle threshold of Probe A; +, rifampicin resistance detected; – rifampicin resistance not detected; \, data not available; NEG, M. tuberculosis not detected.

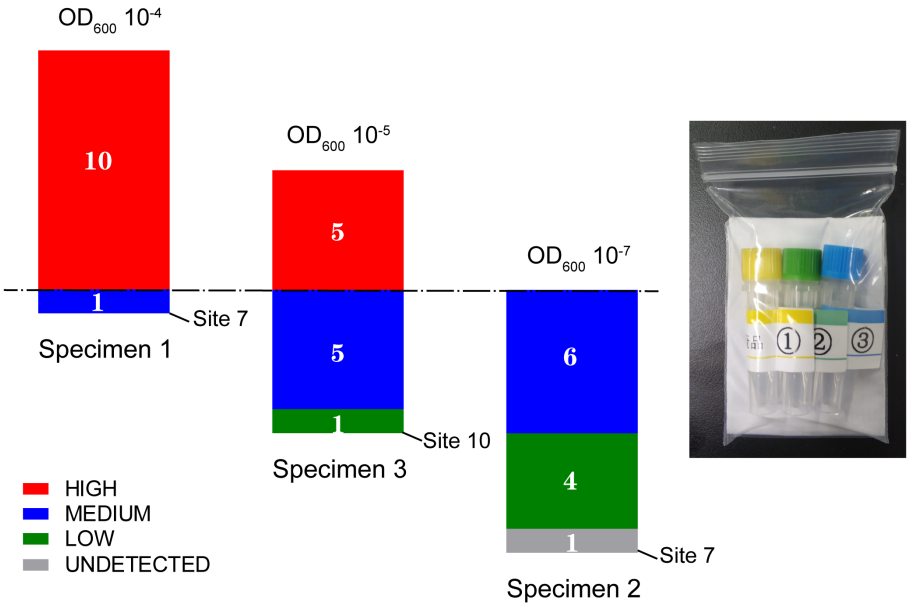

FIGURE 4
M. tuberculosis detection results of three specimens in the panel from the pilot survey in 11 clinical laboratories in Shanghai.

tuberculosis clinical strains identified in Shaanxi province of China, seven patterns of the Xpert system are expected (Yang et al., 2021). The pattern number expanded to nine with 205 rifampicin-resistant isolates identified in Bangladesh, including five single mutations, four double mutations, and no triple mutation (Uddin et al., 2020). Although the diverse mutation pattern suggests geographic variation (Zaw et al., 2018), customs and delivery constraints for transporting pathogens prevent access to obtain foreign isolates, thus confining the diversity possible to only locally available clinical strains. To overcome these barriers in ensuring appropriate EQA, the panel developed in this study includes 12 types of mutations corresponding to 12 distinct probe patterns in the Xpert MTB/RIF assay: five single mutations, five double mutations, and two triple mutations, with the aid of 11 primers. To our knowledge, this number exceeds the reported patterns expected in any survey performed to date, covering the probe patterns that can be expected in most TB-affected regions. More patterns that can be achieved by simply introducing additional primers, if needed, as shown in the study. Theoretically, the library can mimic any mutant in the core region, providing sufficient diversity of quality controls to customize panels for the designated EQA.

B. subtilis and *E. coli* were used as heterologous hosts for the library constructed in this study, and are extensively implemented as chassis for the biosynthesis of antibiotics (Liu et al., 2016), anti-tumor compounds (Tang et al., 2022), biomass (Liu et al., 2022), and therapeutics (Lynch et al., 2022), demonstrating good records regarding biosafety. Thus, a conventional laboratory is adequate for preparation of our panel, in contrast to the mandatory requirement of biosafety level III infrastructure sets for handling *M. tuberculosis*. This facilitates local manufacture of the panel in resource-limited countries, which also carry a high burden of TB. In addition, the slow-growth property of *M. tuberculosis* results in a time-consuming production process and subsequent inactivation verification. For confirmation of the inactivation of the pathogen, 42 days was required for dried culture spots using microbial growth incubation tubes (Becton, Dickinson, Sparks, MD, USA) (Scott et al., 2011) and 84 days was required for a dried tube specimen panel (Gumma et al., 2019). However, less than seven days was needed for our panels based on *B. subtilis* or *E. coli*, from inoculation to preparation to inactivation.

As shown in the pilot survey, the panel based on *E. coli* fully meets the EQA requirement for Xpert MTB/RIF by monitoring its probe patterns and responding to the concentration variation of the bacillus. The Ct values of the probes or semi-quantitative results of the panel were positively associated with bacterial OD_{600} values, offering a useful means in detecting discordance. Moreover, the OD value of bacilli can be easily adjusted and measured with a spectrophotometer, which is readily available in a conventional laboratory, even in resource-limited settings, compared with the requirement of more complex flow cytometry for existing *M. tuberculosis* panels (Scott et al., 2011). The requirement of a cold chain for transport and the inconvenience in dispensing the samples into the cartridge, two problems that plagued heterogeneous panels (Scott et al., 2014), has been resolved. Our panel involves a package fit for single use (Figure 4) and a matrix with appropriate fluidity; no transfer problems were reported in the present survey. Moreover, a cold chain is not required for allocation since the panel can be expected to remain stable, either for more than 20 days at room temperature, or 10 days at 37°C, which provides a particular advantage, especially for improving access to resource-limited regions and countries (Scott et al., 2014). The panel was stable for more than one year at 4°C and a tube of culture (3 ml) is adequate for conducting more than 10,000 tests, further demonstrating improved convenience and accessibility.

Although we demonstrated that the library based on *E. coli* or *B. subtilis* is suitable as a quality control material for the Xpert MTB/RIF assay, though the difference between the bacillus and mycobacteria chassis remains a potential concern, especially given their distinct cell wall features, which may affect DNA extraction (Picard et al., 2009). Mycobacteria are classified as gram-positive bacteria but with an outer membrane covering the cell wall, resembling the characteristics of gram-negative bacteria (Rohde, 2019). In this study, both gram-negative and gram-positive model bacteria, *E. coli* and *B. subtilis*, respectively, were tested as chassis cells; neither of these hosts prevented Xpert MTB/RIF from reading the mutant library. We speculate that the extraction procedure in the kit is sufficient for either *E. coli* or *B. subtilis* as well as for *M. tuberculosis*. It is worth noting that *Bacillus subtilis* subsp. *globigii*, a subspecies of *B. subtilis*, is used as the sample processing control in the Xpert MTB/RIF assay cartridge (Helb et al., 2010; World Health Organization, 2011). Nevertheless, a chassis that is more similar to *M. tuberculosis* would still be preferred. In light of the convenience in switching the chassis of the library, as shown in this study, it may be possible to use mutants based on *Mycobacterium smegmatis*, which is generally considered a non-pathogenic mycobacterium and grows faster than *M. tuberculosis* (Tyagi and Sharma, 2002; Sundarsingh et al., 2020); thus, we plan to test *M. smegmatis* as a possible chassis for this panel in further studies. Another discrepancy between the heterologous library and the target pathogen involves the vector of the target sequence. Multiple plasmid copies were used in construction of our library, whereas the pathogen harbors only one copy of the target sequence of Xpert MTB/RIF in the chromosome. Thus, further investigation is warranted to determine how this difference affects detection, and if a single-copy plasmid or integrative vector would be superior (such as providing better reproducibility in the "very low" rank). Importantly, successors of the Xpert MTB/RIF assay continue to expand the targeting sequences for various purposes such as detecting resistance to more drugs in the Xpert MTB/XDR assay (Naidoo and Dookie, 2022) and increasing the sensitivity of *M. tuberculosis* detection in the Xpert MTB/RIF Ultra assay, which incorporates the multicopy amplification targets "IS6110" and "IS1081" (Chakravorty et al., 2017). Thus, in developing the library for these assays, additional target sequences will need to be added as well as assigned to the vectors with a suitable copy number (single, multiple, or combined). Another limitation is that this pilot survey only covered a limited number of laboratories in Shanghai, China. As such, this study should be scaled up and performed in more rounds to more comprehensively investigate the features of the new library panel.

In summary, we have constructed a heterogeneous library for Xpert MTB/RIF assay quality control based on non-pathogenic bacteria, which overcomes the obstacles associated with the detected pathogen, including the biosafety risk, time-consuming preparation and verification, constrained laboratory infrastructure, and limited target sequence polymorphisms. The panel is based on a library that is suitable for applications in EQA and offers accessible quality control materials for the Xpert MTB/RIF assay, even in resource-limited regions, which tend to have higher TB burdens. Importantly, this work demonstrates the feasibility of the approach to use heterologous hosts as an alternative to pathogens, which can help to mitigate safety concerns and expand quality control for assays targeting infectious pathogens more broadly.

Data availability statement

The original contributions presented in the study are included in the article/Supplementary Material. Further inquiries can be directed to the corresponding author.

Author contributions

YF designed the study and performed the experiments and interpretation of data. XH and ZG conducted experiments of some representative bacteria. XW, HW, and WH contributed to part of the data analysis. All authors contributed to the article and approved the submitted version.

Funding

This study was supported by National Science and Technology Major Project for the Control and Prevention of Major Infectious Diseases in China (grant number 2017ZX10302201) and Shanghai Municipal Health Commission (grant number 201940341).

Acknowledgments

We thank Dr. Fangyou Yu and Dr. Xiaocui Wu, Clinical Laboratory of Shanghai Pulmonary Hospital, for experimental instrument support. We thank Dr. Xiaoli Xue, Shanghai Institute of Plant Physiology and Ecology, Chinese Academy of Sciences, for critical reading of the manuscript. The authors are grateful to the Clinical Laboratory of Shanghai Pulmonary Hospital for providing the necessary facilities to carry out this work.

Conflict of interest

The authors declare that the research was conducted in the absence of any commercial or financial relationships that could be construed as a potential conflict of interest.

Publisher's note

that may be evaluated in this article, or claim that may be made by its manufacturer, is not guaranteed or endorsed by the publisher.

Supplementary material

The Supplementary Material for this article can be found online at: https://www.frontiersin.org/articles/10.3389/fcimb.2023.1128337/full#supplementary-material

SUPPLEMENTARY FIGURE 1
Effect of KroVin 600 on the test results according to the cycle threshold (Ct) value of probe A.

SUPPLEMENTARY FIGURE 2
Xpert MTB/RIF assay results of the library based on *E. coli* (GeneXpert Dx System, partial). Mismatched probes are framed in rectangles.

SUPPLEMENTARY FIGURE 3
Xpert MTB/RIF assay results of the library based on *E. coli* (GeneXpert Dx System, Chinese version, partial). Mismatched probes are framed in rectangles.

SUPPLEMENTARY FIGURE 4
Stability of specimens at 37°C.

SUPPLEMENTARY FIGURE 5
Xpert MTB/RIF assay results of the library based on *B. subtilis* (GeneXpert Infinity System, partial). Mismatched probes are framed in rectangles.

References

Albert, H., Nathavitharana, R. R., Isaacs, C., Pai, M., Denkinger, C. M., and Boehme, C. C. (2016). Development, roll-out and impact of xpert MTB/RIF for tuberculosis: What lessons have we learnt and how can we do better? *Eur. Respir. J.* 48, 516–525. doi: 10.1183/13993003.00543-2016

Chakravorty, S., Simmons, A. M., Rowneki, M., Parmar, H., Cao, Y., Ryan, J., et al. (2017). The new xpert MTB/RIF ultra: Improving detection of *Mycobacterium tuberculosis* and resistance to rifampin in an assay suitable for point-of-care testing. *MBio.* 8, e00812-17. doi: 10.1128/mBio.00812-17

Dartois, V. A., and Rubin, E. J. (2022). Anti-tuberculosis treatment strategies and drug development: Challenges and priorities. *Nat. Rev. Microbiol.* 20, 685–701. doi: 10.1038/s41579-022-00731-y

Dong, B., He, Z., Li, Y., Xu, X., Wang, C., and Zeng, J. (2022). Improved conventional and new approaches in the diagnosis of tuberculosis. *Front. Microbiol.* 13. doi: 10.3389/fmicb.2022.924410

Gumma, V., DeGruy, K., Bennett, D., Nguyen Thi Kim, T., Albert, H., Bond, K. B., et al. (2019). Impact of external quality assurance on the quality of xpert MTB/RIF testing in Viet nam. *J. Clin. Microbiol.* 57, e01669-18. doi: 10.1128/JCM.01669-18

Helb, D., Jones, M., Story, E., Boehme, C., Wallace, E., Ho, K., et al. (2010). Rapid detection of *Mycobacterium tuberculosis* and rifampin resistance by use of on-demand, near-patient technology. *J. Clin. Microbiol.* 48, 229–237. doi: 10.1128/JCM.01463-09

Klein, K., DeGruy, K., Rey, Z., Hall, P., Kim, A., Gutreuter, S., et al. (2020). A global proficiency testing programme for Xpert(R) MTB/RIF using dried tube specimens 2013-2015. *Afr. J. Lab. Med.* 9, 1167. doi: 10.4102/ajlm.v9i1.1167

Li, M. C., Wang, X. Y., Xiao, T. Y., Lin, S. Q., Liu, H. C., Qian, C., et al. (2022). *rpoB* mutations are associated with variable levels of rifampin and rifabutin resistance in *Mycobacterium tuberculosis*. *Infect. Drug Resist.* 15, 6853–6861. doi: 10.2147/IDR.S386863

Liebenberg, D., Gordhan, B. G., and Kana, B. D. (2022). Drug resistant tuberculosis: Implications for transmission, diagnosis, and disease management. *Front. Cell Infect. Microbiol.* 12. doi: 10.3389/fcimb.2022.943545

Liu, Q., Shen, Q., Bian, X., Chen, H., Fu, J., Wang, H., et al. (2016). Simple and rapid direct cloning and heterologous expression of natural product biosynthetic gene cluster in *Bacillus subtilis via* Red/ET recombineering. *Sci. Rep.* 6, 34623. doi: 10.1038/srep34623

Liu, J., Wang, X., Dai, G., Zhang, Y., and Bian, X. (2022). Microbial chassis engineering drives heterologous production of complex secondary metabolites. *Biotechnol. Adv.* 59, 107966. doi: 10.1016/j.biotechadv.2022.107966

Lynch, J. P., Goers, L., and Lesser, C. F. (2022). Emerging strategies for engineering *Escherichia coli nissle* 1917-based therapeutics. *Trends Pharmacol. Sci.* 43, 772-786. doi: 10.1016/j.tips.2022.02.002

Mokrousov, I., Otten, T., Vyshnevskiy, B., and Narvskaya, O. (2003). Allele-specific *rpoB* PCR assays for detection of rifampin-resistant *Mycobacterium tuberculosis* in sputum smears. *Antimicrob. Agents Chemother.* 47, 2231–2235. doi: 10.1128/AAC.47.7.2231-2235.2003

Naidoo, K., and Dookie, N. (2022). Can the GeneXpert MTB/XDR deliver on the promise of expanded, near-patient tuberculosis drug-susceptibility testing? *Lancet Infect. Dis.* 22, e121–e127. doi: 10.1016/S1473-3099(21)00613-7

Picard, F. J., Gagnon, M., Bernier, M. R., Parham, N. J., Bastien, M., Boissinot, M., et al. (2009). Internal control for nucleic acid testing based on the use of purified *Bacillus atrophaeus* subsp. *globigii* spores. *J. Clin. Microbiol.* 47, 751–757. doi: 10.1128/JCM.01746-08

Rohde, M. (2019). The gram-positive bacterial cell wall. *Microbiol. Spectr.* 7, GPP3-0044-2018. doi: 10.1128/microbiolspec.GPP3-0044-2018

Scott, L., Albert, H., Gilpin, C., Alexander, H., DeGruy, K., and Stevens, W. (2014). Multicenter feasibility study to assess external quality assessment panels for xpert MTB/RIF assay in south Africa. *J. Clin. Microbiol.* 52, 2493–2499. doi: 10.1128/JCM.03533-13

Scott, L. E., Gous, N., Cunningham, B. E., Kana, B. D., Perovic, O., Erasmus, L., et al. (2011). Dried culture spots for xpert MTB/RIF external quality assessment: Results of a phase 1 pilot study in south Africa. *J. Clin. Microbiol.* 49, 4356–4360. doi: 10.1128/JCM.05167-11

Shea, J., Halse, T. A., Kohlerschmidt, D., Lapierre, P., Modestil, H. A., Kearns, C. H., et al. (2021). Low-level rifampin resistance and *rpoB* mutations in *Mycobacterium tuberculosis*: An analysis of whole-genome sequencing and drug susceptibility test data in new York. *J. Clin. Microbiol.* 59, e01885-20. doi: 10.1128/JCM.01885-20

Sundarsingh, T. J. A., Ranjitha, J., Rajan, A., and Shankar, V. (2020). Features of the biochemistry of *Mycobacterium smegmatis*, as a possible model for *Mycobacterium tuberculosis*. *J. Infect. Public Health* 13, 1255–1264. doi: 10.1016/j.jiph.2020.06.023

Tang, J. W., Liu, X., Ye, W., Li, Z. R., and Qian, P. Y. (2022). Biosynthesis and bioactivities of microbial genotoxin colibactins. *Nat. Prod. Rep.* 39, 991–1014. doi: 10.1039/d1np00050k

Thirumurugan, R., Kathirvel, M., Vallayyachari, K., Surendar, K., Samrot, A. V., and Muthaiah, M. (2015). Molecular analysis of *rpoB* gene mutations in rifampicin resistant *Mycobacterium tuberculosis* isolates by multiple allele specific polymerase chain reaction in puducherry, south India. *J. Infect. Public Health* 8, 619–625. doi: 10.1016/j.jiph.2015.05.003

Tyagi, J. S., and Sharma, D. (2002). *Mycobacterium smegmatis* and tuberculosis. *Trends Microbiol.* 10, 68–69. doi: 10.1016/s0966-842x(01)02296-x

Uddin, M. K. M., Rahman, A., Ather, M. F., Ahmed, T., Rahman, S. M. M., Ahmed, S., et al. (2020). Distribution and frequency of *rpoB* mutations detected by xpert MTB/RIF assay among Beijing and non-Beijing rifampicin resistant *Mycobacterium tuberculosis* isolates in Bangladesh. *Infect. Drug Resist.* 13, 789–797. doi: 10.2147/IDR.S240408

World Health Organization (2011). *Policy statement: Automated real-time nucleic acid amplification technology for rapid and simultaneous detection of tuberculosis and rifampicin resistance: Xpert MTB/RIF system* (Geneva: World Health Organization).

World Health Organization (2020a). *Global tuberculosis report 2020* (Geneva: World Health Organization).

World Health Organization (2020b). *WHO consolidated guidelines on tuberculosis. module 3: Diagnosis – rapid diagnostics for tuberculosis detection* (Geneva: World Health Organization).

World Health Organization (2021). *Global tuberculosis report 2021* (Geneva: World Health Organization).

Wu, Z., Rueda, Z. V., Li, T., Zhang, Z., Jiang, Y., Sha, W., et al. (2020). Effect of the xpert MTB/RIF on the detection of pulmonary tuberculosis cases and rifampicin resistance in shanghai, China. *BMC Infect. Dis.* 20, 153. doi: 10.1186/s12879-020-4871-9

Xue, G. P., Johnson, J. S., and Dalrymple, B. P. (1999). High osmolarity improves the electro-transformation efficiency of the gram-positive bacteria *Bacillus subtilis* and *Bacillus licheniformis*. *J. Microbiol. Methods* 34, 183–191. doi: 10.1016/S0167-7012(98)00087-6

Yang, J., Zhang, T., Xian, X., Li, Y., Wang, R., Wang, P., et al. (2021). Molecular characteristics and drug resistance of *Mycobacterium tuberculosis* isolate circulating in shaanxi province, northwestern China. *Microb. Drug Resist.* 27, 1207–1217. doi: 10.1089/mdr.2020.0496

Zaw, M. T., Emran, N. A., and Lin, Z. (2018). Mutations inside rifampicin-resistance determining region of *rpoB* gene associated with rifampicin-resistance in *Mycobacterium tuberculosis*. *J. Infect. Public Health* 11, 605–610. doi: 10.1016/j.jiph.2018.04.005

frontiers | Frontiers in Cellular and Infection Microbiology

TYPE Original Research
PUBLISHED 03 April 2023
DOI 10.3389/fcimb.2023.1125079

OPEN ACCESS

EDITED BY
Michael McClelland,
University of California, Irvine, United States

REVIEWED BY
Nadine Christine Lemaitre,
Centre Hospitalier Universitaire (CHU) d'Amiens, France
Yolanda González Hernández,
National Institute for Respiratory Diseases, Mexico

*CORRESPONDENCE
Suzanne M. Hingley-Wilson
s.hingley-wilson@surrey.ac.uk
Augustina Angelina Sylverken
asylverken@knust.edu.gh

SPECIALTY SECTION
This article was submitted to Molecular Bacterial Pathogenesis, a section of the journal Frontiers in Cellular and Infection Microbiology

RECEIVED 15 December 2022
ACCEPTED 17 March 2023
PUBLISHED 03 April 2023

CITATION
Owusu W, van Vliet AHM, Riddell NE, Stewart G, Akwani WC, Aryeetey S, Arthur RA, Sylverken AA and Hingley-Wilson SM (2023) A multiplex PCR assay for the differentiation of *Mycobacterium tuberculosis* complex reveals high rates of mixed-lineage tuberculosis infections among patients in Ghana.
Front. Cell. Infect. Microbiol. 13:1125079.
doi: 10.3389/fcimb.2023.1125079

A multiplex PCR assay for the differentiation of *Mycobacterium tuberculosis* complex reveals high rates of mixed-lineage tuberculosis infections among patients in Ghana

Wellington Owusu[1], Arnoud H. M. van Vliet[2], Natalie E. Riddell[3], Graham Stewart[1], Winifred C. Akwani[1], Sherihane Aryeetey[4], Rejoice Agyeiwaa Arthur[4], Augustina Angelina Sylverken[4,5]* and Suzanne M. Hingley-Wilson[1]*

[1]Department of Microbial Sciences, School of Biosciences, Faculty of Health and Medical Sciences, University of Surrey, Guildford, United Kingdom, [2]Department of Comparative Biomedical Sciences, School of Veterinary Medicine, Faculty of Health and Medical Sciences, University of Surrey, Guildford, United Kingdom, [3]Department of Biochemical Sciences, School of Biosciences and Medicine, University of Surrey, Guildford, United Kingdom, [4]Kumasi Centre for Collaborative Research in Tropical Medicine, Kwame Nkrumah University of Science and Technology, Kumasi, Ghana, [5]Department of Theoretical and Applied Biology, Kwame Nkrumah University of Science and Technology, Kumasi, Ghana

In low-resource settings with high tuberculosis (TB) burdens, lack of rapid diagnostic methods for detection and differentiation of *Mycobacterium tuberculosis* complex (MTBC) is a major challenge affecting TB management. This study utilized comparative genomic analyses of MTBC lineages; *M. tuberculosis*, *M. africanum* Lineages 5/6 and *M. bovis* to identify lineage-specific genes. Primers were designed for the development of a Multiplex PCR assay which was successful in differentiating the MTBC lineages. There was no cross-reaction with other respiratory pathogens tested. Validation of the assay using clinical samples was performed with sputum DNA extracts from 341 clinically confirmed active TB patients. It was observed that 24.9% of cases were caused by *M. tuberculosis*, while *M. africanum* L5 & L6 reported 9.0% and 14.4%, respectively. *M. bovis* infection was the least frequently detected lineage with 1.8%. Also, 27.0% and 17.0% of the cases were PCR negative and unspeciated, respectively. However, mixed-lineage TB infections were recorded at a surprising 5.9%. This multiplex PCR assay will allow speciation of MTBC lineages in low-resource regions, providing rapid differentiation of TB infections to select appropriate medication at the earliest possible time point. It will also be useful in epidemiological surveillance studies providing reliable information on the prevalence of TB lineages as well as identifying difficult to treat cases of mixed-lineage tuberculosis infections.

KEYWORDS

***Mycobacterium tuberculosis* complex, bioinformatic analyses, multiplex polymerase chain reaction, mixed-lineage tuberculosis infections, tuberculosis diagnosis, Ghana**

Introduction

Human tuberculosis (TB) is a communicable disease caused by some members of the Mycobacterium tuberculosis complex (MTBC), mainly; *Mycobacterium tuberculosis* (Mtb), *Mycobacterium africanum* (Maf) and *Mycobacterium bovis* (Mbo). It is one of the leading causes of death from a single infectious organism, infecting about a quarter of the world's population (WHO, 2020). It remains a global pandemic, despite the availability of interventional control measures such as the use of a live attenuated vaccine (BCG) and multi-drug therapy. The situation has been further aggravated by the lack of rapid and reliable, point-of-care diagnostic methods for low-resource areas, and the use of various forms of insufficient treatment procedures among poor resource countries (WHO, 2020).

TB in an individual is often assumed to be caused by a single clonal MTBC lineage, although mixed infections have been previously noted (Hingley-Wilson et al., 2013). Advances in molecular-based approaches in TB studies also demonstrated multiple lineages causing TB in the same patient (Van Rie et al., 2005; Huyen et al., 2012; Zetola et al., 2014) and the occurrence of mixed-lineage TB infections in high TB endemic regions has been reported (Cohen et al., 2011). In TB management, mixed-lineage TB infections have been strongly associated with poor treatment outcome (Zetola et al., 2014).

West-Africa has one of the highest incidences of TB world-wide with a unique set of circulating MTBC species namely: *M. tuberculosis, M. africanum* and *M. bovis*. While *M. tuberculosis* is generally the predominant pathogen for human TB, unusually almost 50% of all TB cases in West Africa are caused by *M. africanum* (Mostowy et al., 2004). In The Gambia, 39% of TB cases are caused by *M. africanum* (de Jong et al., 2010a). In Ghana, *M. africanum* rates remain stable at around 20%, with one of the highest rates of infections in the Northern part of Ghana (De Jong et al., 2009). While the reservoir of infection for *M. tuberculosis* is the latently infected human population, a non-human reservoir of infection for *M. africanum* in Ghana has been postulated, likely to be more concentrated in Northern Ghana (Otchere et al., 2018).

The gold standard of TB diagnosis is the isolation of MTBC by culture and the use of biochemical tests (Gholoobi et al., 2014). However, these methods are very laborious and time-consuming which further risk aggravating the condition of patients due to delayed treatment. In addition, with culturing-based techniques in a mixed infection, the fastest growing is often noted as a single infection (Hingley-Wilson et al., 2013). Species differentiation is often challenged with misidentification. For instance, *M. africanum* Lineage 5 (MafL5) and Lineage 6 (MafL6) exhibit growth characteristics which are intermediates of both *M. tuberculosis* and *M. bovis* (de Jong et al., 2010b). Since 2010, WHO recommended the use of GeneXpert assay in diagnostic facilities as a first-line TB diagnostic tool (Goig et al., 2019). It detects MTBC through the identification of insertion sequence (*IS6110)* as well as identifying rifampicin resistant genes. Although an improved modified GeneXpert Ultra version has been produced with high sensitivity and specificity, it is unable to differentiate the individual MTBC lineages to inform selection of appropriate medication.

In low-resource regions, MTBC lineages are often not differentiated prior to treatment due to reasons such as unavailability of high cost, non-portable genome sequencing machines and length of time for culture results. This can lead to inappropriate treatment regimens, for example, *M. bovis* is intrinsically resistant to pyrazinamide, one of the frontline drugs used collectively for standard TB treatment (Oryan et al., 2022). Indeed, patient exposure to prolonged pyrazinamide treatment can result in hepatotoxicity and polyarthralgia (Papastavros et al., 2002) and should therefore be avoided if not required. Additionally, antibiotic treatment duration of *M. bovis* infections is recommended for 9 months (rather than the standard 6 months) because of the absence of pyrazinamide efficacy (Lan et al., 2016). In general, TB treatment durations shorter than recommendation may lead to incomplete sterilization of an infection and increase the risk of the development of antibiotic resistance (Khalif Ali et al., 2017; Ali et al., 2019). It is therefore important to investigate and identify lineage-specific TB molecular markers for designing diagnostic assays with high level of sensitivity and specificity to inform selection of appropriate medication to limit morbidity and drug resistance.

Using the comparative genomics workflow previously described by Akwani et al., 2022, MTBC lineage-specific genes identified were transferred into the development of multiplex PCR assay for TB lineage differentiation. This will enhance precise disease diagnosis, improve epidemiological surveillance studies and help inform selection of appropriate TB drug regimens at early time point especially in low resource settings with high TB incidence.

Materials and methods

Selection and processing of genome sequences

Genome sequences of *M. tuberculosis, M. africanum* and *M. bovis* in the form of sequence reads and assembled genomes were obtained from NCBI, Genbank and EMBL-EBI repositories using fastq-dump instructions (SRA-Tools-NCBI, 2021). In addition, reference sequences were also obtained. An overall total of 7,456 genome sequences comprising *M. tuberculosis* (6802), *M. africanum* (244), *M. bovis* (391) and other animal-adapted MTBCs (19) were assessed (Supplementary Table S1). Genome assembly was performed with Shovil Megahit toolkit version 1.2.9. To evaluate the consistency of the assembled genomes, quality assessment was performed with QUAST version. 4.6.3 (Gurevich et al., 2013). The inclusion criteria for checks included: largest contig must be greater than 100kb, N50 >25kb, L50 < 50 and the genomic size between 4.0 and 4.8 Mbp. A total of 120 genomes of *M. tuberculosis*, *M. africanum* and *M. bovis* were used for the pangenome analysis leading to the identification of lineage-specific genes as shown in Figure 1.

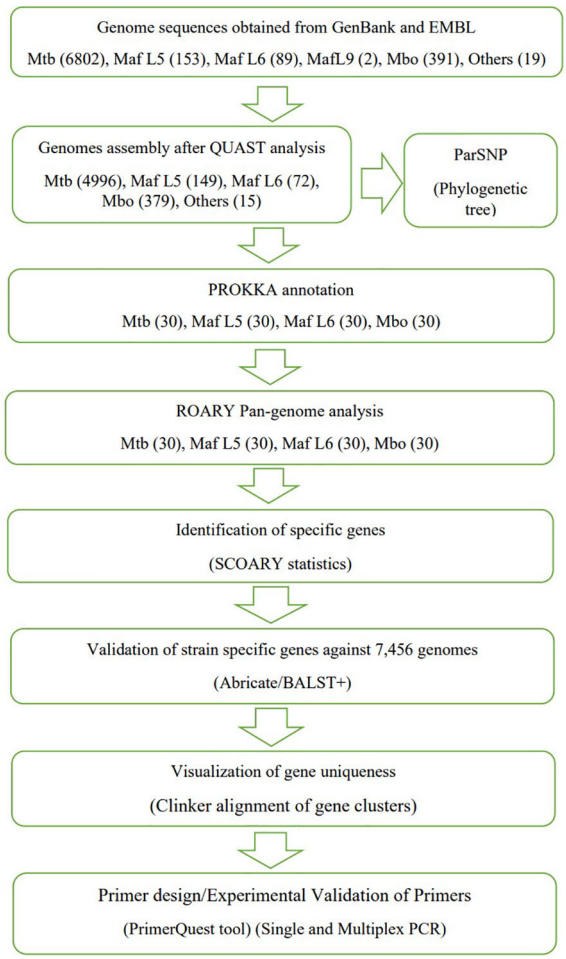

FIGURE 1
An overview of Scheme of work towards identification of lineage-specific genes for PCR primers development (similar to comparative genomic workflow previously described by Akwani et al., 2022).

Phylogenetic analysis of MTBC

ParSNP v. 1.2 was used as described previously (Pornsukarom et al., 2018) using the "-a 13 – x" settings to generate a phylogenetic tree of MTBC lineages. Classification of lineages was achieved based on the phylogenetic tree constructed. The output was visualised with FigTree version 1.4.3.

Comparative genomic analysis and identification of lineage-specific genes

Genomes were annotated using Prokka v1.14 (Seemann, 2014), while pangenomes were analyzed using Roary v3.12 (Page et al., 2015) at default settings and 90% BLAST cut-offusing randomly selected 120 genomes comprising *M. tuberculosis* (30), *M. africanum* L5 (30), *M. africanum* L6 (30) and *M. bovis* (30) (Supplementary Table S1). Scoary analysis (Brynildsrud et al., 2016) was used to examine the association between accessory (lineage-specific) genes and phenotypic traits. The number of lineage-specific genes was trimmed using statistical results from Bonferroni corrected p-value of ≤ 0.05. Also, lineage-specific genes were selected only if present in greater than 90% of the respective lineages and less than 10% in the other lineages. Further screening of the lineage-specific genes was performed by BLAST+ version 2.13.0 against all 7,456 MTBC genomes *via* Abricate v.1.0.9 (https://github.com/tseemann/abricate) with minimum coverage of 70% and minimum identity of 80% for a correct match. Genomic regions were compared to identify uniqueness using Clinker alignment of complete genomes (Gilchrist & Chooi, 2021).

Isolation of genomic DNA

The following reagents were obtained through BEI Resources, NIAID, NIH: genomic DNA from *M. africanum* strains NLA009502090, NR-49655 and *M. africanum* strain NLA000017316, NR-49652. Heat-killed *M. tuberculosis* (H37Rv) and *M. bovis* (AF2122/97) were obtained from liquid cultures prepared in the containment level 3 (CL3) lab before being transferred to the CL2 lab for DNA extraction. Genomic DNA of mycobacterial strains was extracted using the cetyltrimethylammonium bromide (CTAB)-chloroform method as described previously (Belisle et al., 2009). The concentration and purity of DNA was determined by the NanoDrop 2000 at absorbance of 260nm and purity A_{260}/A_{280} ratio of 1.7 to 2.0.

Primer design

Candidate genes identified were selected for primer design, using the PrimerQuest Tool developed by Integrated DNA Technologies (https://eu.idtdna.com/Primerquest). The FASTA format of each nucleotide sequence was inputted with PCR 2 primer options. Each primer was assigned a specific product size ranging from 100 to 1000 bp. Details of primers have been shown in Table 1.

Preparation of PCR assay

For the single PCR assays, a final volume of 25 µl was setup. Each setup contained 12.5 µl of 2x GoTaq® Hot Start Green Master Mix (400 µM polymerase, 400 µM of dNTPs, 4 mM $MgCl_2$ and pH 8.5 buffer), produced by Promega, UK, 1µl each of 10µM forward and reverse primers, 1 µl DNA (< 250 ng), 1 µl DMSO and nuclease free water. The non-template control consisted of the master mix, specific primers and nuclease free water, while 1 µl of *E.coli* DNA was used as negative control. For the multiplex PCR assays, a 50µl reaction volume was achieved with the following constituents: 25 µl of 2x GoTaq® Hot Start Green Master Mix, 5 µl of 10 µM of forward/reverse primers (1 µl of each lineage-specific primer), 1µl DNA (<250 ng), 2 µl DMSO and nuclease free water. An all-in-one multiplex PCR had 4 µl of DNA (1µl from each lineage). The reaction mix contained an excess of primers and nucleotides to ensure reaction continuity without limitation. The amplification

10.3389/fcimb.2023.1125079

TABLE 1 MTBC lineage-specific genes and primer sequences.

MTBC	Gene	Type of Primer	Sequence	Length	Tm	Amplicon (bp)
Mtb	*Rv1977*	forward	GTTTCCCGAGATCAGCTCAA	20	62	418
		reverse	CATCATCATCGTGCGGTACA	20	62	
	Rv2073c	forward	CGCTGCTCCGGTAGTAATTT	20	62	558
		reverse	CGCCCGATGACGAATCC	17	62	
	Rv2074	forward	GCGATGGTCAACACCACTA	19	62	133
		reverse	GGTCGAAGGTGAAACCTACC	20	62	
Maf (L5)	*Rv3347c*	forward	CGCGGAAGCCTTAGGAAAT	19	62	275
		reverse	ACGACCCGTTTATCAGCATC	20	62	
Maf (L6)	*Rv0186 (BglS)*	forward	CCGCAACTTCGAGTACCTTT	20	62	381
		reverse	ATACCGTTGTGGTGCTTGAG	20	62	
MTB Complex	*Rv3903c* (positive control)	forward	CGGATCGAACCACCAGAATC	20	62	636
		reverse	GGCCGGATTGTCTGTAAAGT	20	62	
Mbo*	*pncA*	forward	ATGCGGGCGTTGATCATCGTC	21	62	186
		reverse	CGGTGTGCCGGAGAAGTCG	19	62	

**M.bovis* primers designed from pyrazinamidase (pncA) by de los Monteros et al., 1998 were employed. The pncA gene carries a mutation within the genome of *M. bovis* but conserved in other MTBCs. There is a point mutation at the 169 nucleotide position which is occupied by guanine instead of cytosine.

was carried out in the SimpliAmp Thermal cycler at an initial denaturation of 2 mins at 95°C; 30 cycles of 30 sec at 95°C; 1 min at 62°C; 1 min at 72°C and a final extension at 72°C for 5 min. The separation of PCR products was performed using 2% gel agarose electrophoresis at 80 V for 1.30 hrs. A 100 bp DNA ladder was used as indicator. Visualization of gel was performed under ultraviolet light of Microtek MiBio Fluo version1.04.

Ethical clearance

Ethical approval for the use of human sputum samples was granted by the Committee on Human Research and Publication Ethics (CHRPE) at the School of Medical Science of Kwame Nkrumah University of Science and Technology (KNUST), Ghana: (CHRPE/AP/396/22).

Results

Stratification and identification of lineage-specific genes of the MTBC

A selection of 120 MTBC genomes (30 *M. tuberculosis*, 30 *M. africanum* L5, 30 *M. africanum* L6 and 30 *M. bovis*) from GenBank and EMBL repositories, were subjected to comparative genomic analysis. The phylogenetic relationship between the MTBCs was established with ParSNP which constructs a phylogenetic tree using core genome SNPs. In Figure 2, divisions were observed in four large clusters representing *M. tuberculosis*, *M. africanum* L5, *M. africanum* L6 and *M. bovis*. Pangenome analysis was performed on the same set of genomes to obtain the distribution of gene families within the MTBCs. A Roary matrix shows the clustering of 7,610 genes into either core genes (commonly shared by all members) or accessory genes (found in only few members) (Figure 1). It could be seen that almost all the genes are skewed toward the core gene section while

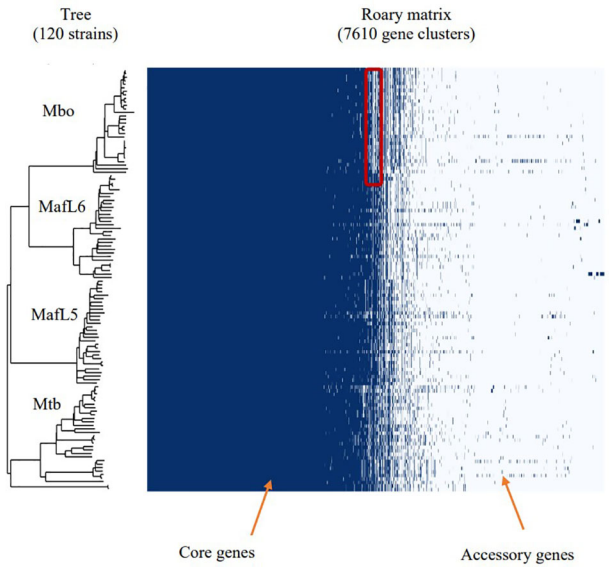

FIGURE 2
Phylogenetic tree together with pangenome distribution of genes within the MTBC – *M. tuberculosis*, *M. africanum* and *M. bovis*. The phylogenetic tree was constructed *via* identification of core genome SNPs using ParSNP tool. Roary matrix obtained from pangenome analysis shows the distribution of core and accessory genes within the MTBC. The highlighted section of the *M. bovis* genomes shows deletions which are characteristic of *M. bovis* as RD4, RD7, RD8, RD9 and RD12 deletions.

only a few were categorised as accessory genes. This type of gene distribution highlights the high level of clonality of the MTBC.

Further analysis was conducted on the pangenome outcome to ascertain the relationship between accessory genes and trait (lineages) using Scoary statistics. The definition of lineage-specific genes was set as being present in more than 90% of specific species and less than 10% in the other lineages. A total of 56 lineage-specific genes were obtained comprising 16 *M. africanum* L5, 10 *M. africanum* L6, 10 *M. tuberculosis* and 20 *M. bovis* specific genes (Supplementary Table S2). A final screening of these lineage-specific genes was performed by BLAST against 7,456 MTBC genomes *via* Abricate with a minimum coverage of 70% and minimum identity of 80% for a correct match as shown in Table 2. The candidate genes specific for *M. tuberculosis* were *Rv1977, Rv2073c and Rv2074.* The *Rv0186*-betaglucosidase was unique for *M. africanum* L6 while *Rv3903c* was conserved in all the MTBCs, thus serving as positive control marker. The Rv*3347c* was unique for *M. africanum* L5 *via* Clinker alignment of gene clusters shown in Figure 3. Although BLAST hits did not show any unique gene for *M. bovis*, the *pncA* gene highlighted to be distinctive in *M. bovis* by de los Monteros et al., 1998 was used.

Comparison of genomic regions by clinker

The uniqueness of lineage-specific genes was visualized by comparing gene clusters *via* Clinker software as shown in Figure 3. Variable regions of genes were observed to aid primers design.

Single PCR assays showing MTBC lineage-specificity

The primerQuest tool was used to design and assign all primers to different PCR product sizes for the purpose of differentiating the MTBCs in a multiplex PCR assay. Primers were screened and selected on the bases of sensitivity, specificity and compatibility. The *M. tuberculosis* specific primers designed from *Rv1977, Rv2073c* and *Rv2074* produced single amplification products of 418 bp, 558 bp and 133 bp specifically in reactions with *M. tuberculosis* DNA and not with other members of the MTBC (Figures 4A–C). Primers to the *Rv3347c* gene unique to *M. africanum* L5 produced a product band size of 275 bp specifically in reaction with *M. africanum* L5 DNA (Figure 4D), while *M. africanum* L6- *BgIS* primers amplified a fragment of 381 bp specifically from *M. africanum* L6 DNA (Figure 4E). For *M. bovis pncA* primers designed by de los Monteros et al., 1998 were used and produced an *M. bovis*-specific amplicon of 186 bp (Figure 4F). The positive control primers (*Rv3903c)* were also assigned to 636 bp (Figure 4G).

Multiplex PCR assay differentiating MTBC

Two forms of multiplex PCR assays were performed in a 50 µl reaction for each: Multiplex primers tested on each DNA sample (Figure 5A) and an "All in one" reaction i.e., combination of all primers with mixture of all DNA samples (Figure 5B). All expected amplification products were observed without any extra products formations.

Limits of detection (LOD) of PCR assays

PCR experiments were performed using the identified lineage-specific primers against their respective DNA samples to identify the least amount of DNA required for amplification. *M. africanum* L5, *M. africanum* L6 and *M. bovis* recorded LOD of 0.003 ng/µl which equates to 620 genome copy numbers, while *M. tuberculosis* was detected at 0.012 ng/µl or 2479 copy numbers as shown in Table 3.

Specificity of MTBC primers against other pathogens

In view of misdiagnoses of tuberculosis with other respiratory pathogens such as a range of non-tuberculous mycobacteria (NTM)

TABLE 2 Summary of Abricate BLAST results showing MTBC lineage-specific genes.

Gene ID	MafL5	MafL6	Mbo	Mtb	*Others	Name of gene in official H37Rv	Remarks
MAFGCA_01990	0.0	98.6	0.0	0.0	0.0	*Bgls (Rv0186)*	L6 specific
MTBH37Rv_02010	100.0	0.0	98.9	100.0	100.0		not L6
MTBH37Rv_13290	100.0	100.0	0.0	99.6	75.0		not Mbo
MTBH37Rv_13300	100.0	100.0	0.0	100.0	75.0		not Mbo
MTBH37Rv_15940	0.0	100.0	0.0	99.6	100.0		not L5/Mbo
MTBH37Rv_20850	0.7	0.0	0.0	100.0	8.3	*Rv1977*	Mtb-specific
MTBH37Rv_21880	0.7	0.0	0.0	100.0	8.3	*Rv2073c*	Mtb-specific
MTBH37Rv_21890	0.7	0.0	0.0	100.0	8.3	*Rv2074*	Mtb-specific
MTBH37Rv_41080	100.0	100.0	99.1	99.6	91.7	*Rv3903c*	positive control gene

*Others = genomes of animal-adapted ecotypes of the MTBC (M. microti, M. pennipedii, M. orygis, M. caprae, M. mungi).

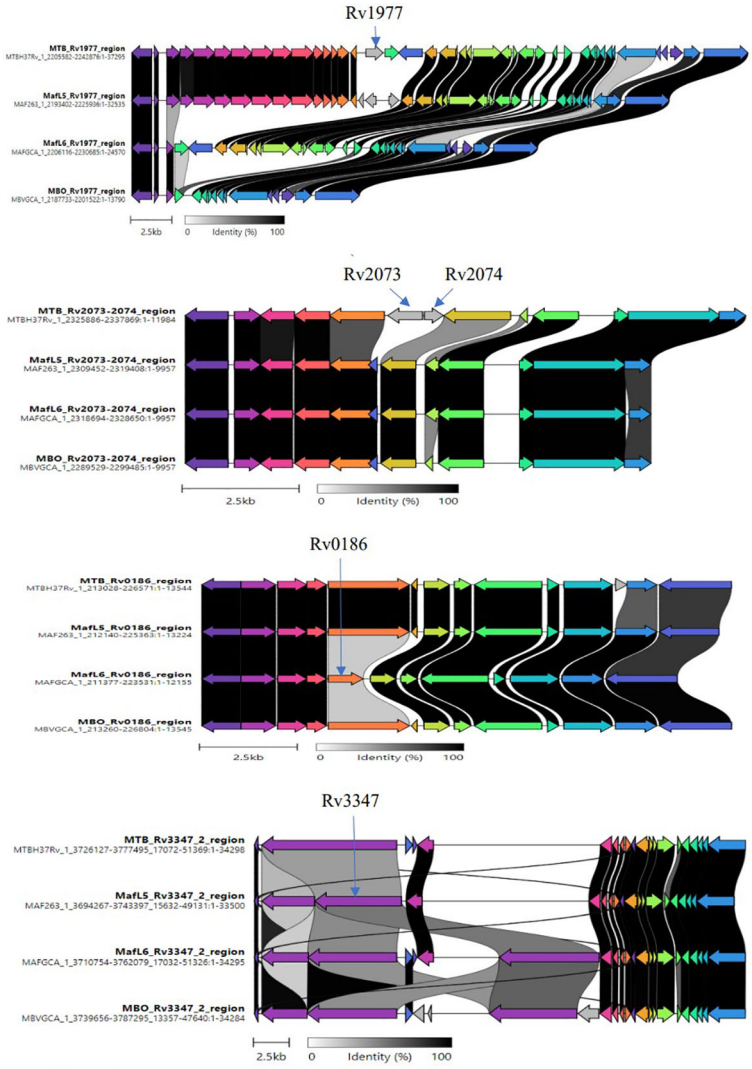

FIGURE 3
Clinker showing variations of lineage-specific genes *via* alignment of gene clusters. Variable regions of the identified unique genes were examined through the alignment of gene clusters from members of the MTBC (*M. tuberculosis, M. africanum* L5/L6, *M. bovis*).

(Yılmaz et al., 2017), cross-reactivity experiments involving testing primers against other microorganisms was conducted. NTMs obtained from Reference Centre for Mycobacteria, Borstel-Germany were used for the cross-reactivity study. The MTBC primers did not show any cross reactivity since negative PCR test results were obtained against all non-MTBC DNAs (Supplementary Table S4). Furthermore, PCR test results of other respiratory pathogens comprising a cocktail of bacteria and viruses (22 targets) also recorded negative (Supplementary Table S5). Details of various bacterial and viral analytes are shown in Supplementary Table S3.

Validation of multiplex PCR assay using clinical samples

A total of 341 retrospective sputum samples from TB patients in Ghana were used for the validation of PCR assays. These samples have been confirmed TB positive using sputum smear microscopy, GeneXpert MTB/RIF assay and culture (BD BACTEC Mycobacterium Growth Indicator Tube- MGIT) methods based on previous studies conducted on TB drug resistance surveillance in Ghana (Sylverken et al., 2021). Sputum samples were decontaminated by treating with 4% N-Acetyl-L-Cysteine-Sodium-Hydroxide (NALC-NaOH) before neutralizing with 1X phosphate-buffered saline (PBS). DNA extraction was performed using the GenoLYSE extraction kit and followed by the multiplex PCR assay procedure described earlier. The results showed that *M. tuberculosis* contributes to a quarter (24.9%) of the cases, *M. africanum* L5 and *M. africanum* L6 were identified with 9.1% and 14.4% respectively, while *M. bovis* recorded only 1.8% of the cases. Interestingly, there was an observation of mixed-lineage TB infections at 5.9%. Also, 27.0% and 17.0% of the cases were PCR negative and unspeciated respectively, which may have been due to the extremely low concentration of DNA in some samples.

10.3389/fcimb.2023.1125079

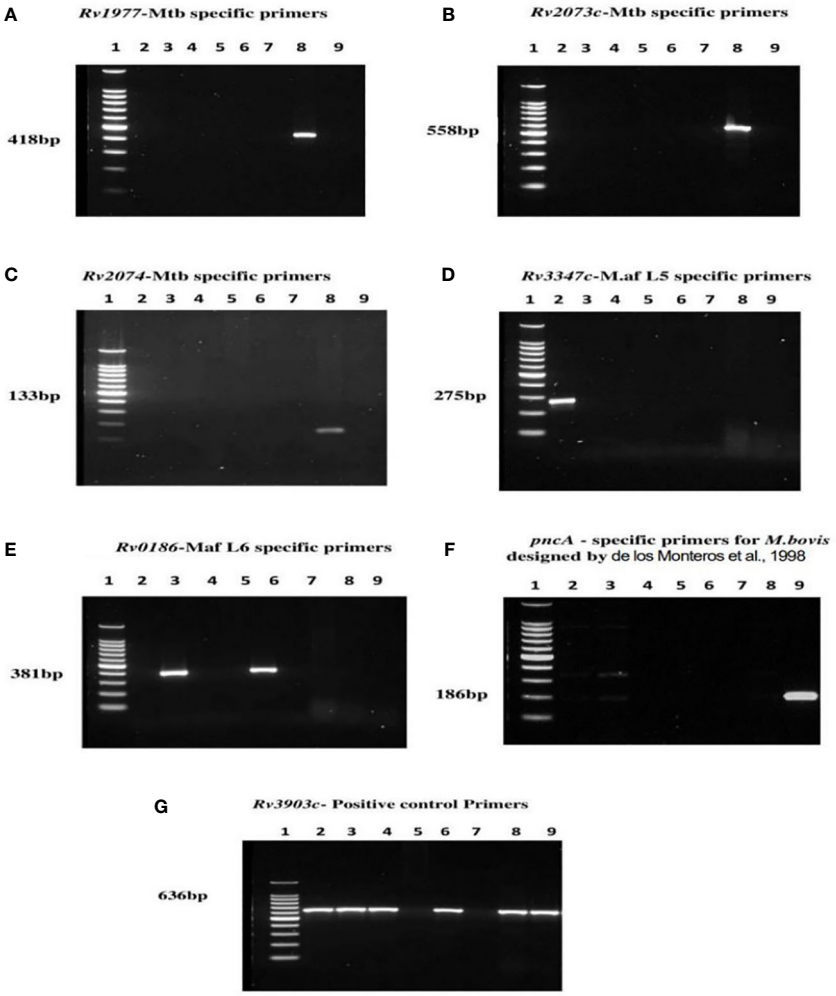

FIGURE 4
PCR results of MTBC specific lineages after optimization of various product sizes; Lane 1= DNA ladder, 2= *M. africanum* L5, 3= *M. africanum* L6 (isolate a), 4=BCG, 5= *E. coli*, 6= *M. africanum* L6 (isolate b), 7= water, 8= *M. tuberculosis* and 9= *M. bovis*. Each of the primers was tested against genomic DNA of all MTBCs for specificity. DNA of *E. coli* and nuclease-free water were used as negative and non-template controls respectively. Optimum separation of PCR products was achieved with 2% agarose gel at 80V, 1hr:30mins. Primers designed from genes; **(A)** *Rv1977*, **(B)** *Rv2073c*, and **(C)** *Rv2074* amplifying at 418 bp, 558 bp and 133 bp respectively were specific for Mtb. The *M. africanum* L5 and *M. africanum* L6 primers were set at 275 bp and 381bp respectively as shown in **(D, E)**. Primers developed from *pncA* gene by de los Monteros et al., 1998 were used for *M. bovis* identification **(F)** at 186 bp. The **(G)** *Rv3903c* primers at 636 bp served as positive control since it was conserved in all MTBCs.

Discussion

The ability to differentiate between the lineages of the MBTC is very important in TB management because it provides reliable information for epidemiological surveillance and treatment choice. In this study, MTBC have been phylogenetically classified leading to the identification of lineage-specific genes. These lineage-specific genes have been explored for the development of a multiplex PCR assay which distinguishes between members of the MTBC.

In low resource regions, Ziehl-Neelsen acid-fast staining microscopy is the most common technique used to diagnose TB (Denkinger et al., 2013). It requires about 5,000 – 10,000 bacilli per ml of sputum for successful detection (Ausina Ruiz et al., 2013). Thus, its limitations are low sensitivity as well as the inability to differentiate between different mycobacterial species. Although culture, biochemical tests and sequencing are considered gold standard for identification and differentiation (Gholoobi et al., 2014), these are expensive, laborious and time-consuming. Additionally, obtaining results from these methods are sometimes unreliable due to difficulty in identification of some lineages (*M. africanum* lineages exhibit growth characteristics which are intermediates of *M. tuberculosis* and *M. bovis*) (de Jong et al., 2010a). The advent of genome sequencing techniques has provided relevant data for performing extensive genomic analyses. As a result, several molecular-based assays have been designed to detect MTBCs. These methods are highly sensitive and specific because unique gene sequences are targeted for amplification. Researchers have discovered gene markers such as IS*6110, hsp65, dnaJ, psbA, lepA* and *MPT64* to detect MTBCs against other respiratory pathogens such NTMs (Chin et al., 2018). A recent multiplex PCR assay (Akwani et al., 2022) demonstrated successful separation of *Mycobacterium abscessus* complex subspecies from

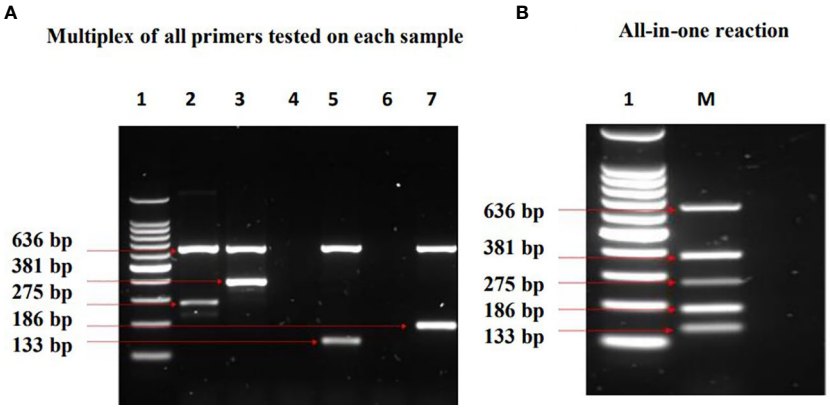

FIGURE 5
Results of Multiplex PCR assays which show identification of the MTBC lineages investigated. Lane 1= DNA ladder, 2= *M. africanum* L5, 3= *M. africanum* L6 (isolate a), 4= *E. coli*, 5= *M. tuberculosis*, 6= water, 7= *M. bovis*, M=mixture of all samples. In **(A)** multiplex of all primers tested on each DNA sample, two bands were observed in each of the MTBC as expected. The band at 636 bp (positive control) is conserved in all the MTBCs, whereas the other band depicts the respective lineage-specific band. Bands at 275 bp and 381 bp denote *M. africanum* L5 and L6 specificity respectively, while Mtb was represented at 133 bp. *M. bovis* was identified at 186 bp. In **(B)** All in one reaction; the compatibility and specificity of the assay was ascertained by combining all primers with mixtures of *M. tuberculosis, M. africanum* L5 & L6, and *M. bovis.* The outcome depicts a successful differentiation of the MTBCs without any inhibition.

other NTMs as well as *M. tuberculosis*, although evaluation of assay performance in clinical samples needs to be carried out. Since 2010, WHO has recommended the use of GeneXpert MTB/RIF assay as the first-line diagnostic tool which detects MTBC together with rifampicin resistance (Goig et al., 2019). This is a molecular approach based on detection of the repetitive elements *IS6110* and IS*1081* and rifampicin resistance region. However, misdiagnoses of TB using the GeneXpert assay have been observed in NTM species at a high bacterial load (Pang et al., 2017). In TB endemic areas with infections caused by a diversity of MTBC species, a suitable differential diagnostic approach will be required since GeneXpert lacks the ability to distinguish between MTBC lineages.

In West Africa, MTBC classification has been achieved using spoligotyping technique which involves the amplification of direct repeat copies, followed by hybridization into intergenic spacers experiments (De Jong et al., 2009; de Jong et al., 2010b; Ofori-Anyinam et al., 2016; Otchere et al., 2018; Otchere et al., 2019). This is a two-step approach which is expensive, laborious and time-consuming. In Ghana, a single multiplex PCR experiment was conducted on the MTBC differentiation using primers from spacer regions 33 and 34 of the DR copies of MTBC, *IS6110* and the *hsp65* (Yeboah-Manu et al., 2001). Although this assay is not successful in separation of *M. tuberculosis* from *M. africanum* L6, the assay could still be used to complement biochemical testing.

TABLE 3 Results showing LOD of PCR assays.

MTBC	LOD (ng/µl)	LOD (DNA copies/µl)
MafL5	0.003	620
MafL6	0.003	620
Mtb	0.012	2479
Mbo	0.003	620

A 10-fold serial dilution of DNA samples was used for the PCR to observe the least concentration at which amplification could still be achieved. DNA copy numbers were estimated using formula: (weight in ng x 6.0221x 10^{23}molecules/moles)/[(genome length x 660g/mole) x 1 x 10^{9}ng/g].

However, the present study introduces a successful differentiation of MTBCs *via* a single multiplex PCR method which is rapid, cost effective and has a short turnaround time. The different PCR product sizes can be easily used to distinguish between lineages without the need for sequencing. One advantage of this PCR assay is the ease of adapting it to the available hardware as it will work on any PCR platform. This new assay provides a reliable solution to misdiagnoses with other NTM infections reported in some endemic regions (Brown-Elliott et al., 2012; Yılmaz et al., 2017; He et al., 2022). Indeed, our assay did not cross-react with a range of NTMs, respiratory bacterial and viral pathogens (Supplementary Tables S4, S5). We tested our assay using clinical samples (Table 4; Supplementary Figure S1) to demonstrate its utility at revealing the diversity of MTBC lineages in Ghana. The highest number of cases (24.9%) was caused by *M. tuberculosis*, followed by *M. africanum* L5 & L6 (23.5%). *M. bovis* recorded 1.8% which is comparable to 1.5% observed by Otchere et al., 2019. Negative PCR results (27.0%) and unspeciated lineages (17.0%) may require further confirmation *via* genome sequencing, although samples have been previously detected as MTBCs by liquid cultures, followed by confirmations using purity tests (on blood agar) and rapid test kit (TB cID) (Sylverken et al., 2021). However, since these are retrospective samples stored over time, sample integrity may have been compromised through repeated freeze/thaw cycles which were beyond our control. Following the reports of mixed MTBC infections among high TB burden settings (Van Rie et al., 2005; Huyen et al., 2012; Zetola et al., 2014), this study detected 20 (5.9%) cases of mixed-lineage TB infections. Poor treatment outcomes have been strongly associated with mixed-lineage TB infections (Zetola et al., 2014). Therefore, the effect of mixed-lineage TB infections in TB management cannot be

TABLE 4 Results of multiplex PCR validation using samples from 341 active TB patients in Ghana.

Target	Number	Percentage (%)
M. tuberculosis	85	24.9
M. bovis	6	1.8
M. africanum L5	31	9.1
M. africanum L6	49	14.4
M. africanum L5/*M. tuberculosis*	6	1.8
M. africanum L5/*M. africanum* L6	5	1.5
M. africanum L6/*M. tuberculosis*	5	1.5
M. bovis/*M. africanum* L6	2	0.6
M. bovis/*M. tuberculosis*	2	0.6
Unspeciated species (only positive for control marker)	58	17.0
MTBC negative	92	27.0
TOTAL	341	100

overlooked as treatment failures are often observed in various regions of Ghana (Agyare et al., 2021).

In summary, this assay is not an alternate replacement for GeneXpert which is currently the first-line TB diagnostic tool recommended by WHO. However, it will be beneficial to low-resource regions where TB is caused by diverse members of the MTBC providing rapid diagnosis to inform appropriate TB drug selection, reduce treatment relapse and the development of antimicrobial resistance. It will also be useful in epidemiological surveillance studies providing reliable information on TB lineage prevalence as well as identifying cases of mixed-lineage tuberculosis infections.

Data availability statement

The original contributions presented in the study are included in the article/Supplementary Material. Further inquiries can be directed to the corresponding authors.

Author contributions

The concept and study design were established by SH-W, AS, NR, and GS. Bioinformatic analyses was performed by AvV. Assay optimization by WO, WA, and SH-W. Assay validation using clinical samples was performed in Ghana by RA, SA, and AS. Manuscript writing and editing were done by WO, AS, AvV, GS, and SH-W. All authors contributed to the article and approved the submitted version.

Funding

This research was financially supported by the Vice Chancellor's Studentship Award from the University of Surrey and the Global Challenges Research Fund.

Acknowledgments

We would like to say thank you to Reference Centre for Mycobacteria, Borstel-Germany for providing NTM strains used in the cross-reactivity experiment as well as the management of TB DRS Ghana project for supporting with clinical sputum samples. Thank you to BEI resources for providing the *M. africanum* DNA samples used in this study.

Conflict of interest

The authors declare that the research was conducted in the absence of any commercial or financial relationships that could be construed as a potential conflict of interest.

Publisher's note

Supplementary material

The Supplementary Material for this article can be found online at: https://www.frontiersin.org/articles/10.3389/fcimb.2023.1125079/full#supplementary-material

References

Agyare, S. A., Osei, F. A., Odoom, S. F., Mensah, N. K., Amanor, E., Martyn-Dickens, C., et al. (2021). Treatment outcomes and associated factors in tuberculosis patients at atwima nwabiagya district, Ashanti region, Ghana: A ten-year retrospective study. *Tuberc. Res. Treat.* 2021, 1–9. doi: 10.1155/2021/9952806

Akwani, W. C., van Vliet, A. H. M., Joel, J. O., Andres, S., Diricks, M., Maurer, F. P., et al. (2022). The use of comparative genomic analysis for the development of subspecies-specific PCR assays for mycobacterium abscessus. *Front. Cell. Infect. Microbiol.* 12. doi: 10.3389/FCIMB.2022.816615/BIBTEX

Ali, M. H., Alrasheedy, A. A., Kibuule, D., Godman, B., and Hassali, M. A. (2019). Assessment of multidrug-resistant tuberculosis (MDR-TB) treatment outcomes in sudan; findings and implications. *Expert Rev. Anti Infect. Ther.* 17, 927–937. doi: 10.1080/14787210.2019.1689818

Ausina Ruiz, V., Fernández-Rivas, G., and Vilaplana Messeguer, C. (2013). Selected culture and drug-susceptibility testing methods for drug-resistant mycobacterium tuberculosis screening in resource-constrained settings. *Expert Rev. Mol. Diagn.* 13, 247–249. doi: 10.1586/erm.13.10

Belisle, J. T., Mahaffey, S. B., and Hill, P. J. (2009). "Isolation of mycobacterium species genomic DNA," in *Mycobacteria protocols*, *2nd ed*. Eds. T. Parish and A. C. Brown (Totowa, NJ: Humana Press), 1–12.

Brown-Elliott, B. A., Nash, K. A., and Wallace, R. J. (2012). Antimicrobial susceptibility testing, drug resistance mechanisms, and therapy of infections with nontuberculous mycobacteria. *Clin. Microbiol. Rev.* 25, 545–582. doi: 10.1128/CMR.05030-11

Brynildsrud, O., Bohlin, J., Scheffer, L., and Eldholm, V. (2016). Rapid scoring of genes in microbial pan-genome-wide association studies with scoary. *Genome Biol.* 17, 1–9. doi: 10.1186/S13059-016-1108-8/FIGURES/4

Chin, K. L., Sarmiento, M. E., Norazmi, M. N., and Acosta, A. (2018). DNA Markers for tuberculosis diagnosis. *Tuberculosis* 113, 139–152. doi: 10.1016/j.tube.2018.09.008

Cohen, T., Wilson, D., Wallengren, K., Samuel, E. Y., and Murray, M. (2011). Mixed-strain mycobacterium tuberculosis infections among patients dying in a hospital in KwaZulu-natal, south Africa. *J. Clin. Microbiol.* 49, 385. doi: 10.1128/JCM.01378-10

de Jong, B. C., Adetifa, I., Walther, B., Hill, P. C., Antonio, M., Ota, M., et al. (2010a). Differences between tuberculosis cases infected with *Mycobacterium africanum* , West African type 2, relative to Euro-American *Mycobacterium tuberculosis*: An update. *FEMS Immunol. Med. Microbiol.* 58, 102–105. doi: 10.1111/j.1574-695X.2009.00628.x

De Jong, B. C., Antonio, M., Awine, T., Ogungbemi, K., De Jong, Y. P., Gagneux, S., et al. (2009). Use of spoligotyping and large sequence polymorphisms to study the population structure of the mycobacterium tuberculosis complex in a cohort study of consecutive smear-positive tuberculosis cases in the Gambia. *J. Clin. Microbiol.* 47, 994–1001. doi: 10.1128/JCM.01216-08

de Jong, B. C., Antonio, M., and Gagneux, S. (2010b). Mycobacterium africanum-review of an important cause of human tuberculosis in West Africa. *PloS Negl. Trop. Dis.* 4, e744. doi: 10.1371/journal.pntd.0000744

de los Monteros, L. E. E., Galán, J. C., Gutiérrez, M., Samper, S., García Marín, J. F., Martín, C, et al. (1998). Allele-specific PCR method based on pncA and oxyR sequences for distinguishing mycobacterium bovis from mycobacterium tuberculosis: Intraspecific m. bovis pncA sequence polymorphism. *J. Clin. Microbiol.* 36, 239–242. doi: 10.1128/JCM.36.1.239-242.1998

Denkinger, C. M., Kik, S. V., and Pai, M. (2013). Robust, reliable and resilient: designing molecular tuberculosis tests for microscopy centers in developing countries. *Expert Rev. Mol. Diagn.* 13, 763–767. doi: 10.1586/14737159.2013.850034

Gholoobi, A., Masoudi-Kazemabad, A., and Meshkat, Z. (2014). Comparison of culture and PCR methods for diagnosis of mycobacterium tuberculosis in different clinical specimens. *Jundishapur. J. Microbiol.* 7, 8939. doi: 10.5812/jjm.8939

Gilchrist, C. L. M., and Chooi, Y. H. (2021). Clinker & clustermap.js: Automatic generation of gene cluster comparison figures. *Bioinformatics* 37, 2473–2475. doi: 10.1093/BIOINFORMATICS/BTAB007

Goig, G. A., Torres-Puente, M., Mariner-Llicer, C., Villamayor, L. M., Chiner-Oms, Á., Gil-Brusola, A., et al. (2019). Towards next-generation diagnostics for tuberculosis: identification of novel molecular targets by large-scale comparative genomics. *Bioinformatics* 36, 985–989. doi: 10.1093/bioinformatics/btz729

Gurevich, A., Saveliev, V., Vyahhi, N., and Tesler, G. (2013). QUAST: quality assessment tool for genome assemblies. *Bioinformatics* 29, 1072–1075. doi: 10.1093/BIOINFORMATICS/BTT086

He, Y., Wang, J. L., Zhang, Y. A., and Wang, M. S. (2022). Prevalence of culture-confirmed tuberculosis among patients with nontuberculous mycobacterial disease. *Infect. Drug Resist.* 15, 3097–3101. doi: 10.2147/IDR.S363765

Hingley-Wilson, S. M., Casey, R., Connell, D., Bremang, S., Evans, J. T., Hawkey, P. M., et al. (2013). Undetected multidrug-resistant tuberculosis amplified by first-line therapy in mixed infection. *Emerg. Infect. Dis.* 19, 1138–1141. doi: 10.3201/1907.130313

Huyen, M. N. T., Kremer, K., Lan, N. T. N., Cobelens, F. G. J., Buu, T. N., Dung, N. H., et al. (2012). Mixed tuberculosis infections in rural south Vietnam. *J. Clin. Microbiol.* 50, 1586–1592. doi: 10.1128/JCM.00434-12

Khalif Ali, M., Karanja, S., Karama, M., and Kenyatta, J. (2017). Factors associated with tuberculosis treatment outcomes among tuberculosis patients attending tuberculosis treatment centres in 2016-2017 in Mogadishu, Somalia. *Pan. Afr. Med. J.* 28, 197. doi: 10.4314/pamj.v28i1

Lan, Z., Bastos, M., and Menzies, D. (2016). Treatment of human disease due to mycobacterium bovis: A systematic review. *Eur. Respir. J.* 48, 1500–1503. doi: 10.1183/13993003.00629-2016

Mostowy, S., Onipede, A., Gagneux, S., Niemann, S., Kremer, K., Desmond, E. P., et al. (2004). Genomic analysis distinguishes mycobacterium africanum. *J. Clin. Microbiol.* 42, 3594–3599. doi: 10.1128/JCM.42.8.3594-3599.2004

Ofori-Anyinam, B., Kanuteh, F., Agbla, S. C., Adetifa, I., Okoi, C., Dolganov, G., et al. (2016). Impact of the mycobaterium africanum West Africa 2 lineage on TB diagnostics in West Africa: Decreased sensitivity of rapid identification tests in the Gambia. *PloS Negl. Trop. Dis.* 10, e0004801. doi: 10.1371/journal.pntd.0004801

Oryan, A., Yazdi, H. S., Alidadi, S., and Doostmohammadi, S. (2022). Use of a gyrB PCR-RFLP method to diagnose tuberculosis and identify the causative mycobacterium sp. in cattle and humans. *Comp. Immunol. Microbiol. Infect. Dis.* 82, 101767. doi: 10.1016/J.CIMID.2022.101767

Otchere, I. D., Coscollá, M., Sánchez-Busó, L., Asante-Poku, A., Brites, D., Loiseau, C., et al. (2018). Comparative genomics of mycobacterium africanum lineage 5 and lineage 6 from Ghana suggests distinct ecological niches. *Sci. Rep.* 8, 1–11. doi: 10.1038/s41598-018-29620-2

Otchere, I. D., van Tonder, A. J., Asante-Poku, A., Sánchez-Busó, L., Coscollá, M., Osei-Wusu, S., et al. (2019). Molecular epidemiology and whole genome sequencing analysis of clinical mycobacterium bovis from Ghana. *PloS One* 14, e0209395. doi: 10.1371/journal.pone.0209395

Page, A. J., Cummins, C. A., Hunt, M., Wong, V. K., Reuter, S., Holden, M. T. G., et al. (2015). Roary: Rapid large-scale prokaryote pan genome analysis. *Bioinformatics* 31, 3691–3693. doi: 10.1093/BIOINFORMATICS/BTV421

Pang, Y., Lu, J., Su, B., Zheng, H., and Zhao, Y. (2017). Misdiagnosis of tuberculosis associated with some species of nontuberculous mycobacteria by GeneXpert MTB/RIF assay. *Infection* 45, 677–681. doi: 10.1007/s15010-017-1044-x

Papastavros, T., Dolovich, L. R., Holbrook, A., Whitehead, L., and Loeb, M. (2002). Adverse events associated with pyrazinamide and levofloxacin in the treatment of latent multidrug-resistant tuberculosis. *Can. Med. Assoc. J.* 167, 131.

Pornsukarom, S., van Vliet, A. H. M., and Thakur, S. (2018). Whole genome sequencing analysis of multiple salmonella serovars provides insights into phylogenetic relatedness, antimicrobial resistance, and virulence markers across humans, food animals and agriculture environmental sources. *BMC Genomics* 19, 801. doi: 10.1186/s12864-018-5137-4

PrimerQuest Tool *IDT*. Available at: https://eu.idtdna.com/Primerquest/Home/Index (Accessed June 18, 2022).

Seemann, T. (2014). Prokka: Rapid prokaryotic genome annotation. *Bioinformatics* 30, 2068–2069. doi: 10.1093/BIOINFORMATICS/BTU153

SRA-Tools-NCBI (2021). Available at: https://ncbi.github.io/sra-tools/fastq-dump.html (Accessed June 22, 2021).

Sylverken, A. A., Kwarteng, A., Twumasi-Ankrah, S., Owusu, M., Arthur, R. A., Dumevi, R. M., et al. (2021). The burden of drug resistance tuberculosis in ghana; results of the first national survey. *PloS One* 16, e0252819. doi: 10.1371/JOURNAL.PONE.0252819

Van Rie, A., Victor, T. C., Richardson, M., Johnson, R., van der Spuy, G. D., Murray, E. J., et al. (2005). Reinfection and mixed infection cause changing mycobacterium tuberculosis drug-resistance patterns. *Am. J. Respir. Crit. Care Med.* 172, 636. doi: 10.1164/RCCM.200503-449OC

WHO (2020) *Global tuberculosis report 2020: executive summary*. Available at: http://apps.who.int/bookorders (Accessed January 5, 2021).

Yeboah-Manu, D., Yates, M. D., and Wilson, S. M. (2001). Application of a simple multiplex PCR to aid in routine work of the mycobacterium reference laboratory. *J. Clin. Microbiol.* 39, 4166–4168. doi: 10.1128/JCM.39.11.4166-4168.2001

Yılmaz, N., Uçar, E. Y., and Sağlam, L. (2017). Mycobacterium tuberculosis and nontuberculous mycobacteria coinfection of the lungs. *Turkish Thorac. J.* 18, 23. doi: 10.5152/TURKTHORACJ.2017.16034

Zetola, N. M., Shin, S. S., Tumedi, K. A., Moeti, K., Ncube, R., Nicol, M., et al. (2014). Mixed mycobacterium tuberculosis complex infections and false-negative results for rifampin resistance by GeneXpert MTB/RIF are associated with poor clinical outcomes. *J. Clin. Microbiol.* 52, 2422. doi: 10.1128/JCM.02489-13

frontiers | Frontiers in Cellular and Infection Microbiology

TYPE Original Research
PUBLISHED 18 July 2023
DOI 10.3389/fcimb.2023.1192002

OPEN ACCESS

EDITED BY
Laura Cerqueira,
University of Porto, Portugal

REVIEWED BY
Mehmet Doganay,
Lokman Hekim University, Türkiye
Fabrice Compain,
L'Institut Mutualiste Montsouris, France

*CORRESPONDENCE
Paul-Antoine Chatelard
pachatelard@saintjosephsaintluc.fr

RECEIVED 22 March 2023
ACCEPTED 27 June 2023
PUBLISHED 18 July 2023

CITATION
Chatelard P-A, Rousseau N, Parmeland L, Metral P, Pariset C and Vivier E (2023) Shortening identification times: comparative observational study of three early blood culture testing protocols. *Front. Cell. Infect. Microbiol.* 13:1192002. doi: 10.3389/fcimb.2023.1192002

Shortening identification times: comparative observational study of three early blood culture testing protocols

Paul-Antoine Chatelard[1]*, Nathalie Rousseau[2], Laurence Parmeland[2], Pierre Metral[3], Caroline Pariset[4] and Emmanuel Vivier[1,5]

[1]Centre Hospitalier Saint Joseph Saint Luc, Médecine Intensive Réanimation, Lyon, France, [2]Centre Hospitalier Saint Joseph Saint Luc, Laboratoire de biologie médicale, Lyon, France, [3]Centre Hospitalier Saint Joseph Saint Luc, Département d'Information Médicale, Lyon, France, [4]Centre Hospitalier Saint Joseph Saint Luc, Maladies Infectieuses, Lyon, France, [5]Centre Hospitalier Saint Joseph Saint Luc, Unité de Recherche Clinique, Lyon, France

Background: While early appropriate antibiotic therapy is a proven means of limiting the progression of infections, especially bacteremia, empirical antibiotic therapy in sepsis is ineffective up to 30%. The aim of this study was to compare early blood culture testing protocols in terms of their ability to shorten the delay between blood sampling and appropriate antibiotic therapy.

Methods: In this french observational study, we compared three blood culture testing protocols. Positive blood cultures were tested using either GenMark ePlex panels (multiplex PCR period), a combination of MRSA/SA PCR, β-Lacta and oxidase tests (multitest period), or conventional identification and susceptibility tests only (reference period). Conventional identification and susceptibility tests were performed in parallel for all samples, as the gold standard.

Results: Among the 270 patients with positive blood cultures included, early and conventional results were in good agreement, especially for the multitest period. The delay between a blood culture positivity and initial results was 3.8 (2.9–6.9) h in the multiplex PCR period, 2.6 (1.3–4.5) h in the multitest period and 3.7 (1.8–8.2) h in the reference period ($p<0.01$). Antibiotic therapy was initiated or adjusted in 68 patients based on early analysis results. The proportion of patients receiving appropriate antibiotic therapy within 48 h of blood sampling was higher in the multiplex PCR and multitest periods, (respectively 90% and 88%) than in the reference period (71%).

Conclusion: These results suggest rapid bacterial identification and antibiotic resistance tests are feasible, efficient and can expedite appropriate antibiotic therapy.

KEYWORDS

bacteremia, MRSA/SA PCR, ePlex assay, β-Lacta test, oxidase test

Background

Bloodstream infections are associated with high morbidity and mortality and the increase in multidrug resistant pathogens has made them increasingly difficult to treat (Rhodes et al., 2017; Robineau et al., 2018; Cassini et al., 2019). Identifying causative pathogens is crucial to optimize treatment and patient outcomes (Seifert, 2009); however, conventional identification and antimicrobial susceptibility tests are time-consuming, with results only available 48–72 h after blood culture collection (Miller et al., 2018; CASFM/EUCAST, 2019). Although empirical antibiotic therapy can be adjusted based on the Gram stain and bacterial species results 24–48 h after bacterial growth positivity, a further 24–48 h is required for definitive susceptibility results to confirm or correct the antibiotic therapy. This delay between blood sampling and appropriate antibiotic therapy is a cornerstone in the management of patients with sepsis and should be reduced as much as possible (Rivers et al., 2001; Rhodes et al., 2017). Up to 20 or 30% of patients with sepsis are initially treated with inappropriate empirical antibiotic therapy (Yokota et al., 2014), and delayed or inappropriate antibiotic therapy is strongly associated with mortality (Kollef, 2000; Leone et al., 2003; Kumar, 2010; Rhodes et al., 2017; Robineau et al., 2018). New, potentially more efficient techniques based on multiplex PCR (m-PCR), targeted gene sequencing or enzymatic activity testing are particularly interesting in this context.

In this study, we compared in three consecutive periods, three blood culture testing strategies based on m-PCR and multiple rapid tests with conventional Gram staining, to investigate whether the new approaches are feasible and shorten the time to appropriate antibiotic therapy. The main objective of the study was to determine the feasibility and performance of multiple rapid tests and m-PCR tests in clinical practice and compare the effectiveness of the two methods. The secondary objective was to determine whether either approach reduced the delay between blood sampling and appropriate antibiotic therapy.

Materials and methods

Study design

This observational study included all patients older than 18 years with positive blood cultures treated in two non-university hospitals in Lyon, France between 1 March and 20 September 2019. Between 1 March and 30 April 2019 (the m-PCR period), blood cultures were tested using GenMark ePlex blood culture identification panels, between 30 April and 21 July 2019 (the reference period), blood cultures were tested by conventional methods, and between 22 July and 20 September 2019 (the multitest period), a combination of rapid MRSA/SA PCR, β-Lacta and oxidase tests (Figure 1). All early analysis (m-PCR, rapid tests and Gram stain), were performed 24 hours a day and 7 days a week. The same number of cultures were analyzed in each period. For safety reasons and to evaluate the performance of the rapid techniques, conventional identification and susceptibility tests were performed in parallel on all samples as the gold standard. All tests were performed in the same laboratory (Saint-Joseph-Saint-Luc Hospital, Lyon, France). Additional details are provided in the Supplemental Material.

Abbreviations: ICU, intensive care unit; MRSA, methicillin-resistant *Staphylococcus aureus*; PCR, polymerase chain reaction; m-PCR, multiplex polymerase chain reaction; SA, *Staphylococcus aureus*; SAPS 2, simplified acute physiology score 2.

Laboratory procedures

All blood samples were immediately incubated on a round-the-clock basis in a BACT/ALERT 3D instrument (BioMérieux, France) and Gram staining was immediately performed on positive cultures. Bacterial identification and antimicrobial susceptibility tests were then performed on positive blood cultures by microbiology laboratory staff during working hours (Mon.–Fri., 8 a.m. to 7 p.m.; Sat., 8 a.m. to 1 p.m.) using a VITEK 2 system (BioMérieux, France).

During the m-PCR period, blood cultures were tested using the ePlex blood culture identification panel system (GenMark Diagnostics, Carlsbad, CA, USA) (Schmitz and Tang, 2018). The ePlex blood culture identification panel (EU CE-IVD certification in 2017) consists of three separate cartridges for gram positive, gram negative, and fungal pathogens, and several genus- and/or species-level probes. The gram-positive and gram-negative cartridges also include several probes of key antimicrobial resistance genes (Table 1).

During the multiple rapid test (multitest) period, blood cultures were tested based on Gram stain results using a combination of three rapid tests with a decision algorithm to select the best possible combination based on Gram-staining results (Figure 1): Bactident oxidase tests (Merck, Darmstadt, Germany) β-Lacta tests (Bio-Rad, Marnes la Coquette, France) for gram negative bacteria, and MRSA/SA tests for clustered gram positive cocci (GeneXpert MRSA/SA test, Cepheid, Sunnyvale, CA).

During the reference period, the gram stain was considered as the "early analysis" and was communicated to the physicians to help them to adapt empirical antibiotic therapy. The term was also changed in Table 2.

Clinical guidelines

All blood culture results were immediately communicated to the attending physician. Treatment protocols and guidelines were established for each period by a working group of clinical biochemists, infectious diseases specialists, and intensive care physicians (Supplemental Table 2). The protocols were accessible on the computer system of the two hospitals. These measures were implemented alongside the rapid techniques to optimize their impact on patient outcomes (Banerjee et al., 2015; Vardakas et al., 2015; Barlam et al., 2016; Timbrook et al., 2017; De Waele et al., 2018).

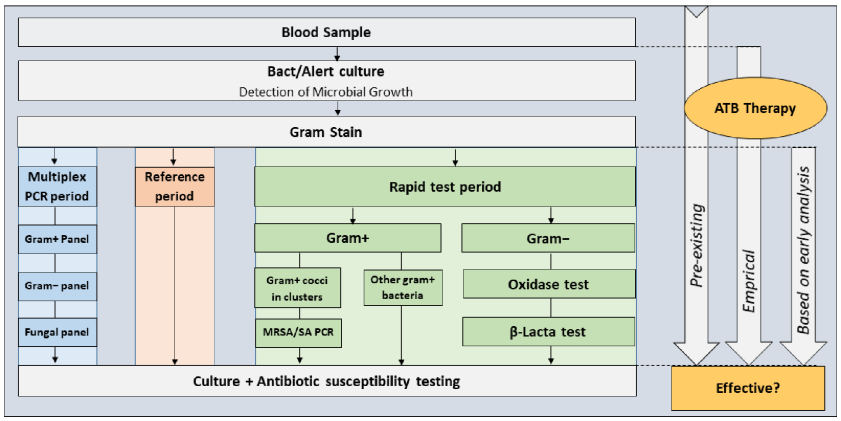

FIGURE 1
Testing flow diagram.

Data collection and outcomes

The following data were collected from the patients' electronic medical records: age, gender, identified pathogens, infection sites, ICU admission, SAPS 2 score, need for vasopressor therapy, invasive mechanical ventilation or renal replacement therapy, length of hospital stay and mortality. All microbiological results were collected. The final results of the conventional identification and susceptibility tests were used as reference to assess the results of the m-PCR and rapid tests. The times of blood sampling, positive blood culture alerts, early analysis results and final results were recorded. The timing and choice of antibiotics were recorded and defined for each step: pre-existing antibiotic therapy (started before blood sampling), empirical antibiotic therapy (initiated between the sample collection and antibiogram result) and antibiotic therapy based on early analysis results (started and selected based on early analysis results and antibiotic treatment guidelines, see Supplemental Tables 1 and 2). Antibiotic therapy wad considered effective according to the definitive result of the antibiogram.

TABLE 1 Microorganisms and resistance genes detected by the different cartridges in the ePlex blood culture identification panel.

Identification	GRAM positive Panel	GRAM negative Panel	FONGIC Panel
Microorganisms	*Bacillus cereus* group *Bacillus subtilis* group *Corynebacterium* Cutibacterium acnes (P. acnes) Enterococcus Enterococcus faecalis Enterococcus faecium Lactobacillus Listeria Listeria monocytogenes Micrococcus Staphylococcus Staphylococcus aureus Staphylococcus epidermidis Staphylococcus lugdunensis Streptococcus Streptococcus agalactiae Streptococcus anginosus group Streptococcus pneumoniae Streptococcus pyogenes Pan Gram-negative Pan Candida	*Acinetobacter baumannii* *Bacteroides fragilis* *Citrobacter* *Cronobacter sakazakii* *Enterobacter (non-cloacae* complex) *Enterobacter cloacae* complex *Escherichia coli* *Fusobacterium nucleatum* *Fusobacterium necrophorum* *Haemophilus influenzae* *Klebsiella oxytoca* *Klebsiella pneumoniae* group *Morganella morganii* *Neisseria meningitidis* Proteus *Proteus mirabilis* Pseudomonas aeruginosa Salmonella Serratia Serratia marcescens Stenotrophomonas maltophilia Pan Gram-Positive Pan Candida	*Candida albicans* *Candida dubliniensis* *Candida famata* *Candida glabrata* *Candida guilliermondii* *Candida kefyr* *Candida lusitaniae* *Candida krusei* *Candida parapsilosis* *Candida tropicalis* *Cryptococcus neoformans* *Cryptococcus gattii* *Fusarium* *Malassezia furfur* *Rhodotorula* *Trichosporon*
Resistance genes	*MecA* *MecC* *VanA* *VanB*	*CTX-M* *IMP* *KPC* *NDM* *OXA-23* *OXA-48* *VIM*	

10.3389/fcimb.2023.1192002

TABLE 2 Patient characteristics and microbiological results.

	m-PCR period (n= 90)	Reference period (n= 90)	Multitest period (n= 90)	*p*
Age (years)	70 ± 20	70 ± 16	71 ± 20	0.487
< 65 years	26 (29)	30 (33)	25 (28)	0.690
65–80 years	30 (33)	35 (39)	25 (28)	0.287
≥ 80 years	34 (38)	25 (28)	40 (44)	0.065
Male	47 (52)	51 (57)	45 (50)	0.659
Contamination	9 (10)	8 (9)	7 (8)	0.872
Nosocomial infection	22 (24)	33 (37)	31 (34)	0.172
Pneumonia	22 (24)	12 (13)	21 (23)	0.125
Urinary tract infection	16 (18)	28 (31)	22 (24)	0.115
Septic shock	16 (18)	9 (10)	16 (18)	0.244
ICU admission	28 (31)	20 (22)	26 (29)	0.380
SAPS II score on admission	40 ± 13	38 ± 15	52 ± 22	0.040
Catecholamines	16 (18)	9 (10)	19 (21)	0.117
Invasive ventilation	16 (18)	8 (9)	14 (16)	0.203
Renal replacement therapy	7 (8)	4 (4)	8 (9)	0.479
In-hospital deaths	12 (13)	6 (7)	13 (14)	0.209
Length of hospital stay (days)	9 (4–23)	9 (4–18)	13 (4–25)	0.212
All pathogens identified	90 (100)	90 (100)	84 (93)	0.417
Gram-positive	45 (45)	44 (44)	51 (55)	0.410
Gram-negative	54 (54)	55 (55)	40 (43)	0.193
Yeasts	1 (1)	1 (1)	2 (2)	0.776
Time from blood sampling to positive blood culture (hours)	16.9 (13–22.1)	13.7 (11.9–21.5)	15.9 (13–21.3)	0.057
Time from positive blood culture to early analysis results (hours)	3.8 (2.9–6.9)	3.7 (1.8–8.2)	2.6 (1.3–4.5)	<0.01
Time from positive blood culture to final results (hours)	51.8 (43.8–66.5)	49.3 (37.5–58)	48.9 (40.1–54.6)	0.181
Time from blood sampling to final results (hours)	68.9 (61.2–93.4)	62.8 (56.9–74.3)	64.5 (58.7–75)	0.031

Data are reported as mean ± standard deviation, median (interquartile range) or frequency (%).

The primary outcome measures were the feasibility of the methods and the diagnostic performance of the rapid tests relative to conventional tests (sensitivity, specificity, positive and negative predictive values). We also evaluated the time between blood culture positivity and test results for each approach.

The clinical impact of each technique was assessed in terms of the time from blood culture collection to the introduction of appropriate antibiotic therapy. These delays were compared between patients treated in the different periods and for subgroups of patients with confirmed bacteremia and with or without appropriate antibiotic therapy at the release of early analysis results. Patient outcomes were evaluated in terms of ICU admission, length of hospital stay and in-hospital mortality. Duration of exposure to broad-spectrum antibiotics was also considered.

Statistical analysis

Continuous variables were expressed as median (interquartile range), and categorical variables were expressed as numbers and percentages. Between-group comparisons were performed using ANOVA tests (if the data were normally distributed) or Kruskal-Wallis tests (if the distribution was skewed) for continuous variables and using chi-square tests for categorical variables. A p-value <0.05 was deemed significant. All analyses were performed with the software SPSS (version 20.0, SPS Inc, Chicago, Illinois). The diagnostic performance of the rapid tests (sensitivity and specificity) were calculated using the results of the conventional tests as the gold standard (see Supplemental Material).

10.3389/fcimb.2023.1192002

Results

Population and pathogens

Two hundred and seventy patients were included in total, 90 in each of the three periods, from the medical, geriatric, surgical, emergency, and intensive care units. All patients had a positive blood culture with an unknown pathogenic microorganism in the preceding 48 hours. Patient characteristics and biochemical results are summarized in Table 2. Patients treated in the multitest period had higher SAPS 2 scores. The bloodstream infections were mostly due to a single pathogen but 21/270 (8%) involved multiple pathogens. The main sources of the infection were the urinary tract (24% of cases) and the lungs (19%), and the most common pathogens were *Escherichia coli* and *Staphylococcus aureus* (found in 24% and 10% of blood cultures, respectively). The gram distribution was similar in the three periods (51% of gram-negative bacteria and 47% of gram-positive bacteria). A small proportion of cases (1% in each period) involved fungal infections (Table 2). The median time between blood sampling and blood culture positivity tend to be shorter in the reference period than in the other two periods (13.7 h vs 15.9 and 16.9 h, $p = 0.06$)

Feasibility and performance of the rapid tests

The performance of the m-PCR tests was variable with sensitivities for bacterial identification and antibiotic resistance of 93% and 78%, respectively, specificities of 40% and 100%, positive predictive values of 89% and 100%, and negative predictive values of 55% and 98%, respectively (see Supplemental Material 3). The performance of the multiple rapid tests was excellent with sensitivities, specificities, and negative and positive predictive values of 100% for bacterial identification and susceptibility results. The multitest method was also the fastest with delays between blood sampling and early analysis results of 3.8 (2.9–6.9) h, 3.7 (1.8–8.2) h and 2.6 (1.3–4.5) h in the m-PCR, reference and multitest periods, respectively ($p < 0,01$; Table 2).

Adjustment of antibiotic therapy based on rapid test results

Empirical antibiotic therapy was initiated in 229 patients (85%) before early analysis results were available and was inappropriate in 44 of these patients (19%) before early analysis results (Figure 2). For these patients, the delay between blood sampling and analysis results. For these patients, the time from blood sampling to the initiation of appropriate antibiotic therapy did not differ between the three periods. Antibiotic therapy was initiated or adjusted based on early analysis results in 78 patients in total (introduced in 34 patients without prior antibiotic therapy and adjusted in 44 patients with inappropriate empirical antibiotic therapy). Among these 78 patients, the delay between blood sampling and appropriate antibiotic therapy was 9.5 h (29%) shorter in the m-PCR period and 8.9 h (27%) shorter in the multitest period than in the reference period. The use of m-PCR or multiple rapid tests was associated with a higher likelihood of patients receiving appropriate antibiotic therapy within 24 and 48 h of blood sampling. Among patients with no or inappropriate antibiotic therapy prior to early analysis results, the proportions receiving appropriate antibiotic therapy in the m-PCR, rapid test and reference periods increased to 60%, 50% and 42%, respectively, within 24 h of blood sampling, and 90%, 88% and 71% within 48 h of blood sampling. (Table 3).

Patient outcomes and antibiotic consumption

The in-hospital mortality rate was 11.5% overall (31/270) and was slightly lower (but not statistically significant) in the reference period (7%) than in the m-PCR and multitest periods (13% and 14%, respectively, p = 0.209). The median length of hospital stay

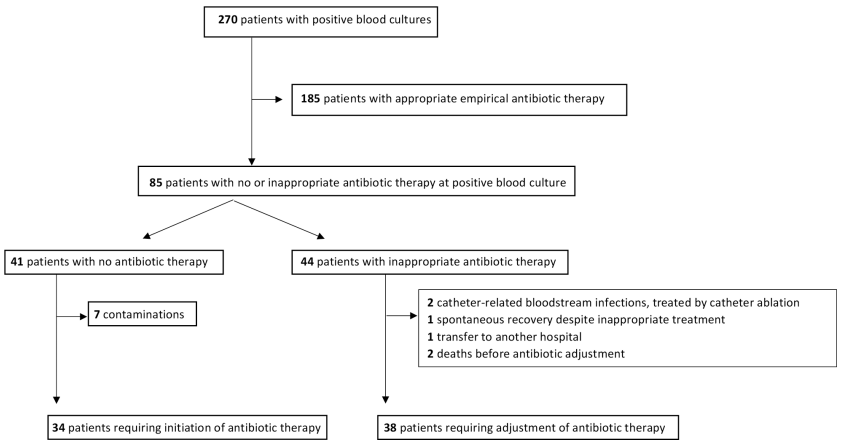

FIGURE 2
Treatment flow diagram.

TABLE 3 Treatment implications and delays (contaminations excluded).

	m-PCR period	Reference period	Multitest period	*p*
All patients (n=246)				
Time (hours) from blood sampling to appropriate antibiotic therapy	2.8 (0.5–17.5)	6 (1.6–20.3)	6.4 (1–18.7)	0.196
Appropriate antibiotic therapy < 24 h after blood sampling	69/81 (85)	62/82 (76)	66/83 (80)	0.421
Appropriate antibiotic therapy < 48 h after blood sampling	77/81 (95)	69/82 (84)	76/83 (92)	0.105
No AT before rapid test results (n=34)	10/81 (12)	12/82 (15)	12/83 (14)	0.972
Time (hours) from blood sampling to appropriate antibiotic therapy (n=30)*	22.1 (18.1–24.9)	25 (20.3–33.1)	23.4 (15.9–24.6)	0.416
Empirical antibiotic therapy before early analysis (n=212)	71/81 (88)	70/82 (85)	71/83 (86)	0.972
Inappropriate antibiotic therapy before early analysis (n=44)	12/71 (17)	17/70 (24)	15/71 (21)	0.555
Time (hours) from blood sampling to appropriate antibiotic therapy (n=38)**	28.5 (20.7–36.5)	47.6 (22.4–58.1)	24 (18.2–35.3)	0.264
AT introduction or adjustment after early analysis (n=68)				
Time (hours) from blood sampling to appropriate antibiotic therapy (hours)	23.4 (19.9–29.7)	32.9 (20.3–51.5)	24 (17.7–30.8)	0.454
Appropriate antibiotic therapy < 24 h after blood sampling	12/20 (60%)	10/24 (42%)	12/24 (50%)	0.480
Appropriate antibiotic therapy < 48 h after blood sampling	18/20 (90%)	17/24 (71%)	21/24 (88%)	0.180

Data are reported as mean ± standard deviation, median (interquartile range) or frequency (%).
*4/34 patients never received antibiotic therapy (one transient bacteriemia in the reference period, one transfer to another hospital before antibiotic therapy was initiated in the reference period, and palliative care for two patients in the multitest period).
**6/44 patients never received antibiotic therapy (two deaths in the m-PCR and reference periods, one lung infection resolved under inappropriate antibiotic therapy in the m-PCR period, two catheter infections treated by catheter ablation in the reference and multitest periods, and one transfer to another hospital before appropriate antibiotic therapy in the reference period.

was 9 (4–22.5) days and did not differ between periods. Broad-spectrum antibiotic consumption was similar in the three periods (Supplemental Table 4).

Discussion

Rapid techniques

Faster identification of bacterial species and antibiotic resistance could allow earlier administration of appropriate narrow-spectrum antibiotics and should thereby help improve patient outcomes, reduce costs, adverse effects, and the emergence of antibiotic resistant organisms (Caliendo et al., 2013; Garnier et al., 2017). This has prompted manufacturers to develop m-PCR systems designed to rapidly identify causative organisms in sepsis and common antibiotic resistance genes. Molecular diagnostic assays are now available that can be used directly on positive blood culture bottles, providing results much faster than conventional cultures and antimicrobial susceptibility testing (Liesenfeld et al., 2014; Salimnia et al., 2016; Huang et al., 2019; Oberhettinger et al., 2020). The good diagnostic performance of m-PCR is well-established (Banerjee et al., 2015; Southern et al., 2015; Walker et al., 2016; Schmitz and Tang, 2018; Bryant et al., 2020; Carroll et al., 2020; Krifors et al., 2020), but just like for other rapid techniques, few studies have shown any significant clinical impact (Timbrook et al., 2017; Rodrigues et al., 2019). The ePlex blood culture identification panel is a hybrid m-PCR system that identifies a panel of genes from pathogenic organisms or associated with antibiotic resistance. This panel has been shown to identify around 95% of frequently encountered pathogens with a sensitivity and specificity of more than 90% (Huang et al., 2019; Bryant et al., 2020; Carroll et al., 2020; Krifors et al., 2020; Oberhettinger et al., 2020). The present results confirm the rapid nature of the test but suggest that its efficacy may be lower than previously reported (particularly for antibiotic resistance findings).

The other rapid testing protocol investigated in this study involved multiple rapid tests (Parmeland et al., 2021) with a decision algorithm to select the best possible combination based on Gram-staining results. The GeneXpert MRSA/SA PCR test is a genotypic test able to detect methicillin-resistant *Staphylococcus* with a sensitivity and specificity close to 100% in blood cultures (Parta et al., 2009; Brown and Paladino, 2010; Davies et al., 2012). The β-Lacta test is a phenotypic test that detects β-lactamase–producing enterobacteria with third generation-cephalosporin resistance with a reported sensitivity around 85% and a specificity of more than 95% in previous studies (Renvoise et al., 2013; Compain et al., 2015; Garnier et al., 2017; Hasso et al., 2017). The oxidase test is also a phenotypic test used to detect gram-negative bacteria producing cytochrome oxidase, typically *Pseudomonas* species in bacteremia. The performance and utility of this test remains to be established, but its sensitivity and specificity have been found to be around 95% and 100% respectively, when performed on blood cultures (Sepúlveda et al., 1990; Cobos-Triguero et al., 2017; Parmeland et al., 2021). Neither the β-Lacta test nor the oxidase test require additional sample preparation steps, consumables, or specialist training. The results of the present study suggest they can be easily integrated into laboratory workflows.

Performance and feasibility

The diagnostic performance of the ePlex blood culture identification panel was poorer than previously reported (Schmitz and Tang, 2018; Huang et al., 2019; Bryant et al., 2020; Carroll et al., 2020; Krifors et al., 2020; Oberhettinger et al., 2020), with a sensitivity of just 78% for antibiotic resistances and a very low specificity and negative predictive value for pathogen identification. The resistance identification results should be interpreted with caution since the patients in this study mostly had community-acquired bacteremia with a relatively low prevalence of antibiotic resistance. It is noteworthy however that there were two false negative results with the ePlex assay for methicillin-resistant staphylococci, which could have had serious clinical consequences. The low specificity in pathogen identification is mainly due to the poor performance of the panGram gene search, which was implicated in 89% of false positive results. This panGram gene search was not systematically included in the diagnostic performance analyses in previous studies. Finally, the low sensitivity of this approach in pathogen identification is related to a few cases of bacteremia with opportunistic but not particularly virulent pathogens not included in the ePlex panel (Table 4).

In contrast, the diagnostic performance of the three rapid tests was excellent, with sensitivities and specificities of 100%. While the performance and clinical benefit of the GeneXpert MRSA/SA PCR test is well established, this is not the case for the β-Lacta and oxidase tests (Parta et al., 2009; Brown and Paladino, 2010; Davies et al., 2012). The β-Lacta test is known to be less sensitive to enterobacteria resistant to third-generation cephalosporins by AmpC overproduction, which hydrolyzes the probe enzyme, HMRZ-86, less efficiently than extended-spectrum β-lactamases and carbapenemases do (Renvoise et al., 2013; Morosini et al., 2014). It should be noted that we reported none hypercephalosporinase in the sample, which could contribute to the very good diagnostic performances we obtained in the study. In terms of implementation, these rapid tests were found to be easy-to-use and did not slow down the biochemical testing workflow for positive blood cultures. The time from positive blood culture to rapid test results was equal or shorter than the time from positive blood culture to Gram stain results in the reference period. Surprisingly the multitest test protocol was 1 h faster on average than the ePlex assays. This may be because laboratory technicians interpreted Gram stain results sooner when they knew other tests depended on them.

Therapeutic implication

One of the objectives of this study was to determine whether rapid tests could reduce the time to appropriate antibiotic therapy, avoiding the wait for conventional culture results, which are only provided during working hours in the two hospitals in the study. The cases in this study included both community and hospital-acquired bacteremia with typical rates of inadequate empirical antibiotic therapy (23%) and in-hospital mortality (11%) (Robineau et al., 2018). Our results support the use of rapid techniques for blood culture testing, since they were associated with shorter delays from blood collection to appropriate antibiotic therapy and a greater likelihood of appropriate antibiotic therapy within 24 h of blood sampling (Caliendo et al., 2013; Banerjee et al., 2015; Timbrook et al., 2017; Miller et al., 2018; Oberhettinger et al., 2020). None of these associations were statistically significant, but the effect of the rapid tests is masked somewhat by the time between blood sampling and positive blood culture results having been 2–3 h shorter in the reference period than in the m-PCR and multitest periods.

The use of rapid techniques was not associated with reduced morbidity or mortality, possibly because the study was underpowered to detect this. Another limitation of the study may be that the severity of patients' symptoms differed, but not significantly, between the three periods. This could explain why no significant difference was observed in the consumption of broad-spectrum antibiotics.

TABLE 4 List of discrepancies between ePlex blood culture identification panel and culture methods.

	Details	n
Pathogen not in ePlex panel (n = 8)	*Granulicatella adiacens*	1
	Methylobacterium mesophilicum	1
	Sphingomonas paucimobilis	1
	Prevotella melaninogenica	1
	Moraxella	1
	Parvimonas micra	1
	Alcaligenes xylosoxidans	1
	Clostridium paraputrificum	1
Pathogen in panel but not detected (n=5)	*Fusobacterium necrophorum*	1
	Pseudomonas aeruginosa	1
	Staphylococcus aureus	1
	Coagulase negative staphylococcus	1
	Enterococcus faecalis	1
Resistance not in ePlex panel (n=2)	*Hypercephalosporinase (Pseudomonas A.)* *Ofloxacine resistance*	1 1
Resistance in panel but not detected (n=2)	*MecA (S. aureus and S. hominis)*	2

ePlex assay results differed from conventional culture results in 12 pathogens (8 off-panel microorganisms and 5 negative PCR results for a microorganism in the panel) and for 4 forms of antibiotic resistance [the MecA gene, included in the panel (false negatives), in two cases and hypercephalosporinase resistance in a *Pseudomonas aeruginosa* and ofloxacin resistance in *Escherichia coli* (true negatives)].

Conclusion

In these patients with positive blood cultures, the diagnostic performance of multiple rapid tests performed according to a

decision algorithm was excellent and superior to that of ePlex assay m-PCR tests. Both rapid techniques were easily incorporated into the laboratory workflow alongside conventional cultures and led to patients receiving appropriate antibiotic therapy sooner. Larger studies with a greater prevalence of resistant pathogens are required to estimate the impact of these tests on length of hospital stay and mortality.

Data availability statement

The raw data supporting the conclusions of this article will be made available by the authors, without undue reservation.

Ethics statement

The studies involving human participants were reviewed and approved by Declaration of Helsinki. Written consent was not required because of the observational nature of the study. All patients received general information about research activities and data management policies. Written informed consent for participation was not required for this study in accordance with the national legislation and the institutional requirements.

Author contributions

P-AC, EV, NR, LP, and CP designed the study. P-AC and NR organized and performed the data collection. P-AC and EV performed the statistical analysis. P-AC, EV, NR, LP, and CP analyzed and interpreted the data. P-AC and EV wrote the manuscript. All authors had full access to the study data, contributed to drafting the manuscript or critically revised its content, approved the final version of the manuscript, and take responsibility for the integrity of the data and the accuracy of the data analysis. EV is the guarantor of the paper. All authors contributed to the article and approved the submitted version.

Funding

This work was supported by general hospital funding.

Acknowledgments

The authors would like to thank Saint Joseph Saint Luc laboratory staff for participating in the study.

Conflict of interest

The GenMark ePlex system was provided free-of-charge to Saint Joseph Saint Luc hospital by the manufacturer.

Publisher's note

Supplementary material

The Supplementary Material for this article can be found online at: https://www.frontiersin.org/articles/10.3389/fcimb.2023.1192002/full#supplementary-material

References

Banerjee, R., Teng, C. B., Cunningham, S. A., Ihde, S. M., Steckelberg, J. M., Moriarty, J. P., et al. (2015). Randomized trial of rapid multiplex polymerase chain reaction–based blood culture identification and susceptibility testing. *Clin. Infect. Dis.* 61 (7), 1071–1080. doi: 10.1093/cid/civ447

Barlam, T. F., Cosgrove, S. E., Abbo, L. M., MacDougall, C., Schuetz, A. N., Septimus, E. J., et al. (2016). Executive summary: implementing an antibiotic stewardship program: guidelines by the infectious diseases society of America and the society for healthcare epidemiology of America. *Clin. Infect. Dis.* 62 (10), 1197–1202. doi: 10.1093/cid/ciw217

Brown, J., and Paladino, J. A. (2010). Impact of rapid methicillin-resistant staphylococcus aureus polymerase chain reaction testing on mortality and cost effectiveness in hospitalized patients with bacteraemia: a decision model. *PharmacoEconomics.* 28 (7), 567–575. doi: 10.2165/11533020-000000000-00000

Bryant, S., Almahmoud, I., Pierre, I., Bardet, J., Touati, S., Maubon, D., et al. (2020). Evaluation of microbiological performance and the potential clinical impact of the ePlex® blood culture identification panels for the rapid diagnosis of bacteremia and fungemia. *Front. Cell Infect. Microbiol.* 10, 594951. doi: 10.3389/fcimb.2020.594951

Caliendo, A. M., Gilbert, D. N., Ginocchio, C. C., Hanson, K. E., May, L., Quinn, T. C., et al. (2013). Better tests, better care: improved diagnostics for infectious diseases. *Clin. Infect. Dis.* 57 (suppl 3), S139–S170. doi: 10.1093/cid/cit578

Carroll, K. C., Reid, J. L., Thornberg, A., Whitfield, N. N., Trainor, D., Lewis, S., et al. (2020). Clinical performance of the novel GenMark dx ePlex blood culture ID gram-positive panel. *J. Clin. Microbiol.* 58 (4), e01730–e01719. doi: 10.1128/JCM.01730-19

CASFM/EUCAST (2019) *CASFM/EUCAST V1.1.* Available at: https://www.sfm-microbiologie.org/2019/01/07/casfm-eucast-2019.

Cassini, A., Högberg, L. D., Plachouras, D., Quattrocchi, A., Hoxha, A., Simonsen, G. S., et al. (2019). Attributable deaths and disability-adjusted life-years caused by infections with antibiotic-resistant bacteria in the EU and the European economic area in 2015: a population-level modelling analysis. *Lancet Infect. Dis.* 19 (1), 56–66. doi: 10.1016/S1473-3099(18)30605-4

Cobos-Triguero, N., Zboromyrska, Y., Morata, L., Alejo, I., de la Calle, C., Vergara, A., et al. (2017). Time-to-positivity, type of culture media and oxidase test performed on positive blood culture vials to predict pseudomonas aeruginosa in patients with gram-negative bacilli bacteraemia. *Rev. Espanola Quimioter Publicacion Of Soc. Espanola Quimioter.* 30 (1), 9–13.

Compain, F., Bensekhri, H., Rostane, H., Mainardi, J. L., and Lavollay, M. (2015). β LACTA test for rapid detection of enterobacteriaceae resistant to third-generation cephalosporins from positive blood cultures using briefly incubated solid medium cultures. *J. Med. Microbiol.* 64 (10), 1256–1259. doi: 10.1099/jmm.0.000157

Davies, J., Gordon, C. L., Tong, S. Y. C., Baird, R. W., and Davis, J. S. (2012). Impact of results of a rapid staphylococcus aureus diagnostic test on prescribing of antibiotics

for patients with clustered gram-positive cocci in blood cultures. *J. Clin. Microbiol.* 50 (6), 2056–2058. doi: 10.1128/JCM.06773-11

De Waele, J. J., Akova, M., Antonelli, M., Canton, R., Carlet, J., De Backer, D., et al. (2018). Antimicrobial resistance and antibiotic stewardship programs in the ICU: insistence and persistence in the fight against resistance. a position statement from ESICM/ESCMID/WAAAR round table on multi-drug resistance. *Intensive Care Med.* 44 (2), 189–196. doi: 10.1007/s00134-017-5036-1

Garnier, M., Rozencwajg, S., Pham, T., Vimont, S., Blayau, C., Hafiani, M., et al. (2017). Evaluation of early antimicrobial therapy adaptation guided by the BetaLACTA® test: a case-control study. *Crit. Care* 21 (1), 161. doi: 10.1186/s13054-017-1746-6

Hasso, M., Porter, V., and Simor, A. E. (2017). Evaluation of the β-lacta test for detection of extended-Spectrum-β- lactamase (ESBL)-producing organisms directly from positive blood cultures by use of smudge plates. *J. Clin. Microbiol.* 55 (12), 3. doi: 10.1128/JCM.01354-17

Huang, T. D., Melnik, E., Bogaerts, P., Evrard, S., and Glupczynski, Y. (2019). Evaluation of the ePlex blood culture identification panels for detection of pathogens in bloodstream infections. *J. Clin. Microbiol.* 57 (2), e01597–18. doi: 10.1128/JCM.01597-18

Kollef, M. H. (2000). Inadequate antimicrobial treatment: an important determinant of outcome for hospitalized patients. *Clin. Infect. Dis.* 31 (Supplement_4), S131–S138. doi: 10.1086/314079

Krifors, A., Rådberg, G., Golbob, S., Omar, Z., Svensson, C., Heimer, D., et al. (2020). The clinical impact of implementing GenMark ePlex blood culture panels for around-the-clock blood culture identification; a prospective observational study. *Infect. Dis.* 52 (10), 705–712. doi: 10.1080/23744235.2020.1775882

Kumar, A. (2010). Early antimicrobial therapy in severe sepsis and septic shock. *Curr. Infect. Dis. Rep.* 12 (5), 336–344. doi: 10.1007/s11908-010-0128-x

Leone, M., Bourgoin, A., Cambon, S., Dubuc, M., Albanèse, J., and Martin, C. (2003). Empirical antimicrobial therapy of septic shock patients: adequacy and impact on the outcome*. *Crit. Care Med.* 31 (2), 462–467. doi: 10.1097/01.CCM.0000050298.59549.4A

Liesenfeld, O., Lehman, L., Hunfeld, K. P., and Kost, G. (2014). Molecular diagnosis of sepsis: new aspects and recent developments. *Eur. J. Microbiol. Immunol.* 4 (1), 1–25. doi: 10.1556/EuJMI.4.2014.1.1

Miller, J. M., Binnicker, M. J., Campbell, S., Carroll, K. C., Chapin, K. C., Gilligan, P. H., et al. (2018). A guide to utilization of the microbiology laboratory for diagnosis of infectious diseases: 2018 update by the infectious diseases society of America and the American society for microbiologya. *Clin. Infect. Dis.* 67 (6), e1–94. doi: 10.1093/cid/ciy381

Morosini, M. I., Garcia-Castillo, M., Tato, M., Gijon, D., Valverde, A., Ruiz-Garbajosa, P., et al. (2014). Rapid detection of -Lactamase-Hydrolyzing extended-spectrum cephalosporins in enterobacteriaceae by use of the new chromogenic lacta test. *J. Clin. Microbiol.* 52 (5), 1741–1744. doi: 10.1128/JCM.03614-13

Oberhettinger, P., Zieger, J., Autenrieth, I., Marschal, M., and Peter, S. (2020). Evaluation of two rapid molecular test systems to establish an algorithm for fast identification of bacterial pathogens from positive blood cultures. *Eur. J. Clin. Microbiol. Infect. Dis.* 39 (6), 1147–1157. doi: 10.1007/s10096-020-03828-5

Parmeland, L., Bourru, T., Kyungu, V., Rousseau, N., Gleize, M., De Beauvoir, C., et al. (2021). A rapid and inexpensive protocol to screen for third generation cephalosporin-resistant and non-fermenting gram-negative rods directly in positive blood cultures. *Diagn. Microbiol. Infect. Dis.* 101 (2), 115428. doi: 10.1016/j.diagmicrobio.2021.115428

Parta, M., Goebel, M., Matloobi, M., Stager, C., and Musher, D. M. (2009). Identification of methicillin-resistant or methicillin-susceptible *Staphylococcus aureus* in blood cultures and wound swabs by GeneXpert. *J. Clin. Microbiol.* 47 (5), 1609–1610. doi: 10.1128/JCM.00351-09

Renvoise, A., Decre, D., Amarsy-Guerle, R., Huang, T. D., Jost, C., Podglajen, I., et al. (2013). Evaluation of the lacta test, a rapid test detecting resistance to third-generation cephalosporins in clinical strains of enterobacteriaceae. *J. Clin. Microbiol.* 51 (12), 4012–4017. doi: 10.1128/JCM.01936-13

Rhodes, A., Evans, L. E., Alhazzani, W., Levy, M. M., Antonelli, M., Ferrer, R., et al. (2017). Surviving sepsis campaign: international guidelines for management of sepsis and septic shock: 2016. *Intensive Care Med.* 43 (3), 304–377. doi: 10.1007/s00134-017-4683-6

Rivers, E., Nguyen, B., Havstad, S., Ressler, J., Muzzin, A., Knoblich, B., et al. (2001). Early goal-directed therapy in the treatment of severe sepsis and septic shock. *N Engl. J. Med.* 345 (19), 1368–1377. doi: 10.1056/NEJMoa010307

Robineau, O., Robert, J., Rabaud, C., Bedos, J. P., Varon, E., Péan, Y., et al. (2018). Management and outcome of bloodstream infections: a prospective survey in 121 French hospitals (SPA-BACT survey). *Infect. Drug Resist.* 11, 1359–1368. doi: 10.2147/IDR.S165877

Rodrigues, C., Siciliano, R. F., Filho, H. C., Charbel, C. E., de Carvalho Sarahyba da Silva, L., Baiardo Redaelli, M., et al. (2019). The effect of a rapid molecular blood test on the use of antibiotics for nosocomial sepsis: a randomized clinical trial. *J. Intensive Care* 7 (1), 37. doi: 10.1186/s40560-019-0391-3

Salimnia, H., Fairfax, M. R., Lephart, P. R., Schreckenberger, P., DesJarlais, S. M., Johnson, J. K., et al. (2016). Evaluation of the FilmArray blood culture identification panel: results of a multicenter controlled trial. *J. Clin. Microbiol.* 54 (3), 687–698. doi: 10.1128/JCM.01679-15

Schmitz, J. E., and Tang, Y. W. (2018). The GenMark ePlex ®: another weapon in the syndromic arsenal for infection diagnosis. *Future Microbiol.* 13 (16), 1697–1708. doi: 10.2217/fmb-2018-0258

Seifert, H. (2009). The clinical importance of microbiological findings in the diagnosis and management of bloodstream infections. *Clin. Infect. Dis.* 48 (s4), S238–S245. doi: 10.1086/598188

Sepúlveda, J. L., Stager, C. E., and Davis, J. R. (1990). Rapid presumptive identification of gram-negative rods directly from blood cultures by simple enzymatic tests. *J. Clin. Microbiol.* 28 (2), 177–181. doi: 10.1128/jcm.28.2.177-181.1990

Southern, T. R., VanSchooneveld, T. C., Bannister, D. L., Brown, T. L., Crismon, A. S., Buss, S. N., et al. (2015). Implementation and performance of the BioFire FilmArray® blood culture identification panel with antimicrobial treatment recommendations for bloodstream infections at a midwestern academic tertiary hospital. *Diagn. Microbiol. Infect. Dis.* 81 (2), 96–101. doi: 10.1016/j.diagmicrobio.2014.11.004

Timbrook, T. T., Morton, J. B., McConeghy, K. W., Caffrey, A. R., Mylonakis, E., and LaPlante, K. L. (2017). The effect of molecular rapid diagnostic testing on clinical outcomes in bloodstream infections: a systematic review and meta-analysis. *Clin. Infect. Dis.* 64 (1), 15–23. doi: 10.1093/cid/ciw649

Vardakas, K. Z., Anifantaki, F. I., Trigkidis, K. K., and Falagas, M. E. (2015). Rapid molecular diagnostic tests in patients with bacteremia: evaluation of their impact on decision making and clinical outcomes. *Eur. J. Clin. Microbiol. Infect. Dis.* 34 (11), 2149–2160. doi: 10.1007/s10096-015-2466-y

Walker, T., Dumadag, S., Lee, C. J., Lee, S. H., Bender, J. M., Cupo Abbott, J., et al. (2016). Clinical impact of laboratory implementation of verigene BC-GN microarray-based assay for detection of gram-negative bacteria in positive blood cultures. *J. Clin. Microbiol.* 54 (7), 1789–1796. doi: 10.1128/JCM.00376-16

Yokota, P. K. O., Marra, A. R., Martino, M. D. V., Victor, E. S., Durão, M. S., Edmond, M. B., et al. (2014). Impact of appropriate antimicrobial therapy for patients with severe sepsis and septic shock – a quality improvement study. *PloS One* 9 (11), e104475. doi: 10.1371/journal.pone.0104475

frontiers | Frontiers in Cellular and Infection Microbiology

TYPE Original Research
PUBLISHED 10 August 2023
DOI 10.3389/fcimb.2023.1239269

OPEN ACCESS

EDITED BY
Laura Cerqueira,
University of Porto, Portugal

REVIEWED BY
Arianna Tavanti,
University of Pisa, Italy
Ashraf Kariminik,
Islamic Azad University Kerman, Iran

*CORRESPONDENCE
Dong Qu
qudong2012@126.com
Yi Wang
wildwolf0101@163.com
Juan Zhou
zhoujuan2015@126.com

RECEIVED 13 June 2023
ACCEPTED 25 July 2023
PUBLISHED 10 August 2023

CITATION
Liu S, Huang S, Li F, Sun Y, Fu J, Xiao F, Jia N, Huang X, Sun C, Zhou J, Wang Y and Qu D (2023) Rapid detection of *Pseudomonas aeruginosa* by recombinase polymerase amplification combined with CRISPR-Cas12a biosensing system. *Front. Cell. Infect. Microbiol.* 13:1239269. doi: 10.3389/fcimb.2023.1239269

Rapid detection of *Pseudomonas aeruginosa* by recombinase polymerase amplification combined with CRISPR-Cas12a biosensing system

Shuang Liu[1], Siyuan Huang[1], Fang Li[1], Yuanyuan Sun[1], Jin Fu[2], Fei Xiao[2], Nan Jia[2], Xiaolan Huang[2], Chunrong Sun[2], Juan Zhou[2*], Yi Wang[2*] and Dong Qu[1*]

[1]Department of Critical Medicine, Children's Hospital Affiliated Capital Institute of Pediatrics, Beijing, China, [2]Experimental Research Center, Capital Institute of Pediatrics, Beijing, China

Pseudomonas aeruginosa (*P. aeruginosa*) is an important bacterial pathogen involved in a wide range of infections and antimicrobial resistance. Rapid and reliable diagnostic methods are of vital important for early identification, treatment, and stop of *P. aeruginosa* infections. In this study, we developed a simple, rapid, sensitive, and specific detection platform for *P. aeruginosa* infection diagnosis. The method integrated recombinase polymerase amplification (RPA) technique with clustered regularly interspaced short palindromic repeat (CRISPR)–CRISPR-associated protein 12a (Cas12a) biosensing system and was termed *P. aeruginosa*–CRISPR–RPA assay. The *P. aeruginosa*–CRISPR–RPA assay was subject to optimization of reaction conditions and evaluation of sensitivity, specificity, and clinical feasibility with the serial dilutions of *P. aeruginosa* genomic DNA, the non–*P. aeruginosa* strains, and the clinical samples. As a result, the *P. aeruginosa*–CRISPR–RPA assay was able to complete *P. aeruginosa* detection within half an hour, including RPA reaction at 42°C for 20 min and CRISPR-Cas12a detection at 37°C for 10 min. The diagnostic method exhibited high sensitivity (60 fg per reaction, ~8 copies) and specificity (100%). The results of the clinical samples by *P. aeruginosa*–CRISPR–RPA assay were consistent to that of the initial result by microfluidic chip method. These data demonstrated that the newly developed *P. aeruginosa*–CRISPR–RPA assay was reliable for *P. aeruginosa* detection. In summary, the *P. aeruginosa*–CRISPR–RPA assay is a promising tool to early and rapid diagnose *P. aeruginosa* infection and stop its wide spread especially in the hospital settings.

KEYWORDS

Pseudomonas aeruginosa*, recombinase polymerase amplification, RPA, CRISPR-Cas12a, *oprL

Introduction

Pseudomonas aeruginosa (*P. aeruginosa*) is a Gram-negative, rod-shaped aerobe/facultative anaerobe belonging to the genus *Pseudomonas* of family *Pseudomonadaceae*. Metabolically, *P. aeruginosa* is versatile and can adapt to a wide range of niches, including soil, aquatic environment, plants, animals, and human beings (Silby et al., 2011; Gellatly and Hancock, 2013; Moradali et al., 2017). *P. aeruginosa* is an important opportunistic pathogen of human beings, especially for the vulnerable patients with cystic fibrosis (CF) lungs (Turner et al., 2015), obstructive pulmonary diseases (Eklöf et al., 2020), and other immunocompromised and hospitalized patients (Malhotra et al., 2019). It infects three-quarters of patients with CF and leads to high morbidity and mortality rate (Surette, 2014). Meanwhile, *P. aeruginosa* is the predominant pathogen causing otitis media (Mittal et al., 2015), keratitis (Hilliam et al., 2020), endocarditis (Sheppard, 1991), bacteremia (Fabre et al., 2019), burn and wound infections (Salerian, 2020), urinary tract infections (Yin et al., 2022), and more. However, treatment of *P. aeruginosa* infection in clinical setting has confronted with great challenge due to its resistance to different antibiotics and antiseptic (Lister et al., 2009; Chevalier et al., 2017). A combination of intrinsic, acquired, and adaptive ability of *P. aeruginosa* to counter antibiotic attack (Pang et al., 2019) and its extensive reservoirs in nosocomial and community environments (Ratnam et al., 1986; van Asperen et al., 1995; Yakupogullari et al., 2008; Quick et al., 2014) complicated the effective treatment and control of *P. aeruginosa* infection and rendered it a healthcare concern (Rosenthal et al., 2016). *P. aeruginosa* has become one of the notorious "ESKAPE" pathogens (Pendleton et al., 2013) and been considered as the "critical" category of the World Health Organization's priority list of bacterial pathogens for which research and development of new antibiotics is urgently needed (Tacconelli et al., 2018). Under this context, development of rapid, accurate, and sensitive detection method for *P. aeruginosa* is of vital importance and urgently required for early diagnosis of *P. aeruginosa* infection and effective control its wide spread.

In clinical settings and routine laboratories, specimen culture is the most common and gold standard for *P. aeruginosa* identification (Rytter et al., 2020). Use of culture-based method is able to determine antibiotic susceptibility; however, obtaining the results usually takes a minimum time of 48 h, which may delay antibiotic treatment and compromise patient outcome (Rytter et al., 2020). In this regard, more rapid and sensitive diagnostic tests for *P. aeruginosa* detection are still urgently needed. During the past decades, a plenty of polymerase chain reaction (PCR)–based techniques, including conventional PCR and real-time PCR methods, have been widely developed and applied in pathogen identification including *P. aeruginosa* (Williams et al., 2010; Lim et al., 2021). Although sensitive and specific, these methods usually rely on sophisticated instruments and well-trained technicians, which commonly equipped in the well-established laboratories and normally cost more than 1 h to report results. More recently, several isothermal nucleic acid amplification techniques that overcome the limitations of PCR-based methods have been reported for *P. aeruginosa* detection, such as recombinase polymerase amplification (RPA) assay (Yang et al., 2021), multiple–cross-displacement amplification (MCDA) assay (Li et al., 2020; Wang et al., 2020), and loop-mediated isothermal amplification assay (Takano et al., 2019). These tools could rapidly, accurately, sensitively, and specifically identify and characterize *P. aeruginosa* only with a simple an apparatus that could maintain a constant temperature (Wang et al., 2015), which demonstrated the potential to be applied in resource-limited or rural regions. However, the results identification and reporting systems of the isothermal amplification techniques normally rely on indicator, fluorescent dye or fluorescent probe, and amplification bias and non-specific amplification inherent in exponential strategies (Zhao et al., 2015). Therefore, the urgent need for new nucleic acid detection techniques with rapidity, accuracy, and high sensitivity still exists.

Discovery of the clustered regularly interspaced short palindromic repeats (CRISPR) and CRISPR-associated protein (Cas) (CRISPR-Cas) system has revolutionized the biosensing field and sparked great interest in nucleic acid detection technologies (Li et al., 2019). The CRISPR-Cas biosensing system could transfer the sequence information of targets to detectable signals (such as fluorescence or colorimetric values) by employing the collateral cleavage activities of the Cas effectors (Cas12a, Cas12b, Cas13, and Cas14), conferring this technology high sensitivity and specificity of detection and simplicity to develop, which also exhibits great potential in point-of-care tests (Gootenberg et al., 2018; Myhrvold et al., 2018; Bonini et al., 2021; Jirawannaporn et al., 2022; Kumaran et al., 2023; Zheng et al., 2023). In particular, by coupling isothermal amplification procedure, the detection performance of CRISPR-Cas biosensing system is greatly improved, and the target type also can be converted (Li et al., 2019; Zhang et al., 2023). Recently, the CRISPR-Cas–based biosensing detection platforms, such as SHERLOCK (Specific High Sensitivity Enzymatic Reporter Unlocking, RPA combination with Cas13a) (Myhrvold et al., 2018) and DETECTR (DNA Endonuclear Targeted Crispr Trans Reporter, RPA combination with Cas12a) (Chen et al., 2018), have been rapidly developed and already commercial available for pathogen detection.

In this study, a CRISPR-Cas12a–based RPA detection platform (CRISPR-RPA) targeting the *oprL* gene was developed and validated for rapid, accurate, sensitive, and specific diagnosis of *P. aeruginosa* infection. This two-step detection platform included *oprL* gene amplification using RPA assay at 42°C within 20 min and CRISPR-Cas12a detection at 37°C for 10 min. The result was interpreted using real-time fluorescence analysis using the single-strand DNA (ssDNA) reporter (5′-FAM-TTATTAT-BHQ1-3′). The detection performance of the *P. aeruginosa*–CRISPR–RPA assay was confirmed with DNA templates of *P. aeruginosa* strains, other respiratory pathogen strains, and clinical samples.

Materials and methods

Reagents and apparatus

Recombinase polymerase–based amplification kit for isothermal amplification was purchased from Msunflowers Biotech Co., Ltd. (Beijing, China). The 100-bp DNA marker and the EasyPure® Genomic DNA Kit for genomic DNA extraction and purification were obtained from TransGene Biotech Co., Ltd. (Beijing, China). EnGen® Lba Cas12a (Cpf1) and NEBuffer r2.1 were purchased from New England Biolabs (Beijing, China). The ABI 7500 FAST real-time PCR platform (Applied Biosystems, USA) was used as the fluorescence reader. An imaging system (Gel Doc XR C, Bio-Rad, USA) was used for gel image taken.

Bacterial strains and clinical samples

A total of 25 strains, including eight *P. aeruginosa* strains and 17 non–*P. aeruginosa* strains, were used in this study (Table 1). Genomic DNA of all the strains was extracted and purified using the EasyPure® Genomic DNA Kit according to the manufacturer's instruction, and species identification was confirmed by PCR amplification of the 16S rRNA gene with primer pair 27F/1492R (Neilan et al., 1997). In addition, 96 bronchoalveolar lavage fluid (BALF) samples suspected of respiratory infection were included in this study as well. DNA templates of these BALF samples were obtained by using the nucleic acid extraction reagent of Capital BioTech Co., Ltd. (Sichuan, China). All the DNA templates were stored at −20°C before use.

TABLE 1 Bacterial strains used in this study.

Bacteria	Strain no. (source of strain)[a]	No. of strains
Pseudomonas aeruginosa	Isolated strains (CDC)	8
Enterococcus faecium	Isolated strains (CDC)	1
Shigella sonnei	Isolated strains (CDC)	1
Citrobacter freundii	Isolated strains (CDC)	2
Moraxella catarrhalis	Isolated strains (CDC)	1
Escherichia coli	Isolated strains (CDC)	1
Salmonella enteritidis	Isolated strains (CDC)	2
Bacillus cereus	Isolated strains (CDC)	1
Klebsiella pneumoniae	Isolated strains (CDC)	1
Streptococcosis suis	Isolated strains (CDC)	2
Stenotrophomonas maltophilia	Isolated strains (CDC)	1
Corynebacterium striatum	Isolated strains (CDC)	1
Streptococcus salivarius	Isolated strains (CDC)	1
Streptococcus pyogenes	Isolated strains (CDC)	1
Nocardia asteroids	Isolated strains (CDC)	1

[a]CDC, Chinese center for disease control and prevention.

Primer and crRNA design

Primers for *P. aeruginosa* detection targeting *oprL* gene (GenBank: Z50191.1) (De Vos et al., 1997; Wang et al., 2020) were designed by using the Primer-Blast tool of National Center for Biotechnology Information (NCBI) on the basis of RPA reaction mechanism (Piepenburg et al., 2006). Two forward primers (F1 and F2) and six reverse primers (R1 to R6) were obtained, resulting to six pairs of primers (F1R1, F1R2, F2R3, F2R4, F2R5, and F2R6). Each primer pair was subjected to specificity assessment using the BLAST tool. After primers screen, the CRISPR RNA (crRNA) and probe were designed according to the principle of CRISPR-Cas12a effector. The probe was an ssDNA reporter that labeled with 5-Carboxyfluorescein (FAM) fluorophore and Black Hole Quencher 1 (BHQ1) quencher at the 5′ and 3′ end, respectively. Sequences and locations of all the oligonucleotides and crRNA were shown in Table 2 and Figure 1, and all of them were synthesized by TianyiHuiyuan Biotech Co., Ltd. (Beijing, China).

Standard RPA amplification

According to the manufacturer's instruction, amplification of the *oprL* gene was performed in a 50-μL reaction mixture at 39°C for 40 min. In brief, 29.5 μL of A buffer and 2 μL of each of forward and reverse primer (10 μM) were added into a tube containing lyophilized RPA enzyme mix until fully dissolved, and, then, 2 μL of template and 2.5 μL of magnesium acetate (B buffer) were added before incubated at 39°C for 40 min. The RPA products were examined by using electrophoresis on 2% agarose gel, and the images were taken by using an imaging system.

CRISPR-Cas12a detection

The CRISPR-Cas12a detection procedure included two steps: formation of CRISPR-Cas12a–crRNA binary complex and CRISPR-Cas12a trans-cleavage reaction. The CRISPR-Cas12a–crRNA binary complex was prepared by incubating 100 nM CRISPR-Cas12a and 100 nM crRNA in 2× NEBuffer r2.1 at 37°C for 10 min and then immediately used or stored at 4°C for no more than 24 h. The CRISPR-Cas12a trans-cleavage reaction was carried out at 37°C for 10 min in a 100-μL mixture, including 18 μL of CRISPR-Cas12a–crRNA binary complex, 50 μL of 2× NEBuffer r2.1, 2.5 μL of probe (10μM), 2 μL of RPA products, and 27.5 μL of distilled water (DW). The result was monitored in a real-time manner by the real-time fluorescence detector.

Optimization of *P. aeruginosa*–CRISPR–RPA assay

To determine the optimal reaction temperature at RPA reaction stage, RPA products amplified at temperatures ranging from 37°C to 42°C (interval of 1°C) were tested. Furthermore, the optimal

TABLE 2 Primers, crRNA, and probe design in this study.

Primers	Sequences (5′-3′)	Length
F1	AACAATGGCGGCAACGTTCCTCCTTCCGG	29 nt
F2	GTCGCGTCGAGCTGAAGAAGTAAGAAGTC	29 nt
R1	ATCTGCTGGAGCTGCATGAACAGTTCGCC	29 nt
R2	AGCCAACTCGTCCTGCATCTGCTGGAGCT	29 nt
R3	CAACGCCGTCATACACAGGAACTTCCGCC	29 nt
R4	TGTTGGCGGCAACGCCGTCATACACAGGA	29 nt
R5	GGAAGGAGGAACGTTGCCGCCATTGTTGG	29 nt
R6	ATCTGCTGGAGCTGCATGAACAGTTCGCC	29 nt
crRNA	UAAUUUCUACUAAGUGUAGAUCCGGAGGUGGGGUGACAACCCC	43 mer
Probe	FAM-TATTATTATTATTATTT-BHQ1	17 mer

reaction time for RPA reaction was detected by performing RPA reaction at optimal temperature for 10 to 40 min (interval of 10 min), respectively. The optimal RPA reaction conditions were decided according to the brightness and sharpness of target band on gel electrophoresis images.

To optimize the performance of CRISPR-Cas12a trans-cleavage reaction, a series of reaction conditions were examined as well, including the reaction volume (50 μL versus 100 μL), the trans-cleavage temperature (37°C to 42°C, with an interval of 1°C) and time (10 to 20 min, with an interval of 5 min). The optimum conditions were determined according to the fluorescence intensity with different volume, at different temperature or within different time.

In addition, to verify the true component that works in the CRISPR-Cas12a trans-cleavage reaction mixture, reactions with different combinations of CRISPR-Cas12a, crRNA, probe, and RPA products were carried out. Result was recorded by the real-time fluorescence detector.

Sensitivity and specificity of the *P. aeruginosa*–CRISPR–RPA assay

To determine the sensitivity of the CRISPR-RPA assay for *P. aeruginosa* detection, genomic DNA of *P. aeruginosa* strains was 10-fold serially diluted from 6 ng to 0.6 fg as templates, with negative control and blank control detected simultaneously. Moreover, a total of 17 non–*P. aeruginosa* strains (Table 1) were employed in this study for specificity evaluation. Each test was repeated three times to ensure stability.

GAACCGTCGCGTCGAGCTGAAGAAGTAAGAAGTCGTTATGCCCAAGCACCTGCGTGTCCTGA
CGTTCCTCGCGCTCAGCCTGCCATTAGCGGCCAGGGCGGAAGTTCCTGTGTATGACGGCGTTG
CCGCCAACAATGGCGGCAACGTTCCTCCTTCCGGGTATGGCACGGCAGGTGCCGGCGGCGCC
TTTACCGGGAGGTGGGGTGACAACCCCCACCTCCGTGCAGGGCGAACTGTTCATGCAGCTCC
AGCAGATGCAGGACGAGTTGGCTCGCCTGCGTGGCACGCTCGAGCGAGAGGTTGCCCGCATG
GCTTCGGTTTGGCAGAGGCCTGCGGGGAGCCGCTGTAATCCACCTTCC

FIGURE 1
Sequences and locations of the oprL gene of *P. aeruginosa* used to design the RPA primers and crRNA. Locations of RPA primers are underlined, and crRNA is in the box. The right arrow and left arrow represent the sense and complementary sequence used in this study, respectively.

Clinical validity of the *P. aeruginosa*–CRISPR–RPA assay

The *P. aeruginosa*–CRISPR–RPA assay was performed with a total of 96 BALF samples to evaluate its feasibility in clinical settings. The BALF samples were collected from patients suspected of respiratory infection in the Capital Institute of Pediatrics and had been examined for pathogen identification using microfluidic chip (MFC) technology. Of the 96 BALF samples, 19 were detected as *P. aeruginosa*–positive with MFC method. The performance of the *P. aeruginosa*–CRISPR–RPA assay was compared with that of the MFC method for *P. aeruginosa* detection.

Results

Confirmation of the *P. aeruginosa*–CRISPR–RPA assay for *P. aeruginosa* detection

A total of six pairs of primers were designed and employed to amplify partial sequence of the *oprL* gene. According to the results of gel electrophoresis image (Figure S1), primer pair F2/R6 resulted in bright and single band and exhibited excellent amplification effect. Thus, primers F2 and R6 was used for the following RPA reaction with a length of 250 bp.

With primer pair F2/R6, only the reaction tube with *P. aeruginosa* genomic DNA as template displayed a bright target band in the gel electrophoresis image and generated fluorescence, whereas no band or fluorescence was produced in the negative control (with genomic DNA of *Escherichia coli* as template) and blank control (DW) reaction products (Figure 2). Thus, the primer

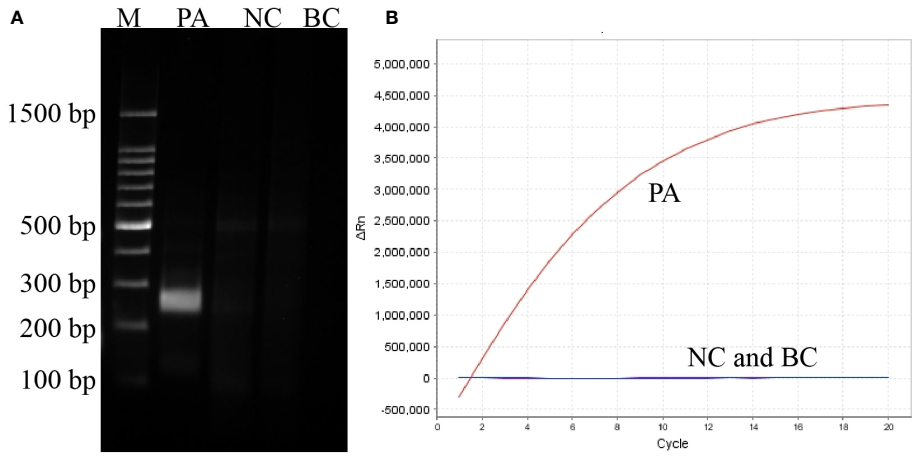

FIGURE 2
Establishment and confirmation of *P. aeruginosa*–CRISPR–RPA for *P. aeruginosa* detection. **(A)** RPA products amplified with primer pair F2/R6 are detected by agarose gel electrophoresis. **(B)** CRISPR-Cas12a biosensing system is used for detection of the target product. PC, positive control of *P. aeruginosa* strain; NC, negative control of *Klebsiella pneumonia*; BC, blank control of distilled water.

F2/R6 and the developed *P. aeruginosa*–CRISPR–RPA assay were available to detect *P. aeruginosa* strains.

Optimization conditions for *P. aeruginosa*–CRISPR–RPA assay

The *P. aeruginosa*–CRISPR–RPA assay was a two-step method and consisted of RPA pre-amplification and CRISPR-Cas12a detection two procedures. First, the optimum temperature and time of RPA pre-amplification step were determined by performing RPA reaction at temperatures ranging from 37°C to 42°C (with 1°C interval) and with time from 10 to 40 min (with 10 min interval), respectively. As shown in Figures S2A, B, a reaction temperature of 42°C and a reaction time of 20 min exhibited better amplification efficiency and thus were more suitable for RPA reaction. Then, the CRISPR-Cas12a detection step was optimized by performing tans-cleavage reaction within 50- or 100-μL volume, at 37 to 42°C (with 1°C interval) and with time from 10 to 20 min (with 5 min interval), respectively, and the trans-cleavage efficiency under different conditions was compared. According to the fluorescence intensity images (Figures S2C–E), a reaction volume of 100 μL, a temperature of 37°C, and a reaction time of 10 min generated higher fluorescence intensity and thus were better candidates for CRISPR-Cas12a detection for *P. aeruginosa*–RPA products. Therefore, 42°C and 30 min for *P. aeruginosa*–RPA reaction as well as 100 μL of reaction mixture, 37°C, and 10 min for CRISPR-Cas12a detection of *P. aeruginosa*–RPA products were selected for the subsequent *P. aeruginosa*–CRISPR–RPA assay. Moreover, the functional components within the reaction mixture were also confirmed by detecting the fluorescence intensity with each combination. As shown in Figure S3, only the combination contained all the components (CRISPR-Cas12a, crRNA, probe, and RPA product) displayed a positive result.

Sensitivity and specificity evaluation of the *P. aeruginosa*–CRISPR–RPA assay

The sensitivity of the *P. aeruginosa*–CRISPR–RPA assay was estimated by detecting the serially diluted genomic DNA of *P. aeruginosa* strain. As shown in Figure 3B, when dilution concentration exceeded 60 fg, apparent fluorescence intensity was generated by the real-time fluorescence detector, indicating that the *P. aeruginosa*–CRISPR–RPA assay was able to detect low as 60 fg *P. aeruginosa* genomic DNA per reaction. Compared with agarose gel electrophoresis after *P. aeruginosa*–RPA pre-amplification (6 pg, Figure 3A), the *P. aeruginosa*–CRISPR–RPA assay was obviously more sensitive to diagnose *P. aeruginosa* infection.

The specificity of the *P. aeruginosa*–CRISPR–RPA assay was assessed by using genomic DNA templates extracted from 17 non–*P. aeruginosa* strains. The result of fluorescence detector indicated that no fluorescence was generated from the 17 non–*P. aeruginosa* strains and the blank control (DW), whereas the eight *P. aeruginosa* strains produced significant fluorescence (Figure 4). Thus, the *P. aeruginosa*–CRISPR–RPA assay did not cross-react with other common respiratory pathogens, indicating a high specificity (100%).

Clinical validity of the *P. aeruginosa*–CRISPR–RPA assay

To examine the performance of the *P. aeruginosa*–CRISPR–RPA assay in clinical practice, the detection platform was applied in clinical samples from patients with suspected respiratory infection. Of the 96 BALF samples, 19 were diagnosed as *P. aeruginosa*–positive, which were detected as *P. aeruginosa*–positive by the MFC method as well; whereas, the other 77 samples were negative for *P. aeruginosa* by both the *P. aeruginosa*–CRISPR–RPA assay and MFC method (Figure 5; Table 3). The detection result of the 96 clinical samples was identical between the *P. aeruginosa*–CRISPR–RPA

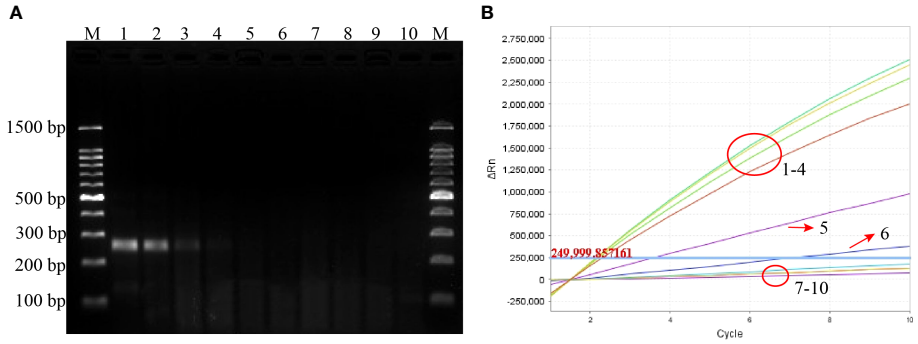

FIGURE 3
Sensitivity evaluation of the *P. aeruginosa*–CRISPR–RPA assay. Sensitivity assay was performed by using agarose gel electrophoresis **(A)** and CRISPR-Cas12a biosensing system **(B)** to detect the RPA products using gradient-diluted *P. aeruginosa* genomic DNA. Numbers 1–8 refer to the serial dilutions of *P. aeruginosa* genomic DNA from 6 ng to 0.6 fg, number 9 refers to the negative control (*E. coli*), and number 10 refers to the blank control (DW). Fluorescence intensity higher than 250,000 was considered as positive result.

assay and MFC method. These results demonstrated that the *P. aeruginosa*–CRISPR–RPA assay developed here was a reliable tool for *P. aeruginosa* detection in clinical settings.

Discussion

P. aeruginosa was one of the most common pathogens of hospital-acquired pneumonia (HAP) (16.9%–22.0%) (Moradali et al., 2017; Reynolds and Kollef, 2021) and also accounted for at least 1.0% of community-acquired pneumonia (Fine et al., 1996). Moreover, it was reported that 27.7% of the *P. aeruginosa* strains isolated from patient with HAP admitted in Intensive Care Unit (ICU) were of carbapenem resistance (Botelho et al., 2019). The high disease burden caused by *P. aeruginosa* and the increasing trend of antimicrobial resistance even multi-drug resistance of *P. aeruginosa* strains challenged the public health globally, and improvements to increase *P. aeruginosa* identification rate and time were urgently needed.

The CRISPR-Cas biosensing system has inspired numerous research activity in the diagnostic area on nucleic acid detection platform development (Li et al., 2019; Li et al., 2021; Jia et al., 2023), and the recently well-developed nucleic acid detection methods (such as SHERLOCK, HOLMES, DETECTR, and HUDSON) have manifested this. These methods were mainly developed with various CRISPR-Cas effectors (such as 12a, 12b, 13a, and 13b), which normally possess trans-cleavage activity, and activation of the trans-cleavage activity commonly required the formation of Cas effector/crRNA/target DNA ternary complex (Li et al., 2018a; Li et al., 2019). For example, the CRISPR-Cas12a effector could target

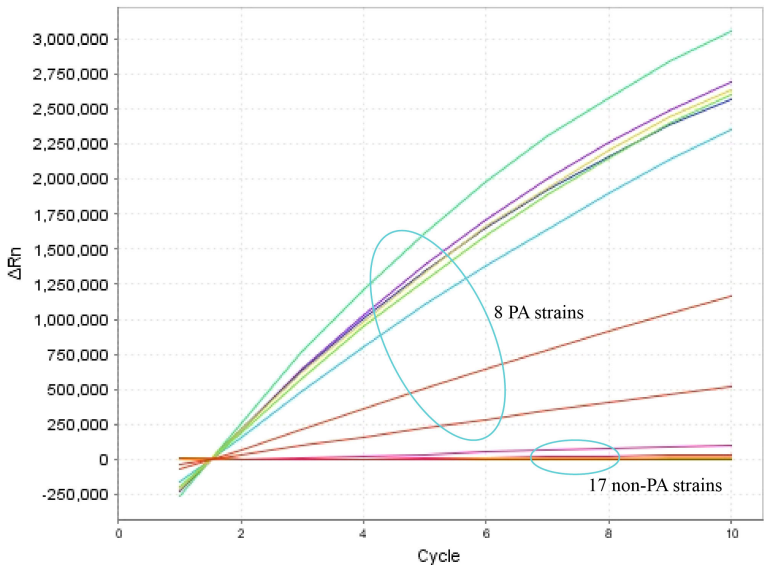

FIGURE 4
Specificity evaluation of the *P. aeruginosa*–CRISPR–RPA assay. Specificity assay was conducted by detecting the fluorescence intensity of 17 non–*P. aeruginosa* strains and eight *P. aeruginosa* strains by the real-time fluorescence detector. Fluorescence intensity higher than 250,000 was considered as positive result.

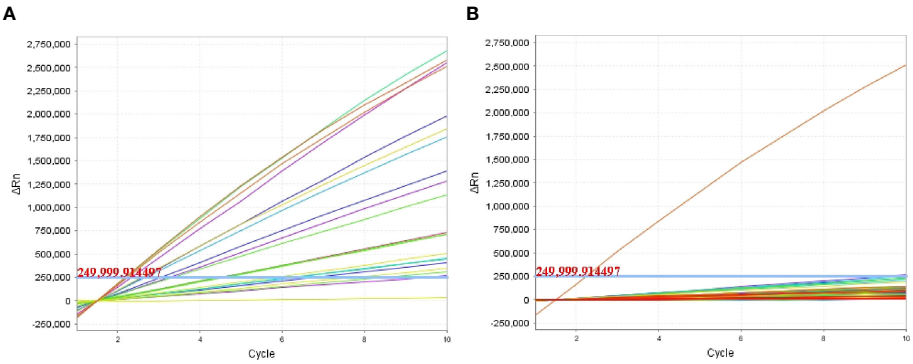

FIGURE 5
Clinical validity of the *P. aeruginosa*–CRISPR–RPA assay. A total of 96 BALF samples initial diagnosed by microfluidic chip (MFC) method were examined by the *P. aeruginosa*–CRISPR–RPA assay to confirm its application in clinical settings. Fluorescence intensity of the 19 P. *aeruginosa*–positive samples **(A)** and 77 P. *aeruginosa*–negative samples **(B)** were reported by the real-time fluorescence detector. Fluorescence intensity higher than 250,000 was considered as positive result.

DNA and trans-cleave any collateral ssDNA (Zetsche et al., 2015). Only after recognizing the target sequence that complementary to the crRNA sequence and juxtaposed with a suitable protospacer-adjacent motif (PAM, TTTN), the trans-cleavage activity of the CRISPR-Cas12a effector was able to be activated, following the paired fluorescence/quencher-labeled ssDNA probe cleaved and a fluorescent readout generated, which could be monitored by the real-time fluorescence detector (Li et al., 2018b). Owing to its merits of being highly efficient, sensitive, ultra-specific, and time-efficient, the CRISPR-Cas biosensing system has attracted much attention for its application in molecular diagnostic field. Therefore, in this study, we integrated the CRISPR-Cas12a biosensing system with RPA isothermal amplification techniques to optimize the *P. aeruginosa* identification rate and efficiency.

Compared with other nucleic acid amplification techniques, RPA was more preferable due to its simplicity, sensitivity, extremely rapidity, operation at low and constant temperature and with simple instruments, and no need for multiple primers (Lobato and O'Sullivan, 2018). In this study, the RPA pre-amplification step could be completed within 20 min at 42°C only with a simple water bath that could sustain a constant temperature. Because the reagents of RPA were freeze-dried and stored in the reaction tube, the RPA kit was especially convenient to store and employed. Thus, in this study, by combining with CRISPR-Cas12a detection platform, the *P. aeruginosa*–CRISPR–RPA assay was able to be performed independent of sophisticated equipment and foregoing the need for maintenance of a cold chain, which were attractive for use in point-of-care diagnostics and rural areas. Moreover, after optimization, the detection procedure of *P. aeruginosa*–CRISPR–RPA assay could be completed within half an hour, including 20 min for RPA reaction and 10 min for CRISPR-Cas12a detection, which was apparently rapid than that of PCR-based method and other isothermal amplification methods. In general, the *P. aeruginosa*–CRISPR–RPA assay in this study ensured its high sensitivity by pre-amplification the target nucleic acid using the attractive RPA method and guaranteed its high specificity with both the specific RPA primers and gRNA, together with paired fluorescence/quencher-labeled ssDNA probe, producing accurate and easy-to-interpret readouts.

The new established *P. aeruginosa*–CRISPR–RPA assay was proven sensitive to detect *P. aeruginosa* strains. It can detect as low as 60 fg (~8 copies) of *P. aeruginosa* genomic DNA per reaction, obviously more sensitive than the RPA-only method that detected by agarose gel electrophoresis method (6 pg). When compared with the previously reported *P. aeruginosa*–MCDA assay (100 fg) (Wang et al., 2020), the *P. aeruginosa*–CRISPR–RPA assay also exhibited higher sensitivity. However, the sensitivity of the *P. aeruginosa*–CRISPR–RPA assay was slight lower than the RPA-LFS assay developed by Yang et al. in 2021 (3.05 copies per reaction) (Yang et al., 2021). Thus, further optimization of the *P. aeruginosa*–CRISPR–RPA assay is still needed to improve the detection sensitivity, and more comparisons will be carried out to provide better reference to the clinicians for rapid and accurate diagnosis of *P. aeruginosa*–associated infections.

The specificity of the *P. aeruginosa*–CRISPR–RPA assay was evaluated by 17 non–*P. aeruginosa* strains, most of which were common respiratory pathogens. After detected by the *P. aeruginosa*–CRISPR–RPA assay, none of the 17 non–*P.*

TABLE 3 Performance comparison between the *P. aeruginosa*–CRISPR–RPA assay and microfluidic chip (MFC) method for *P. aeruginosa* detection in clinical samples.

Methods	*P. aeruginosa*–CRISPR–RPA		Comparison of two methods		
MFC	Positive	Negative	Sensitivity (%)	Specificity (%)	Kappa
Positive	19	0	100	100	1
Negative	0	77			

aeruginosa strains displayed a positive result except for the eight *P. aeruginosa* strains, manifesting that the *P. aeruginosa*–CRISPR–RPA assay was specific enough for diagnosis of *P. aeruginosa* infection. However, an obvious drawback of the specificity evaluation test was that no other members of genus *Pseudomonas* strains was tested here; thus, it will be supplemented if available in the future. After all, the *P. aeruginosa*–CRISPR–RPA assay was highly specific to detect *P. aeruginosa* strains and had no cross-reactivity with other pathogens.

Finally, the clinical validity of the *P. aeruginosa*–CRISPR–RPA assay was evaluated using 96 BALF samples initially diagnosed by MFC method. The *P. aeruginosa*–CRISPR–RPA assay reported 19 P. *aeruginosa*–positive samples and 77 negative samples, all of which was consisted with results by the MFC method, implying the *P. aeruginosa*–CRISPR–RPA assay was reliable for *P. aeruginosa* detection. Moreover, the *P. aeruginosa*–CRISPR–RPA assay was able to report the results of these clinical samples within half an hour, whereas that by MFC method needs about an hour, further demonstrating the superiority of the *P. aeruginosa*–CRISPR–RPA assay. It was well-known that conventional culture–based technique was more proper to be employed to validate the new established *P. aeruginosa*–CRISPR–RPA assay; however, no original clinical BALF samples was available; thus, comparison of the performance of this new method with culture-based technique could only be carried out in the future studies. Together, it could be concluded that the validity was a promising tool for the rapid and accurate diagnosis of *P. aeruginosa* infection.

Certainly, there are still some limitations in this study: (1) the genetic information of the eight *P. aeruginosa* strains was not available, which may affect the evaluation of the new established detection system in correctly *P. aeruginosa* identification; (2) the background fluorescence signal is occasional high, which may lead to false-positive results; (3) the carryover contamination cause by opening the RPA amplification tube may produce background signals; and (4) more clinical samples should be tested for clinical validation. Of course, there are also some improvements that can be made in the future, including using more genetically diverse strains for the method establishment and verification, interpreting the result of *P. aeruginosa*–CRISPR–RPA assay under blue light if the drawback of high background signals solved; moreover, conducting the whole detection procedure within one step if further optimizations were provided, which also can avoid the production of aerosol pollution.

In summary, we reported the development and validation of a CRISPR-Cas12a–based detection platform for *P. aeruginosa* identification and termed it *P. aeruginosa*–CRISPR–RPA assay. The two-step *P. aeruginosa*–CRISPR-RPA assay was capable of detecting *P. aeruginosa* only within half an hour with simple instruments. After detecting the serial dilutions of *P. aeruginosa* genomic DNA, other non–*P. aeruginosa* strains and clinical samples with the *P. aeruginosa*–CRISPR-RPA assay, it can be concluded that the *P. aeruginosa*–CRISPR–RPA assay possesses the merits of rapidity, reliability, easy to perform, higher sensitivity, and specificity. Thus, the *P. aeruginosa*–CRISPR–RPA assay established here was a reliable and promising tool for early and rapid diagnosis of *P. aeruginosa* infection and stop of its wide spread especially in the hospital settings.

Data available statement

The original contributions presented in the study are included in the article/Supplementary Material. Further inquiries can be directed to the corresponding authors.

Ethics statement

The studies involving humans were approved by ethic committee of Capital Institute of Pediatrics. The studies were conducted in accordance with the local legislation and institutional requirements. The human samples used in this study were acquired from primarily isolated as part of your previous study for which ethical approval was obtained. Written informed consent for participation was not required from the participants or the participants' legal guardians/next of kin in accordance with the national legislation and institutional requirements.

Author contributions

SL performed the experiments, analyzed the data, and drafted the manuscript. SH, FL, and YS helped perform the experiments and organize the data. JF, FX, NJ, XH, and CS provided experimental reagents and materials. JZ and YW supervised this study and revised the manuscript. DQ conceived, supervised and funded this study, and revised manuscript. All authors contributed to the article and approved the submitted version.

Acknowledgments

This study was funded by Beijing Nova Program (Grant Nos. Z211100002121042), National Key Research and Development Program of China (Grant Nos. 2021YFC2301101 and 2021YFC2301102), and National Natural Science Foundation of China (82200115).

Conflict of interest

The authors declare that the research was conducted in the absence of any commercial or financial relationships that could be construed as a potential conflict of interest.

Publisher's note

All claims expressed in this article are solely those of the authors and do not necessarily represent those of their affiliated organizations, or those of the publisher, the editors and the reviewers. Any product that may be evaluated in this article, or claim that may be made by its manufacturer, is not guaranteed or endorsed by the publisher.

Supplementary material

The Supplementary Material for this article can be found online at: https://www.frontiersin.org/articles/10.3389/fcimb.2023.1239269/full#supplementary-material

References

Bonini, A., Poma, N., Vivaldi, F., Biagini, D., Bottai, D., Tavanti, A., et al. (2021). A label-free impedance biosensing assay based on CRISPR/Cas12a collateral activity for bacterial DNA detection. *J. Pharm. BioMed. Anal.* 204, 114268. doi: 10.1016/j.jpba.2021.114268

Botelho, J., Grosso, F., and Peixe, L. (2019). Antibiotic resistance in Pseudomonas aeruginosa - Mechanisms, epidemiology and evolution. *Drug Resist. Update* 44, 100640. doi: 10.1016/j.drup.2019.07.002

Chen, J. S., Ma, E., Harrington, L. B., Da Costa, M., Tian, X., Palefsky, J. M., et al. (2018). CRISPR-Cas12a target binding unleashes indiscriminate single-stranded DNase activity. *Science* 360 (6387), 436–439. doi: 10.1126/science.aar6245

Chevalier, S., Bouffartigues, E., Bodilis, J., Maillot, O., LesouHaitier, O., Feuilloley, M. G. J., et al. (2017). Structure, function and regulation of Pseudomonas aeruginosa porins. *FEMS Microbiol. Rev.* 41 (5), 698–722. doi: 10.1093/femsre/fux020

De Vos, D., Lim, A. Jr., Pirnay, J. P., Struelens, M., Vandenvelde, C., Duinslaeger, L., et al. (1997). Direct detection and identification of Pseudomonas aeruginosa in clinical samples such as skin biopsy specimens and expectorations by multiplex PCR based on two outer membrane lipoprotein genes, oprI and oprL. *J. Clin. Microbiol.* 35 (6), 1295–1299. doi: 10.1128/jcm.35.6.1295-1299.1997

Eklöf, J., Sørensen, R., Ingebrigtsen, T. S., Sivapalan, P., Achir, I., Boel, J. B., et al. (2020). Pseudomonas aeruginosa and risk of death and exacerbations in patients with chronic obstructive pulmonary disease: an observational cohort study of 22 053 patients. *Clin. Microbiol. Infect.* 26 (2), 227–234. doi: 10.1016/j.cmi.2019.06.011

Fabre, V., Amoah, J., Cosgrove, S. E., and Tamma, P. D. (2019). Antibiotic therapy for Pseudomonas aeruginosa bloodstream infections: how long is long enough? *Clin. Infect. Dis.* 69 (11), 2011–2014. doi: 10.1093/cid/ciz223

Fine, M. J., Smith, M. A., Carson, C. A., Mutha, S. S., Sankey, S. S., Weissfeld, L. A., et al. (1996). Prognosis and outcomes of patients with community-acquired pneumonia. A meta-analysis. *Jama* 275 (2), 134–141. doi: 10.1001/jama.1996.03530260048030

Gellatly, S. L., and Hancock, R. E. (2013). Pseudomonas aeruginosa: new insights into pathogenesis and host defenses. *Pathog. Dis.* 67 (3), 159–173. doi: 10.1111/2049-632x.12033

Gootenberg, J. S., Abudayyeh, O. O., Kellner, M. J., Joung, J., Collins, J. J., and Zhang, F. (2018). Multiplexed and portable nucleic acid detection platform with Cas13, Cas12a, and Csm6. *Science* 360 (6387), 439–444. doi: 10.1126/science.aaq0179

Hilliam, Y., Kaye, S., and Winstanley, C. (2020). Pseudomonas aeruginosa and microbial keratitis. *J. Med. Microbiol.* 69 (1), 3–13. doi: 10.1099/jmm.0.001110

Jia, N., Zhou, J., Xiao, F., Zheng, B., Huang, X., Sun, C., et al. (2023). A CRISPR-Cas12a-Based platform for ultrasensitive, rapid, and highly specific detection of Mycoplasma pneumonia in clinical application. *Front. Bioeng Biotechnol.* 11. doi: 10.3389/fbioe.2023.1022066

Jirawannaporn, S., Limothai, U., Tachaboon, S., Dinhuzen, J., Kiatamornrak, P., Chaisuriyong, W., et al. (2022). Rapid and sensitive point-of-care detection of Leptospira by RPA-CRISPR/Cas12a targeting lipL32. *PloS Negl. Trop. Dis.* 16 (1), e0010112. doi: 10.1371/journal.pntd.0010112

Kumaran, A., Jude Serpes, N., Gupta, T., James, A., Sharma, A., Kumar, D., et al. (2023). Advancements in CRISPR-based biosensing for next-gen point of care diagnostic application. *Biosensors (Basel)* 13 (2), 202. doi: 10.3390/bios13020202

Li, D. X., Shu, G. L., Wang, W. J., Wu, Y., and Niu, H. C. (2020). Simple, rapid and sensitive detection of Pseudomonas aeruginesa by colorimetric multiple cross displacement amplification. *Curr. Med. Sci.* 40 (2), 372–379. doi: 10.1007/s11596-020-2169-1

Li, L., Li, S., Wu, N., Wu, J., Wang, G., Zhao, G., et al. (2019). HOLMESv2: A CRISPR-cas12b-assisted platform for nucleic acid detection and DNA methylation quantitation. *ACS Synth Biol.* 8 (10), 2228–2237. doi: 10.1021/acssynbio.9b00209

Li, S. Y., Cheng, Q. X., Liu, J. K., Nie, X. Q., Zhao, G. P., and Wang, J. (2018a). CRISPR-Cas12a has both cis- and trans-cleavage activities on single-stranded DNA. *Cell Res.* 28 (4), 491–493. doi: 10.1038/s41422-018-0022-x

Li, S. Y., Cheng, Q. X., Wang, J. M., Li, X. Y., Zhang, Z. L., Gao, S., et al. (2018b). CRISPR-Cas12a-assisted nucleic acid detection. *Cell Discov.* 4, 20. doi: 10.1038/s41421-018-0028-z

Li, S., Huang, J., Ren, L., Jiang, W., Wang, M., Zhuang, L., et al. (2021). A one-step, one-pot CRISPR nucleic acid detection platform (CRISPR-top): Application for the diagnosis of COVID-19. *Talanta* 233, 122591. doi: 10.1016/j.talanta.2021.122591

Lim, H. J., Kang, E. R., Park, M. Y., Kim, B. K., Kim, M. J., Jung, S., et al. (2021). Development of a multiplex real-time PCR assay for the simultaneous detection of four bacterial pathogens causing pneumonia. *PloS One* 16 (6), e0253402. doi: 10.1371/journal.pone.0253402

Lister, P. D., Wolter, D. J., and Hanson, N. D. (2009). Antibacterial-resistant Pseudomonas aeruginosa: clinical impact and complex regulation of chromosomally encoded resistance mechanisms. *Clin. Microbiol. Rev.* 22 (4), 582–610. doi: 10.1128/cmr.00040-09

Lobato, I. M., and O'Sullivan, C. K. (2018). Recombinase polymerase amplification: Basics, applications and recent advances. *Trends Analyt Chem.* 98, 19–35. doi: 10.1016/j.trac.2017.10.015

Malhotra, S., Hayes, D. Jr., and Wozniak, D. J. (2019). Cystic fibrosis and Pseudomonas aeruginosa: the host-microbe interface. *Clin. Microbiol. Rev.* 32 (3), e00138-18. doi: 10.1128/cmr.00138-18

Mittal, R., Lisi, C. V., Gerring, R., Mittal, J., Mathee, K., Narasimhan, G., et al. (2015). Current concepts in the pathogenesis and treatment of chronic suppurative otitis media. *J. Med. Microbiol.* 64 (10), 1103–1116. doi: 10.1099/jmm.0.000155

Moradali, M. F., Ghods, S., and Rehm, B. H. (2017). Pseudomonas aeruginosa lifestyle: A paradigm for adaptation, survival, and persistence. *Front. Cell Infect. Microbiol.* 7. doi: 10.3389/fcimb.2017.00039

Myhrvold, C., Freije, C. A., Gootenberg, J. S., Abudayyeh, O. O., Metsky, H. C., Durbin, A. F., et al. (2018). Field-deployable viral diagnostics using CRISPR-Cas13. *Science* 360 (6387), 444–448. doi: 10.1126/science.aas8836

Neilan, B. A., Wilton, A. N., and Jacobs, D. (1997). A universal procedure for primer labelling of amplicons. *Nucleic Acids Res.* 25 (14), 2938–2939. doi: 10.1093/nar/25.14.2938

Pang, Z., Raudonis, R., Glick, B. R., Lin, T. J., and Cheng, Z. (2019). Antibiotic resistance in Pseudomonas aeruginosa: mechanisms and alternative therapeutic strategies. *Biotechnol. Adv.* 37 (1), 177–192. doi: 10.1016/j.bioteChadv.2018.11.013

Pendleton, J. N., Gorman, S. P., and Gilmore, B. F. (2013). Clinical relevance of the ESKAPE pathogens. *Expert Rev. Anti Infect. Ther.* 11 (3), 297–308. doi: 10.1586/eri.13.12

Piepenburg, O., Williams, C. H., Stemple, D. L., and Armes, N. A. (2006). DNA detection using recombination proteins. *PloS Biol.* 4 (7), e204. doi: 10.1371/journal.pbio.0040204

Quick, J., Cumley, N., Wearn, C. M., Niebel, M., Constantinidou, C., Thomas, C. M., et al. (2014). Seeking the source of Pseudomonas aeruginosa infections in a recently opened hospital: an observational study using whole-genome sequencing. *BMJ Open* 4 (11), e006278. doi: 10.1136/bmjopen-2014-006278

Ratnam, S., Hogan, K., March, S. B., and Butler, R. W. (1986). Whirlpool-associated folliculitis caused by Pseudomonas aeruginosa: report of an outbreak and review. *J. Clin. Microbiol.* 23 (3), 655–659. doi: 10.1128/jcm.23.3.655-659.1986

Reynolds, D., and Kollef, M. (2021). The epidemiology and pathogenesis and treatment of Pseudomonas aeruginosa infections: an update. *Drugs* 81 (18), 2117–2131. doi: 10.1007/s40265-021-01635-6

Rosenthal, V. D., Al-Abdely, H. M., El-Kholy, A. A., AlKhawaja, S. A. A., Leblebicioglu, H., Mehta, Y., et al. (2016). International Nosocomial Infection Control Consortium report, data summary of 50 countries for 2010-2015: Device-associated module. *Am. J. Infect. Control* 44 (12), 1495–1504. doi: 10.1016/j.ajic.2016.08.007

Rytter, H., Jamet, A., Coureuil, M., Charbit, A., and Ramond, E. (2020). Which current and novel diagnostic avenues for bacterial respiratory diseases? *Front. Microbiol.* 11. doi: 10.3389/fmicb.2020.616971

Salerian, A. J. (2020). Burn wound infections and Pseudomonas aeruginosa. *Burns* 46 (1), 257–258. doi: 10.1016/j.burns.2019.07.008

Sheppard, M. (1991). Pseudomonas aeruginosa endocarditis. *J. Hosp Infect.* 19 (4), 283. doi: 10.1016/0195-6701(91)90246-5

Silby, M. W., Winstanley, C., Godfrey, S. A., Levy, S. B., and Jackson, R. W. (2011). Pseudomonas genomes: diverse and adaptable. *FEMS Microbiol. Rev.* 35 (4), 652–680. doi: 10.1111/j.1574-6976.2011.00269.x

Surette, M. G. (2014). The cystic fibrosis lung microbiome. *Ann. Am. Thorac. Soc.* 11 Suppl 1, S61–S65. doi: 10.1513/AnnalsATS.201306-159MG

Tacconelli, E., Carrara, E., Savoldi, A., Harbarth, S., Mendelson, M., Monnet, D. L., et al. (2018). Discovery, research, and development of new antibiotics: the WHO priority list of antibiotic-resistant bacteria and tuberculosis. *Lancet Infect. Dis.* 18 (3), 318–327. doi: 10.1016/s1473-3099(17)30753-3

Takano, C., Seki, M., Kim, D. W., Gardner, H., McLaughlin, R. E., Kilgore, P. E., et al. (2019). Development of a novel loop-mediated isothermal amplification method to detect guiana extended-spectrum (GES) β-lactamase genes in Pseudomonas aeruginosa. *Front. Microbiol.* 10. doi: 10.3389/fmicb.2019.00025

Turner, K. H., Wessel, A. K., Palmer, G. C., Murray, J. L., and Whiteley, M. (2015). Essential genome of Pseudomonas aeruginosa in cystic fibrosis sputum. *Proc. Natl. Acad. Sci. U.S.A.* 112 (13), 4110–4115. doi: 10.1073/pnas.1419677112

van Asperen, I. A., de Rover, C. M., Schijven, J. F., Oetomo, S. B., Schellekens, J. F., van Leeuwen, N. J., et al. (1995). Risk of otitis externa after swimming in recreational fresh water lakes containing Pseudomonas aeruginosa. *Bmj* 311 (7017), 1407–1410. doi: 10.1136/bmj.311.7017.1407

Wang, J., Chen, H., Lin, X., Ji, C., and Chen, B. (2020). Multiple cross displacement amplification-a more applicable technique in detecting Pseudomonas aeruginosa of ventilator-associated pneumonia (VAP). *Crit. Care* 24 (1), 306. doi: 10.1186/s13054-020-03003-4

Wang, Y., Wang, Y., Ma, A. J., Li, D. X., Luo, L. J., Liu, D. X., et al. (2015). Rapid and sensitive isothermal detection of nucleic-acid sequence by multiple cross displacement amplification. *Sci. Rep.* 5, 11902. doi: 10.1038/srep11902

Williams, H. L., Turnbull, L., Thomas, S. J., Murphy, A., Stinear, T., Armstrong, D. S., et al. (2010). A diagnostic PCR assay for the detection of an Australian epidemic strain of Pseudomonas aeruginosa. *Ann. Clin. Microbiol. Antimicrob.* 9, 18. doi: 10.1186/1476-0711-9-18

Yakupogullari, Y., Otlu, B., Dogukan, M., Gursoy, C., Korkmaz, E., Kizirgil, A., et al. (2008). Investigation of a nosocomial outbreak by alginate-producing pan-antibiotic-resistant Pseudomonas aeruginosa. *Am. J. Infect. Control* 36 (10), e13–e18. doi: 10.1016/j.ajic.2008.07.006

Yang, H., Wang, Y., Yang, Q., Fan, H., Wang, L., Zhang, T., et al. (2021). and sensitive detection method for Pseudomonas aeruginosa using visualized recombinase polymerase amplification and lateral flow strip technology. *Front. Cell Infect. Microbiol.* 11. doi: 10.3389/fcimb.2021.698929

Yin, R., Cheng, J., Wang, J., Li, P., and Lin, J. (2022). Treatment of Pseudomonas aeruginosa infectious biofilms: challenges and strategies. *Front. Microbiol.* 13. doi: 10.3389/fmicb.2022.955286

Zetsche, B., Gootenberg, J. S., Abudayyeh, O. O., Slaymaker, I. M., Makarova, K. S., Essletzbichler, P., et al. (2015). Cpf1 is a single RNA-guided endonuclease of a class 2 CRISPR-Cas system. *Cell* 163 (3), 759–771. doi: 10.1016/j.cell.2015.09.038

Zhang, J. X., Xu, J. H., Yuan, B., Wang, X. D., Mao, X. H., Wang, J. L., et al. (2023). Detection of Burkholderia pseudomallei with CRISPR-Cas12a based on specific sequence tags. *Front. Public Health* 11. doi: 10.3389/fpubh.2023.1153352

Zhao, Y., Chen, F., Li, Q., Wang, L., and Fan, C. (2015). Isothermal amplification of nucleic acids. *Chem. Rev.* 115 (22), 12491–12545. doi: 10.1021/acs.chemrev.5b00428

Zheng, J., Liu, L., Li, X., Xu, Z., Gai, Z., Zhang, X., et al. (2023). Rapid and simple detection of Burkholderia gladioli in food matrices using RPA-CRISPR/cas12a method. *Foods* 12 (9), 1760. doi: 10.3390/foods12091760

frontiers | Frontiers in Cellular and Infection Microbiology

TYPE Brief Research Report
PUBLISHED 02 November 2023
DOI 10.3389/fcimb.2023.1301446

OPEN ACCESS

EDITED BY
Laura Cerqueira,
University of Porto, Portugal

REVIEWED BY
Anna Benini,
University of Verona, Italy
Tiziano Angelo Schweizer,
University Hospital Zürich, Switzerland

*CORRESPONDENCE
Wanil Kim
wkim@gnu.ac.kr
Min-Chul Cho
minchulcho7397@gmail.com

†These authors have contributed equally to this work

RECEIVED 25 September 2023
ACCEPTED 19 October 2023
PUBLISHED 02 November 2023

CITATION
Tak L-J, Shin M-K, Yoo J-I, Cho M-C and Kim W (2023) Development of droplet digital PCR-based detection of bacterial pathogens in prosthetic joint infection: a preliminary study using a synthesized model plasmid.
Front. Cell. Infect. Microbiol. 13:1301446.
doi: 10.3389/fcimb.2023.1301446

Development of droplet digital PCR-based detection of bacterial pathogens in prosthetic joint infection: a preliminary study using a synthesized model plasmid

Lee-Jung Tak[1], Min-Kyoung Shin[2], Jun-Il Yoo[3], Min-Chul Cho[4*†] and Wanil Kim[5*†]

[1]Department of Convergence Medical Science, Gyeongsang National University, Jinju, Republic of Korea, [2]Department of Microbiology, Department of Convergence Medical Science, and Institute of Health Sciences, School of Medicine, Gyeongsang National University, Jinju, Republic of Korea, [3]Department of Orthopedic Surgery, Inha University Hospital, Incheon, Republic of Korea, [4]Departments of Laboratory Medicine, Korea University Guro Hospital, Korea University College of Medicine, Seoul, Republic of Korea, [5]Department of Biochemistry, Department of Convergence Medical Science, and Institute of Health Sciences, School of Medicine, Gyeongsang National University, Jinju, Republic of Korea

Periprosthetic joint infection (PJI) can be diagnosed to characterize the microorganisms constituting a biofilm, which is an essential procedure for proper treatment. The gold standard method for detecting and identifying the causative microorganism is culture of microorganisms from patients-derived sample.; however, this method takes a long time and has low sensitivity. To compensate for these limitations, identification methods based on real-time PCR (RT-PCR) have been widely used. However, RT-PCR also has limitations, including low sensitivity and the requirement of a standard curve for quantification. Therefore, to prevent significant proliferation of pathogenic bacteria, it is important to detect a limited number of infectious bacteria during early stages of PJI. In the present study, we developed droplet digital PCR-based detection of bacterial pathogens in PJI. And we evaluated the analytical performance of the assay using a model plasmid, based on the 16S ribosomal DNA sequence of target bacteria commonly found in PJI. We also prepared genomic DNA extracted from *E. coli*, *S. aureus*, and *S. epidermidis* to test whether ddPCR provides better sensitivity and quantification of the target sequences. ddPCR detected 400 attograms of target DNA, which was more than 10 times less than that detected by real-time PCR using synthesized plasmid. In addition, ddPCR detected target regions from genomic DNA of 50 femtograms for *E. coli*, 70 femtograms for *S. epidermidis*, and 90 femtograms for *S. aureus*. The results indicate that ddPCR has the potential to decrease the microbial detection limit and provide precise detection, signifying its effectiveness for early PJI.

KEYWORDS

ddPCR, periprosthetic joint infection, diagnosis, bacteria, infection

Introduction

The prevalence of artificial joint transplantation is increasing owing to increased life expectancy and changing lifestyles among the older population (Kurtz et al., 2007). Periprosthetic joint infections (PJI) result in inflammation of the synovial membrane and bone following artificial joint replacement surgery. The number of publications on periprosthetic joint infection continues to grow as the number of PJIs and transplants increases (Li et al., 2020). PJI has been reported to occur in 1%–2% of primary arthroplasties and 4% of revision surgeries (Ong et al., 2009; Aggarwal et al., 2013). PJI is a devastating complication associated with high morbidity rates, prolonged hospitalization, and the need for additional surgery with antimicrobial treatment (Schwarz et al., 2019; Pannu et al., 2021).

PJI can occur either in the early post-implantation phase, typically within the first 4 weeks, or later, usually between 3 months and 3 years after implantation. Early infections are caused by highly virulent pathogens, such as *Staphylococcus aureus*, *Streptococci*, and *Enterococci*, while delayed infections are caused by less virulent organisms (Izakovicova et al., 2019; Gatti et al., 2022). There are many microorganisms causing PJI, such as *Staphylococcus aureus*, coagulase-negative *Staphylococcus*, *Streptococcus* species, Enterococcus species, and gram-negative bacteria (Choong et al., 2007; Kuiper et al., 2014; Patel, 2023). Pathogenic microorganisms adhere to the implants and form microcolonies and biofilms via cell proliferation and intercellular adhesion (Parvizi et al., 2011). The most common bacteria responsible for the formation of such biofilms are *Staphylococcus aureus* and *Staphylococcus epidermidis* (Choong et al., 2007).

Diagnosis of PJI can be performed in multiple steps, including laboratory testing, imaging, and joint aspiration (Izakovicova et al., 2019). The 2018 Evidence-Based Stepwise Algorithm for Diagnosis of PJI is a clinical decision-making tool that provides a systematic approach to the diagnosis of PJI. The algorithm is based on the 2018 Musculoskeletal Infection Society (MSIS) criteria for the diagnosis of PJI, which are the most widely accepted diagnostic criteria for PJI. The algorithm consists of four steps: 1) clinical evaluation, 2) laboratory testing, 3) Imaging studies, 4) Joint aspiration and culture. The 2018 Evidence-Based Stepwise Algorithm for Diagnosis of PJI is a valuable tool for clinicians who are diagnosing PJI. The algorithm provides a systematic approach to the diagnosis of PJI, which can help to improve the accuracy of diagnosis and the quality of care for patients with PJI (Parvizi et al., 2011; Osmon et al., 2013).

Because the identification of microbes is essential for the appropriate treatment of PJI, PJI can be further diagnosed through the detection of pathogenic microbes in the affected tissue, synovial aspirate, and blood. However, the limitations of the detection of microbes in fluids include a high detection limit, difficulty in initial diagnosis, and lack of a method for the simultaneous detection of various pathogenic microbes. The primary and most important method for detecting the causative microorganism is the direct culture of patient-derived samples. Since the introduction of sonication culture, the sensitivity of PJI diagnosis has drastically increased (Rodriguez-Merchan, 2022). However, culturing tissue samples obtained during joint aspiration (i.e., synovial fluid) or surgery remains time-consuming and has low sensitivity. Culture-negative results have been observed in numerous PJI cases, leading to unnecessary antibiotic use or even unnecessary surgery (Berbari et al., 2007; Trampuz et al., 2007; Bellova et al., 2019). If culture-negative PJI are still clinically suspected, a presumptive diagnosis is made using other indirect markers, such as C-reactive protein (CRP), erythrocyte sedimentation rate (ESR), leukocyte esterase, and alpha-defensin (Palan et al., 2019).

Through broad-range PCR method, it might be possible to roughly confirm whether the cause of PJI is a bacterium or fungus prior to accurate bacterial identification of the species. The differential detection of these bacterial and fungal infections provides important information for clinicians in selecting appropriate drugs and determining treatment directions.

Among the PCR-based molecular diagnostic methods, real-time PCR has been widely used instead of traditional PCR. Because this method quantifies the amount of DNA via the cycle threshold (Ct) value, which is defined as the number of cycles for the amplicon-derived fluorescence to exceed the background, a standard curve should be generated for quantitative analyses, which makes this method non-preferred (Kralik and Ricchi, 2017). Significant deviations could also occur in the results owing to differences in many variables, such as amplification efficiency, template processing, and machine error in each trial.

Recently, droplet digital PCR (ddPCR) was introduced for clinical diagnostics. ddPCR divides a mixed volume of polymerase, primers, and templates into tens of thousands of droplets, so that the number of target amplifications can be counted in a digital-like on-and-off manner (Hindson et al., 2011). This method enables absolute quantification of the targets without standard curve generation, as well as quantification of a small number of targets with better sensitivity and accuracy than conventional diagnostic tools (Hindson et al., 2011; Pinheiro et al., 2012). Thus, ddPCR has garnered significant interest in the clinical field, particularly in cases with limited access to *in vivo* samples with mutated genes in hemato-oncology and infectious disease pathogens (Miotke et al., 2014; Li et al., 2018). However, the use of ddPCR for detecting PJI has not yet been reported. Here, we suggest the potential application of ddPCR for diagnosing significant pathogenic microbes with high sensitivity and accuracy, so that the method could be used in the clinical determination of PJI.

Materials and methods

Determination of target region and primers

The primers and probes targeting common sequences on 16S rRNA of PJI significant microbes are described in previous study (Horz et al., 2005). Briefly, a universal primer sequence was determined using the 'Probe Match' of ARB phylogenetic software, a database for maintaining and managing sequence data. The universal PCR primer and probe sequences were determined through in silico 16S ribosomal RNA gene sequence

analysis of 43 sub-strains of *S. aureus*, 7 sub-strains of *S. epidermidis*, and 4 sub-strains of *E. coli*. Common 16S ribosomal RNA regions for targeting were selected from reference genomes of *Escherichia coli* (Genbank ID: MF.372553.1), *Staphylococcus aureus* (Genbank ID: MN524176.1), and *Staphylococcus epidermidis* (Genbank ID: OP481211.1).

Plasmid DNA transformation and Midi prep

A model plasmid was synthesized based on the 16S ribosomal DNA sequences of target bacteria commonly present in PJI. The target DNA fragment was inserted into pUCosmo-Amp provided by Cosmogenetech (Cosmogenetech, Daejeon, Korea). 1μl of plasmid DNA was added to DH5α chemically competent *E. coli* (Enzynomics, Daejeon, Korea), followed by inoculation on an ampicillin selection plate and incubated overnight at 37°C. Midi prep of the plasmids was performed with 250 ml culture of the transformed bacteria, and DNA was then obtained using the NucleoBond® Xtra Midi Plus kit (MACHEREY-NAGEL, Düren, NW, Germany). DNA quantification was measured at 260 nm using a QIAxpert spectrophotometer (QIAGEN, Hilden, Germany).

Design of primers and probes

Primers and probes were designed using the 16S ribosomal RNA sequences inserted into plasmid DNA and are shown in the below. FAM was selected as the receptor dye of the probe, and BHQ-1 was chosen as the quencher dye.

Forward primer: 5`-TCCTACGGGAGGCAGCAGT-3`
Reverse primer: 5`-GGACTACCAGGGTATCTAATCCTGTT-3`
Probe: 5`-[Fam]CGTATTACCGCGGCTGCTGGCAC[BHQ-1]-3`

Qualitative conventional PCR

Template DNA was continuously diluted 10 times to a concentration of 400ag. A sample containing primers only was used as a negative control. PCR was performed using a Go-Taq (Promega, Madison, WI, USA) and a VeritiPro thermal cycler (Thermo Fisher scientific Inc., Waltham, MA, USA). The amplification program was one cycle for 5 minutes (95°C), followed by 30 cycles of 30 seconds at 95°C, 30 seconds at 55°C, and 30 seconds at 72°C. The amplicon was also visualized under gel electrophoresis for size control. Electrophoresis was performed at 50 volts using 2% agarose gel (FMC bioproduct, Philadelphia, Pennsylvania, USA). The agarose gel was stained and visualized using MaXidoc Gel Imaging System (DAIHAN scientific, Wonju, Korea).

Real-time PCR

Real-time PCR was performed with PCR Master Mix (GenDEPOT, Barker, Texas, USA) using the Rotor-Gene Q device (QIAGEN, Hilden, Germany). Samples were diluted in the same manner as qualitative PCR. Amplification was performed for 5 minutes at 95°C for activation, followed by 30 cycles of 30 seconds at 95°C, 30 seconds at 55°C, and 30 seconds at 72°C. CT values were plotted using Graphpad Prism software (Graphpad Software Inc, San Diego, CA, USA).

Droplet-digital PCR

Target DNA was also quantified using a QX200 droplet digital PCR instrument (Bio-Rad, Hercules, CA, USA). We prepared 20μl of ddPCR reaction mix containing ddPCR Supermix for Probes (no dUTP) (Bio-Rad, Hercules, CA, USA), DNA template, and primer/probe. A 40 μL emulsified mixture was prepared by combining 20 μL PCR mix and probe droplet formation oil (Bio-Rad, Hercules, CA, USA). All the procedures were performed on a QX200 Droplet Digital PCR System (Bio-Rad, Hercules, CA, USA). After droplet generation, the emulsified mixture was transferred to a clean 96-well plate and sealed with the PX1 PCR plate sealer (Bio-Rad, Hercules, CA, USA) at 180°C for 5 seconds. The emulsified mixture was then PCR amplified. The VeritiPro Thermal Cycler equipment was used for amplification (Thermo Fisher Scientific Inc., Waltham, MA, USA). The thermal cycling involved 40 cycles of 30 seconds at 94°C and 1 minute at 60°C, followed by a 10-minute incubation at 95°C to terminate the PCR reaction. The instrument had a ramp rate of 2°C/sec for all steps. QuantaSoft was used to determine the number of positive droplets (Bio-Rad, Hercules, CA, USA).

Bacteria genomic DNA extraction

Escherichia coli (*E. coli* KBN12P06660), *Staphylococcus aureus* (*S. aureus* KBN12P06533), and *Staphylococcus epidermidis* (*S. epidermidis* KBN12P06690) were provided from the Fastidious Specialized Pathogen Resources Bank (a member of the National Culture Collection for Pathogens), Gyeongsang National University Hospital, Jinju, Korea. All bacteria strains used in the study were obtained from clinical samples. Bacterial DNA was extracted using PureLink™ Genomic DNA Mini Kit (Thermo Fisher scientific Inc., Waltham, MA, USA) according to the manufacturer's instruction.

Results

Determination of primer design and target

We utilized a common 16S rRNA sequence from a previous study (Horz et al., 2005) and conducted all the analyses in this study. This sequence included the common 16S rRNA of *E. coli*, *S. aureus*, and *S. epidermidis*, which are the most frequent and representative pathogenic bacteria detected in PJI (Figure 1A). Primers and probes were designed and based on this sequence, along with the FAM dye and BHQ-1 quencher. Next, a model plasmid was created by synthesizing the target sequence and inserting it into a simple plasmid (Figure 1B).

Construction of synthesized 16s rRNA sequence inserted plasmid for the analysis of limit of detection

Ampicillin-resistant pUCosmo-Amp™ provided by Cosmogenetech was used as the vector, and purified DNA was serially diluted to determine the minimum detection threshold. To reduce the time required for the extraction of genomic DNA from microorganisms and compensate for the purity and low yield of the final product owing to the many intermediate steps, we analyzed the detection of common 16S sequences based on the synthesized model plasmids. The number of transformed colonies decreased as the DNA was diluted (Figure 2A). 400 ng of the plasmid DNA was serially diluted and transformed into DH5α *E. coli*, and the colony number was quantified. Transformation with 400 fg of the plasmid ($2.4x10^5$ plasmids) yielded 70 colonies; however, we could not find any colonies under 400 fg.

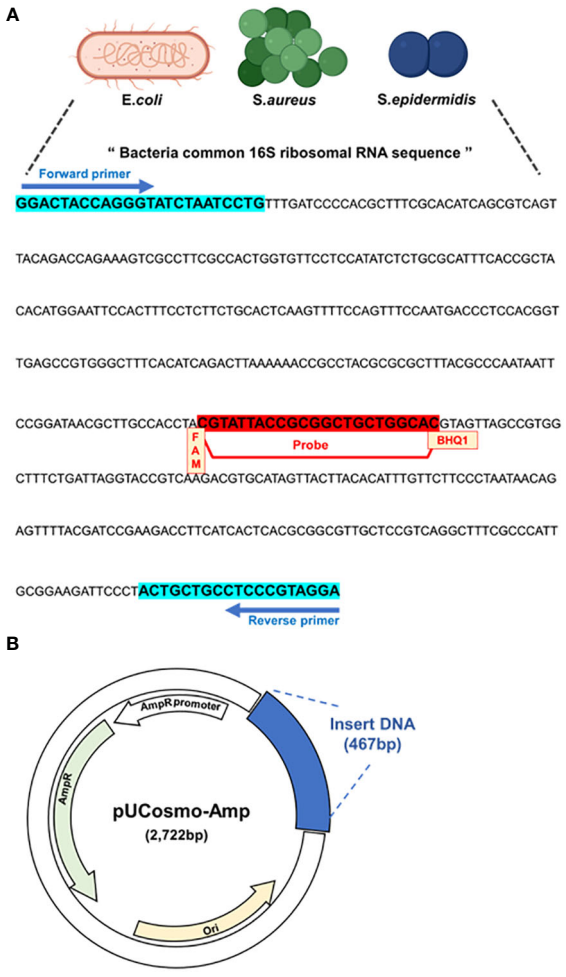

FIGURE 1
Model plasmid and primer design. **(A)** Primers and probe that target common sequences on 16S rRNA of PJI significant bacteria, *E coli*, S. *aureus* and S. *epidermidis*. The probe has FAM as the receptor dye and BHQ-1 as the quencher dye. **(B)** Schematic of model plasmid. The target DNA fragment was inserted into ampicillin-resistant pUCosmo-Amp plasmid provided by Cosmogentech. The plasmid was then added to DH5α chemically competent *E coli*, transformed, and then used in the experiment.

Test using conventional PCR

Next, we PCR-amplified the diluted DNA to assess the minimal number of plasmids with a detectable signal on agarose gel electrophoresis (Figure 2B). DNA of the concentration of 400 pg was 1/10 diluted and amplified using Taq polymerase, followed by visualization on a 2% agarose gel. The result shows that 400 fg of DNA (2.4×10^5 plasmids) was the minimum detectable concentration, which is consistent with the transformation analysis in Figure 2A. Band quantification using ImageJ also decreased as the DNA diluted. Therefore, there was no difference in the detection limit between the PCR and bacterial transformation methods for the target 16S rRNA sequence.

Analysis of limit of detection using real-time PCR

Next, we performed quantitative real-time PCR to assess the detection limit of the diluted plasmids (Figure 2C). As the DNA concentration decreased, the threshold cycle number (Ct) increased, and there was no significant difference between the no-template control and the 400 ag (attogram) DNA. When 40 fg or less of DNA was used for the analysis, a plateau was not reached, but there was a clear graphical difference from the no-template control (NTC). However, the amplification curve for 4fg DNA was not significantly different from that of NTC. Therefore, we assume the minimum amount of target DNA that can be detected by real-time PCR to 40 fg or more.

Analysis of LOD using ddPCR

Subsequently, the detection threshold was determined by ddPCR analyses with serially diluted DNA (Figure 2D). We found that 400 ag of the plasmid DNA (240 plasmid copies) generated an average of 74 positive droplets. However, the difference in the number of droplets between 4fg and 400ag was insignificant. Therefore, we concluded that the ddPCR assay could detect 4fg, which corresponds to 2400 copies of target sequence fragments. Taken together, these results suggest that the detection of target sequences through ddPCR is advantageous for quantitative analysis compared to conventional real-time PCR analysis and has the potential to lower the minimum detection limit.

Comparison of LOD of real-time PCR with that of ddPCR using bacterial genomic DNA

We tested the detection limits of gDNA extracted from *E. coli*, *S. aureus*, and *S. epidermidis* at different dilutions. First, we confirmed

10.3389/fcimb.2023.1301446

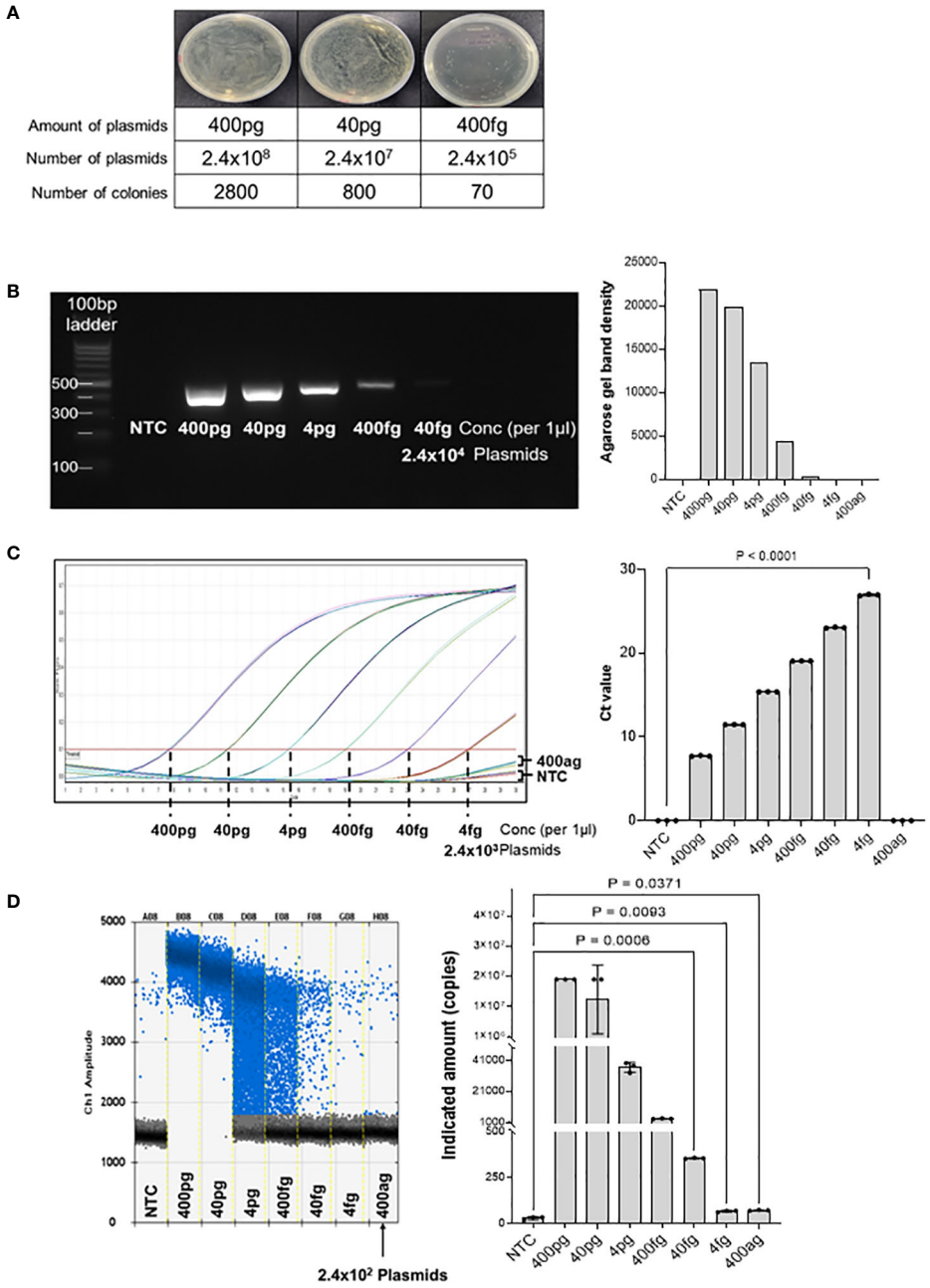

FIGURE 2
Threshold determination with model plasmid. **(A)** The model plasmid containing the target sequences was serially diluted and transformed into *E coli* to quantify the number of colonies. The results show that 400 fg of model plasmid was the minimum amount to detect visible colonies on the plate. The number of colonies was quantified using Image J program. **(B)** The model plasmid was PCR-amplified using Taq polymerase and visualized by electrophoresis on a 2% agarose gel. As the concentration decreased, the band density also decreased. There was no band on the no template control and concentration below 400 fg. **(C)** Quantitative real-time PCR was performed for 30 cycles to determine the Ct (cycle threshold) of the diluted model plasmid. The results were visualized using GraphPad software. 400 fg of DNA reached a plateau at the end of the cycles, which was significantly different from the control. 4 fg of DNA did not reach a plateau for Ct analysis compared to the control, but was visually different from the control. **(D)** Digital droplet PCR was performed to determine the detection limit of the diluted plasmids. The raining drops between 4 pg and 40 fg range could be optimized, but since the purpose of this method is to detect any bacteria in the samples qualitatively, this would not be a significant flaw of this method. The LOD of the ddPCR-based detection was 100 pg, corresponding to $2.4x10^2$ plasmids. The fluorescence value generated by DNA amplification was assessed as the indicated amount, and positive droplets containing target DNA were counted using a droplet reader and displayed in blue. The measured positive droplet was converted to a calculated value according to Poisson's Law of Dispersion in the analysis program and displayed in the graph. Results are shown as mean ± SD, one-way ANOVA test. NTC, no template control; pg, picogram; fg, femtogram; ag, attogram; conc, concentration.

the detection limit of the PCR-amplified diluted DNA by agarose gel electrophoresis (Figure 3A). The minimum detectable concentrations were 50 pg in *E. coli*, 9 pg in *S. aureus*, and 700 fg *S. epidermidis*. Band quantification using ImageJ also showed a decrease in band intensity with DNA dilution. In the PCR amplification results, the detection limits for *E. coli* and *S. aureus* were higher than those in our model plasmid experiment, whereas the detection limits for *S. epidermidis* were confirmed to be similar.

Quantitative real-time PCR was performed to confirm the detection limit of the diluted microorganisms (Figure 3B). As the concentration of the microorganisms decreased, the Ct value increased. Significant differences were observed between the no-template control and *E. coli* at 500 fg, *S.aureus* at 900, and *S. epidermidis* at 700 fg. The DNA amplification curves of less than 50 fg for *E. coli*, 90 fg for *S. aureus*, and 70 fg for *S. epidermidis* were not significantly different from those of NTC, nor were the Ct values. Therefore, we suggest that the minimum amount of microbial DNA detected by real-time PCR is 500 fg in *E. coli*, 900 fg in *S. aureus*, and 700 fg in *S. epidermidis*.

Considering that ddPCR can efficiently reduce the detection limit in model plasmid experiments, we performed ddPCR analysis with serially diluted microorganism DNA (Figure 3C). In *E. coli*, 50 fg of plasmid DNA (31,000 plasmid copies) generated an average of 66 positive droplets. However, the number of droplets generated at < 5 fg was negligible. Next, in *S. aureus*, 900 fg of plasmid DNA (5.5 x10^5 plasmid copies) generated an average of 1246 positive droplets. Compared to 90–900 ag (attogram), 900 fg of *S. aureus* DNA generated significantly more positive droplets than the no-template control. We found that *S. epidermidis* DNA generated an average of 114 positive droplets (43,000 plasmid copies) at a concentration of 70 fg. However, the number of droplets generated at 7 fg and 700 ag was insignificant. Thus, the limit of detection (LOD) of ddPCR was determined to be 50 fg for *E. coli*, 900 fg for *S. aureus*, and 70 fg for *S. epidermidis*.

Discussion

One prominent method for diagnosing PJI involves detecting infectious bacteria by real-time PCR. Among the microbes that cause PJI, bacteria account for over 97% of the cases, with fungi accounting for the remaining cases (Benito et al., 2016). In bacteria, there is a common region suitable for universal amplification of 16rRNA (Plouzeau et al., 2015). Similarly, in fungi, conserved regions within the 18S, 5.8S, and 28S ribosomal subunits can be targeted for universal amplification (Petti, 2007). Thus, the application of broad-range PCR, which can be amplified and detected by targeting the common regions of these bacteria, is feasible (Bemer et al., 2014).

In this study, we confirmed that the designed primer set and probe targeting the 16S ribosomal RNA sequences worked properly in tests using conventional PCR and real-time PCR prior to the main ddPCR experiment. The melting temperatures of the primers and probes were optimized using conventional real-time PCR. To facilitate the limit-of-detection analysis, we constructed a plasmid containing an artificially synthesized 16s rRNA sequence. In experiments using this plasmid, the LOD of real-time PCR and ddPCR were confirmed to be 40 fg and 4 fg, respectively, confirming that the LOD of ddCPR was approximately 10 times lower than that of real-time PCR. In addition, to perform LOD analysis in a situation similar to an actual clinical situation, we extracted and tested the gDNA of *S. aureus, S. epidermidis, and E. coli*, which have been reported as the main causative bacteria of PJI. In the LOD experiment using bacterial gDNA, the LOD differed slightly for each strain. The LODs of real-time PCR was 500 fg for *E. coli*, 900 fg for *S. aureus*, and 700 fg for *S. epidermidis*, whereas the LODs of ddPCR was 50 fg for *E. coli*, 900fg for *S. aureus*, and 70 fg for *S. epdermidis* confirming that the LOD of ddPCR was approximately 10/1 compared to real-time PCR.

Although culture is still the gold standard for diagnosis of PJI, in order to increase sensitivity and diagnose PJI as quickly as possible, molecular diagnosis based on real-time PCR has recently been widely used as an auxiliary tool for diagnosis of PJI (Rougemont et al., 2004). However, these real-time PCR-based molecular diagnostic methods do not show satisfactory results in terms of sensitivity, accuracy, or replicability when the concentration of the infectious agent is low during the early stages of infection (Li et al., 2018). The ddPCR technique used in our study has the advantage of being more sensitive than real-time PCR and enables more accurate quantitative testing without a separate control material. These characteristics further strengthen the possibility of using ddPCR as a molecular diagnostic method for detecting infectious agents in PJI.

Because there is no specific diagnostic method for PJI, diagnosis of PJI is diagnosed by performing many tests and comprehensively interpreting the results. These include laboratory and imaging studies. Laboratory tests included non-specific inflammatory markers, such as serum C-reactive protein (CRP), erythrocyte sedimentation rate (ESR), procalcitonin, peripheral blood leukocytes, synovial fluid (SF) white blood cells, and bacterial cultures of preoperative SFs and intraoperative tissues (Peel et al., 2012; Saleh et al., 2018). However, these systemic inflammatory markers are often normal in PJIs caused by low-virulence pathogens (Dodson et al., 2010; Piper et al., 2010; Perez-Prieto et al., 2017).

According to the PJI treatment guidelines, when PJI is diagnosed, surgery to replace an artificial joint is required; therefore, it is very important to clearly detect the source of infection to determine the direction of treatment (Izakovicova et al., 2019). In addition, bacteria account for approximately 97–99% of PJI infectious agents, and fungi account for approximately 1–3%, and are caused by mycobacteria at a very low frequency (Benito et al., 2016). When referring to the frequency of such PJI infectious agents, confirming the presence of bacteria in specimens such as joint fluid in patients suspected of having PJI would be very useful for determining the treatment strategy. With this rationale, we developed a diagnostic method that focuses on detecting the bacteria that account for the largest proportion of the causes of PJI. Gram-positive bacteria are the main species detected in PJI after joint replacement surgery, but gram-negative bacteria account for a low percentage (Wang et al., 2018). Among Gram-positive bacteria, *Staphylococcus epidermidis* and *Staphylococcus aureus* had the highest frequency, and among Gram-negative bacteria,

10.3389/fcimb.2023.1301446

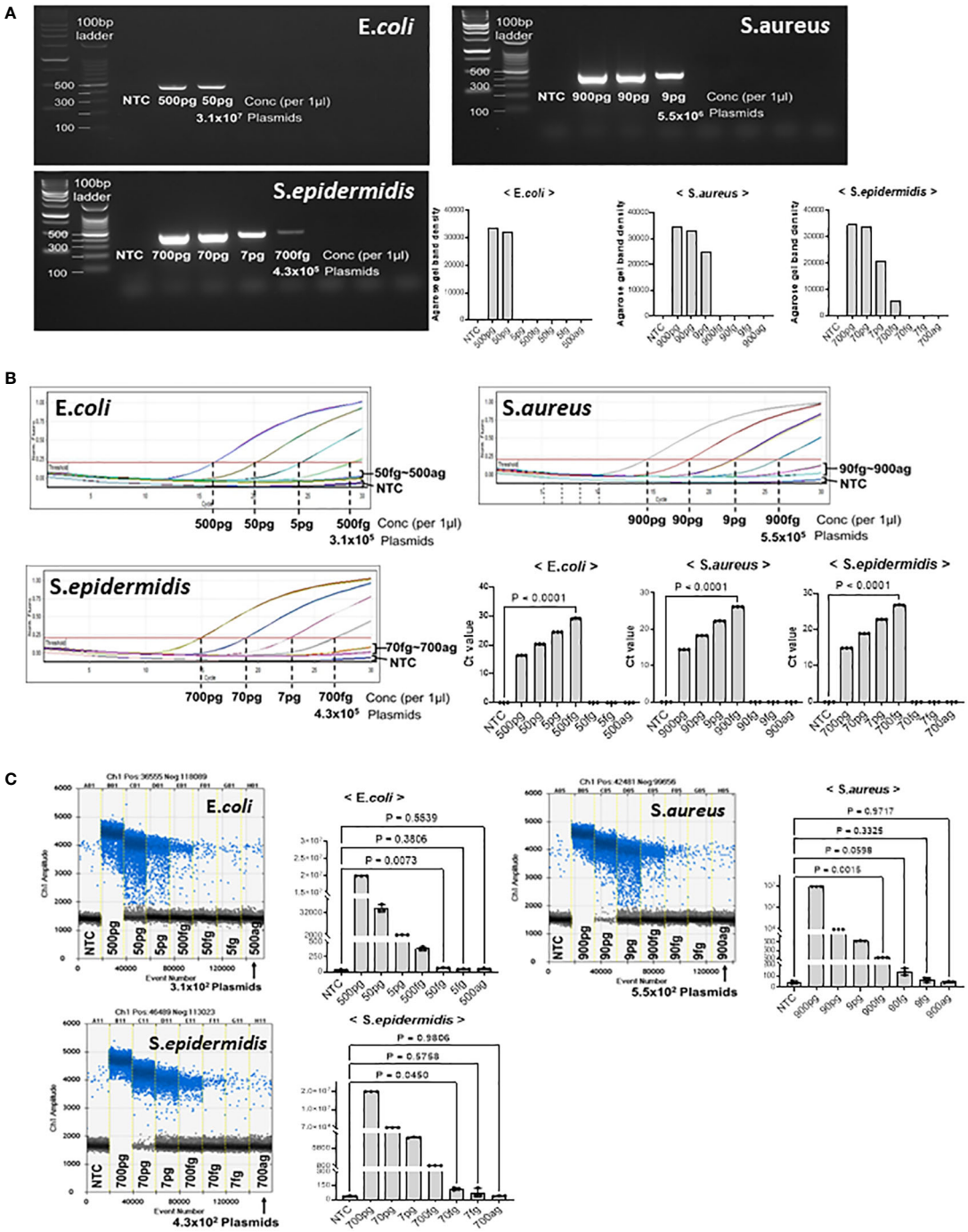

FIGURE 3
Threshold determination with genomic DNA from *E coli*, *S. aureus*, and *S. epidermidis*. PJI-significant bacteria were cultured and collected for genomic DNA purification. Genomic DNA from each bacterium was then serially diluted to determine if our method could amplify and detect target sequences with genomic DNA from cultured bacteria. **(A)** Total genomic DNA was diluted and PCR amplified. The LOD for *E coli* was 50 pg, the LOD for *S. aureus* was 9 pg, and the LOD for *S. epidermidis* was 700 fg. The LOD of the bacteria showed large difference with the same primer sets, which could be due to the different complexity and obstacle around the target sequences. The results were visualized on a 2% agarose gel. The band density was quantified by Image J program. **(B)** Real-time PCR was performed to determine the Ct of bacterial genomic DNA. We determined the LOD even if the DNA amplification did not reach a plateau, if there was a visual difference between the control and the sample on the graph. The real-time PCR analysis for all three bacteria showed significant differences in genomic DNA at the level of hundreds of fg compared to the control. **(C)** ddPCR was performed to determine the LOD with genomic DNA from PJI significant bacteria. For *S. aureus*, ddPCR showed the same LOD as real-time PCR, but for *E coli* and *S. epidermidis*, it was 10 times more sensitive than real-time PCR, detecting 50 fg and 70 fg, respectively. The positive and negative droplets as classified by the thresholds are shown in blue and grey, respectively. The calculated value of the positive droplet according to Poisson's law of dispersion was graphed. Results are shown as mean ± SD, one-way ANOVA test. NTC, no template control; pg, picogram; fg, femtogram; ag, attogram; conc, concentration.

Escherichia coli accounted for the highest frequency (Benito et al., 2016). In our study, the test was conducted using three bacterial strains that accounted for such a high frequency.

In this study, we observed a higher LOD for gDNA samples from cultured bacteria than in purified model plasmid used in other experiments, which could be due to the following reasons. First, some of the target DNA may have been lost during the extraction of genomic DNA from the bacteria. This can be solved in the future by optimizing the extraction process for the appropriate genomic DNA. Second, the target region is surrounded by many non-target regions that may interfere with primer binding. In the future, it may be possible to select and detect the target region through treatment with restriction enzymes (frequent cutters). Third, the target DNA sequence must be contained within the ddPCR droplet for proper results; because the bacterial chromosome exists as a continuous macromolecule, physical space limitations may have occurred. This may be addressed in the future by treatment with the appropriate restriction enzymes.

Overall, in *E. coli* and *S. epidermidis*, the results clearly showed that ddPCR is advantageous for quantitative analysis compared to prior real-time PCR analysis. For *S. aureus*, the LOD was 900 fg, which was similar to that of real-time PCR. However, at 90 fg, the average number of ddPCR-positive droplets was 140, which was significantly higher than that of the control (44 droplets). Although it did not show statistical significance in this report, further studies could optimize the ddPCR parameters so that the assessment of samples under 900fg could be possible in the future. In addition, for *S. aureus*, when comparing ddPCR and real-time PCR, the detection limit with an effective value was 900 fg. However, considering that ddPCR had 140 positive droplets at a 90 fg concentration compared with NTC (44 droplets), it is considered to have a clear difference from the no-template control. Previous studies have reported that the LOD of ddPCR is approximately 1000 times lower than that of real-time PCR, but it was confirmed to be approximately 10 times lower in this study. It can be inferred that this difference is probably caused by a problem with the nucleic acid extraction method, such as DNA loss during the nucleic acid extraction process, or because the protocol of our ddPCR method has not yet been fully optimized. Thus, for future clinical applications of ddPCR detection technology, validation based on different bacteria involved in PJI infection is required. In addition, the optimization and validation of protocols for handling human-derived samples (such as synovial fluid) and obtaining genomic DNA of sufficient quality for testing are needed. The ddPCR can also identify genetic markers associated with resistance to specific pathogens. According to several reports (McEvoy et al., 2018; Zmrzljak et al., 2021) ddPCR has higher sensitivity to detect somatic mutations, enabling the determination of antibiotic resistance caused by a small number of mutations using specific primer sets.

This study had several limitations. First, the ddPCR method we developed was applied to only three bacteria, and has been applied to more diverse bacteria; therefore, it was not confirmed that all bacteria could be detected by the ddPCR method. Second, the ddPCR method developed in this study was evaluated using synthesized DNA sequences and gDNA of cultured bacteria, and clinical specimens, such as joint fluids of patients, could not be evaluated. In this study, we have presented preliminary data confirming the potential of ddPCR for bacterial detection in PJI and have evaluated its analytical performance. However, additional validation with clinical samples is essential to establish the utility of our ddPCR assay for the diagnosis of PJI in real patients

Conclusions

In this study, we developed a method for detecting bacteria in PJI using a ddPCR platform, which is known to be more sensitive than real-time PCR. It was confirmed that the method we developed properly worked in plasmids into which artificially synthesized DNA sequences were inserted and in actual Gram-negative and Gram-positive bacteria. In addition, by comparing this method with the real-time PCR method, it was confirmed that it is a more sensitive method with a low LOD of approximately 1/10. Therefore, the ddPCR-based assay we developed is a highly sensitive diagnostic method that can significantly help in detecting bacteria in patients with PJI.

Data availability statement

The original contributions presented in the study are included in the article/supplementary material. Further inquiries can be directed to the corresponding authors.

Author contributions

L-JT: Conceptualization, Data curation, Formal Analysis, Investigation, Visualization, Writing – original draft. M-KS: Resources, Supervision, Validation, Writing – review & editing. J-IY: Conceptualization, Supervision, Validation, Writing – review & editing. M-CC: Funding acquisition, Methodology, Supervision, Writing – original draft, Writing – review & editing. WK: Conceptualization, Funding acquisition, Investigation, Project administration, Supervision, Validation, Writing – original draft, Writing – review & editing.

Funding

The author(s) declare financial support was received for the research, authorship, and/or publication of this article. This work was supported by biomedical research institute fund (GNUHBRIF-2021-0011) from the Gyeongsang National University Hospital. This work was also supported by the National Research Foundation of Korea (NRF) grant funded by the Korea government (MSIT) (No. 00219399).

Acknowledgments

The pathogen resources (KBN12P06660, KBN12P06533, and KBN12P06690) for this study were provided by the Fastidious Specialized Pathogen Resources Bank (a member of the National Culture Collection for Pathogens, Gyeongsang National University Hospital, Jinju, Korea). The authors thank the reviewers for their

valuable suggestions, which helped to improve the quality of the manuscript.

Conflict of interest

The authors declare that the research was conducted in the absence of any commercial or financial relationships that could be construed as a potential conflict of interest.

Publisher's note

References

Aggarwal, V. K., Rasouli, M. R., and Parvizi, J. (2013). Periprosthetic joint infection: Current concept. *Indian J. Orthop.* 47 (1), 10–17. doi: 10.4103/0019-5413.106884

Bellova, P., Knop-Hammad, V., Konigshausen, M., Mempel, E., Frieler, S., Gessmann, J., et al. (2019). Sonication of retrieved implants improves sensitivity in the diagnosis of periprosthetic joint infection. *BMC Musculoskelet Disord.* 20 (1), 623. doi: 10.1186/s12891-019-3006-1

Bemer, P., Plouzeau, C., Tande, D., Leger, J., Giraudeau, B., Valentin, A. S., et al. (2014). Evaluation of 16S rRNA gene PCR sensitivity and specificity for diagnosis of prosthetic joint infection: a prospective multicenter cross-sectional study. *J. Clin. Microbiol.* 52 (10), 3583–3589. doi: 10.1128/JCM.01459-14

Benito, N., Franco, M., Ribera, A., Soriano, A., Rodriguez-Pardo, D., Sorli, L., et al. (2016). Time trends in the aetiology of prosthetic joint infections: a multicentre cohort study. *Clin. Microbiol. Infect.* 22 (8), 732 e1–732 e8. doi: 10.1016/j.cmi.2016.05.004

Berbari, E. F., Marculescu, C., Sia, I., Lahr, B. D., Hanssen, A. D., Steckelberg, J. M., et al. (2007). Culture-negative prosthetic joint infection. *Clin. Infect. Dis.* 45 (9), 1113–1119. doi: 10.1086/522184

Choong, P. F., Dowsey, M. M., Carr, D., Daffy, J., and Stanley, P. (2007). Risk factors associated with acute hip prosthetic joint infections and outcome of treatment with a rifampinbased regimen. *Acta Orthop.* 78 (6), 755–765. doi: 10.1080/17453670710014527

Dodson, C. C., Craig, E. V., Cordasco, F. A., Dines, D. M., Dines, J. S., Dicarlo, E., et al. (2010). Propionibacterium acnes infection after shoulder arthroplasty: a diagnostic challenge. *J. Shoulder Elbow Surg.* 19 (2), 303–307. doi: 10.1016/j.jse.2009.07.065

Gatti, G., Taddei, F., Brandolini, M., Mancini, A., Denicolò, A., Congestrì, F., et al. (2022). Molecular approach for the laboratory diagnosis of periprosthetic joint infections. *Microorganisms* 10 (8), 1573. doi: 10.3390/microorganisms10081573

Hindson, B. J., Ness, K. D., Masquelier, D. A., Belgrader, P., Heredia, N. J., Makarewicz, A. J., et al. (2011). High-throughput droplet digital PCR system for absolute quantitation of DNA copy number. *Anal Chem.* 83 (22), 8604–8610. doi: 10.1021/ac202028g

Horz, H. P., Vianna, M. E., Gomes, B. P., and Conrads, G. (2005). Evaluation of universal probes and primer sets for assessing total bacterial load in clinical samples: general implications and practical use in endodontic antimicrobial therapy. *J. Clin. Microbiol.* 43 (10), 5332–5337. doi: 10.1128/JCM.43.10.5332-5337.2005

Izakovicova, P., Borens, O., and Trampuz, A. (2019). Periprosthetic joint infection: current concepts and outlook. *EFORT Open Rev.* 4 (7), 482–494. doi: 10.1302/2058-5241.4.180092

Kralik, P., and Ricchi, M. (2017). A basic guide to real time PCR in microbial diagnostics: definitions, parameters, and everything. *Front. Microbiol.* 8. doi: 10.3389/fmicb.2017.00108

Kuiper, J. W., Willink, R. T., Moojen, D. J., van den Bekerom, M. P., and Colen, S. (2014). Treatment of acute periprosthetic infections with prosthesis retention: Review of current concepts. *World J. Orthop.* 5 (5), 667–676. doi: 10.5312/wjo.v5.i5.667

Kurtz, S., Ong, K., Lau, E., Mowat, F., and Halpern, M. (2007). Projections of primary and revision hip and knee arthroplasty in the United States from 2005 to 2030. *J. Bone Joint Surg. Am.* 89 (4), 780–785. doi: 10.2106/JBJS.F.00222

Li, C., Ojeda-Thies, C., Xu, C., and Trampuz, A. (2020). Meta-analysis in periprosthetic joint infection: a global bibliometric analysis. *J. Ortho. Surg. Res.* 15 (1), 251. doi: 10.1186/s13018-020-01757-9

Li, H., Bai, R., Zhao, Z., Tao, L., Ma, M., Ji, Z., et al. (2018). Application of droplet digital PCR to detect the pathogens of infectious diseases. *Biosci. Rep.* 38 (6), BSR20181170. doi: 10.1042/BSR20181170

McEvoy, A. C., Wood, B. A., Ardakani, N. M., Pereira, M. R., Pearce, R., Cowell, L., et al. (2018). Droplet digital PCR for mutation detection in formalin-fixed, paraffin-embedded melanoma tissues: A comparison with sanger sequencing and pyrosequencing. *J. Mol. Diagn.* 20 (2), 240–252. doi: 10.1016/j.jmoldx.2017.11.009

Miotke, L., Lau, B. T., Rumma, R. T., and Ji, H. P. (2014). High sensitivity detection and quantitation of DNA copy number and single nucleotide variants with single color droplet digital PCR. *Anal. Chem.* 86 (5), 2618–2624. doi: 10.1021/ac403843j

Ong, K. L., Kurtz, S. M., Lau, E., Bozic, K. J., Berry, D. J., and Parvizi, J. (2009). Prosthetic joint infection risk after total hip arthroplasty in the Medicare population. *J. Arthroplasty* 24 (6 Suppl), 105–109. doi: 10.1016/j.arth.2009.04.027

Osmon, D. R., Berbari, E. F., Berendt, A. R., Lew, D., Zimmerli, W., Steckelberg, J. M., et al. (2013). Executive summary: diagnosis and management of prosthetic joint infection: clinical practice guidelines by the Infectious Diseases Society of America. *Clin. Infect. Dis.* 56 (1), 1–10. doi: 10.1093/cid/cis966

Palan, J., Nolan, C., Sarantos, K., Westerman, R., King, R., and Foguet, P. (2019). Culture-negative periprosthetic joint infections. *EFORT Open Rev.* 4 (10), 585–594. doi: 10.1302/2058-5241.4.180067

Pannu, T. S., Villa, J. M., and Higuera, C. A. (2021). Diagnosis and management of infected arthroplasty. *SICOT J.* 7, 54. doi: 10.1051/sicotj/2021054

Parvizi, J., Zmistowski, B., Berbari, E. F., Bauer, T. W., Springer, B. D., Della Valle, C. J., et al. (2011). New definition for periprosthetic joint infection: from the Workgroup of the Musculoskeletal Infection Society. *Clin. Orthop. Relat. Res.* 469 (11), 2992–2994. doi: 10.1007/s11999-011-2102-9

Patel, R. (2023). Periprosthetic joint infection. *New Engl. J. Med.* 388 (3), 251–262. doi: 10.1056/NEJMra2203477

Peel, T. N., Buising, K. L., and Choong, P. F. (2012). Diagnosis and management of prosthetic joint infection. *Curr. Opin. Infect. Dis.* 25 (6), 670–676. doi: 10.1097/QCO.0b013e32835915db

Perez-Prieto, D., Portillo, M. E., Puig-Verdie, L., Alier, A., Martinez, S., Sorli, L., et al. (2017). C-reactive protein may misdiagnose prosthetic joint infections, particularly chronic and low-grade infections. *Int. Orthop.* 41 (7), 1315–1319. doi: 10.1007/s00264-017-3430-5

Petti, C. A. (2007). Detection and identification of microorganisms by gene amplification and sequencing. *Clin. Infect. Dis.* 44 (8), 1108–1114. doi: 10.1086/512818

Pinheiro, L. B., Coleman, V. A., Hindson, C. M., Herrmann, J., Hindson, B. J., Bhat, S., et al. (2012). Evaluation of a droplet digital polymerase chain reaction format for DNA copy number quantification. *Anal Chem.* 84 (2), 1003–1011. doi: 10.1021/ac202578x

Piper, K. E., Fernandez-Sampedro, M., Steckelberg, K. E., Mandrekar, J. N., Karau, M. J., Steckelberg, J. M., et al. (2010). C-reactive protein, erythrocyte sedimentation rate and orthopedic implant infection. *PloS One* 5 (2), e9358. doi: 10.1371/journal.pone.0009358

Plouzeau, C., Bemer, P., Valentin, A. S., Hery-Arnaud, G., Tande, D., Jolivet-Gougeon, A., et al. (2015). First experience of a multicenter external quality assessment of molecular 16S rRNA gene detection in bone and joint infections. *J. Clin. Microbiol.* 53 (2), 419–424. doi: 10.1128/JCM.02413-14

Rodriguez-Merchan, E. C. (2022). The function of sonication in the diagnosis of periprosthetic joint infection after total knee arthroplasty. *Arch. Bone Jt Surg.* 10 (9), 735–740. doi: 10.22038/abjs.2020.44329.2212

Rougemont, M., Van Saanen, M., Sahli, R., Hinrikson, H. P., Bille, J., and Jaton, K. (2004). Detection of four Plasmodium species in blood from humans by 18S rRNA gene subunit-based and species-specific real-time PCR assays. *J. Clin. Microbiol.* 42 (12), 5636–5643. doi: 10.1128/JCM.42.12.5636-5643.2004

Saleh, A., George, J., Faour, M., Klika, A. K., and Higuera, C. A. (2018). Serum biomarkers in periprosthetic joint infections. *Bone Joint Res.* 7 (1), 85–93. doi: 10.1302/2046-3758.71.BJR-2017-0323

Schwarz, E. M., Parvizi, J., Gehrke, T., Aiyer, A., Battenberg, A., Brown, S. A., et al. (2019). 2018 International consensus meeting on musculoskeletal infection: research priorities from the general assembly questions. *J. Orthop. Res.* 37 (5), 997–1006. doi: 10.1002/jor.24293

Trampuz, A., Piper, K. E., Jacobson, M. J., Hanssen, A. D., Unni, K. K., Osmon, D. R., et al. (2007). Sonication of removed hip and knee prostheses for diagnosis of infection. *N Engl. J. Med.* 357 (7), 654–663. doi: 10.1056/NEJMoa061588

Wang, F. D., Wang, Y. P., Chen, C. F., and Chen, H. P. (2018). The incidence rate, trend and microbiological aetiology of prosthetic joint infection after total knee arthroplasty: A 13 years' experience from a tertiary medical center in Taiwan. *J. Microbiol. Immunol. Infect.* 51 (6), 717–722. doi: 10.1016/j.jmii.2018.08.011

Zmrzljak, U. P., Košir, R., Krivokapić, Z., Radojković, D., and Nikolić, A. (2021). Detection of somatic mutations with ddPCR from liquid biopsy of colorectal cancer patients. *Genes (Basel).* 12 (2), 289. doi: 10.3390/genes12020289

Frontiers in
Cellular and Infection Microbiology

Investigates how microorganisms interact with their hosts

Explores bacteria, fungi, parasites, viruses, endosymbionts, prions and all microbial pathogens as well as the microbiota and its effect on health and disease in various hosts.

Discover the latest Research Topics

See more →

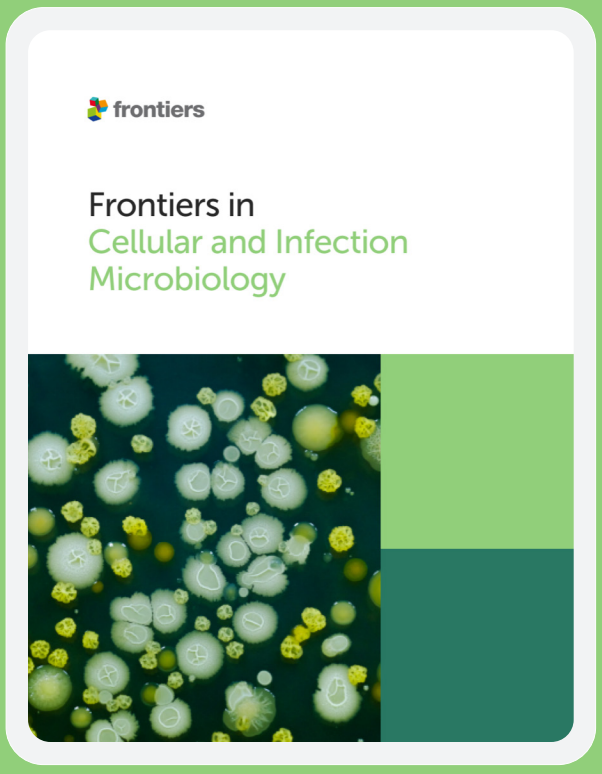

Frontiers

Avenue du Tribunal-Fédéral 34
1005 Lausanne, Switzerland
frontiersin.org

Contact us

+41 (0)21 510 17 00
frontiersin.org/about/contact